NAVAL POSTGRADUATE SCHOOL
Monterey, California

THESIS   20000501 055

PROBABILITY OF SYMBOL ERROR FOR COHERENT
AND NON-COHERENT DETECTION OF M-ARY
FREQUENCY-SHIFT KEYED (MFSK) SIGNALS
AFFECTED BY CO-CHANNEL INTERFERENCE AND
ADDITIVE WHITE GAUSSIAN NOISE (AWGN) IN A
FADING CHANNEL

by

Andreas Argyriou

March 2000

Thesis Advisor:	Jovan Lebaric
Thesis Co-Advisor:	Clark Robertson

Approved for public release; distribution is unlimited.

DTIC QUALITY INSPECTED 3

REPORT DOCUMENTATION PAGE

Form Approved
OMB No. 0704-0188

Public reporting burden for this collection of information is estimated to average 1 hour per response, including the time for reviewing instruction, searching existing data sources, gathering and maintaining the data needed, and completing and reviewing the collection of information. Send comments regarding this burden estimate or any other aspect of this collection of information, including suggestions for reducing this burden, to Washington headquarters Services, Directorate for Information Operations and Reports, 1215 Jefferson Davis Highway, Suite 1204, Arlington, VA 22202-4302, and to the Office of Management and Budget, Paperwork Reduction Project (0704-0188) Washington DC 20503.

1. AGENCY USE ONLY *(Leave blank)*	2. REPORT DATE March 2000	3. REPORT TYPE AND DATES COVERED Master's Thesis

4. TITLE AND SUBTITLE PROBABILITY OF SYMBOL ERROR FOR COHERENT AND NON-COHERENT DETECTION OF M-ARY FREQUENCY-SHIFT KEYED (MFSK) SIGNALS AFFECTED BY CO-CHANNEL INTERFERENCE AND ADDITIVE WHITE GAUSSIAN NOISE (AWGN) IN A FADING CHANNEL	5. FUNDING NUMBERS
6. AUTHOR(S) Andreas Argyriou	

7. PERFORMING ORGANIZATION NAME(S) AND ADDRESS(ES) Naval Postgraduate School Monterey, CA 93943-5000	8. PERFORMING ORGANIZATION REPORT NUMBER

9. SPONSORING / MONITORING AGENCY NAME(S) AND ADDRESS(ES) Research and Development Office	10. SPONSORING / MONITORING AGENCY REPORT NUMBER

11. SUPPLEMENTARY NOTES

The views expressed in this thesis are those of the author and do not reflect the official policy or position of the Department of Defense or the U.S. Government.

12a. DISTRIBUTION / AVAILABILITY STATEMENT Approved for public release; distribution is unlimited.	12b. DISTRIBUTION CODE

13. ABSTRACT *(maximum 200 words)*

The probability of symbol error for coherent and non-coherent detection of M-ary frequency-shift keyed (MFSK) signals affected by other interfering MFSK signals (co-channel interference) and additive white Gaussian noise (AWGN) in a fading channel (Rayleigh and Rician models) is quantified in this thesis. First, theoretical expressions are derived for the symbol error probability as a function of the signal-to-noise ratio SNR and the signal-to-interference/jamming ratio SJR. Next, using SIMULINK and the MATLAB/SIMULINK Communications Toolbox, we develop models to determine the symbol error probability for Monte Carlo type simulations. Finally, we compare the theoretical symbol error probabilities with the simulation's results and identify the differences and their possible causes.

14. SUBJECT TERMS Communications, MFSK coherent -- non-coherent detection, interference, AWGN, fading channel, simulink.	15. NUMBER OF PAGES 307
	16. PRICE CODE

17. SECURITY CLASSIFICATION OF REPORT Unclassified	18. SECURITY CLASSIFICATION OF THIS PAGE Unclassified	19. SECURITY CLASSIFI- CATION OF ABSTRACT Unclassified	20. LIMITATION OF ABSTRACT UL

NSN 7540-01-280-5500

Standard Form 298 (Rev. 2-89)
Prescribed by ANSI Std. 239-18

i

PROBABILITY OF SYMBOL ERROR FOR COHERENT AND NON-COHERENT DETECTION OF M-ARY FREQUENCY-SHIFT KEYED (MFSK) SIGNALS AFFECTED BY CO-CHANNEL INTERFERENCE AND ADDITIVE WHITE GAUSSIAN NOISE (AWGN) IN A FADING CHANNEL

Andreas Argyriou
Captain, Hellenic Air Force
B.Sc., Hellenic Air Force Academy, 1988

Submitted in partial fulfillment of the
requirements for the degree of

MASTER OF SCIENCE IN ELECTRICAL ENGINEERING

from the

NAVAL POSTGRADUATE SCHOOL
March 2000
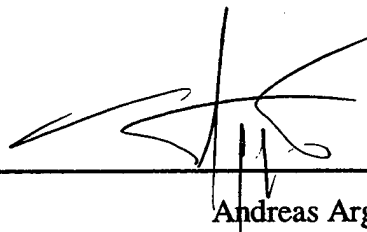
Author: _____
Andreas Argyriou
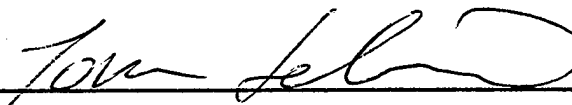
Approved by: _____
Jovan Lebaric, Thesis Advisor
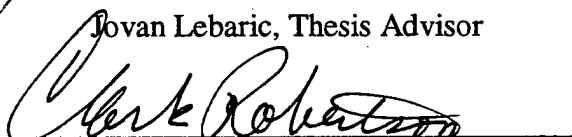
_____
Clark Robertson, Thesis Co-Advisor
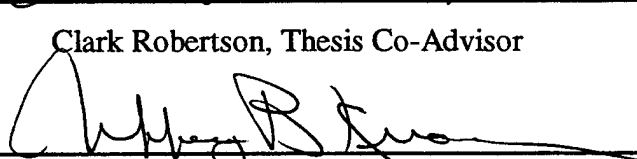
_____
Jeffrey Knorr, Chairman
Department of Electrical and Computer Engineering

iii

ABSTRACT

The probability of symbol error for coherent and non-coherent detection of M-ary frequency-shift keyed (MFSK) signals affected by other interfering MFSK signals (co-channel interference) and additive white Gaussian noise (AWGN) in a fading channel (Rayleigh and Rician models) is quantified in this thesis. First, theoretical expressions are derived for the symbol error probability as a function of the signal-to-noise ratio SNR and the signal-to-interference/jamming ratio SJR. Next, using SIMULINK and the MATLAB/SIMULINK Communications Toolbox, we develop models to determine the symbol error probability for Monte Carlo type simulations. Finally, we compare the theoretical symbol error probabilities with the simulation's results and identify the differences and their possible causes.

TABLE OF CONTENTS

ACKNOWLEDGMENT

I.   INTRODUCTION

A.   THESIS OBJECTIVES

The primary research question of this thesis is how the probability of symbol error for coherent and non-coherent detection of M-ary frequency-shift keyed (MFSK) signals is affected by another, interfering, MFSK signal (co-channel interference), additive white Gaussian noise (AWGN), and a fading channel.

First, theoretical expressions are derived for the probability of symbol error as a function of the signal-to-noise ratio SNR and the signal-to-interference/jamming ratio SJR. Next, using Simulink and Matlab/Simulink Communications Toolbox, we develop models to determine the probability of symbol error for Monte Carlo type simulations. Finally, we verify the theoretical probabilities of symbol error with respect to the simulation's results and identify any discrepancies between them.

B.   BACKGROUND

Interference is the effect of a non-desirable signal on the reception of a desirable signal and can be a major factor limiting the performance of a digital communications system. Co-channel interference is a type of system-generated interference which refers to the degradation caused by a non-desirable signal of the same type as the desirable signal. Co-channel interference is most commonly introduced by other users of the same portion of the RF spectrum operating similar/same types of equipment. The frequency-nonselective, slowly fading channel results in multiplicative distortion of the MFSK transmitted signal. It is important to quantify the effects of co-channel interference and

fading such that measures can be taken to improve the communication system's performance. To do so, we can use computer simulation, which falls into the middle ground between idealized modeling using formulae and hardware prototyping. Designing, implementing and testing hardware is expensive and time consuming, and is becoming more so as communication systems increase in sophistication and complexity, while the computing costs continue to decrease.

Some computer simulations for an MFSK signal operating in the presence of AWGN and co-channel interference have already been performed, and the results are presented in Chapter V of [Ref 1]. This thesis is the continuation and extension of the work presented in [Ref 1]. All the theoretical expressions derived in Chapters IV, V, and VI as well as the closed form solutions in Appendices A, B, and C are believed to be original.

C.   IMPLEMENTATION

All the necessary system modeling is performed in the time domain and based on Simulink Monte Carlo type computer simulations. The probabilities of symbol error that indicate the system's performance are obtained under realistic conditions and assumptions for different values of system's parameters.

Chapters III through VI contain the corresponding mathematical procedure for the case that it is referred to, the models that are used for the simulation, the simulation results, and the verification of the theoretical results with respect to the simulation's results. Finally, conclusions and recommendations for future considerations are presented.

II. M-ARY FREQUENCY SHIFT-KEYING (MFSK)

In a digital communication system, the modulator maps a sequence of binary digits into a set of corresponding signal waveforms. The digital modulation allows us to construct signal waveforms that correspond to multidimensional vectors and signal space diagrams.

One way of creating multidimensional signals is to use M equal energy orthogonal signal waveforms that differ in frequency. Consequently, each transmitted symbol is assigned a specific frequency, and the corresponding MFSK signal is represented as by the following equation:

$$s_m(t) = \sqrt{\frac{2 \cdot E}{T}} \cdot \cos\left[2 \cdot \pi \cdot \left(f_c + m \cdot \Delta f \right) \cdot t + \phi \right] \tag{2.1}$$

where:

m = 1,2,...,M with M equal to the number of transmitted symbols

T is the symbol duration

E is the signal waveform's energy during the time equal to the symbol duration T

Δf is the spacing between any two adjacent frequencies

f_c is the lowest frequency

ϕ is an arbitrary constant for the phase angle.

A. PROBABILITY OF SYMBOL ERROR FOR COHERENT DETECTION OF MFSK SIGNAL CORRUPTED BY AWGN

The symbol error probability for coherent detection of MFSK signal corrupted by AWGN is given by the following expression [Ref 2]:

$$P_{error} = 1 - \frac{1}{\sqrt{2 \cdot \pi}} \cdot \int_{-\infty}^{\infty} e^{-\frac{x^2}{2}} \cdot \left(1 - Q\left(x + \sqrt{\frac{2 \cdot E_s}{N_0}}\right)\right)^{M-1} dx \qquad (2.2)$$

where:

E_s is the energy of each transmitted symbol

N_0 is the on-sided AWGN power spectral density

and the Q-function is given by the following expression:

$$Q(x) = \frac{1}{2} \cdot \left(1 - erf\left(\frac{x}{\sqrt{2}}\right)\right) \qquad (2.3)$$

where the error function (erf) is defined as:

$$erf(x) = \frac{1}{\sqrt{2 \cdot \pi}} \cdot \int_{0}^{x} e^{-x^2} dx \qquad (2.4)$$

The symbol signal-to-noise ratio is defined as:

$$SNR = 10 \cdot \log\left(\frac{E_s}{N_0}\right) \qquad (2.5)$$

From the last expression we get the equivalent expression:

$$\sqrt{\frac{E_s}{N_0}} = 10^{\frac{SNR}{20}} \qquad (2.6)$$

Now, we can express the symbol error probability in terms of the symbol signal-to-noise ratio SNR as follows:

$$P_{error} = 1 - \frac{1}{\sqrt{2 \cdot \pi}} \cdot \int_{-\infty}^{\infty} e^{\frac{-x^2}{2}} \cdot \left(1 - Q\left(x + \sqrt{2 \cdot 10^{\frac{SNR}{20}}}\right)\right)^{M-1} dx \qquad (2.7)$$

Figure 1 is a graph of the probability of symbol error for coherent detection of 2FSK, 4FSK, and 8FSK signals as a function of the symbol SNR. The signal-to-noise ratio is expressed in dB, starting from –5 dB and ending at +20 dB.
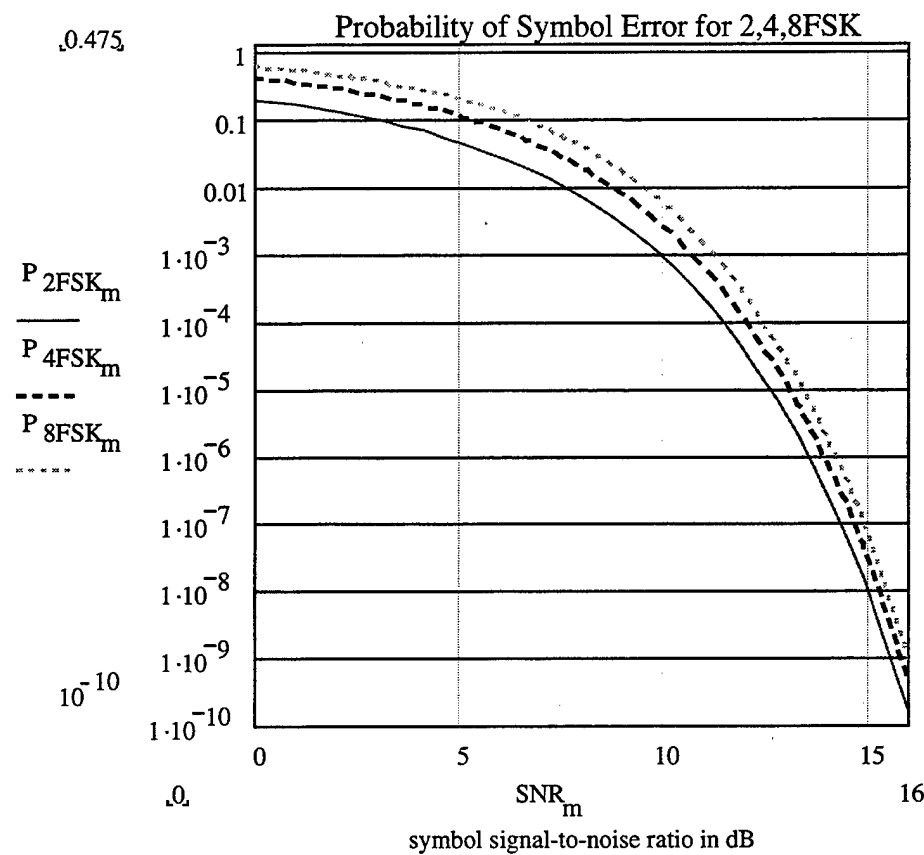
Figure 1. Probability of symbol error for coherent detection of 2, 4, and 8FSK signals.

5

Using MATLAB/SIMULINK and the COMMUNICATIONS TOOLBOX, we can develop corresponding models and perform Monte Carlo type simulations for the above case to verify the theoretical results. The implementation of the models, as well as their performance analysis, are described in [Ref 1].

B. PROBABILITY OF SYMBOL ERROR FOR NONCOHERENT DETECTION OF MFSK SIGNAL CORRUPTED BY AWGN

The symbol error probability for non-coherent detection of MFSK signals corrupted by AWGN is given by the following expression [Ref 2]:

$$P_{error} = \sum_{k=1}^{M-1} \frac{(M-1)!}{k! \cdot (M-1-k)!} \cdot (-1)^{k+1} \cdot \frac{1}{k+1} \cdot e^{\frac{-k}{k+1} \frac{E_s}{N_0}} \qquad (2.8)$$

where:

E_s is the energy of each transmitted symbol

N_0 is the one-sided AWGN power spectral density

M is the number of the transmitted waveforms (symbols)

Now, we can express the symbol error probability in terms of the symbol signal-to-noise ratio SNR as follows:

$$P_{error} = \sum_{k=1}^{M-1} \frac{(M-1)!}{k! \cdot (M-1-k)!} \cdot (-1)^{k+1} \cdot \frac{1}{k+1} \cdot e^{\frac{-k}{(k+1)} \cdot 10^{\frac{SNR}{10}}} \qquad (2.9)$$

Figure 2 is a graph of the probability of symbol error for non-coherent detection of 2FSK, 4FSK, and 8FSK signals as a function of the symbol SNR.

Probability of Symbol Error for 2,4,8FSK
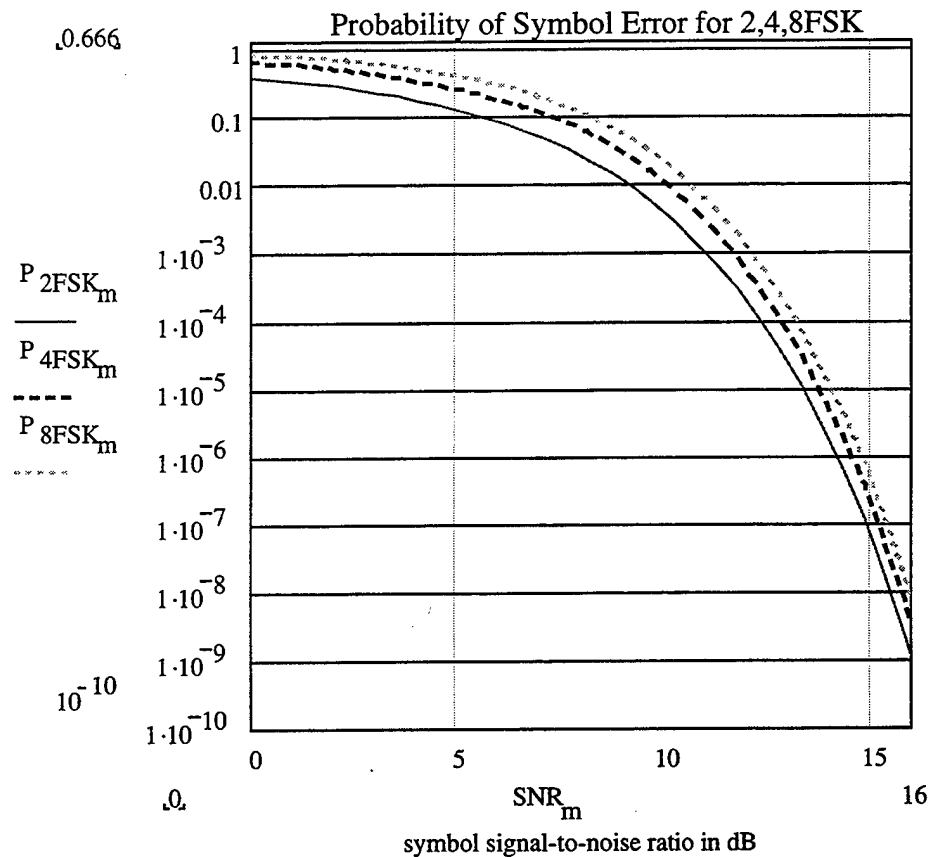
Figure 2. Probability of symbol error for non-coherent detection of 2, 4, and 8FSK signals.

Using MATLAB/SIMULINK and the COMMUNICATIONS TOOLBOX, we can develop corresponding models and perform Monte Carlo type simulations for the above case to verify the theoretical results. The implementation of the models, as well as their performance analysis, is described in [Ref 1].

III. MFSK CORRUPTED BY AWGN AND OPERATING IN A FADING CHANNEL

In this chapter we consider an MFSK signal operating in a noisy and fading channel. First, the theoretical probabilities of symbol error are derived for coherent and non-coherent detection, and then, the simulation results are presented for comparison purposes. The Monte Carlo type simulation is performed in the time domain using MATLAB/SIMULINK models. Two separate cases of channel fading are examined: the frequency-nonselective, slowly fading Rayleigh channel and the frequency-nonselective, slowly fading Rician channel.

A. RAYLEIGH FADING CHANNEL – COHERENT DETECTION

In this section, we derive the symbol error rate performance of MFSK signals when these signals are transmitted over a frequency-nonselective, slowly fading Rayleigh channel. The frequency-nonselective, slowly fading channel results in multiplicative distortion of the MFSK transmitted signal. The condition that the channel fades slowly implies that the multiplicative process may be considered as a constant during at least one signaling time interval. Furthermore, we assume that the channel fading is sufficiently slow that the phase shift introduced by the channel can be estimated from the received signal without error.

1. Theoretical Probability Of Symbol Error For Coherent Detection

We determine the performance of the MFSK communications system by evaluating the decision variables that appear during signal reception. The conditional

probability of symbol error is the standard probability of error for coherent, orthogonal

MFSK signal when AWGN is present:

$$P_{error}(r) = 1 - \frac{1}{\sqrt{2 \cdot \pi}} \cdot \int_{-\infty}^{\infty} e^{\frac{-x^2}{2}} \cdot \left(1 - Q\left(x + \frac{r}{\sigma}\right)\right)^{M-1} dx \qquad (3.1)$$

where:

r is the amplitude of the MFSK signal

σ is the standard deviation of the AWGN

To obtain the symbol error probabilities when r is random, we must average $P_{error}(r)$ over the probability density function of r. Since r is assumed to be Rayleigh distributed, its probability density function is given by:

$$f(r) = \frac{r}{\alpha^2} \cdot e^{\frac{-r^2}{2 \cdot \alpha^2}} \quad \text{for } r \geq 0 \quad \text{and} \quad f(r) = 0 \quad \text{for } r < 0 \qquad (3.2)$$

where:

α^2 is the symbol power of the fading information signal.

In terms of signal's power P_{sig}, we obtain:

$$f(r) = \frac{r}{P_{sig}} \cdot e^{\frac{-r^2}{2 \cdot P_{sig}}} \qquad (3.3)$$

where:

P_{sig} is equal to α^2.

10

Now, we must integrate the product of $P_{error}(r)$ and the probability density function $f(r)$ of the random variable r over all the possible values of r:

$$P_{error} = 1 - \frac{1}{\sqrt{2 \cdot \pi}} \cdot \int_0^\infty \int_{-\infty}^\infty e^{\frac{-x^2}{2}} \cdot \left(1 - Q\left(x + \frac{r}{\sqrt{P_{noise}}}\right)\right)^{M-1} \cdot \left(\frac{r}{P_{sig}} \cdot e^{\frac{-r^2}{2 \cdot P_{sig}}}\right) dx \, dr \qquad (3.4)$$

Using the transformation

$$\frac{r}{\sqrt{P_{sig}}} = y \qquad (3.5)$$

and defining the relationship for the average signal-to-noise power ratio of the information signal as

$$\frac{P_{sig}}{\sigma^2} = 10^{\frac{SNR_{dB}}{10}} \qquad (3.6)$$

we easily get

$$P_{error} = 1 - \frac{1}{\sqrt{2 \cdot \pi}} \cdot \int_0^\infty \int_{-\infty}^\infty e^{\frac{-\left(x^2 + y^2\right)}{2}} \cdot \left(1 - Q\left(x + y \cdot 10^{\frac{SNR_{dB}}{20}}\right)\right)^{M-1} \cdot y \, dx \, dy \qquad (3.7)$$

The above integral has to be evaluated numerically.

Figure 3 is an illustration of the symbol error probabilities for coherent detection of 2, 4, and 8FSK as a function of the average SNR.

11
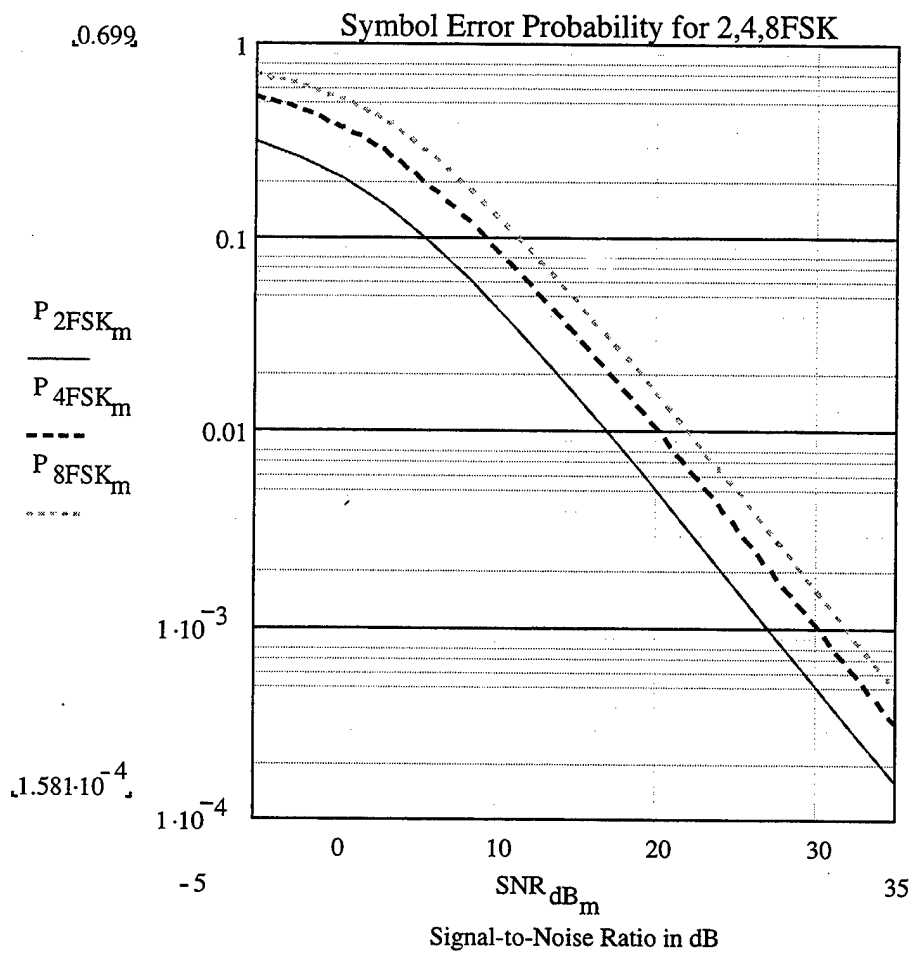
Figure 3. Probability of symbol error for coherent detection of 2, 4, 8FSK signals in Rayleigh fading channel.

We observe that the required SNR to obtain a symbol error probability of 10^{-4} is about +35 dB and more when the channel is Rayleigh fading, while for a non-fading channel the required SNR to obtain symbol error probability of 10^{-4} was about +12 dB.

2. Simulink Model and Block Analysis

The block diagram of the Simulink model, which has been developed for the simulation of coherent MFSK in a Rayleigh fading channel, is shown in Figure 4. The implementation of the blocks of this model is described in [Ref 1] and only the modifications are discussed in this section.
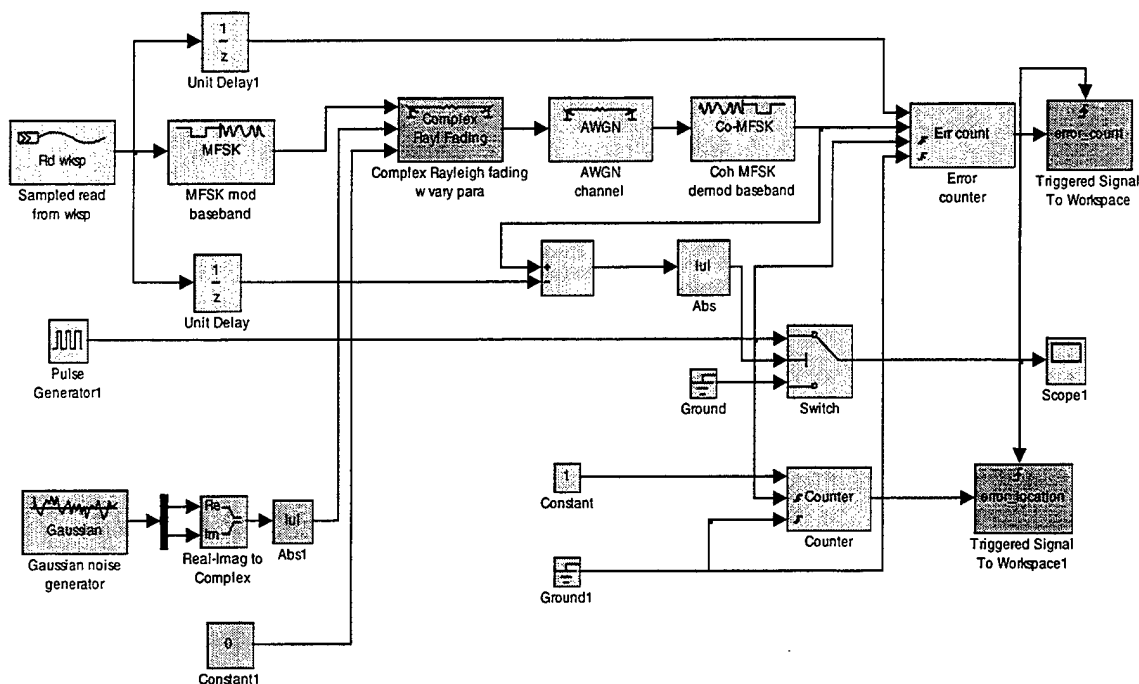
Figure 4. Model for coherent MFSK in a Rayleigh fading channel.

a) Complex Rayl Fading Block

This block introduces Rayleigh fading and has no fixed parameters. The fading envelope and the phase shift of the channel change with the second and third input port values. The first input port value is a unit-amplitude FSK modulated signal. The

13

second input is a Rayleigh distributed random scalar. The third input, which applies the phase variation, is set to zero since it is assumed that the receiver is capable of coherent detection even though the signal is fading.

b) Gaussian Noise Generator

This block generates two Gaussian distributed noise variables with zero mean value. The variance for each noise is equal to the half of power of the diffuse signal component, so that the resulting Rayleigh distributed random variable has a variance exactly equal to the power of the diffuse signal component. First, using the model of Figure 5, we perform a test to determine how SIMULINK evaluates the total signal power.
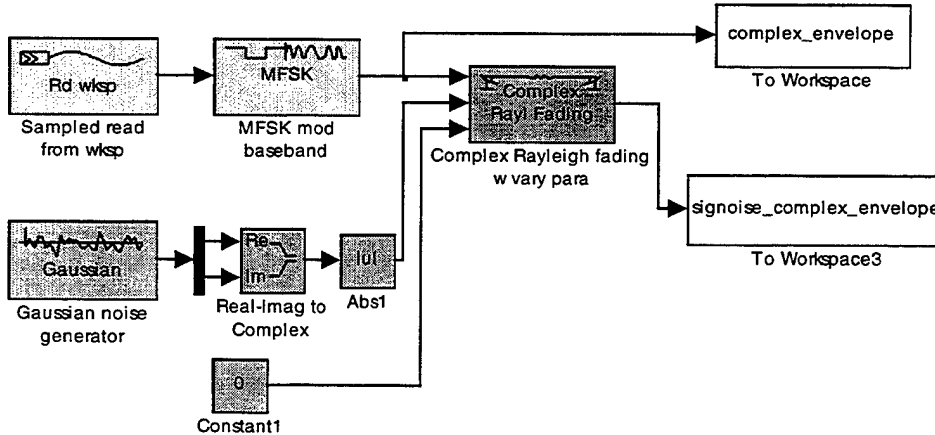
Figure 5. Model for testing the power of the fading signal.

Table 1 is a tabulation of the results obtained for the power of the fading signal, given different values for the Rayleigh RF power in the block Rayleigh noise generator.

14

RAYLEIGH RF POWER INPUT (DIFFUSE COMPONENT ONLY)	POWER OF THE FADING SIGNAL (TEST MEASUREMENT)
1	1.0195
2	2.0390
3	3.0585
4	4.0780
5	5.0975

Table 1. Results for signal's power given different values for Rayleigh RF power.

It is observed that the total RF power of the fading signal is preserved. Related to this, note that the noise variance parameter (noise_var) of the AWGN channel block needs to be multiplied by a factor of two because of the bandpass to lowpass transformation. The output vector size of this block is the same as the vector size of the seed and determines the variation of the fading envelope for the Complex Rayleigh Fading Block.

3.   Simulation Analysis And Performance Verification

In this section, simulation results are presented in order to verify the performance of the MFSK system for coherent detection in a Rayleigh fading channel. Each simulation runs until at least 100 errors are observed [Ref 1]. The observed error number is a random variable subjected to statistical variations. In general, a different number of errors occur each time a simulation is run with a different set of seeds for data, noise and envelope fading. The data sequences are limited to 10^6 symbols for each simulation to prevent 'out of memory' errors. As long as less than 100 errors are observed, the simulation sequence is repeated until a sufficient number of errors are counted.

15

a) Results For 2FSK

The theoretical as well as the experimental symbol error probabilities for coherently detected 2FSK are presented in Figure 5 as functions of the average signal-to-noise ratio in dB. Most communication systems are designed to obtain symbol error rates equal or less than 10^{-4}. Therefore, we present results for the range of values of the signal-to-noise ratio from -5 dB to 35 dB. For large signal-to-noise ratios, the time needed for the simulation increases significantly.
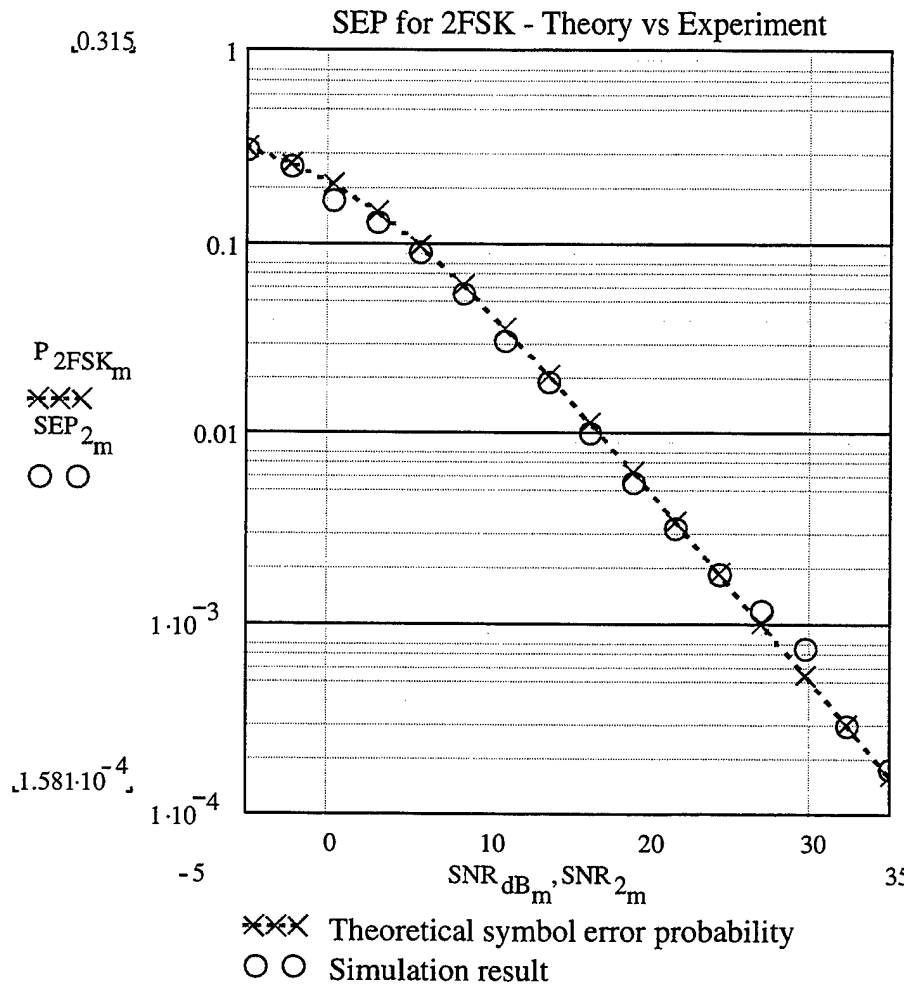
Figure 6. Probability of symbol error (theoretical and experimental) for coherent detection of 2FSK signal corrupted by AWGN in a Rayleigh fading channel.

16

In Figure 7, the difference between the theoretical and experimental symbol error probability is shown.
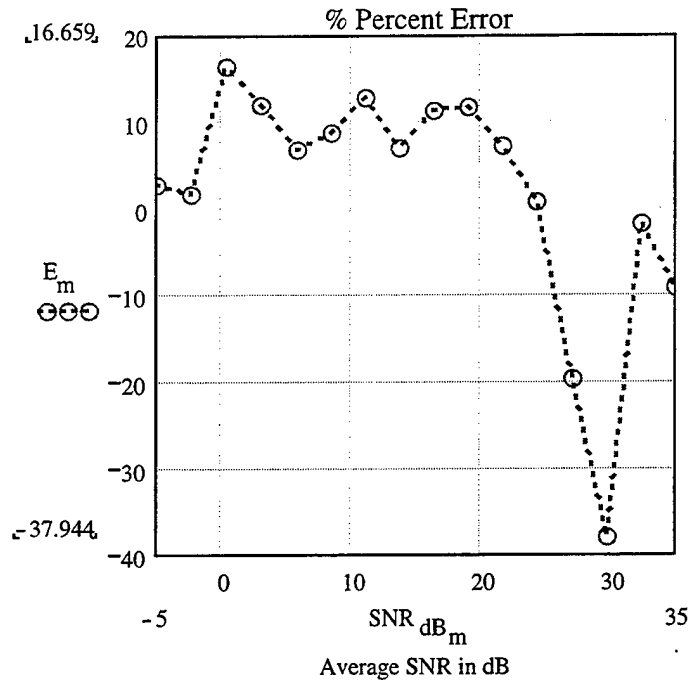
Figure 7. Percent difference (error) between theoretical and simulation results.

We can easily observe that the simulation results for coherent 2FSK in the presence of AWGN and Rayleigh fading channel agree very well with the theory. The summary of the accuracy of the simulation for this case is presented below.

	SYMBOL ERROR PROBABILITY	COHERENT 2FSK
1.	Mean Percent Difference (%)	2.07
2.	Maximum Percent Difference (%)	16.659
3.	Minimum Percent Difference (%)	-37.944
4.	Standard Deviation (%)	13.558

Table 2. Results of the comparison of the theoretical SEP and the SEP obtained by the simulation experiment.

b)   Results For 4FSK

The theoretical as well as the experimental symbol error probabilities for coherently detected 4FSK are presented in Figure 8 as functions of the average signal-to-noise ratio in dB.
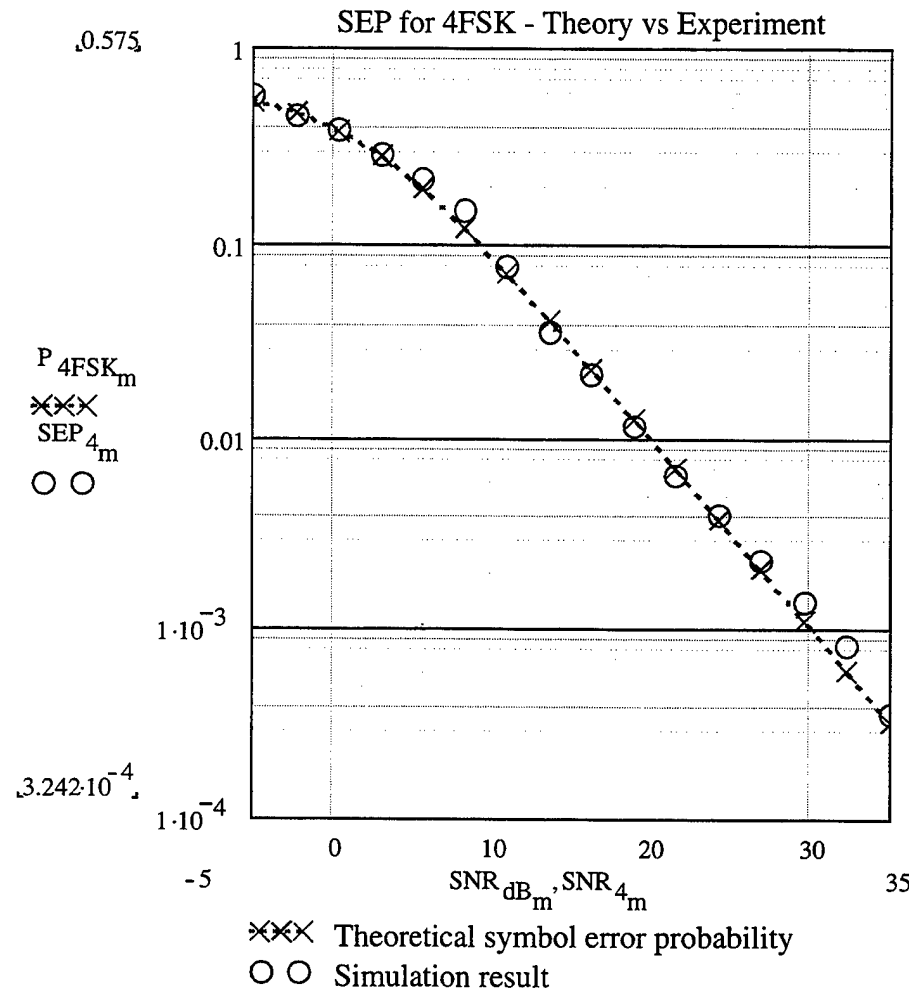
Figure 8. Probability of symbol error (theoretical and experimental) for coherent detection of 4FSK signal corrupted by AWGN in a Rayleigh fading channel.

In Figure 9, the difference between the theoretical and experimental symbol error probability is shown.
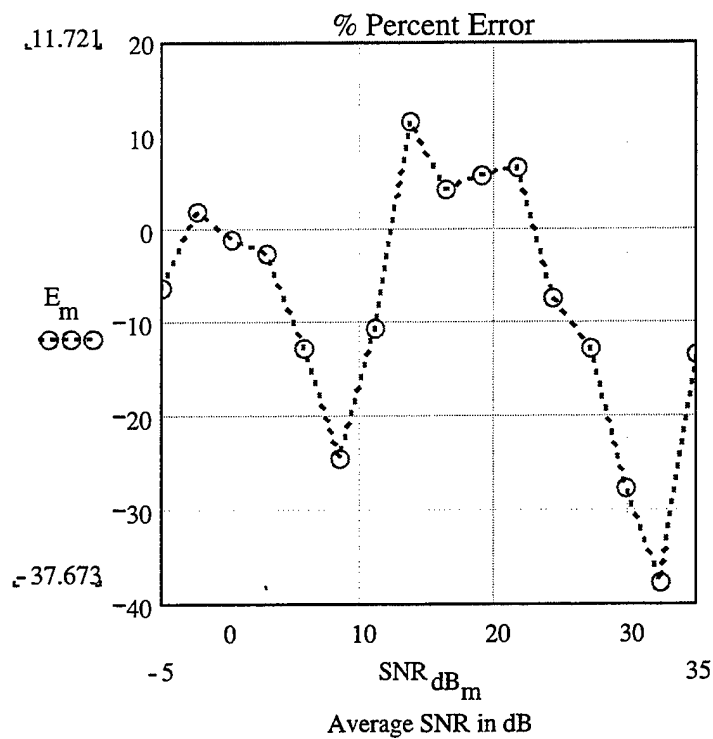
Figure 9. Percent difference (error) between theoretical and simulation results.

Again, we can easily observe that the simulation results for coherent 4FSK in the presence of AWGN and Rayleigh fading channel agree very well with the theory. The summary of the accuracy of the simulation for this case is presented below.

	SYMBOL ERROR PROBABILITY	COHERENT 4FSK
1.	Mean Percent Difference (%)	-7.788
2.	Maximum Percent Difference (%)	11.721
3.	Minimum Percent Difference (%)	-37.673
4.	Standard Deviation (%)	13.075

Table 3. Results of the comparison of the theoretical SEP and the SEP obtained by the simulation experiment.

19

c) Results For 8FSK

The theoretical as well as the experimental symbol error probabilities for coherently detected 8FSK are presented in Figure 10 as functions of the average signal-to-noise ratio in dB.
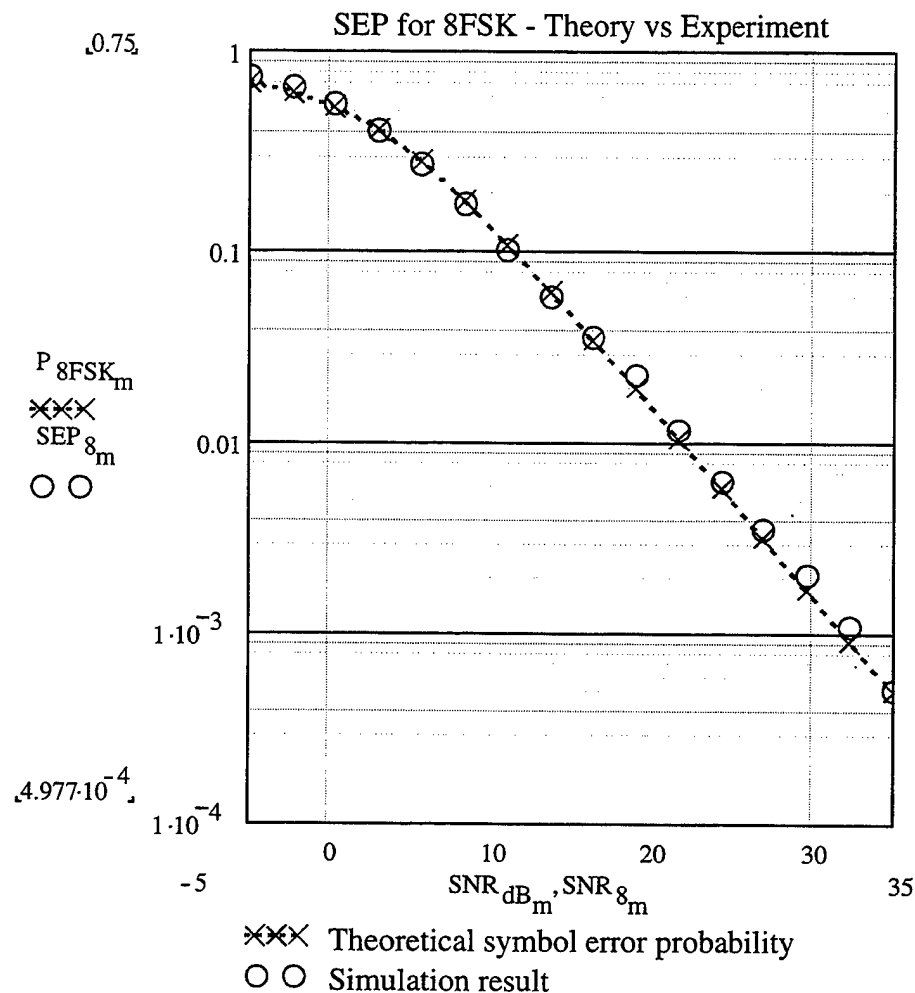
Figure 10. Probability of symbol error (theoretical and experimental) for coherent detection of 8FSK signal corrupted by AWGN in a Rayleigh fading channel.

In Figure 11, the difference between the theoretical and experimental symbol error probability is shown.
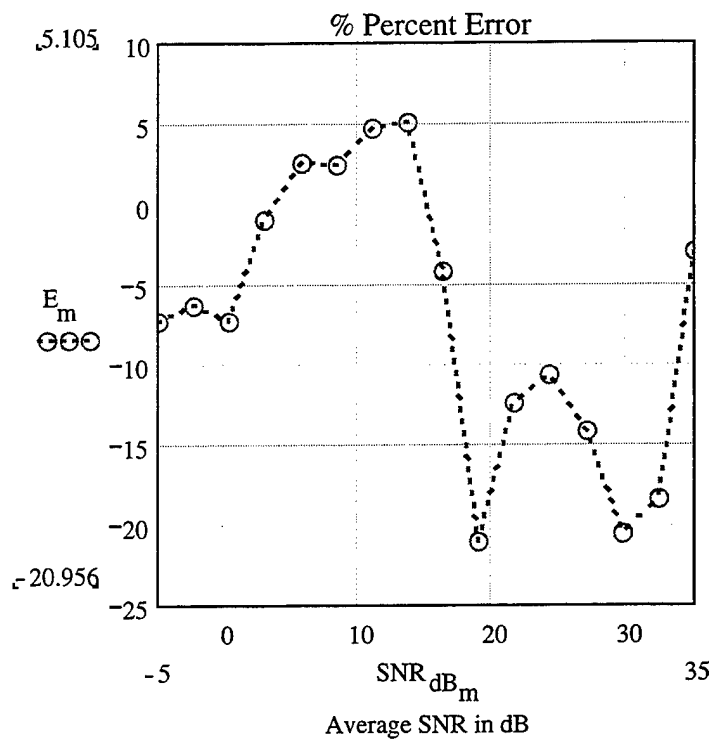
Figure 11. Percent difference (error) between theoretical and simulation results.

Again, we can easily observe that the simulation results for coherent 8FSK in the presence of AWGN and Rayleigh fading channel agree very well with the theory. The summary of the accuracy of the simulation for this case is presented below.

	SYMBOL ERROR PROBABILITY	COHERENT 8FSK
1.	Mean Percent Difference (%)	-6.913
2.	Maximum Percent Difference (%)	5.105
3.	Minimum Percent Difference (%)	-20.956
4.	Standard Deviation (%)	8.409

Table 4. Results of the comparison of the theoretical SEP and the SEP obtained by the simulation experiment.

21

Observing the results for coherent detection of 2, 4, and 8FSK in a Rayleigh fading channel, we note that the simulation underestimates the theory for the 2FSK case while overestimating theory for the cases of 4 and 8FSK. The mean percent error for all the cases is less than 10%, which suggests good simulation accuracy.

The average results for the coherent detection of 2, 4, and 8FSK are:

	SYMBOL ERROR PROBABILITY	AVERAGE RESULTS FOR COHERENT 2, 4, AND 8FSK
1.	Mean Percent Difference (%)	-4.21
2.	Maximum Percent Difference (%)	11.162
3.	Minimum Percent Difference (%)	-32.191
4.	Standard Deviation (%)	11.681

Table 5. Average results for the coherent detection of 2, 4, and 8FSK.

B.   RAYLEIGH FADING CHANNEL – NON-COHERENT DETECTION

In this section, the theoretical performance of non-coherent detection of MFSK is determined and compared to the simulations.

1.   Theoretical Probability Of Symbol Error For Non-Coherent Detection

The conditional probability of symbol error is the standard probability of error for non-coherent, orthogonal MFSK signal when AWGN is present:

$$P_{error}(r) = \sum_{k=1}^{M-1} \frac{(M-1)!}{k! \cdot (M-1-k)!} \cdot (-1)^{k+1} \cdot \frac{1}{k+1} \cdot e^{\frac{-k}{k+1} \cdot \frac{r^2}{2 \cdot \sigma^2}} \qquad (3.8)$$

Integrating the product of the conditional probability of symbol error and the probability density function of the information signal's amplitude r over all possible values of r, we get the unconditional probability of symbol error:

$$P_{error} = \sum_{k=1}^{M-1} \frac{(M-1)!}{k! \cdot (M-1-k)!} \cdot \frac{(-1)^{k+1}}{1 + k \cdot \left(1 + \frac{\alpha^2}{\sigma^2}\right)} \qquad (3.9)$$

where:

α^2 is the power P_{sig} of the fading information signal.

σ is the standard deviation of the AWGN

It is convenient to express the symbol error probability in terms of the average signal-to-noise ratio using the following relationship:

$$\frac{signal\_power}{noise\_power} = \frac{P_{sig}}{P_{noise}} = \frac{\alpha^2}{\sigma^2} = 10^{\frac{SNR_{dB}}{10}} \qquad (3.10)$$

Now, the symbol error probability is given by:

$$P_{error} = \sum_{k=1}^{M-1} \frac{(M-1)!}{k! \cdot (M-1-k)!} \cdot \frac{(-1)^{k+1}}{1 + k \cdot \left(1 + 10^{\frac{SNR_{dB}}{10}}\right)} \qquad (3.11)$$

Figure 12 is an illustration of the symbol error probabilities for non-coherent detection of 2, 4, 8FSK in a Rayleigh fading channel as a function of the average signal to noise ratio.
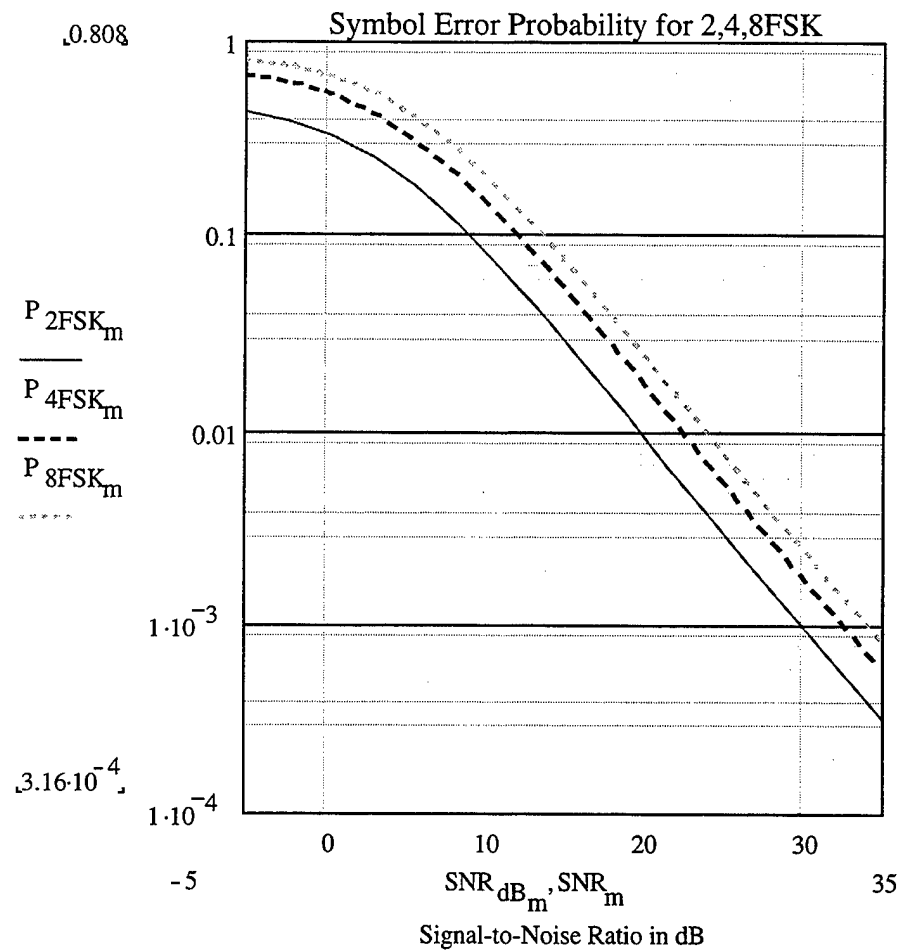
Figure 12. Probability of symbol error for non-coherent detection of 2, 4, 8FSK signals in Rayleigh fading channel.

2. Simulink Model and Block Analysis

The schematic diagram of the Simulink Model, which has been developed for the simulation of non-coherent MFSK signaling in a Rayleigh fading channel, is shown in Figure 13.

24
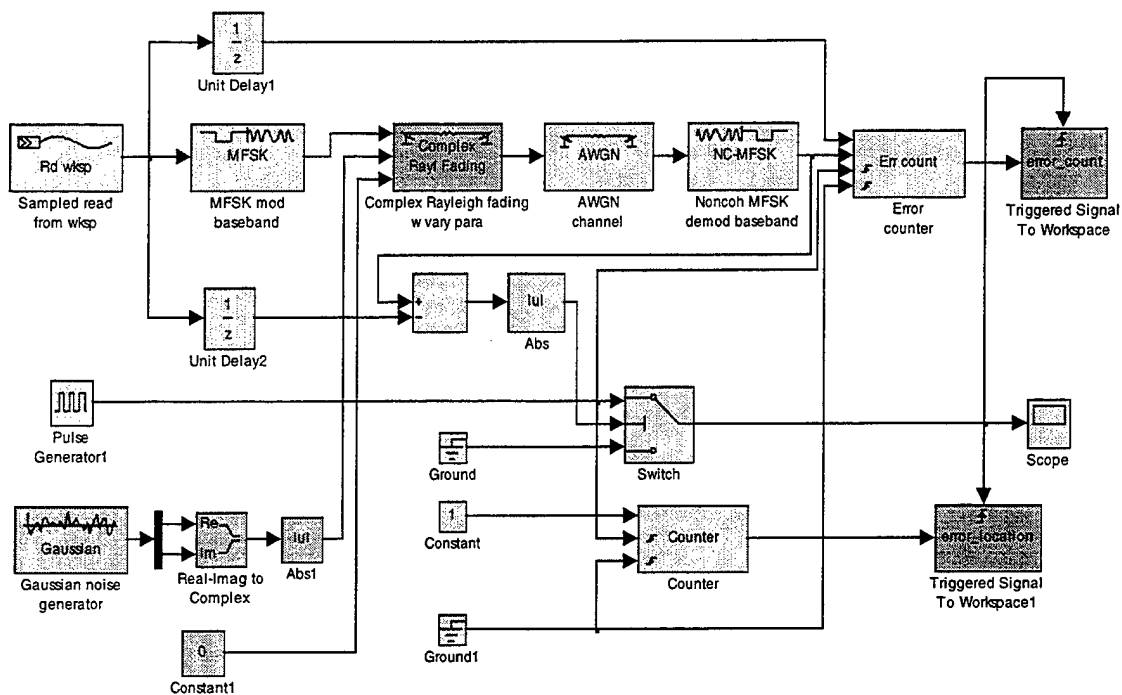
Figure 13. Model for non-coherent detection of MFSK in a Rayleigh fading channel.

The only difference with respect to the coherent case model is that the Coh MFSK demod baseband block has been replaced by the Noncoh MFSK demod baseband block. These blocs are analytically described in [Ref 1].

3. Simulation Analysis And Performance Verification

In this section, simulation results are presented in order to verify the performance of MFSK systems with non-coherent detection in a Rayleigh fading channel. The simulation methods are the same as those of the coherent case.

25

a)   Results For 2FSK

The theoretical as well as the experimental symbol error probabilities for non-coherently detected 2FSK are presented in Figure 14 as functions of the average signal-to-noise ratio in dB.
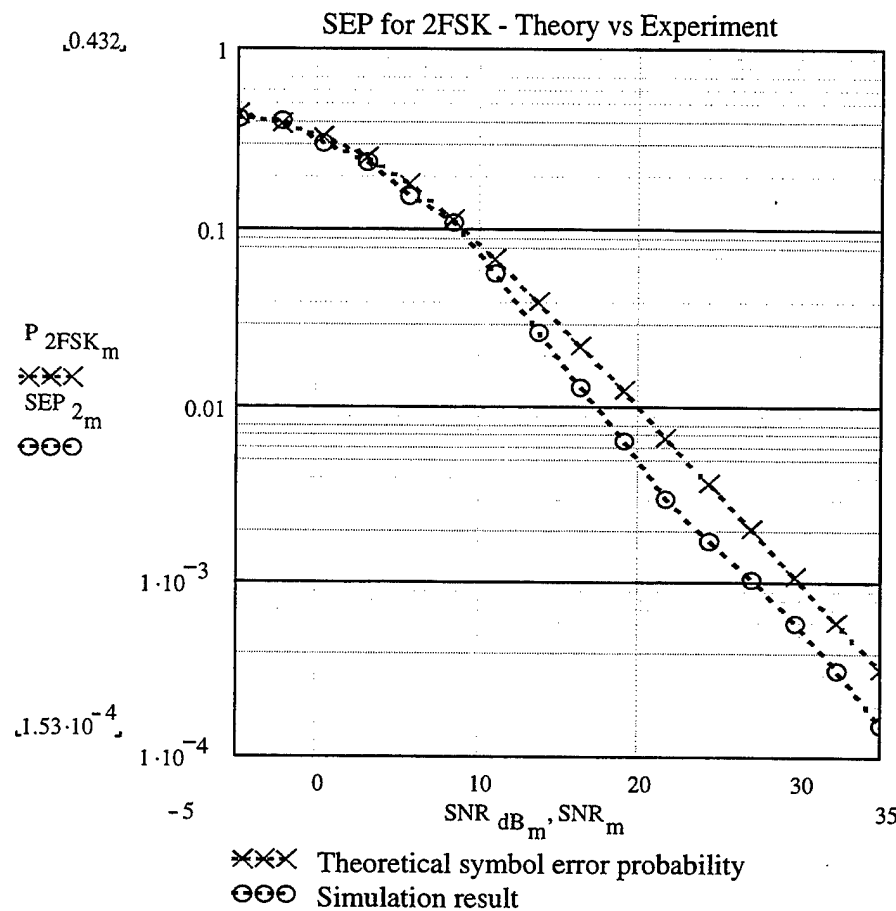

Figure 14. Probability of symbol error (theoretical and simulation) for non-coherent detection of 2FSK signal corrupted by AWGN in a Rayleigh fading channel.

In Figure 15, the difference between the theoretical and the simulation symbol error probability is shown.
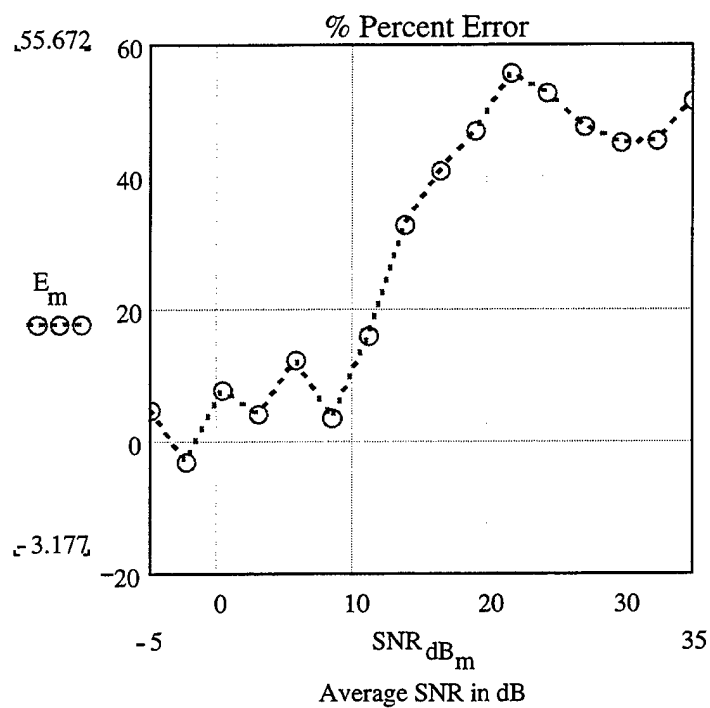
Figure 15. Percent difference (error) between theoretical and simulation results.

The summary of the accuracy of the simulation for this case is presented below.

	SYMBOL ERROR PROBABILITY	NON-COHERENT 2FSK
1.	Mean Percent Difference (%)	29.084
2.	Maximum Percent Difference (%)	55.672
3.	Minimum Percent Difference (%)	-3.177
4.	Standard Deviation (%)	20.799

Table 6. Results of the comparison of the theoretical SEP and the SEP obtained by the simulation.

b) Results For 4FSK

The theoretical and the simulation symbol error probabilities for non-coherently detected 4FSK are presented in Figure 16 as functions of the average signal-to-noise ratio in dB.
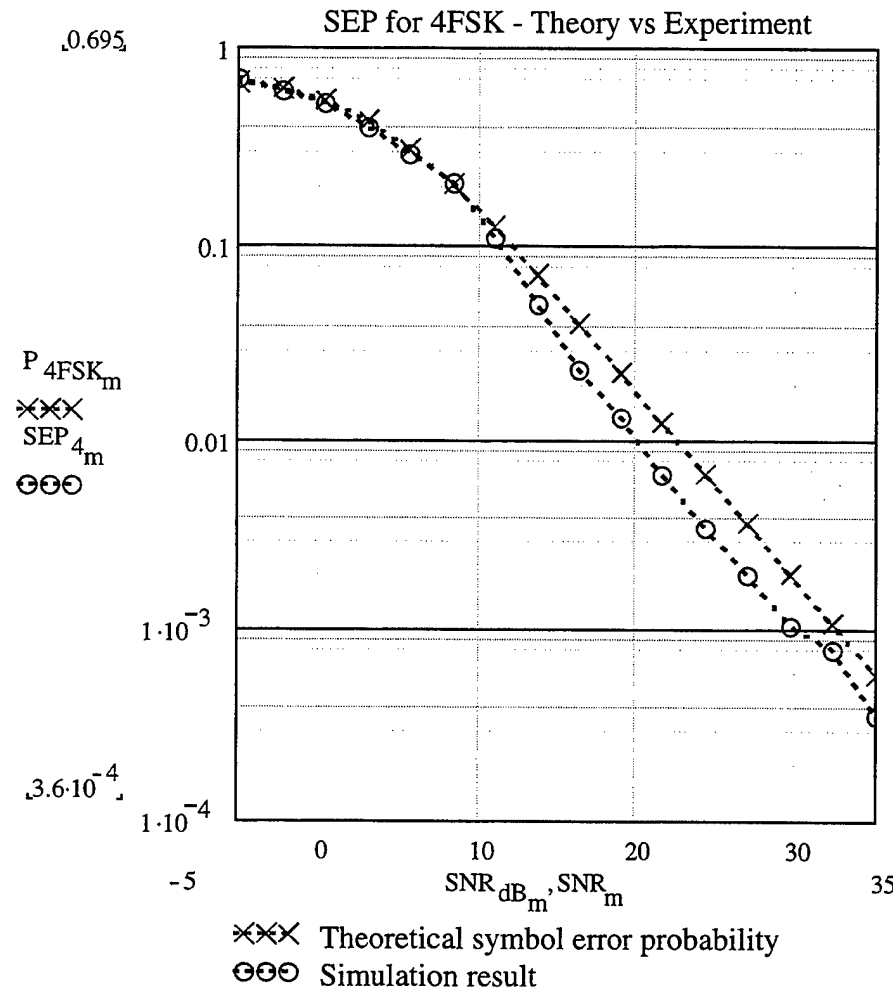
Figure 16. Probability of symbol error (theoretical and simulation) for non-coherent detection of 4FSK signal corrupted by AWGN in a Rayleigh fading channel.

In Figure 17, the difference between the theoretical and the simulation symbol error probability is shown.
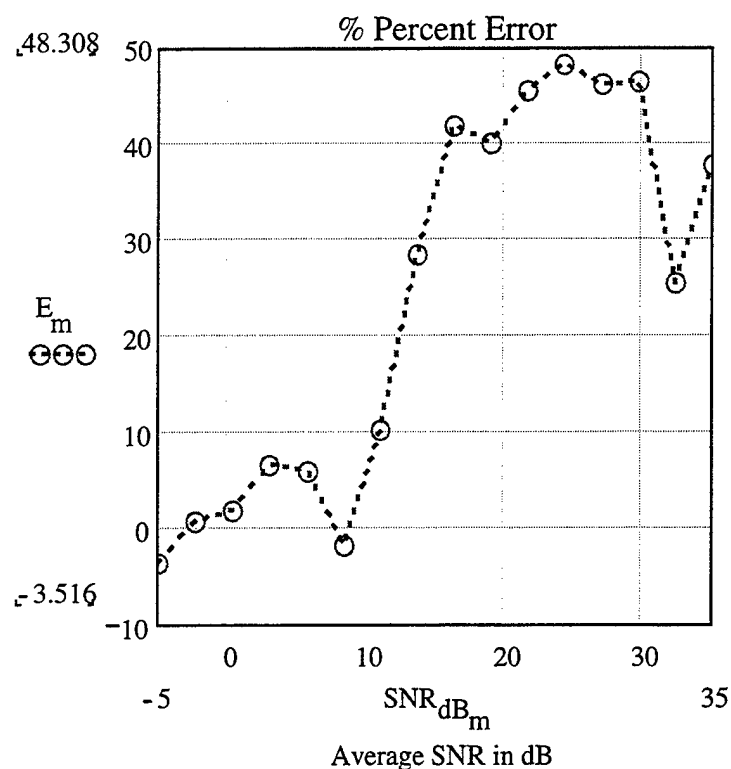
Figure 17. Percent difference (error) between theoretical and simulation results.

The summary of the accuracy of the simulation for this case is presented below.

	SYMBOL ERROR PROBABILITY	NON-COHERENT 4FSK
1.	Mean Percent Difference (%)	23.912
2.	Maximum Percent Difference (%)	48.308
3.	Minimum Percent Difference (%)	-3.516
4.	Standard Deviation (%)	19.52

Table 7. Results of the comparison of the theoretical SEP and the SEP obtained by the simulation.

c)   Results For 8FSK

The theoretical and the simulation symbol error probabilities for non-coherently detected 8FSK are presented in Figure 18 as functions of the average signal-to-noise ratio in dB.
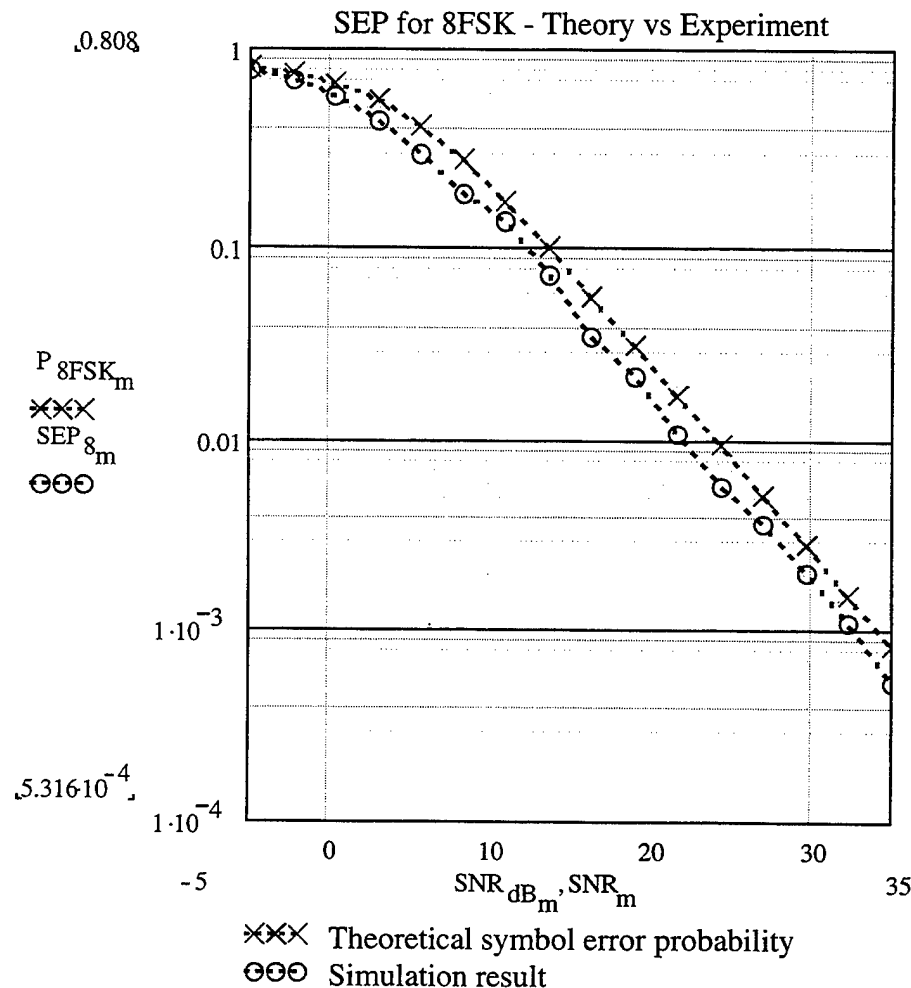
Figure 18. Probability of symbol error (theoretical and simulation) for non-coherent detection of 8FSK signal corrupted by AWGN in a Rayleigh fading channel.

In Figure 19, the difference between the theoretical and the simulation symbol error probability is shown.
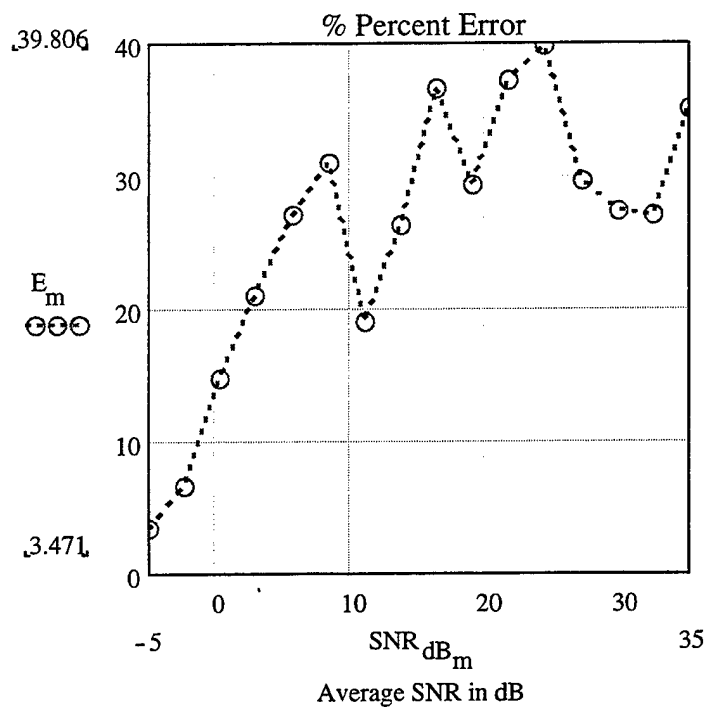
Figure 19. Percent difference (error) between theoretical and simulation results.

The summary of the accuracy of the simulation for this case is presented below.

	SYMBOL ERROR PROBABILITY	NON-COHERENT 8FSK
1.	Mean Percent Difference (%)	25.748
2.	Maximum Percent Difference (%)	39.806
3.	Minimum Percent Difference (%)	3.471
4.	Standard Deviation (%)	10.151

Table 8. Results of the comparison of the theoretical SEP and the SEP obtained by the simulation experiment.

31

Observing the results for non-coherent detection of 2, 4, and 8FSK in a Rayleigh fading channel, we note that the simulation underestimates the theory for all the cases of 2, 4, and 8FSK. The mean percent error for all the cases is much greater compared to the coherent detection.

The average results for the non-coherent detection of 2, 4, and 8FSK are:

	SYMBOL ERROR PROBABILITY	AVERAGE RESULTS FOR NON-COHERENT 2, 4, AND 8FSK
1.	Mean Percent Difference (%)	26.248
2.	Maximum Percent Difference (%)	47.929
3.	Minimum Percent Difference (%)	-1.074
4.	Standard Deviation (%)	16.823

Table 9. Average results for the non-coherent detection of 2, 4, and 8FSK.

Comparing the theory with the simulation, for a given value of symbol error probability, the error in dB ranges from 0 to 1 dB for coherent detection and from 0 to 3 dB for non-coherent detection.

C. RICIAN FADING CHANNEL – COHERENT DETECTION

In this section, we derive the symbol error rate performance of MFSK signals when these signals are transmitted over a frequency-nonselective, slowly fading Rician channel. The assumption again is that channel fades slowly, which implies that the multiplicative process may be considered as a constant during at least one signaling time interval. Furthermore, the channel fading is sufficiently slow that the phase shift introduced by the channel can be estimated from the received signal without error.

1. Theoretical Probability Of Symbol Error For Coherent Detection

The conditional probability of symbol error is the standard probability of error for coherent, orthogonal MFSK signal when AWGN is present:

$$P_{error}(r) = 1 - \frac{1}{\sqrt{2 \cdot \pi}} \cdot \int_{-\infty}^{\infty} e^{-\frac{x^2}{2}} \cdot \left(1 - Q\left(x + \frac{r}{\sqrt{P_{noise}}}\right)\right)^{M-1} dx \qquad (3.12)$$

where:

r is the amplitude of the MFSK signal

$P_{noise} = \sigma^2$ is the power of the AWGN

The above symbol error probability is conditioned on the amplitude r of information signal, since the channel is modeled as a Rician fading channel. The amplitude of the signal is modeled as Rician random variable with the following probability density function:

33

$$f(r) = \begin{vmatrix} \dfrac{r}{P_{dif}} \cdot e^{\dfrac{-\left(r^2 + 2 \cdot P_{dir}\right)}{2 \cdot P_{dif}}} \cdot I0\left(\dfrac{\sqrt{2 \cdot P_{dir}} \cdot r}{P_{dif}}\right) & \text{for } r \geq 0 \\ \\ 0 \text{ for } r < 0 \end{vmatrix} \qquad (3.13)$$

where:

$P_{dir} = \alpha_{dir}^2/2$ is the power of the direct signal component

$P_{dif} = \alpha_{dif}^2$ is the power of the diffuse signal component.

Integrating the product of the conditional probability of symbol error and the probability density function of the information signal's amplitude r over all possible values of r, we get the unconditional probability of symbol error:

$$P_{error} = 1 - \frac{1}{\sqrt{2 \cdot \pi}} \cdot \int_0^\infty \int_{-\infty}^\infty e^{\frac{-x^2}{2}} \cdot \left(1 - Q\left(x + \frac{r}{\sqrt{P_{noise}}}\right)\right)^{M-1} \cdot \left[\frac{r}{P_{dif}} \cdot e^{\frac{-\left(r^2 + 2 \cdot P_{dir}\right)}{2 \cdot P_{dif}}} \cdot I0\left(\frac{\sqrt{2 \cdot \sqrt{P_{dir}}} \cdot r}{P_{dif}}\right)\right] dx\, dr \quad (3.14)$$

First we introduce the following variable transformation:

$$\frac{r}{\sqrt{P_{dif}}} = y \qquad dr = \sqrt{P_{dif}}\, dy \qquad (3.15)$$

and obtain the following expression, which has to be evaluated numerically:

$$P_{error} = 1 - \frac{1}{\sqrt{2 \cdot \pi}} \cdot \int_0^\infty \int_{-\infty}^\infty e^{\frac{-x^2}{2}} \cdot \left(1 - Q\left(x + y \cdot \sqrt{\frac{P_{dif}}{P_{noise}}}\right)\right)^{M-1} \cdot y \cdot e^{-\left(\frac{y^2}{2} + \frac{P_{dir}}{P_{dif}}\right)} \cdot I0\left(\sqrt{2} \cdot \sqrt{\frac{P_{dir}}{P_{dif}}} \cdot y\right) dx\, dy \quad (3.16)$$

34

Next, it is convenient to define the ratio of the powers of the direct and the diffuse component as:

$$R = \frac{P_{dir}}{P_{dif}} \qquad (3.17)$$

For a given value of total signal power, we have:

$$\text{Power}_{dir} + \text{Power}_{dif} = \text{Power}_{signal\_tota} \qquad (3.18)$$

Next, we express the last relationship in terms of the ratio of the powers of direct and diffuse components as:

$$\frac{\text{Power}_{signal\_total}}{\text{Power}_{dif}} = 1 + R \qquad (3.19)$$

The SNR is defined as the ratio of the total signal power to the noise power:

$$SNR = \frac{P_{dir} + P_{dif}}{P_{noise}} = \frac{P_{dif}}{P_{noise}} \cdot (1 + R) \qquad (3.20)$$

Equivalently, we obtain:

$$\sqrt{\frac{P_{dif}}{P_{noise}}} = \sqrt{\frac{SNR}{1 + R}} = \frac{10^{\frac{SNR_{dB}}{20}}}{\sqrt{1 + R}} \qquad (3.21)$$

Substituting equation (3.19) and (3.23) into equation (3.18), we get the following expression for the symbol error probability:

35

$$P_{error} = 1 - \frac{1}{\sqrt{2 \cdot \pi}} \cdot \int_0^\infty \int_{-\infty}^\infty \left[1 - Q\left[x + y \cdot \frac{10^{\frac{SNR_{dB}}{20}}}{\sqrt{1+R}} \right] \right]^{M-1} \cdot y \cdot e^{-\left(\frac{x^2}{2} + \frac{y^2}{2} + R \right)} \cdot I0\left(\sqrt{2 \cdot R \cdot y} \right) dxdy \quad (3.22)$$

Now, we are able to plot the symbol error probability as a function of the signal-to-noise ratio (SNR) and the ratio R of the powers of the direct and diffuse signal components. Figure 20 is a plot of the symbol error probability of a 2FSK signal as a function of the signal-to-noise ratio and for ratios of the powers of the direct and diffuse signal component equal to 1, 4 and 10.
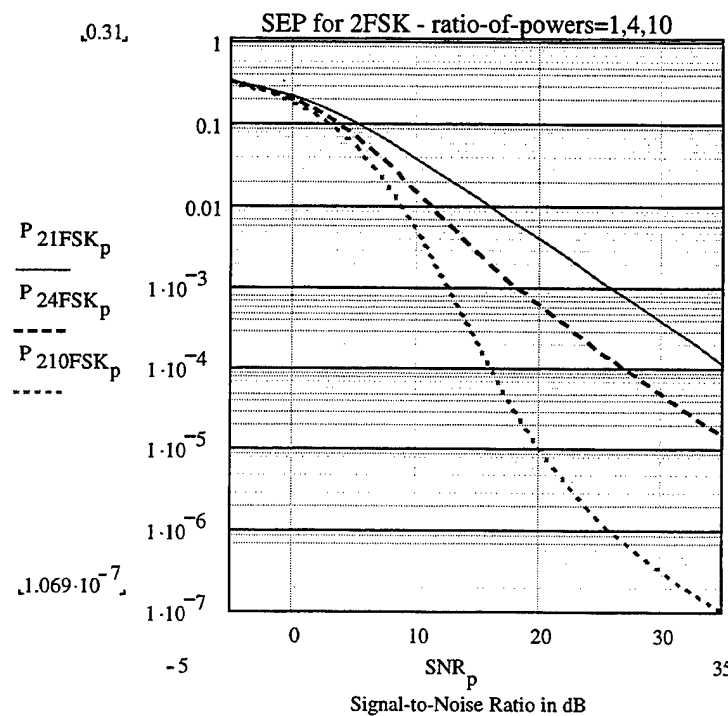
Figure 20. Probability of symbol error for coherent detection of 2FSK signals in Rician

36

fading channel when the ratio of powers is 1, 4, 10.

We observe that the increase of the ratio-of-powers R, which means that the power of the direct signal component increases over the power of the diffuse signal component, does cause significant decrease of the symbol error probability.

Next we plot the probability of symbol error for 2, 4, and 8FSK while the ratio-of-powers remains constant at the value of 1, that is, equal amount of power for the direct and diffuse signal components.
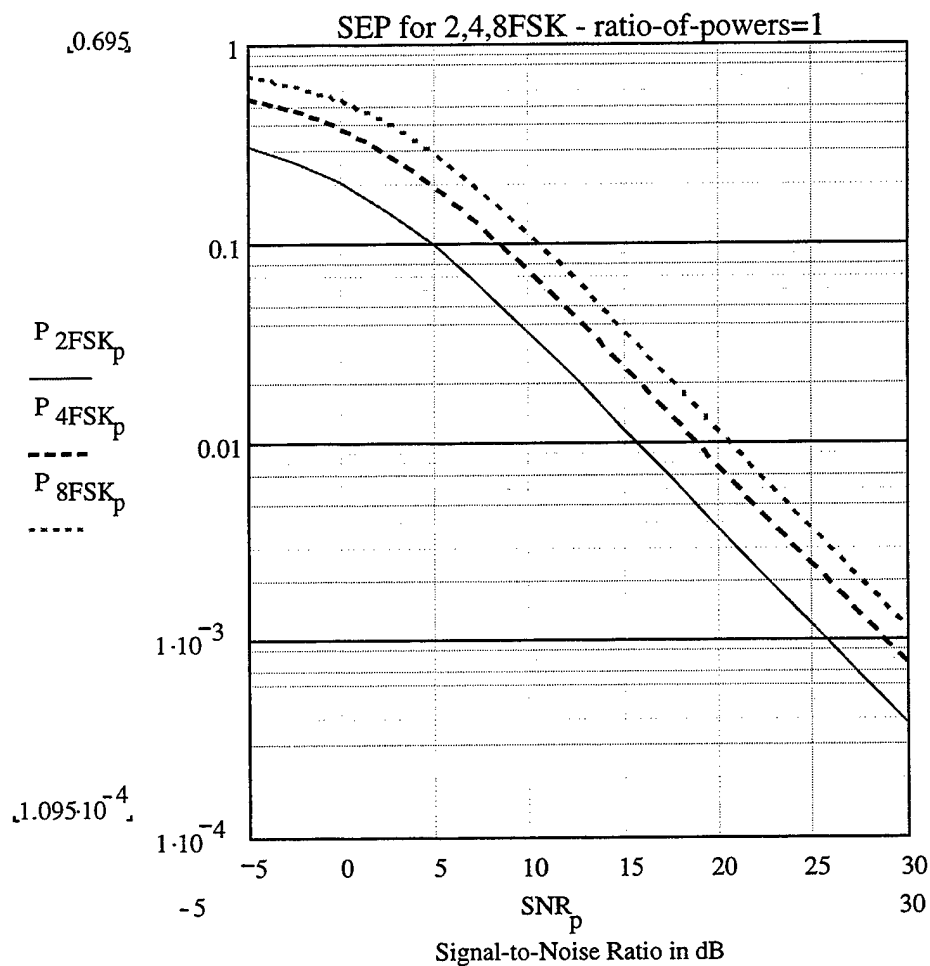
Figure 21. Probability of symbol error for coherent detection of 2, 4, and 8FSK signals in Rician fading channel when the ratio of powers is 1.

37

In the case of equal amount of the direct and diffuse power, the symbol error probability increases as we move from 2FSK to 4FSK and 8FSK signaling. This trend is observed generally for all values of R.

2. Simulink Model and Block Analysis

The schematic diagram of the Simulink model, which has been developed for the simulation of coherent MFSK signaling in a Rician fading channel, is shown in Figure 22.
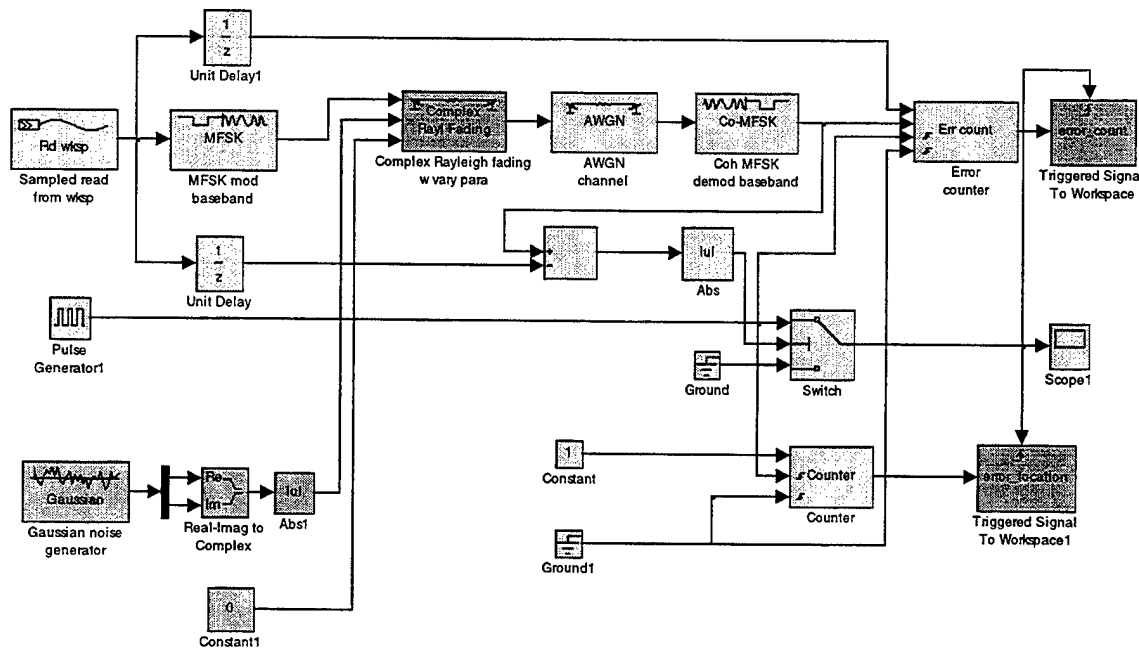
Figure 22. Model for coherent MFSK in a Rician fading channel.

The block diagram of Figure 22 looks the same as the block diagram of the one for the coherent detection of MFSK signal in a Rayleigh fading channel. However, there are essential differences that force the fading of the information signal to follow a Rician distribution.

a)   Gaussian Noise Generator

This block generates two independent Gaussian distributed noise variables. One of the two is a zero mean Gaussian variable, while the other has a mean value equal to the square root of the power of the direct signal component. The variance for each noise is equal to half of power of the diffuse signal component, so that the resulting Rician distributed random variable has variance exactly equal to the power of the diffuse signal component.

The noise variance parameter (noise_var) of the AWGN channel block needs again to be multiplied by a factor of two to account for the bandpass to lowpass transformation.

3.   Simulation Analysis And Performance Verification

In this section, simulation results are presented in order to verify the performance for coherent detection of MFSK in a Rician fading channel. Each simulation runs until at least 100 errors are observed. The data sequences are limited to 10^6 symbols for each simulation to prevent 'out of memory' errors. As long as less than 100 errors are observed, the simulation sequence is repeated until a sufficient number of errors has occurred.

a)   Results For 2FSK

The theoretical and the simulation symbol error probabilities for coherently detected 2FSK are presented in the Figure 23 as functions of the total signal-to-noise ratio in dB.
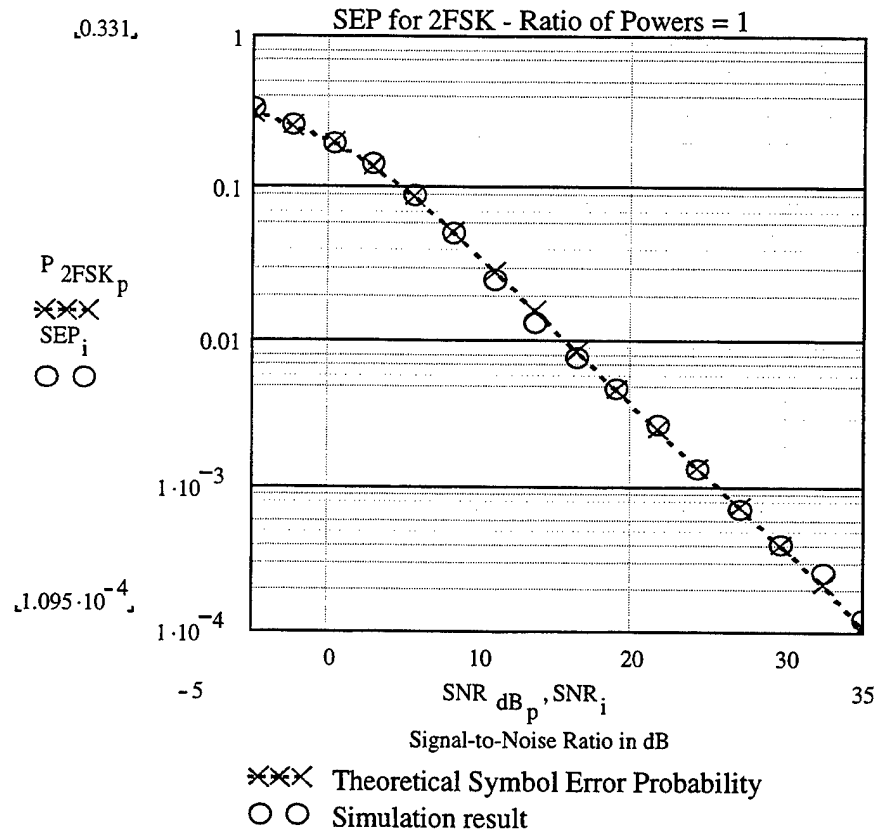
Figure 23. Probability of symbol error (theoretical and experimental) for coherent detection of 2FSK in a Rician fading channel, using ratio of powers 1.

In Figure 24, the difference (percent error) between the theoretical and simulation symbol error probability is shown.
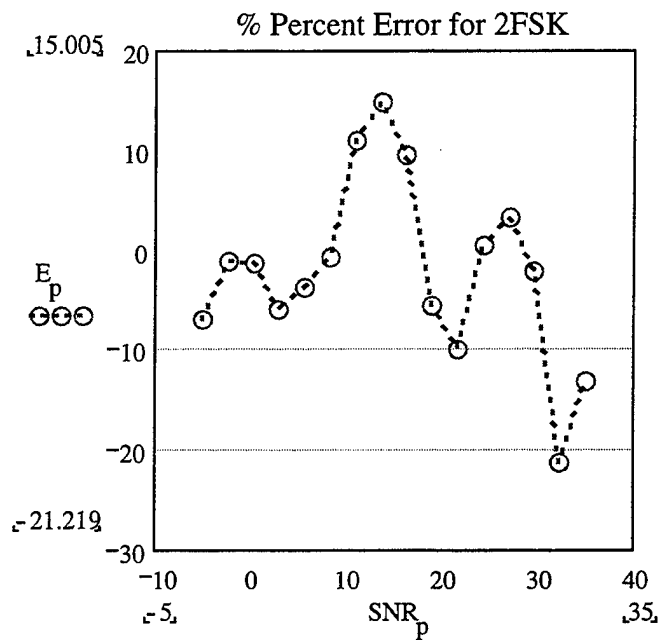
Figure 24. Percent difference (error) between theoretical and simulation results.

The summary of the accuracy of the simulation for this case is presented

in Table 10.

	SYMBOL ERROR PROBABILITY	COHERENT 2FSK
1.	Mean Percent Difference (%)	-1.9
2.	Maximum Percent Difference (%)	15.005
3.	Minimum Percent Difference (%)	-21.219
4.	Standard Deviation (%)	8.826

Table 10. Results of the comparison of the theoretical SEP and the SEP obtained by the simulation.

b)   Results For 4FSK

The theoretical and the simulation symbol error probabilities for coherently detected 4FSK are presented in Figure 25 as functions of the average signal-to-noise ratio in dB. The ratio of powers has been selected as 1.
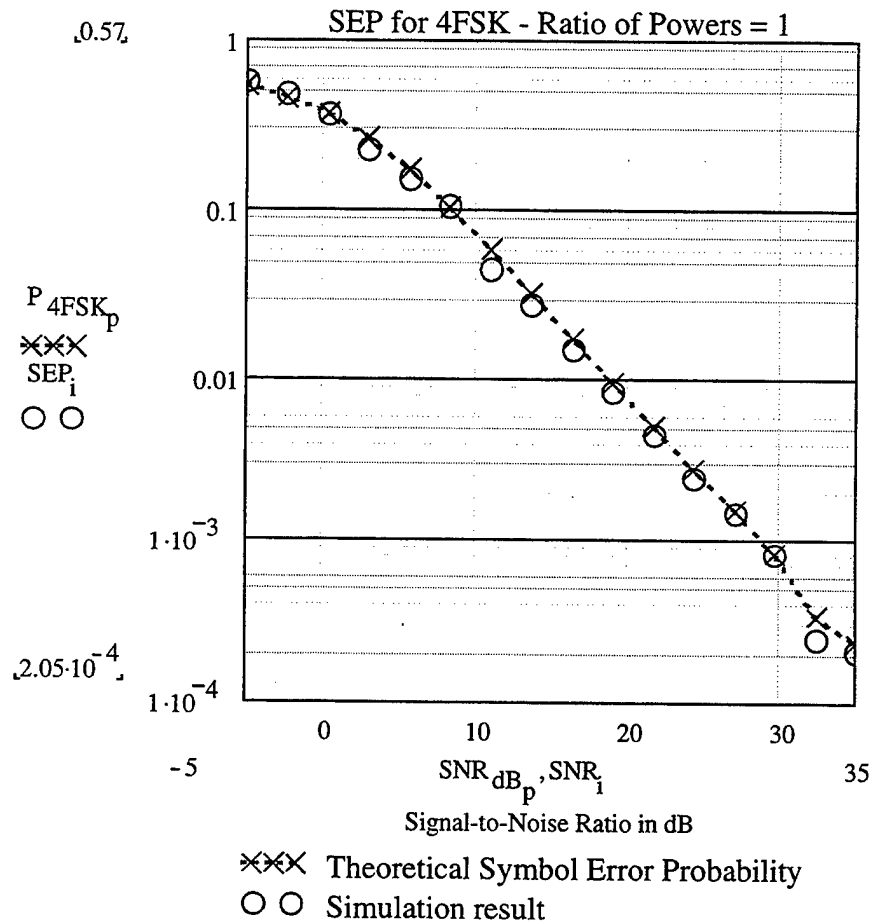
Figure 25. Probability of symbol error (theoretical and simulation) for coherent detection of 4FSK in a Rician fading channel, using the ratio of powers equal to 1.

In Figure 26, the difference between the theoretical and simulation symbol error probability is shown.
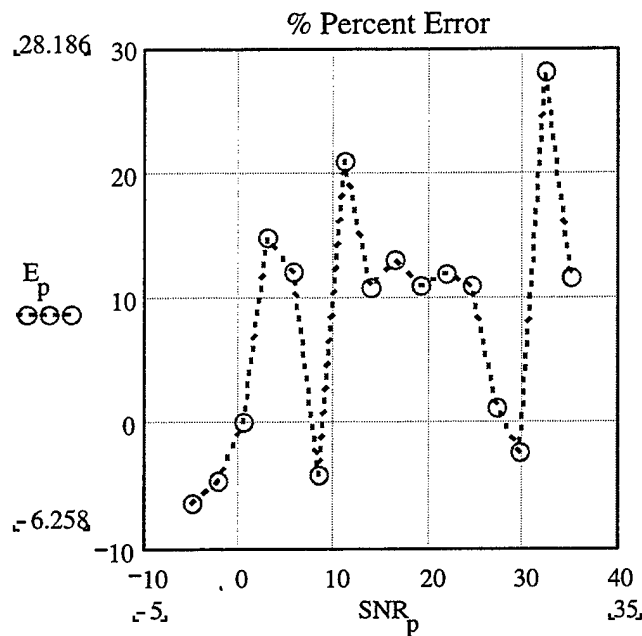
Figure 26. Percent difference (error) between theoretical and simulation results.

The summary of the accuracy of the simulation for this case is presented

in Table 11.

	SYMBOL ERROR PROBABILITY	COHERENT 4FSK
1.	Mean Percent Difference (%)	8.209
2.	Maximum Percent Difference (%)	28.186
3.	Minimum Percent Difference (%)	-6.258
4.	Standard Deviation (%)	9.525

Table 11. Results of the comparison of the theoretical SEP and the SEP obtained by the simulation.

c) Results For 8FSK

The theoretical and the simulation symbol error probabilities for coherently detected 8FSK are presented in Figure 27 as functions of the average signal-to-noise ratio in dB.
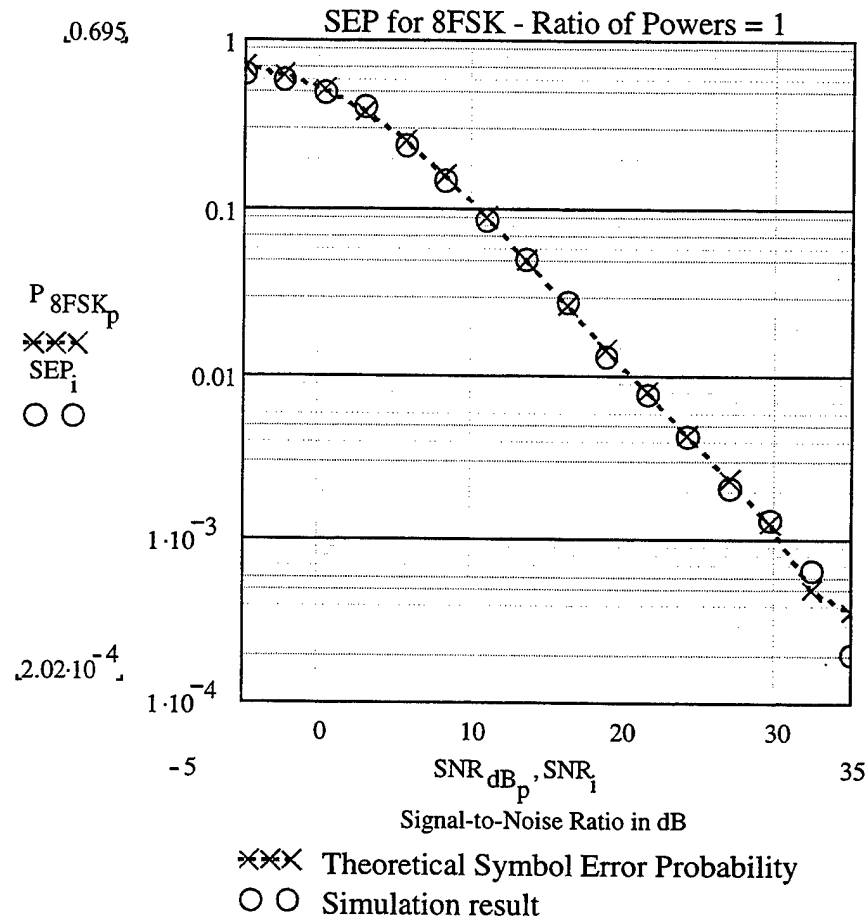
Figure 27. Probability of symbol error (theoretical and simulation) for coherent detection of 8FSK in a Rician fading channel, using the ratio of powers equal to 1.

In Figure 28, the difference between the theoretical and simulation symbol error probability is shown.

44
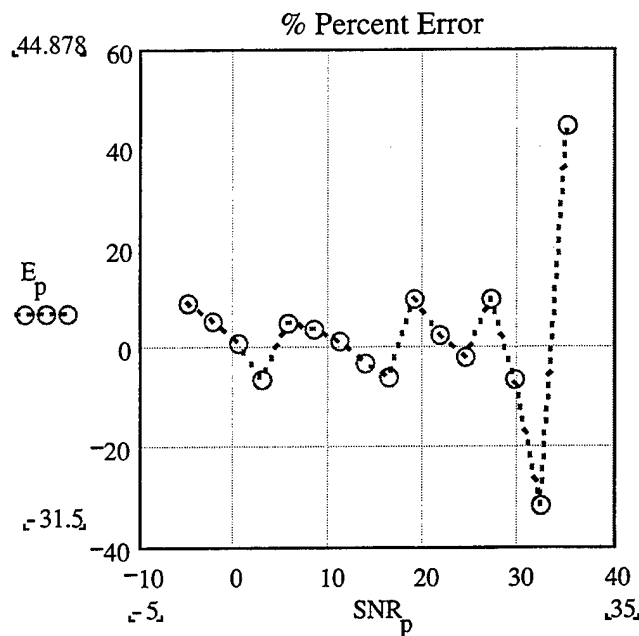
Figure 28. Percent difference (error) between theoretical and simulation results.

The summary of the accuracy of the simulation for this case is presented

in Table 12.

	SYMBOL ERROR PROBABILITY	COHERENT 8FSK
1.	Mean Percent Difference (%)	2.559
2.	Maximum Percent Difference (%)	44.878
3.	Minimum Percent Difference (%)	-31.5
4.	Standard Deviation (%)	14.544

Table 12. Results of the comparison of the theoretical SEP and the SEP obtained by the simulation experiment.

Observing the results for coherent detection of 2, 4, and 8FSK in a Rician fading

channel, we note that the simulation overestimates the theory for the case of 2FSK, and

underestimates the theory for the cases of 4 and 8FSK. The mean percent error for all the cases is less than 10%.

The average results for the coherent detection of 2, 4, and 8FSK are:

	SYMBOL ERROR PROBABILITY	AVERAGE RESULTS FOR COHERENT 2, 4, AND 8FSK
1.	Mean Percent Difference (%)	2.966
2.	Maximum Percent Difference (%)	29.356
3.	Minimum Percent Difference (%)	-19.659
4.	Standard Deviation (%)	10.965

Table 13. Average results for the coherent detection of 2, 4, and 8FSK.

D.   RICIAN FADING CHANNEL – NON-COHERENT DETECTION

In this section, the theoretical performance for non-coherent detection of MFSK in a Rician fading channel is determined and compared to the simulation.

1.   Theoretical Probability Of Symbol Error For Non-Coherent Detection

The probability of symbol error for non-coherent detection of orthogonal MFSK signal in a Rician fading channel is given by [Ref 8]:

$$P_{error} = \sum_{k=1}^{M-1} \frac{(M-1)!}{k!\cdot(M-1-k)!} \cdot \frac{(-1)^{k+1}}{1+k} \cdot \frac{R+1}{R+1+\frac{k}{k+1}\cdot 10^{\frac{SNR_{dB}}{10}}} \cdot e^{-R\left[1-\frac{(R+1)}{R+1+\frac{k}{k+1}\cdot 10^{\frac{SNR_{dB}}{10}}}\right]} \quad (3.23)$$

where R is the ratio of powers of the direct and diffuse signal components $R = \alpha_{dir}^2/2\alpha_{dif}^2$

46

Equivalently, we can write:

$$P_{error} = \sum_{k=1}^{M-1} \frac{(M-1)!}{k! \cdot (M-1-k)!} \cdot \frac{(-1)^{k+1}}{\left(1+k \cdot \left(1+\frac{1}{1+R} \cdot 10^{\frac{SNR_{dB}}{10}}\right)\right)} \cdot e^{\frac{-k \cdot \frac{R}{1+R} \cdot 10^{\frac{SNR_{dB}}{10}}}{\left(1+k \cdot \left(1+\frac{1}{1+R} \cdot 10^{\frac{SNR_{dB}}{10}}\right)\right)}} \qquad (3.24)$$

In Figure 29 the symbol error probability for the 2FSK is shown as a function of the signal-to-noise ratio and for different values of the ratio of the powers of the direct and diffuse signal components.
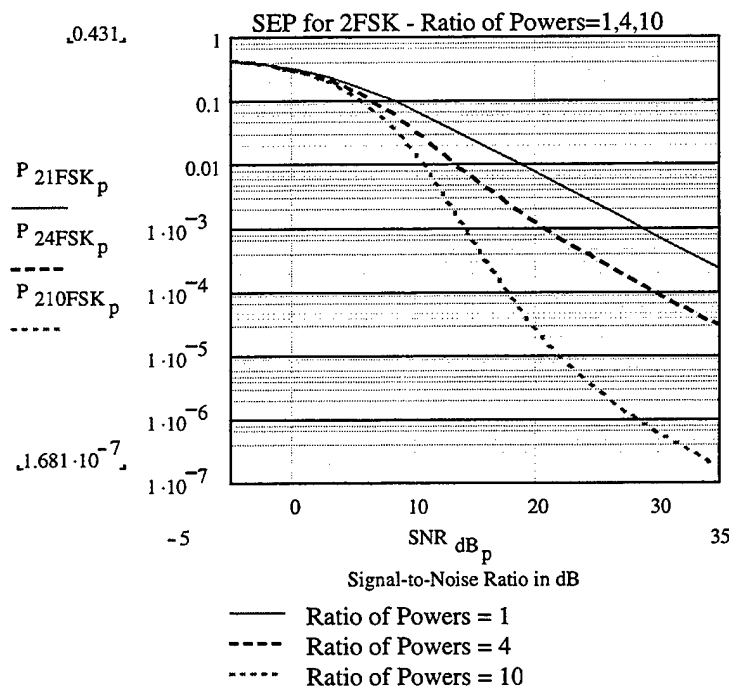
Figure 29. Probability of symbol error for non-coherent detection of 2FSK signals in Rician fading channel when the ratio of powers is 1, 4, and 10.

In Figure 30, we plot the probability of symbol error for 2, 4, and 8FSK while the ratio of powers remains constant at the value of 1.
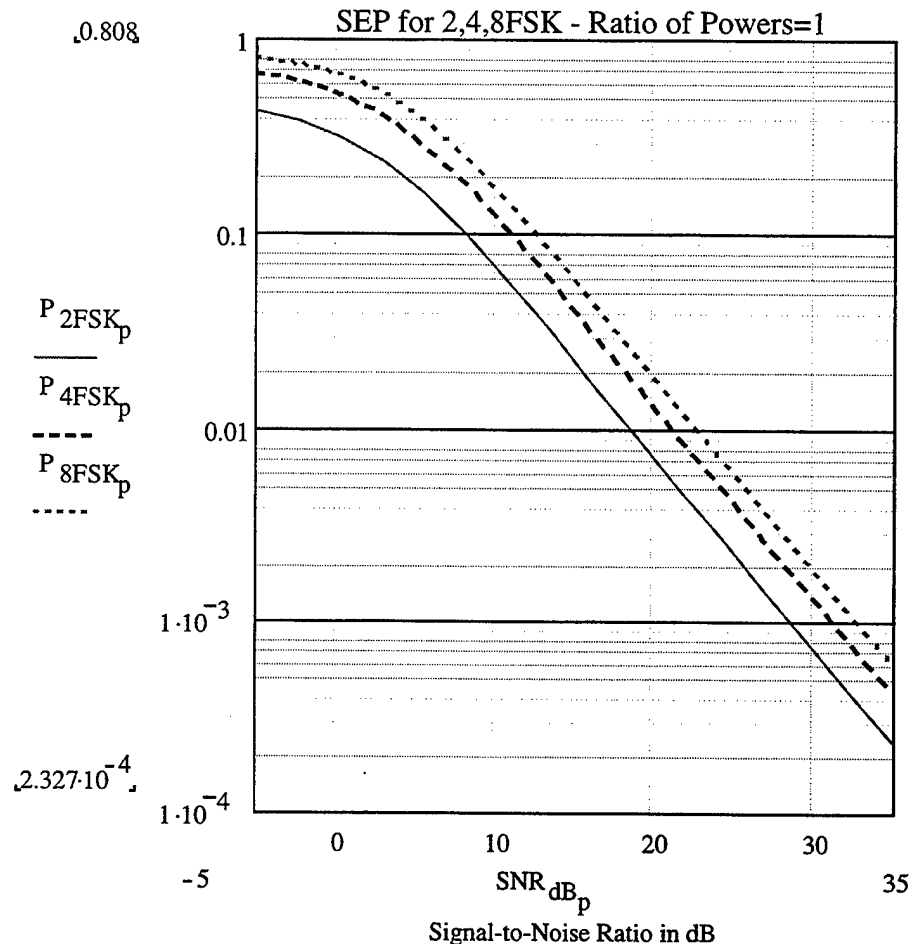
Figure 30. Probability of symbol error for non-coherent detection of 2, 4, 8FSK.

2. Simulink Model and Block Analysis

The schematic diagram of the Simulink model, which has been developed for the simulation of non-coherent detection of MFSK in a Rician fading channel, is not presented here since the only difference with respect to the coherent case is the replacement of the coherent demodulation block by the non-coherent block.

3. Simulation Analysis And Performance Verification

In this section, simulation results are presented in order to verify the performance of non-coherent detection of MFSK in a Rician fading channel.

a)   Results For 2FSK

The theoretical and the simulation symbol error probabilities for non-coherently detected 2FSK are presented in Figure 31 as functions of the total signal-to-noise ratio in dB for R=1.
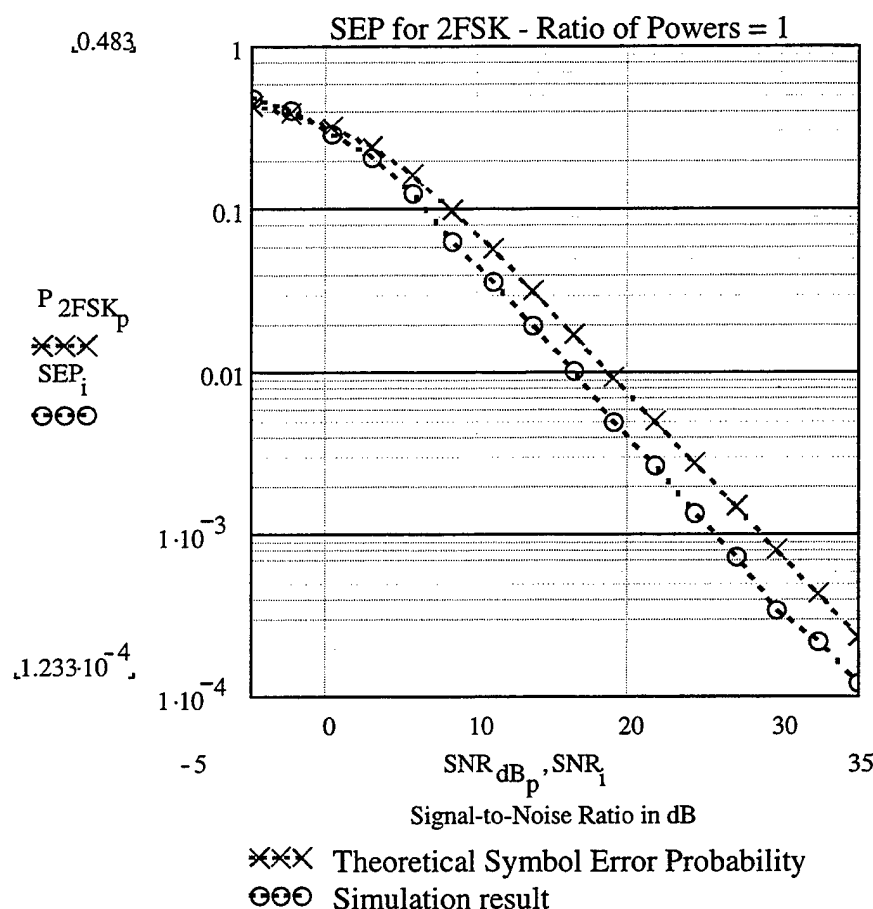
Figure 31. Probability of symbol error (theoretical and simulation) for non-coherent detection of 2FSK in a Rician fading channel, using the ratio of powers equal to 1.

In Figure 32, the difference (percent error) between the theoretical and simulation symbol error probability is shown.
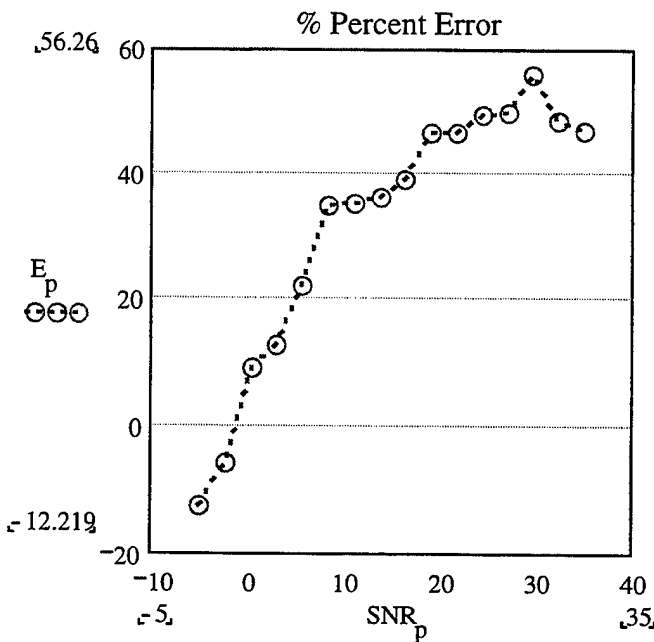

Figure 32. Percent difference (error) between theoretical and simulation results.

The summary of the accuracy of the simulation for this case is presented in Table 14.

	SYMBOL ERROR PROBABILITY	NON-COHERENT 2FSK
1.	Mean Percent Difference (%)	32.418
2.	Maximum Percent Difference (%)	56.26
3.	Minimum Percent Difference (%)	-12.219
4.	Standard Deviation (%)	20.305

Table 14. Results of the comparison of the theoretical SEP and the SEP obtained by the simulation.

b)   Results For 4FSK

The theoretical and the simulation symbol error probabilities for non-coherently detected 4FSK are presented in Figure 33 as functions of the signal-to-noise ratio in dB. The ratio R is selected to be equal to 1.
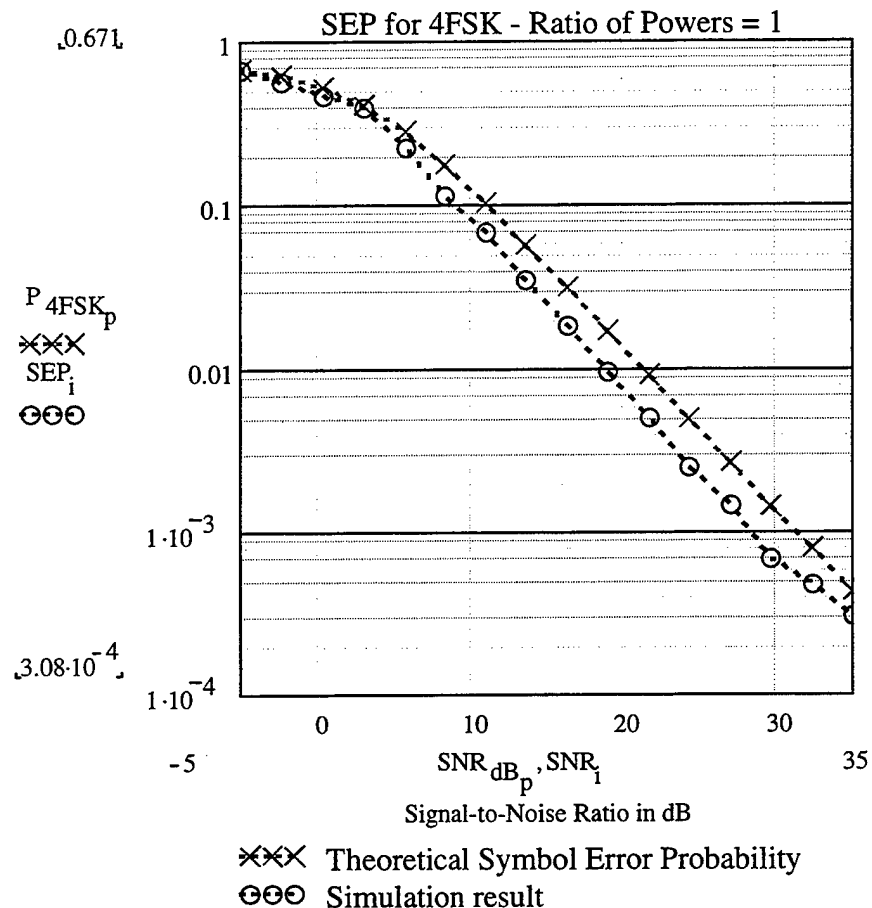

Figure 33. Probability of symbol error (theoretical and simulation) for non-coherent detection of 4FSK in a Rician fading channel, using the ratio of powers equal to 1.

In Figure 34, the difference (percent error) between the theoretical and simulation symbol error probability is shown.

51
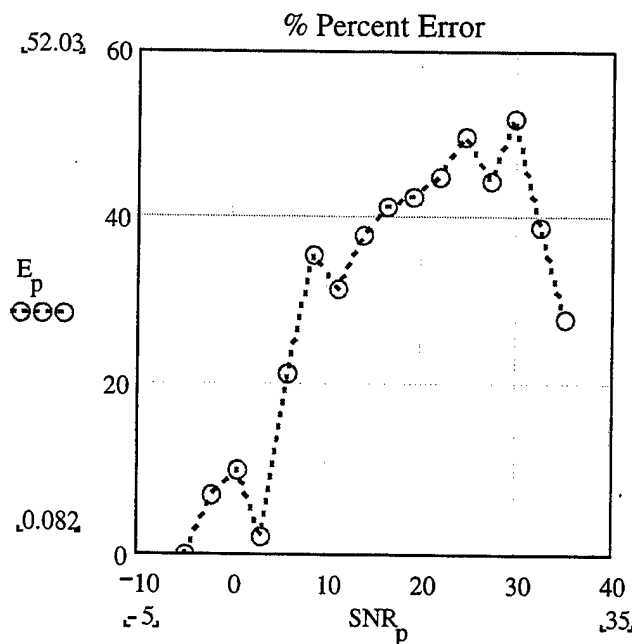
Figure 34. Percent difference (error) between theoretical and simulation results.

The summary of the accuracy of the simulation for this case is presented in Table 15.

	SYMBOL ERROR PROBABILITY	NON-COHERENT 4FSK
1.	Mean Percent Difference (%)	30.456
2.	Maximum Percent Difference (%)	52.03
3.	Minimum Percent Difference (%)	0.082
4.	Standard Deviation (%)	16.708

Table 15. Results of the comparison of the theoretical SEP and the SEP obtained by the simulation.

c) Results For 8FSK

The theoretical and the simulation symbol error probabilities for non-coherently detected 8FSK are presented in Figure 35 as functions of the signal-to-noise ratio in dB for R=1.
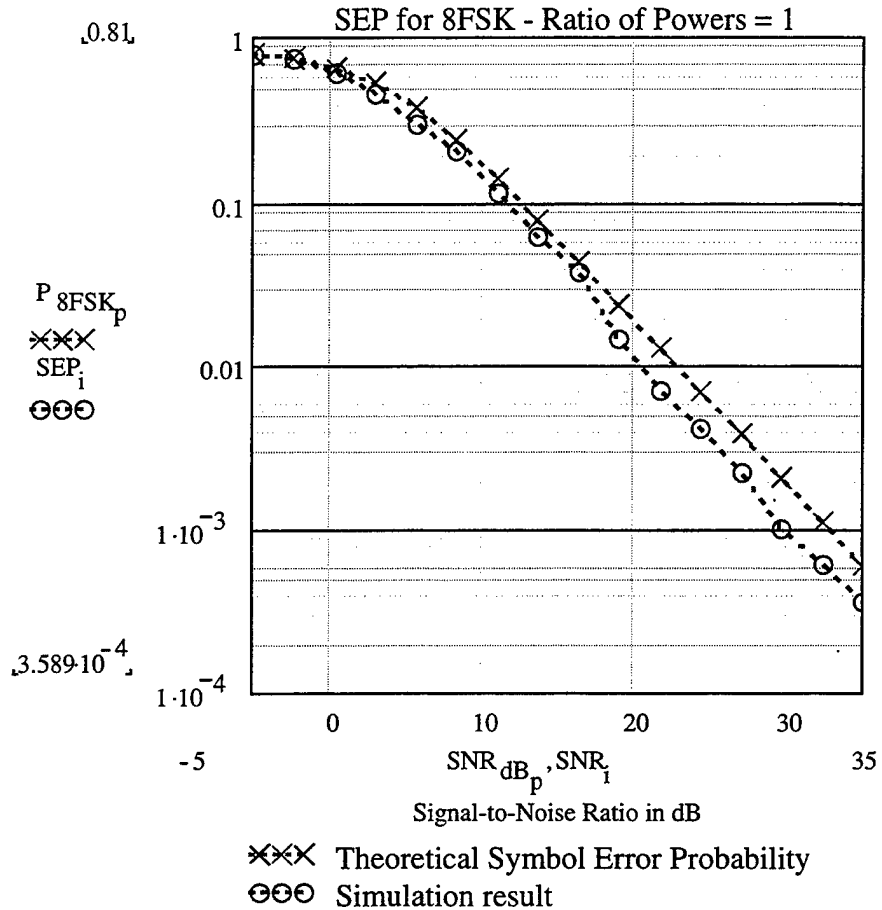
Figure 35. Probability of symbol error (theoretical and simulation) for non-coherent detection of 8FSK in a Rician fading channel, using the ratio of powers equal to 1.

Next, in Figure 36, the difference (percent error) between the theoretical and simulation symbol error probability is shown.
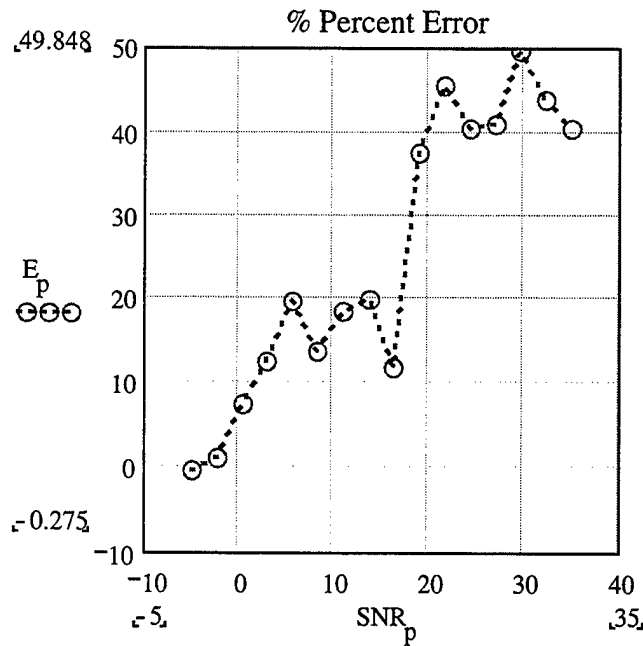
Figure 36. Percent difference (error) between theoretical and simulation results.

The summary of the accuracy of the simulation for this case is presented

in Table 16.

	SYMBOL ERROR PROBABILITY	NON-COHERENT 8FSK
1.	Mean Percent Difference (%)	25.237
2.	Maximum Percent Difference (%)	49.848
3.	Minimum Percent Difference (%)	-0.275
4.	Standard Deviation (%)	16.521

Table 16. Results of the comparison of the theoretical SEP and the SEP obtained by the simulation.

Observing the results for non-coherent detection of 2, 4, and 8FSK in a Rician

fading channel, we note that the simulation underestimates the theory for all the cases of

2, 4, and 8FSK. The mean percent error for all the cases is much greater than the error of the coherent case.

The average results for the non-coherent detection of 2, 4, and 8FSK are:

	SYMBOL ERROR PROBABILITY	AVERAGE RESULTS FOR NON-COHERENT 2, 4, AND 8FSK
1.	Mean Percent Difference (%)	29.37
2.	Maximum Percent Difference (%)	51.379
3.	Minimum Percent Difference (%)	-4.137
4.	Standard Deviation (%)	17.845

Table 17. Average results for the non-coherent detection of 2, 4, and 8FSK.

Comparing the theory with the simulation, for a given value of symbol error probability, the error in dB ranges from 0 to 1 dB for coherent detection and from 0 to 3 dB for non-coherent detection.

IV. MFSK SIGNAL CORRUPTED BY AWGN AND CO-CHANNEL INTERFERENCE

A. INTRODUCTION

Interference is the effect of a non-desirable signal on the reception of a desirable signal and can be a major factor limiting the performance of a digital communications system.

Co-channel interference is a type of system-generated interference which refers to the degradation caused by a non-desirable signal of the same type as the desirable signal. Co-channel interference is most commonly introduced by other users of the same portion of the RF spectrum operating similar/same types of equipment.

In this chapter we derive the theoretical expression of the probability of symbol error for an MFSK signal operating in the presence of AWGN and co-channel interference. The co-channel interference is represented by another MFSK signal added to the desired signal. We consider cases of both coherent and non-coherent detection for 2FSK, 4FSK, and 8FSK communication systems.

The computer simulations for these cases have already been performed, and the results are presented in Chapter V of [Ref 1]. Some of those simulation results may be repeated here for comparison purposes. Later on, the simulation results will be presented for the cases of fading signal/interference, which have not been addressed in [Ref 1].

B. COHERENT DETECTION

We consider MFSK signaling corrupted by AWGN and co-channel interference. The objective is to derive the expression for the symbol error probability, for coherent detection, as a function of SNR and the signal-to-co-channel interference (jamming) ratio SJR and to compare the theoretical results with the simulation results. We will assume that each interfering symbol is synchronized with the transmitted signal symbol (the "worst case" scenario).

1. Theoretical Probability Of Symbol Error For Coherent Detection

In MFSK signaling there are M possible transmitted symbols and we may consider an MFSK receiver as having M "branches", one per symbol. The probability that the interference symbol is on the same branch as the signal symbol (at any given time) is 1/M, and the probability that the interference symbol is at a different branch than the signal symbol is (M-1)/M. The probability that the signal symbol will be received correctly is equal to the probability that:

- **1st case:** the signal and the interference symbols are on the same branch and that the noise in any of the remaining M-1 branches does not exceed the sum of signal and interference symbols, and

- **2nd case:** the signal and the interference symbols are on different branches and neither the sum of the interference and noise nor the noise in any of the remaining M-2 branches exceeds the signal.

a) The Signal And The Interference Symbols Are On The Same Branch

The signal space representation for the transmitted signal (S_i), noise (N), interference (I), and received signal (Y) in the M branches of our receiver is the following:

$$S_i = \begin{bmatrix} 0 \\ 0 \\ \cdot \\ \cdot \\ S \\ \cdot \\ \cdot \\ \cdot \\ 0 \end{bmatrix} \quad N = \begin{bmatrix} n_1 \\ n_2 \\ \cdot \\ \cdot \\ n_i \\ \cdot \\ \cdot \\ \cdot \\ n_M \end{bmatrix} \quad I = \begin{bmatrix} 0 \\ 0 \\ \cdot \\ \cdot \\ J \\ \cdot \\ \cdot \\ \cdot \\ 0 \end{bmatrix} \quad Y = \begin{bmatrix} n_1 \\ n_2 \\ \cdot \\ \cdot \\ S + J + n_i \\ \cdot \\ \cdot \\ \cdot \\ n_M \end{bmatrix} = \begin{bmatrix} y_1 \\ y_2 \\ \cdot \\ \cdot \\ y_i \\ \cdot \\ \cdot \\ \cdot \\ y_M \end{bmatrix} \quad \text{ith symbol}$$

At any time instant the values of branch noises, as well as the transmitted signal and the interference, may be considered as independent random variables. The probability that the noise in any of M-1 branches will not exceed the sum of the signal and interference, that is the probability of correct symbol detection given that y_i is received, is given by:

$$P\{\text{ correct decision } / y\} = \prod_{(j \neq i)} P\left(y_j \leq y_i, \text{given.} y_i\right) = \left(1 - Q\left(\frac{y_i}{\sigma}\right)\right)^{M-1} \tag{4.1}$$

where:

y_j is a Gaussian random variable representing values in any of the remaining M-1 receiver branches different than the ith branch.

To remove the condition on the Gaussian random variable y_i, we must integrate the product of the conditional probability and the probability density function of y_i over all the possible values of y_i. Since y_i is a Gaussian random variable we obtain:

$$P_{correct\_decision} = \int_{-\infty}^{\infty} \left(1 - Q\left(\frac{y_i}{\sigma}\right)\right)^{M-1} \cdot f_{y_i}(y_i) dy_i \qquad (4.2)$$

or equivalently:

$$P_{correct\_decision} = \int_{-\infty}^{\infty} \left(1 - Q\left(\frac{y_i}{\sigma}\right)\right)^{M-1} \cdot \frac{1}{\sqrt{2\cdot\pi\cdot\sigma}} \cdot e^{\frac{-[y_i-(S+J)]^2}{2\cdot\sigma^2}} dy_i \qquad (4.3)$$

Using the transformation

$$x = \frac{y_i - (S + J)}{\sigma} \qquad dx = \frac{dy_i}{\sigma} \qquad (4.4)$$

we obtain:

$$P_{correct\_decision} = \int_{-\infty}^{\infty} \left(1 - Q\left(x + \frac{S+J}{\sigma}\right)\right)^{M-1} \cdot \frac{1}{\sqrt{2\cdot\pi}} \cdot e^{\frac{-x^2}{2}} dx \qquad (4.5)$$

where:

S and J are the amplitudes of desirable and interfering MFSK signals, respectively, and σ is the standard deviation of the AWGN.

So the symbol error probability for this first case is:

$$P1 = 1 - P_{correct\_decision} \tag{4.6}$$

or equivalently

$$P1 = 1 - \frac{1}{\sqrt{2 \cdot \pi}} \cdot \int_{-\infty}^{\infty} e^{\frac{-x^2}{2}} \cdot \left(1 - Q\left(x + \frac{S+J}{\sigma}\right)\right)^{M-1} dx \tag{4.7}$$

The integral of equation (4.7) must be evaluated numerically.

b)   The Signal And The Interference Symbols Are At Different Branches

The signal space representation for the transmitted signal (S_i), noise (N), interference (I) and received signal (Y) in the M branches of the receiver is the following:

$$S_i = \begin{bmatrix} 0 \\ 0 \\ \cdot \\ \cdot \\ S \\ \cdot \\ 0 \\ \cdot \\ 0 \end{bmatrix} \quad N = \begin{bmatrix} n_1 \\ n_2 \\ \cdot \\ \cdot \\ n_i \\ \cdot \\ \cdot n_k \\ \cdot \\ n_M \end{bmatrix} \quad I = \begin{bmatrix} 0 \\ 0 \\ \cdot \\ \cdot \\ 0 \\ \cdot \\ J \\ \cdot \\ 0 \end{bmatrix} \quad Y = \begin{bmatrix} n_1 \\ n_2 \\ \cdot \\ \cdot \\ S + n_i \\ \cdot \\ J + n_k \\ \cdot \\ n_M \end{bmatrix} = \begin{bmatrix} y_1 \\ y_2 \\ \cdot \\ \cdot \\ y_i \\ \cdot \\ \cdot y_k \\ \cdot \\ y_M \end{bmatrix}$$

i^{th} symbol

k^{th} symbol

where $i \neq k$

61

The signal and the interference symbols are now on different branches. The probability that neither the sum of the interference and noise nor the noise in any of the remaining M-2 branches exceeds the signal (that is the probability of correct symbol detection given that y_i was transmitted) is given by:

$$P\{\text{ correct decision }/y_i\} = \prod_{(j\neq i, j\neq k)} P\left(y_j \leq y_i, \text{given.. } y_i\right) \cdot P\left(y_k \leq y_i, \text{given.. } y_i\right) \qquad (4.8)$$

where:

j is the branch that contains only noise

k is the branch that contains interference and noise.

Since y_j and y_k are Gaussian random variables, equivalently, we obtain:

$$P\{\text{ correct decision }/y\} = \left(1 - Q\left(\frac{y_i}{\sigma}\right)\right)^{M-2} \cdot \left(1 - Q\left(\frac{y_i - J}{\sigma}\right)\right) \qquad (4.9)$$

To remove the condition on the random variable y_i, we must integrate the product of the conditional probability and the probability density function of y_i over all the possible values of y_i. Since y_i is a Gaussian random variable, we obtain:

$$P_{\text{correct\_decision}} = \int_{-\infty}^{\infty} \left(1 - Q\left(\frac{y_i}{\sigma}\right)\right)^{M-2} \cdot \left(1 - Q\left(\frac{y_i - J}{\sigma}\right)\right) \cdot \frac{1}{\sqrt{2\pi} \cdot \sigma} \cdot e^{\frac{-(y_i - S)^2}{2\sigma^2}} dy_i \qquad (4.10)$$

Using the transformation:

$$x = \frac{y_i - S}{\sigma} \qquad dx = \frac{dy_i}{\sigma} \qquad (4.11)$$

we obtain:

$$P_{correct\_decision} = \frac{1}{\sqrt{2 \cdot \pi}} \cdot \int_{-\infty}^{\infty} e^{-\frac{x^2}{2}} \cdot \left(1 - Q\left(x + \frac{S}{\sigma}\right)\right)^{M-2} \cdot \left(1 - Q\left(x + \frac{S-J}{\sigma}\right)\right) dx \qquad (4.12)$$

where S and J are the amplitudes of the transmitted and interfering MFSK signals, respectively, and σ is the standard deviation of the AWGN.

So the symbol error probability for this second case is:

$$P2 = 1 - P_{correct\_decision} \qquad (4.13)$$

or equivalently

$$P2 = 1 - \frac{1}{\sqrt{2 \cdot \pi}} \cdot \int_{-\infty}^{\infty} e^{-\frac{x^2}{2}} \cdot \left(1 - Q\left(x + \frac{S}{\sigma}\right)\right)^{M-2} \cdot \left(1 - Q\left(x + \frac{S-J}{\sigma}\right)\right) dx \qquad (4.14)$$

where the above integral must be evaluated numerically.

c) Total Symbol Error Probability

The total symbol error probability, combining the two cases is given by:

$$P_{total} = \frac{1}{M} \cdot P1 + \frac{M-1}{M} \cdot P2 \qquad (4.15)$$

where 1/M is the probability that the transmitted and the interfering symbols are on the same branch and (M-1)/M is the probability that the transmitted and the interfering symbols are on different branches.

A closed form solution is provided in Appendix A for BFSK.

63

2.   Results For 2FSK

Using the relationships

$$\frac{J}{\sigma} = \sqrt{2} \cdot 10^{\frac{SNR - SJR}{20}} \qquad \frac{S}{\sigma} = \sqrt{2} \cdot 10^{\frac{SNR}{20}} \qquad (4.16)$$

we can express the symbol error probability in terms of SNR and SJR. Evaluating and plotting the theoretical and simulation results versus SNR and SJR, as well as the difference (error) between them, we can compare the theoretical performance of coherent 2FSK with the simulation performance.

First, in Figure 37, we plot the theoretical symbol error probability versus SNR with SJR as a parameter for coherent detection of 2FSK. The experimental results are plotted separately, in Figure 38, in order to avoid a complicated and confusing graph.

Next, in Figures 39 and 40, we plot the theoretical and simulation results, respectively, for the symbol error probability of coherent 2FSK but versus SJR with SNR as a parameter.

The values for the signal-to-noise and signal-to-interference ratios are chosen between −5 dB and +13 dB in increments of 1.5 dB.

In Figure 37, 13 curves of the theoretical symbol error probability versus SNR are shown, corresponding to 13 different values of the SJR from −5 dB to +13 dB, where the lower curve corresponds to SJR=+13 dB and the remaining curves are in increments of 1.5 dB.

Note that the symbol error probability decreases as the SNR decreases only for negative values of SJR. This behavior is verified by both theory and simulation.
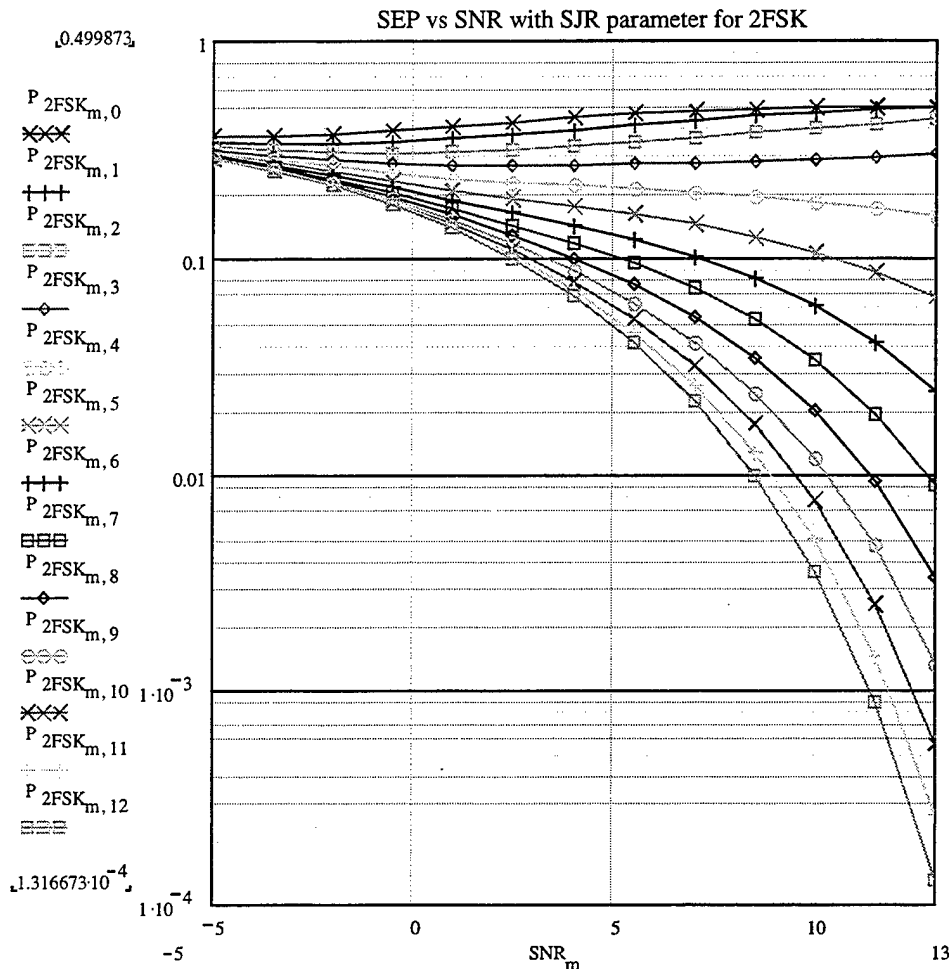
Figure 37. Theoretical symbol error probability versus SNR, with SJR as a parameter for coherent 2FSK.

In Figure 38 we show the simulation results for coherently detected 2FSK in the presence of AWGN and co-channel interference (jamming). The simulation runs until at least 100 errors are observed and the data sequences are limited to 10^6 symbols for each simulation, so that "out of memory" errors are prevented. Whenever less than 100 errors

65

were observed in a simulation, the sequence was repeated until a sufficient number of errors, greater than 100, occurred.

SEP vs SNR with SJR parameter for 2FSK

$SEP_{m,0}$
$SEP_{m,1}$
$SEP_{m,2}$
$SEP_{m,3}$
$SEP_{m,4}$
$SEP_{m,5}$
$SEP_{m,6}$
$SEP_{m,7}$
$SEP_{m,8}$
$SEP_{m,9}$
$SEP_{m,10}$
$SEP_{m,11}$
$SEP_{m,12}$

$SNR2_m$
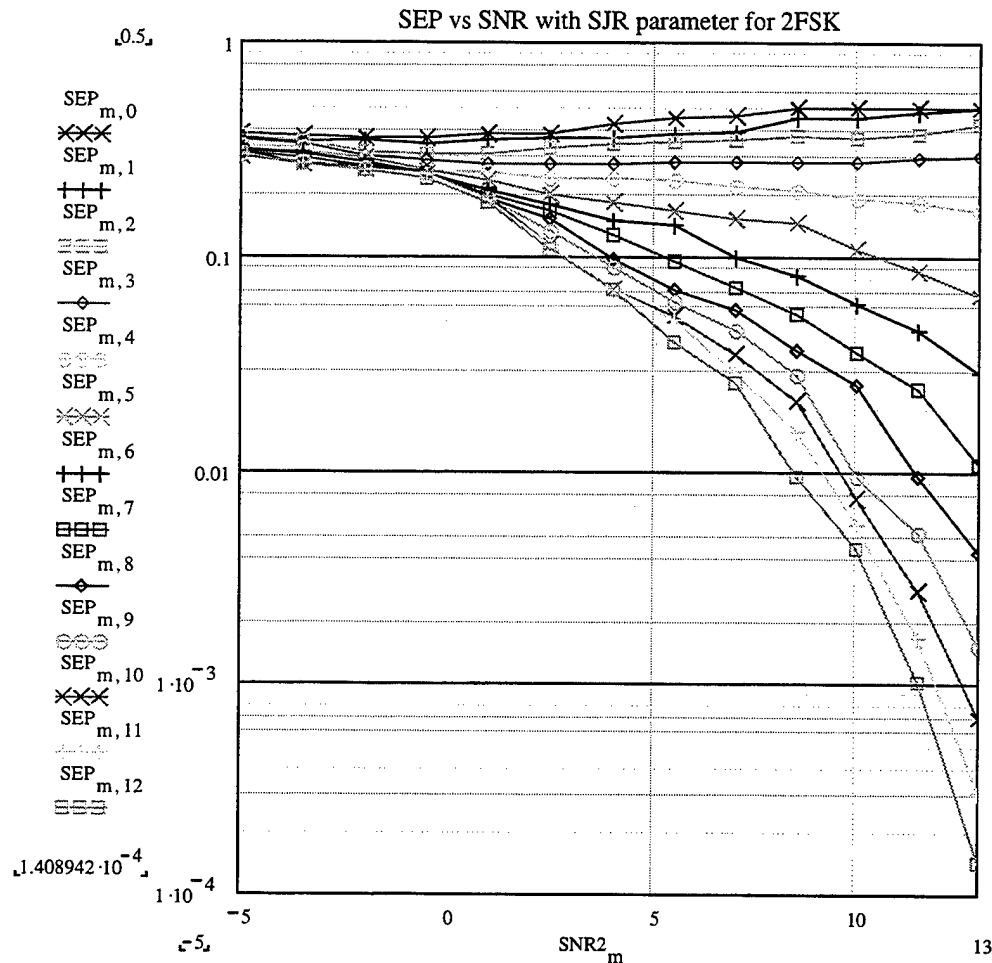
Figure 38. Simulation symbol error probability versus SNR, with SJR as a parameter for coherent 2FSK.

In Figures 39 and 40 the theoretical and simulation results are shown, respectively, for the symbol error probability versus SJR with SNR as a parameter.

From Figure 39, we see that as the signal-to-interference ratio increases, that is, the interference power decreases relative to the signal power, the symbol error probability

66

initially decreases but then tends to a constant value. As the SNR increases, this constant

value also decreases.

SEP vs SJR with SNR parameter for 2FSK

$\lceil 0.499873 \rfloor$ 1

$P_{2FSK_{0,n}}$
$\times\!\!\times\!\!\times$

$P_{2FSK_{1,n}}$
$+\!+\!+$

$P_{2FSK_{2,n}}$

$P_{2FSK_{3,n}}$ 0.1
$-\!\diamond\!-$

$P_{2FSK_{4,n}}$

$P_{2FSK_{5,n}}$
$\times\!\!\times\!\!\times$

$P_{2FSK_{6,n}}$
$+\!+\!+$ 0.01

$P_{2FSK_{7,n}}$
$\boxminus\boxminus\boxminus$

$P_{2FSK_{8,n}}$
$-\!\diamond\!-$

$P_{2FSK_{9,n}}$

$P_{2FSK_{10,n}}$ $1 \cdot 10^{-3}$
$\times\!\!\times\!\!\times$

$P_{2FSK_{11,n}}$

$P_{2FSK_{12,n}}$

$\lceil 1.316673 \cdot 10^{-4} \rfloor$
   $1 \cdot 10^{-4}$

    -6 -4 -2 0   2   4   6   8   10   12

$\lceil -5 \rfloor$ SJR_n 13
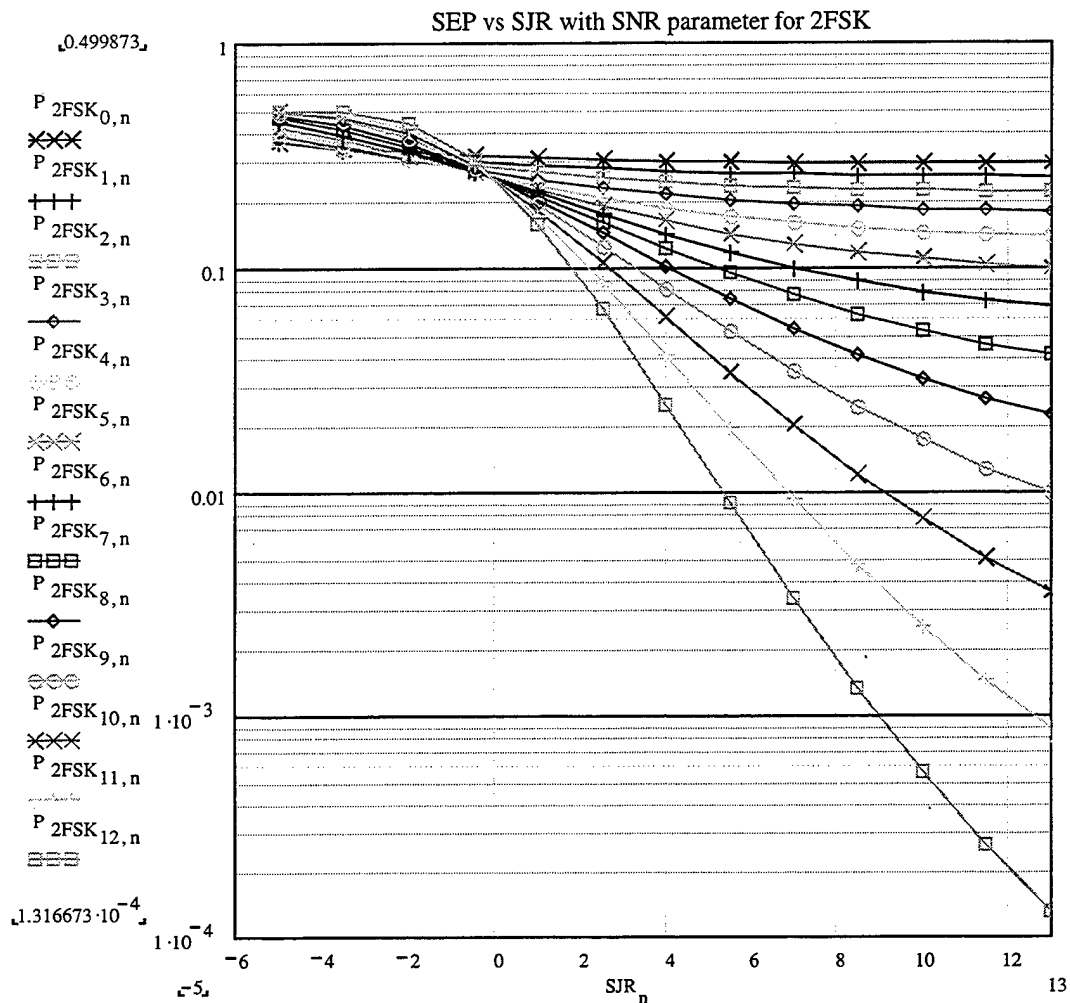
Figure 39. Theoretical symbol error probability versus SJR with SNR as a parameter
for coherent 2FSK.

The last observation indicates that two distinct regions of operation may be
identified. When the interference power is less than the signal power, that is, for SJR>0,
the signal-to-noise ratio dominates performance and the separation between the curves in
Figure 39 increases as SJR increases. For a low SJR, that is, if the interference power is

67

larger than the signal power, the symbol error probability tends to a high constant value regardless of the SNR. This is expected, since, statistically, half of the interference symbols will be opposite to the signal symbols and will be selected by the receiver due to their larger power.
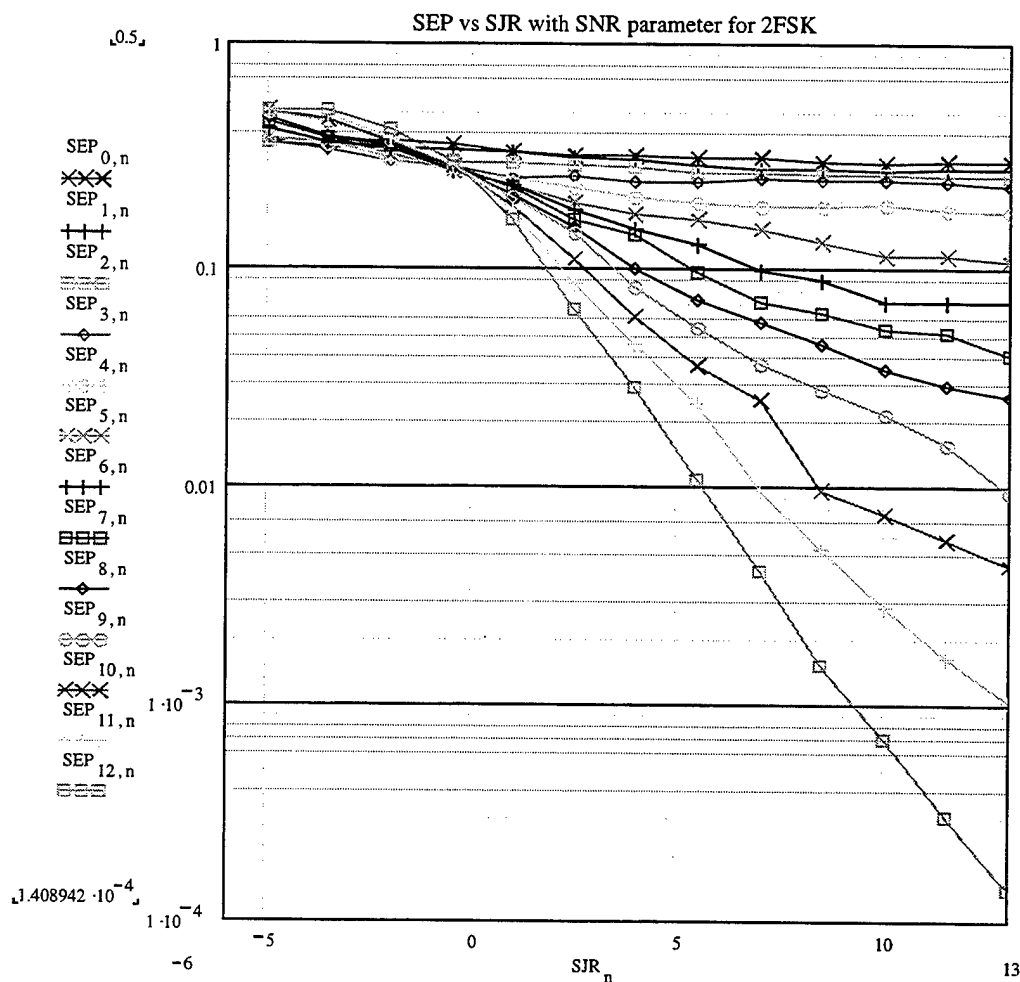
Figure 40. Simulation symbol error probability versus SJR, with SNR as a parameter for coherent 2FSK.

Although the simulation and theoretical curves have the same shape, the specific values for the symbol error probabilities differ from each other, and their relative

difference (in percent) is presented in Table 18. In Figure 41, the average difference or error for each curve is plotted versus SNR and SJR, respectively, for each set of 13 of the previously presented curves.
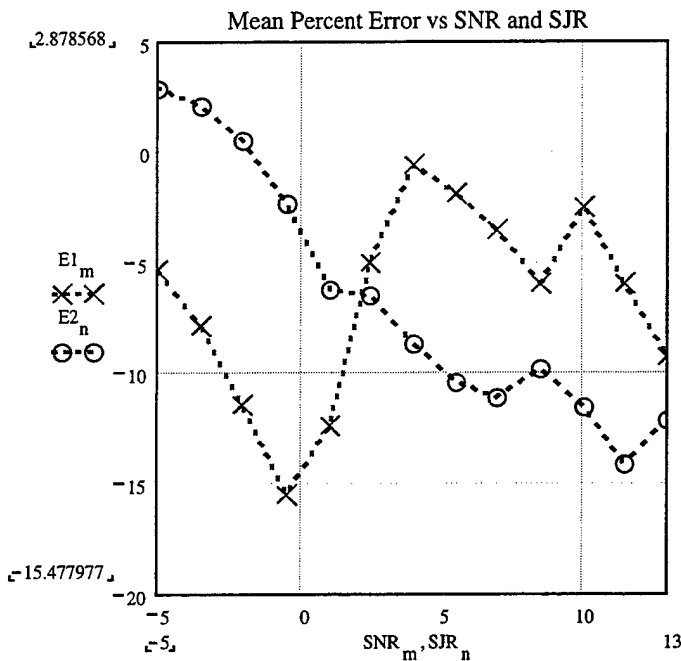
Figure 41. Mean percent difference as a function of SNR and SJR, respectively.

	SYMBOL ERROR PROBABILITY	COHERENT 2FSK
1.	Root Mean Square Difference (%)	11.903
2.	Average Mean Difference (%)	-6.681
3.	Maximum Difference (%)	20.971
4.	Minimum Difference (%)	-35.194
5.	Difference Deviation (%)	9.851

Table 18. Summary of the accuracy of the simulation for coherent 2FSK.

69

3. Results For 4FSK

The probability of symbol error for coherent 4FSK as a function of SNR with SJR as parameter is shown in Figure 42.
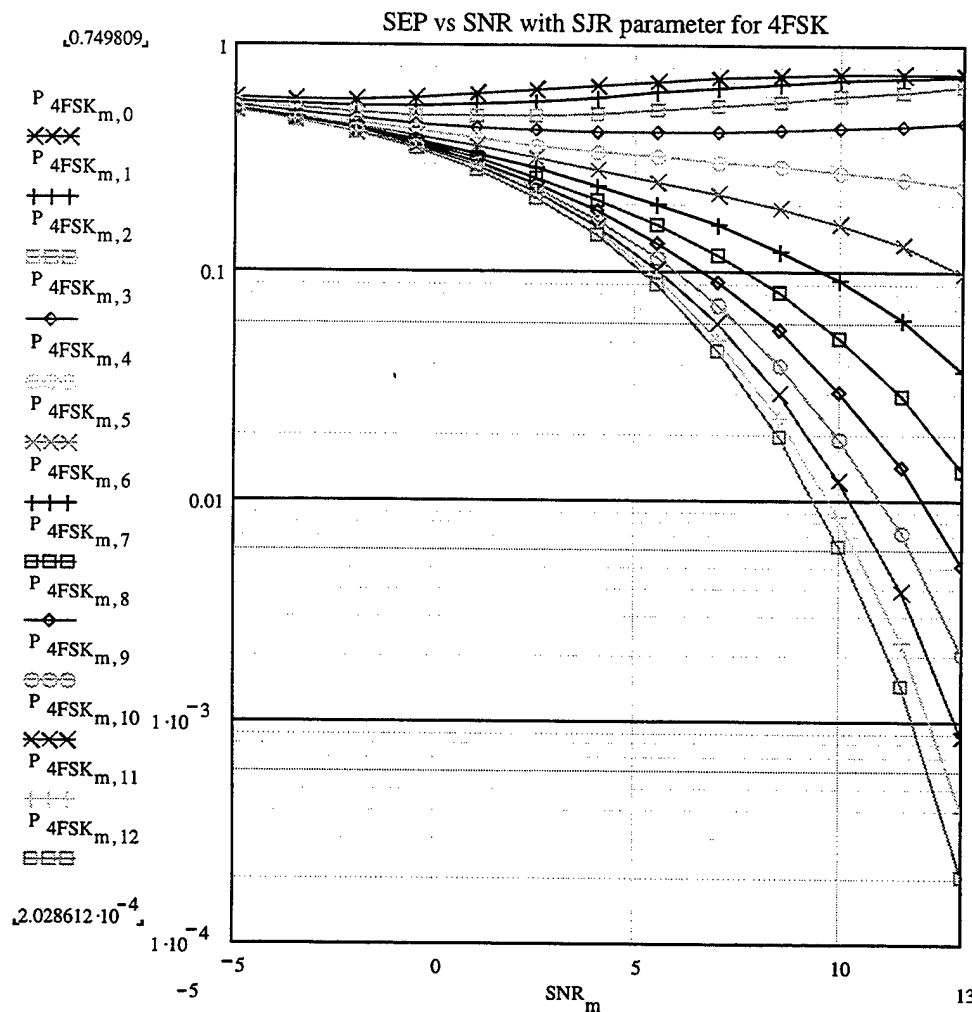
Figure 42. Theoretical symbol error probability versus SNR with SJR as a parameter for coherent 4FSK.

Thirteen curves for SJR values from −5 dB to +13 dB are shown in Figure 42, where the lower curve corresponds to SJR=+13 dB and the remaining curves are in increments of 1.5 dB. We observe that the symbol error probability for small values of

70

SJR is high and almost independent of the SNR. In Figure 43, we plot the simulation

results.
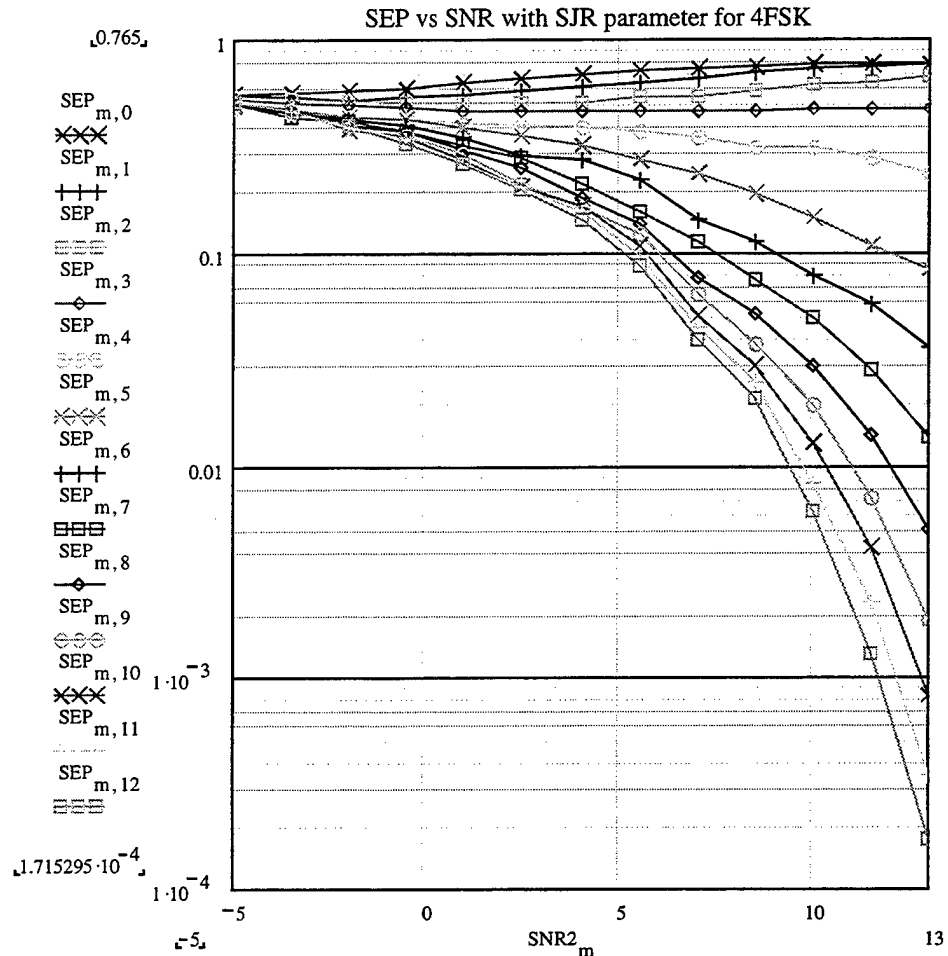
Figure 43. Simulation symbol error probability versus SNR with SJR as a parameter

for coherent 4FSK.

In Figure 44 the theoretical symbol error probability is shown as a function of SJR

with SNR as a parameter.
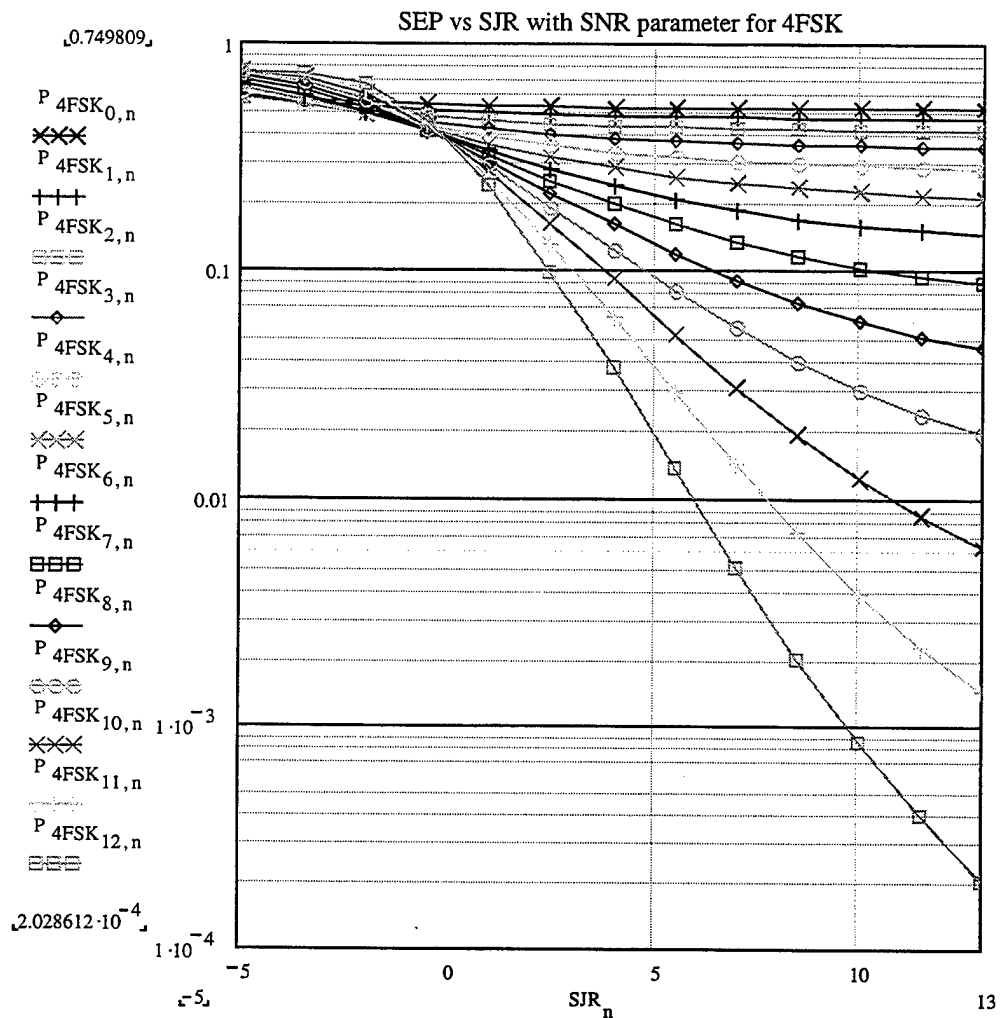
Figure 44. Theoretical symbol error probability versus SJR with SNR as a parameter for coherent 4FSK.

Thirteen curves for SNR values from −5 dB to +13 dB are shown in Figure 44 where the lower curve corresponds to SNR=+13 dB and the remaining curves are in increments of 1.5 dB. We observe that the symbol error probability is high for small values of SJR and almost independent of the SNR. Next, in Figure 45, we plot the simulation results.

72
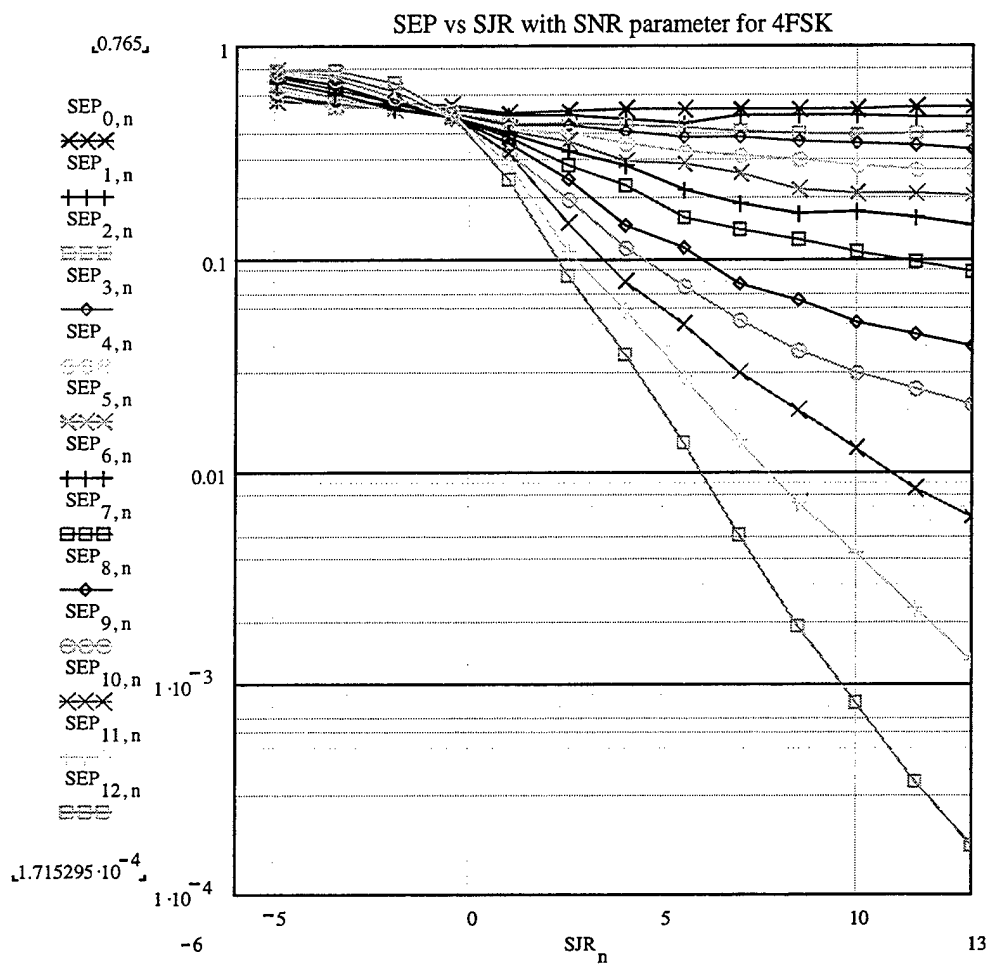
Figure 45. Simulation symbol error probability versus SJR with SNR as a parameter for coherent 4FSK.

In Figure 46, the average difference for each curve is plotted versus SNR and SJR for each set of 13 of the previously presented curves. The relative difference (in percent) between the theory and the simulation is presented in Table 19.

73
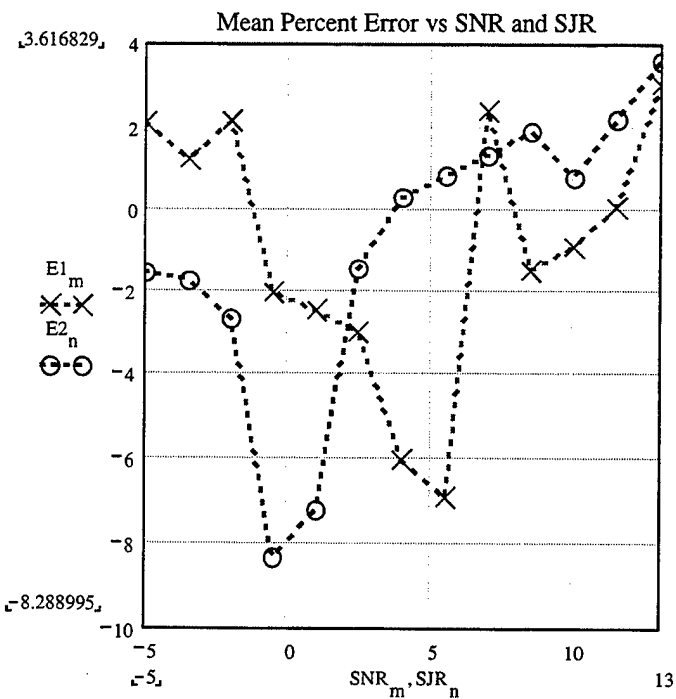
Figure 46. Mean percent difference as a function of SNR and SJR, respectively.

The two curves show how the mean difference ("error") varies with SNR and SJR, respectively. Each value of the mean difference is the average of the differences that correspond to the 13 points on each of the 13 curves for the symbol error probability as a function of SNR (with SJR as parameter) and SJR (with SNR as parameter), respectively.

	SYMBOL ERROR PROBABILITY	COHERENT 4FSK
1.	Root Mean Square Difference (%)	6.888
2.	Average Mean Difference (%)	-0.913
3.	Maximum Difference (%)	16.334
4.	Minimum Difference (%)	-18.625
5.	Difference Deviation (%)	6.828

Table 19. Summary of the accuracy of the simulation for coherent 4FSK.

4. Results for 8FSK

The probability of symbol error for coherent 8FSK as a function of SNR with the

SJR as a parameter is shown in Figure 47.
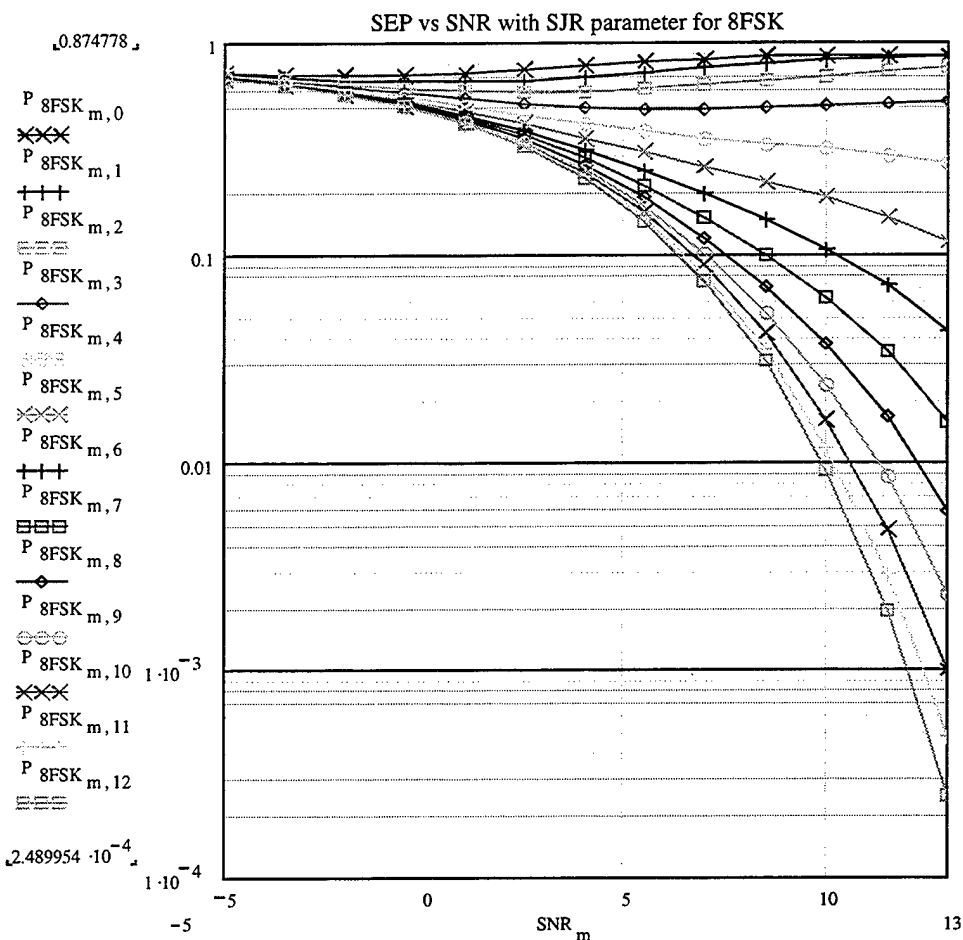
Figure 47. Theoretical symbol error probability versus SNR with SJR as a parameter for coherent 8FSK.

Thirteen curves for SJR values from −5 dB to +13 dB are shown in Figure 47 where the lower curve corresponds to SJR=+13 dB and the remaining curves are in increments of 1.5 dB. We observe again that the symbol error probability is high for

small values of SJR and almost independent of the SNR. Next, in Figure 48, we plot the

simulation results.
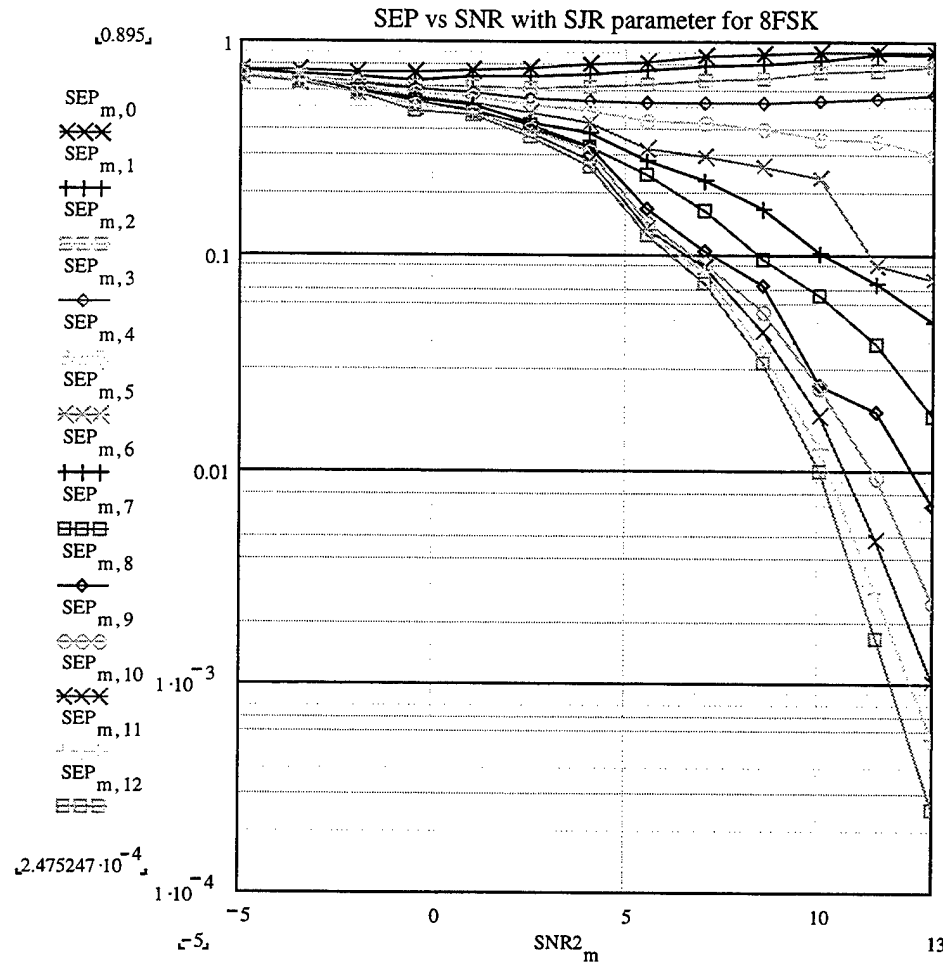
Figure 48. Simulation symbol error probability versus SNR with SJR as a parameter

for coherent 8FSK.

Figure 49 is an illustration of the theoretical symbol error probability versus SJR

with SNR as a parameter.
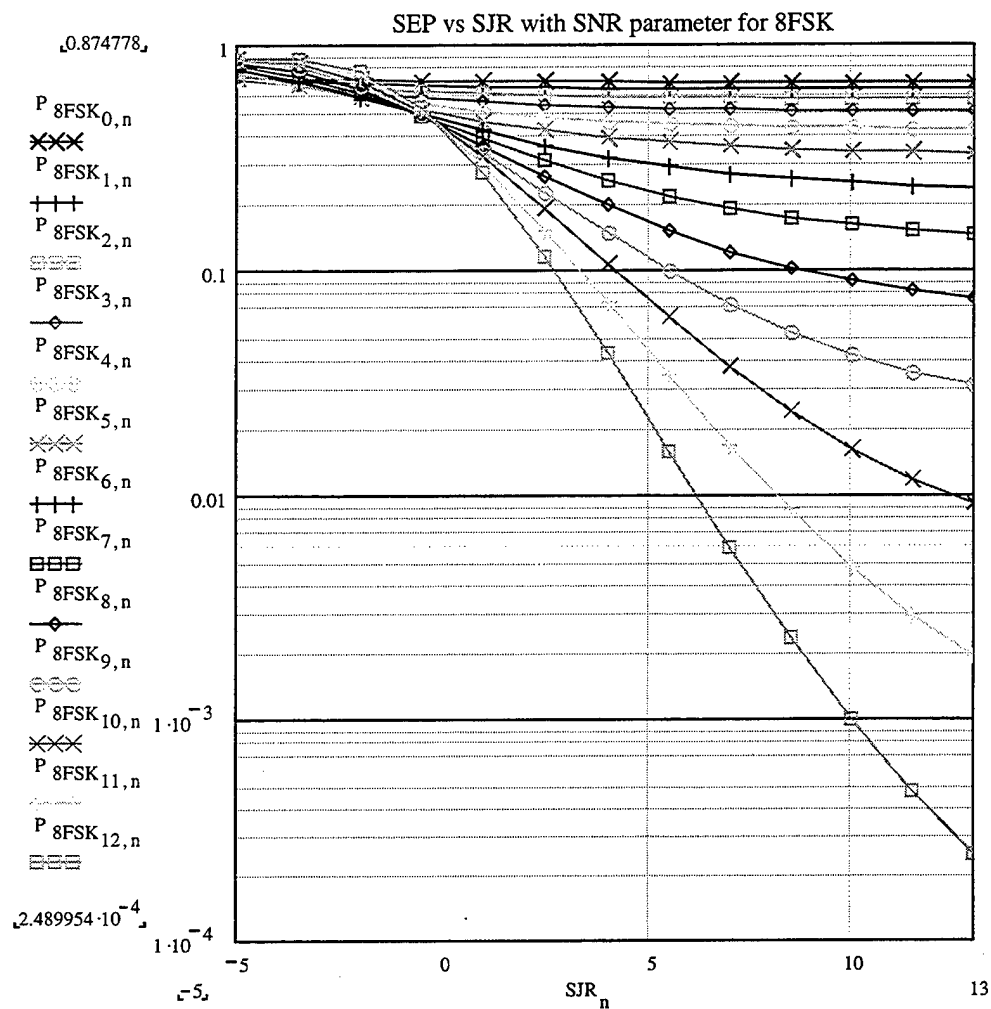
Figure 49. Theoretical symbol error probability versus SJR with SNR as a parameter for coherent 8FSK.

Thirteen curves for SNR values from -5 dB to $+13$ dB are shown in Figure 49 where the lower curve corresponds to SNR$=+13$ dB and the remaining curves are in increments of 1.5 dB. We observe that the symbol error probability is high for small values of SJR and almost independent of SNR. Next, in Figure 50, we plot the simulation results.
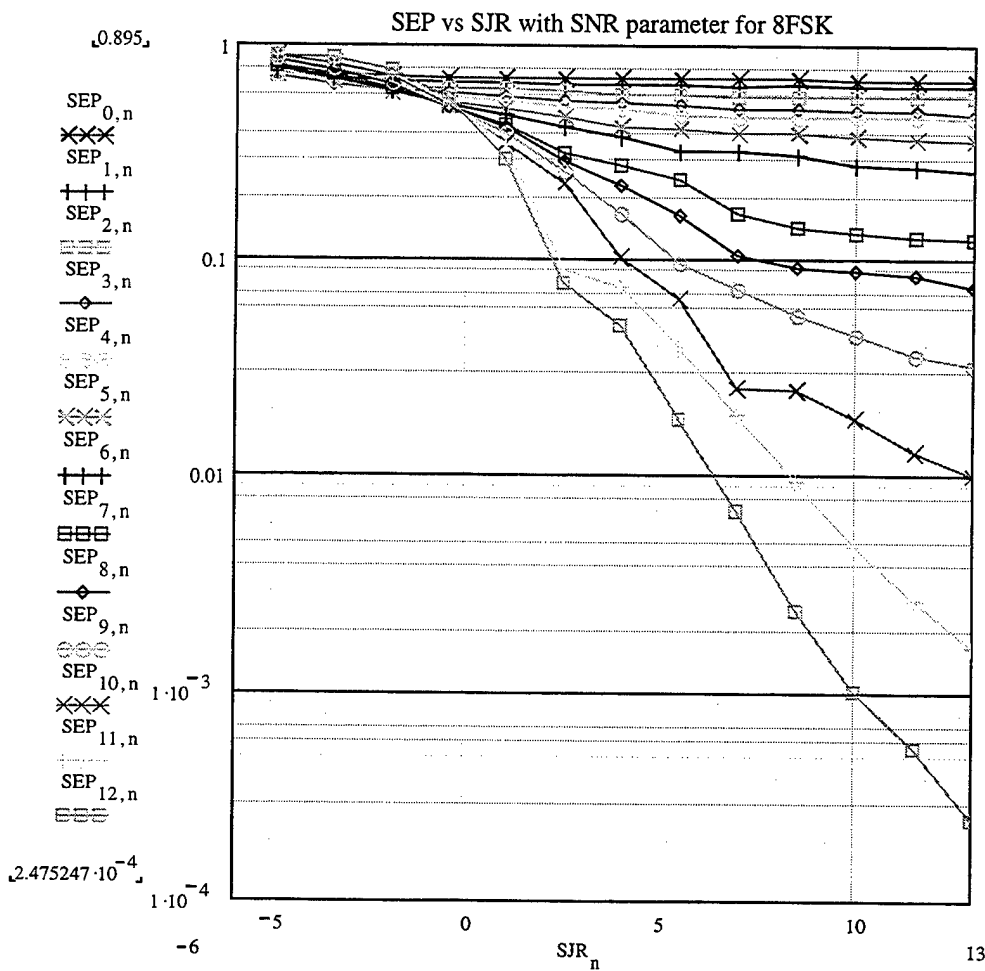
Figure 50. Simulation symbol error probability versus SJR with SNR as a parameter for coherent 8FSK.

First, in Figure 51, the average difference for each curve is plotted versus SNR and SJR, respectively, for each set of 13 of the previously presented curves. The relative difference (in percent) between the theory and the simulation is presented in Table 20.
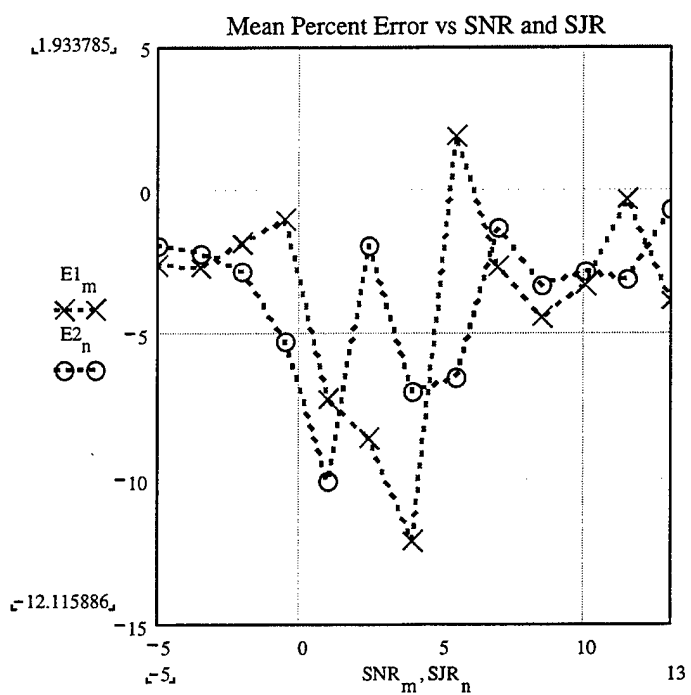
Figure 51. Mean percent difference as a function of SNR and SJR, respectively.

The two curves show how the mean difference varies with SNR and SJR respectively. Each value of the mean difference is the average of the differences that correspond to the 13 points on each of the 13 curves for the symbol error probability as a function of SNR (with SJR as parameter) and SJR (with SNR as parameter), respectively.

	SYMBOL ERROR PROBABILITY	COHERENT 8FSK
1.	Root Mean Square Difference (%)	9.351
2.	Average Mean Difference (%)	-3.714
3.	Maximum Difference (%)	40.608
4.	Minimum Difference (%)	-22.223
5.	Difference Deviation (%)	8.582

Table 20. Summary of the accuracy of the simulation for coherent 8FSK.

C.   NON-COHERENT DETECTION

In this section we consider again MFSK signaling corrupted by AWGN and co-channel interference. First, the expression for the symbol error probability for non-coherent detection is derived as a function of SNR and the signal to co-channel interference (jamming) ratio. Then the theoretical results are compared with the simulation results. We will assume that each interfering symbol is synchronized with the transmitted signal symbol.

1.   Theoretical Probability Of Symbol Error For Non-Coherent Detection

We again consider the two different cases of symbol error probability as we did for the coherent detection analysis. Initially, these two cases will be examined separately and then the combined total symbol error probability will be derived.

a)   The Signal And The Interference Symbols Are On The Same Branch

The signal space representation for the transmitted signal (S_i), noise (N), interference (I), and received signal (Y) for a non-coherent receiver is the following:

$$
S_i = \begin{bmatrix} 0 \\ 0 \\ \cdot \\ \cdot \\ S\cdot\cos(\theta) \\ S\cdot\sin(\theta) \\ \cdot \\ 0 \\ 0 \end{bmatrix} \quad
N = \begin{bmatrix} n_{1c} \\ n_{1s} \\ \cdot \\ \cdot \\ n_{ic} \\ n_{is} \\ \cdot \\ n_{Mc} \\ n_{Ms} \end{bmatrix} \quad
I = \begin{bmatrix} 0 \\ 0 \\ \cdot \\ \cdot \\ J\cdot\cos(\theta) \\ J\cdot\sin(\theta) \\ \cdot \\ 0 \\ 0 \end{bmatrix} \quad
Y = \begin{bmatrix} y_{1c} \\ y_{1s} \\ \cdot \\ \cdot \\ y_{ic} \\ y_{is} \\ \cdot \\ y_{Mc} \\ y_{Ms} \end{bmatrix} \quad \text{ith symbol}
$$

80

In the non-coherent receiver, there is a sine and a cosine path for each of the M branches.

At any time instant the branch noises, as well as the transmitted signal and the interference, can be considered as independent random variables. The probability that the noise in any of M-1 branches will not exceed the sum of the signal and interference, that is, the probability of correct symbol detection given that y_i is received, is given by:

$$P\left(correct\_decision\ given\_y_i\right) = \prod_{(j \neq i)} P\left(y_j \leq y_i, given.\ y_i\right) \qquad (4.17)$$

Our decision variable is:

$$y_j = \sqrt{y_{jc}^2 + y_{js}^2} = \sqrt{n_{jc}^2 + n_{js}^2} \qquad for \quad j \neq i \qquad (4.18)$$

where n_{jc} and n_{js} are gaussian random variables for the sine and cosine path respectively. Consequently, y_j is a Rayleigh random variable with probability density function

$$f\left(y_j\right) = \frac{y_j}{\sigma^2} \cdot e^{\frac{-y_j^2}{2 \cdot \sigma^2}} \qquad for \quad y_j \geq 0 \qquad (4.19)$$

So, the conditional probability of correct symbol detection is:

$$P\left(correct\_decision\ given\_y_i\right) = \left[\int_0^{y_i} \frac{y_j}{\sigma^2} \cdot e^{\frac{-y_j^2}{2 \cdot \sigma^2}}\ dy_j \right]^{M-1} \qquad (4.20)$$

Using the transformation

$$\zeta = \frac{-y_j^2}{2 \cdot \sigma^2} \qquad and \qquad d\zeta = \frac{-y_j}{\sigma^2} \cdot dy_j \qquad (4.21)$$

81

we obtain

$$P\left(\text{correct\_decision given\_}y_i\right) = \left[-\int_0^{\frac{-y_i^2}{2\cdot\sigma^2}} e^{\zeta}d\zeta\right]^{M-1} = \left(1 - e^{\frac{-y_i^2}{2\cdot\sigma^2}}\right)^{M-1} \tag{4.22}$$

The random variable y_i is a Rician random variable, since:

$$y_i = \sqrt{y_{ic}^2 + y_{is}^2} = \sqrt{\left[(S+J)\cdot\cos(\theta) + n_{ic}\right]^2 + \left[(S+J)\cdot\sin(\theta) + n_{is}\right]^2} \tag{4.23}$$

where:

n_{jc} and n_{js} are gaussian random variables for the sine and cosine path respectively.

So, the probability density function of y_i is:

$$f\left(y_i\right) = \frac{y_i}{\sigma^2}\cdot e^{\frac{-\left[y_i^2 + (S+J)^2\right]}{2\cdot\sigma^2}} \cdot I0\left[\frac{(S+J)\cdot y_i}{\sigma^2}\right] \qquad \text{for} \quad y_i \geq 0 \tag{4.24}$$

In order to remove the condition on the probability of correct symbol detection, we have

to integrate the product of the conditional probability and the pdf of the Rician random

variable y_i:

$$P(\text{correct\_decision}) = \int_0^\infty \left(1 - e^{\frac{-y_i^2}{2\cdot\sigma^2}}\right)^{M-1} \frac{y_i}{\sigma^2}\cdot e^{\frac{-\left[y_i^2 + (S+J)^2\right]}{2\cdot\sigma^2}} \cdot I0\left[\frac{(S+J)\cdot y_i}{\sigma^2}\right]dy_i \tag{4.25}$$

82

Using the following two identities

$$\left(1 - e^{\frac{-y_i^2}{2\cdot\sigma^2}}\right)^{M-1} = \sum_{k=0}^{M-1} \frac{(M-1)!}{k!\cdot(M-1-k)!}\cdot(-1)^k\cdot e^{\frac{-k\cdot y_i^2}{2\cdot\sigma^2}} \tag{4.26}$$

$$\int_0^\infty t\cdot e^{-\alpha^2\cdot t^2}\cdot I0(t)\,dt = \frac{1}{2\cdot\alpha^2}\cdot e^{\frac{1}{4\cdot\alpha^2}} \tag{4.27}$$

we obtain the probability for correct decision:

$$P(correct\_decision) = e^{\frac{-(S+J)^2}{2\cdot\sigma^2}}\cdot\sum_{k=0}^{M-1} \frac{(M-1)!}{k!\cdot(M-1-k)!}\cdot(-1)^k\cdot\frac{1}{k+1}\cdot e^{\frac{(S+J)^2}{2\cdot(k+1)\cdot\sigma^2}} \tag{4.28}$$

So, the symbol error probability for the first case is:

$$P1_{error} = 1 - P(correct\_decision) \tag{4.29}$$

or

$$P1_{error} = e^{\frac{-(S+J)^2}{2\cdot\sigma^2}}\cdot\sum_{k=1}^{M-1} \frac{(M-1)!}{k!\cdot(M-1-k)!}\cdot(-1)^{k+1}\cdot\frac{1}{k+1}\cdot e^{\frac{(S+J)^2}{2\cdot(k+1)\cdot\sigma^2}} \tag{4.30}$$

Note that the above expression does not involve numerical integration.

b) The Signal And The Interference Symbols Are On Different Branches

The signal space representation for the transmitted signal (S_i), noise (N), interference (I), and received signal (Y) for non-coherent receiver is:

$$S_i = \begin{bmatrix} 0 \\ 0 \\ \cdot \\ S \cdot \cos(\theta) \\ S \cdot \sin(\theta) \\ \cdot \\ 0 \\ 0 \\ \cdot \\ \cdot \\ 0 \\ 0 \end{bmatrix} \quad N = \begin{bmatrix} n_{1c} \\ n_{1s} \\ \cdot \\ n_{ic} \\ n_{is} \\ \cdot \\ n_{kc} \\ n_{ks} \\ \cdot \\ \cdot \\ n_{Mc} \\ n_{Ms} \end{bmatrix} \quad I = \begin{bmatrix} 0 \\ 0 \\ \cdot \\ 0 \\ 0 \\ \cdot \\ J \cdot \cos(\theta) \\ J \cdot \sin(\theta) \\ \cdot \\ \cdot \\ 0 \\ 0 \end{bmatrix} \quad Y = \begin{bmatrix} y_{1c} \\ y_{1s} \\ \cdot \\ y_{ic} \\ y_{is} \\ \cdot \\ y_{kc} \\ y_{ks} \\ \cdot \\ \cdot \\ y_{Mc} \\ y_{Ms} \end{bmatrix} \begin{array}{l} \\ \\ \\ \text{ith symbol} \\ \\ \\ \text{kth symbol} \end{array} \quad \text{where} \quad i \neq k$$

The signal and the interference symbols are now at different branches. The probability that neither the sum of the interference and noise nor the noise in any of the remaining M-2 branches exceeds the signal (that is the probability of correct symbol detection given that y_i was transmitted) is given by:

$$P\left(\text{correct\_decision, given\_}y_i\right) = \left[\prod_{(j \neq i, j \neq k)} P\left(y_j \leq y_i, \text{given.. } y_i\right) \right] \cdot P\left(y_k \leq y_i, \text{given.. } y_i\right) \quad (4.31)$$

The decision variables are:

$$y_j = \sqrt{y_{jc}^2 + y_{js}^2} = \sqrt{n_{jc}^2 + n_{js}^2} \quad (4.32)$$

84

which is a Rayleigh random variable, and

$$y_k = \sqrt{y_{kc}^2 + y_{ks}^2} = \sqrt{\left(J \cdot \cos(\theta) + n_{kc}\right)^2 + \left(J \cdot \sin(\theta) + n_{ks}\right)^2} \qquad (4.33)$$

which is a Rician random variable.

Therefore, the conditional probability of correct decision is:

$$P\left(\text{correct}, y_i\right) = \left[\int_0^{y_i} \frac{y_j}{\sigma^2} \cdot e^{\frac{-y_j^2}{2 \cdot \sigma^2}} \, dy_j\right]^{M-2} \cdot \left[\int_0^{y_i} \frac{y_k}{\sigma^2} \cdot e^{\frac{-\left[y_k^2 + (S+J)^2\right]}{2 \cdot \sigma^2}} \cdot I0\left[\frac{(S+J) \cdot y_k}{\sigma^2}\right] dy_k\right] \qquad (4.34)$$

Equivalently, it can be written:

$$P\left(\text{correct}, y_i\right) = \left(1 - e^{\frac{-y_i^2}{2 \cdot \sigma^2}}\right)^{M-2} \cdot \int_0^{y_i} \frac{y_k}{\sigma^2} \cdot e^{\frac{-\left[y_k^2 + (S+J)^2\right]}{2 \cdot \sigma^2}} \cdot I0\left[\frac{(S+J) \cdot y_k}{\sigma^2}\right] dy_k \qquad (4.35)$$

To evaluate the integral of the last expression we use the relationship:

$$\int_0^{y_i} \frac{y_k}{\sigma^2} \cdot e^{\frac{-\left[y_k^2 + (S+J)^2\right]}{2 \cdot \sigma^2}} \cdot I0\left[\frac{(S+J) \cdot y_k}{\sigma^2}\right] dy_k = 1 - Q_1\left(\frac{J}{\sigma}, \frac{y_i}{\sigma}\right) \qquad (4.36)$$

where:

Q1 (a, b) is the Marcuum Q-function.

The Marcuum Q-function is given by:

$$Q_1(a,b) = e^{\frac{-\left(a^2 + b^2\right)}{2}} \cdot \sum_{p=0}^{\infty} \left(\frac{a}{b}\right)^p \cdot I_p(a \cdot b) \qquad (4.37)$$

Finally, for the conditional probability of correct decision, we obtain:

$$P\left(\text{correct}, y_i\right) = \left(1 - e^{\frac{-y_i^2}{2 \cdot \sigma^2}}\right)^{M-2} \cdot \left[1 - e^{\frac{-\left(y_i^2 + J^2\right)}{2 \cdot \sigma^2}} \cdot \sum_{p=0}^{\infty} \left(\frac{J}{y_i}\right)^p \cdot I_p\left(\frac{J \cdot y_i}{\sigma^2}\right)\right] \qquad (4.38)$$

The variable y_i is a Rician random variable, since:

$$y_i = \sqrt{y_{ic}^2 + y_{is}^2} = \sqrt{\left(S \cdot \cos(\theta) + n_{ic}\right)^2 + \left(S \cdot \sin(\theta) + n_{is}\right)^2} \qquad (4.39)$$

In order to remove the condition on the correct symbol probability, we have to integrate the product of the above result and the pdf of the random variable y_i over all the possible values of y_i. The unconditional probability for correct decision can now be derived as follows:

$$P_{\text{correct}} = \int_0^\infty \left(1 - e^{\frac{-y_i^2}{2 \cdot \sigma^2}}\right)^{M-2} \cdot \left[1 - e^{\frac{-\left(y_i^2 + J^2\right)}{2 \cdot \sigma^2}} \cdot \sum_{p=0}^{\infty} \left(\frac{J}{y_i}\right)^p \cdot I_p\left(\frac{J \cdot y_i}{\sigma^2}\right)\right] \frac{y_i}{\sigma^2} e^{\frac{-\left(y_i^2 + s^2\right)}{2 \cdot \sigma^2}} \cdot I0\left(\frac{S \cdot y_i}{\sigma^2}\right) dy_i \qquad (4.40)$$

Using the transformation:

$$\frac{y_i}{\sigma} = x \qquad \text{and} \qquad dy_i = \sigma \cdot dx \qquad (4.41)$$

86

we obtain

$$P_{correct} = \int_0^\infty \left(1 - e^{\frac{-x^2}{2}}\right)^{M-2} \cdot \left[1 - e^{\frac{-1}{2}\cdot\left(x^2+\frac{J^2}{\sigma^2}\right)} \cdot \sum_{p=0}^\infty \left(\frac{J}{\sigma\cdot x}\right)^p \cdot I_p\left(\frac{J\cdot x}{\sigma}\right)\right] \cdot e^{\frac{-1}{2}\cdot\left(x^2+\frac{S^2}{\sigma^2}\right)} \cdot I0\left(\frac{S\cdot x}{\sigma}\right) \cdot x\, dx \quad (4.42)$$

Finally, the symbol error probability for this second case is:

$$P2_{error} = 1 - \int_0^\infty \left(1 - e^{\frac{-x^2}{2}}\right)^{M-2} \cdot \left[1 - e^{\frac{-1}{2}\cdot\left(x^2+\frac{J^2}{\sigma^2}\right)} \cdot \sum_{p=0}^\infty \left(\frac{J}{\sigma\cdot x}\right)^p \cdot I_p\left(\frac{J\cdot x}{\sigma}\right)\right] \cdot e^{\frac{-1}{2}\cdot\left(x^2+\frac{S^2}{\sigma^2}\right)} \cdot I0\left(\frac{S\cdot x}{\sigma}\right) \cdot x\, dx \quad (4.43)$$

The above integral must be evaluated numerically.

c)   Total Symbol Error Probability

The total symbol error probability is given by:

$$P_{total} = \frac{1}{M}\cdot P1 + \frac{M-1}{M}\cdot P2 \quad (4.44)$$

where:

1/M is the probability that the transmitted and the interfering symbols are at the same branch and

(M-1)/M is the probability that the transmitted and the interfering symbols are at different branches.

2. Results For 2FSK

In Figure 52, we show the theoretical symbol error probability versus SNR with SJR as a parameter for non-coherent detection of 2FSK. The simulation results are shown separately in Figure 53.
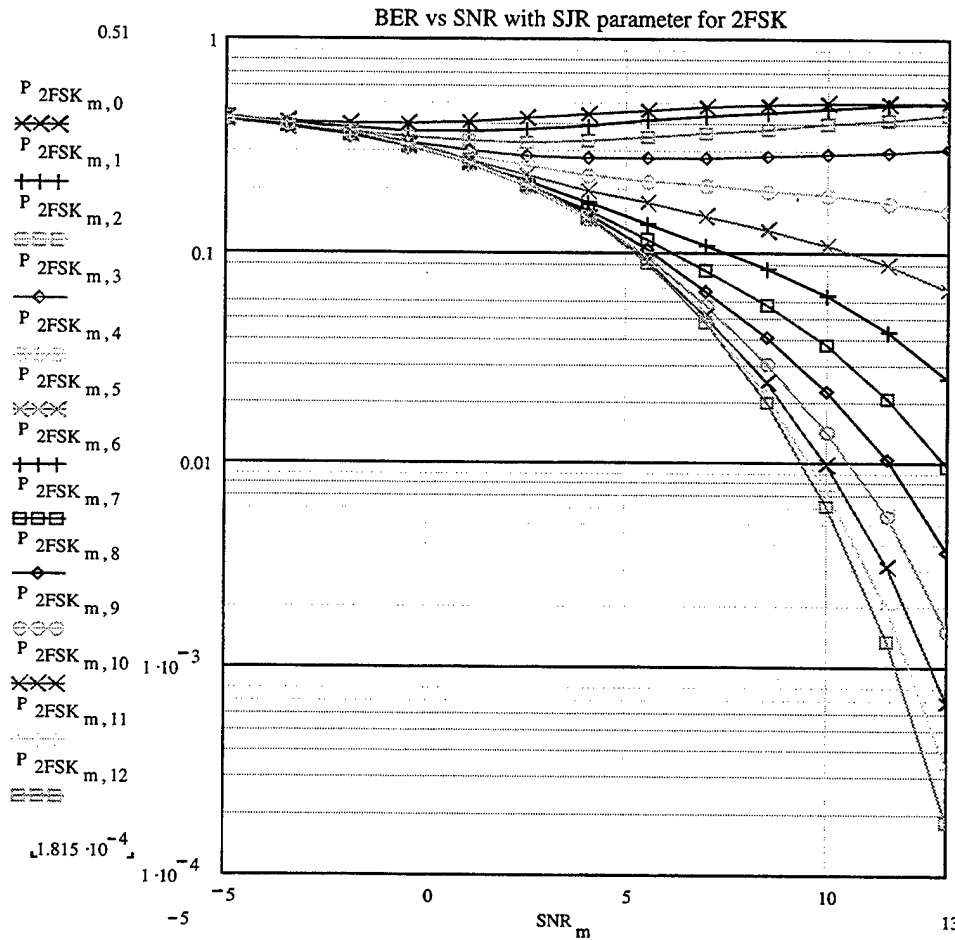
Figure 52. Theoretical symbol error probability versus SNR with SJR as a parameter for non-coherent 2FSK.

In Figure 53, we show the simulation results of non-coherently detected 2FSK signal in the presence of AWGN and co-channel interference (jamming).

88
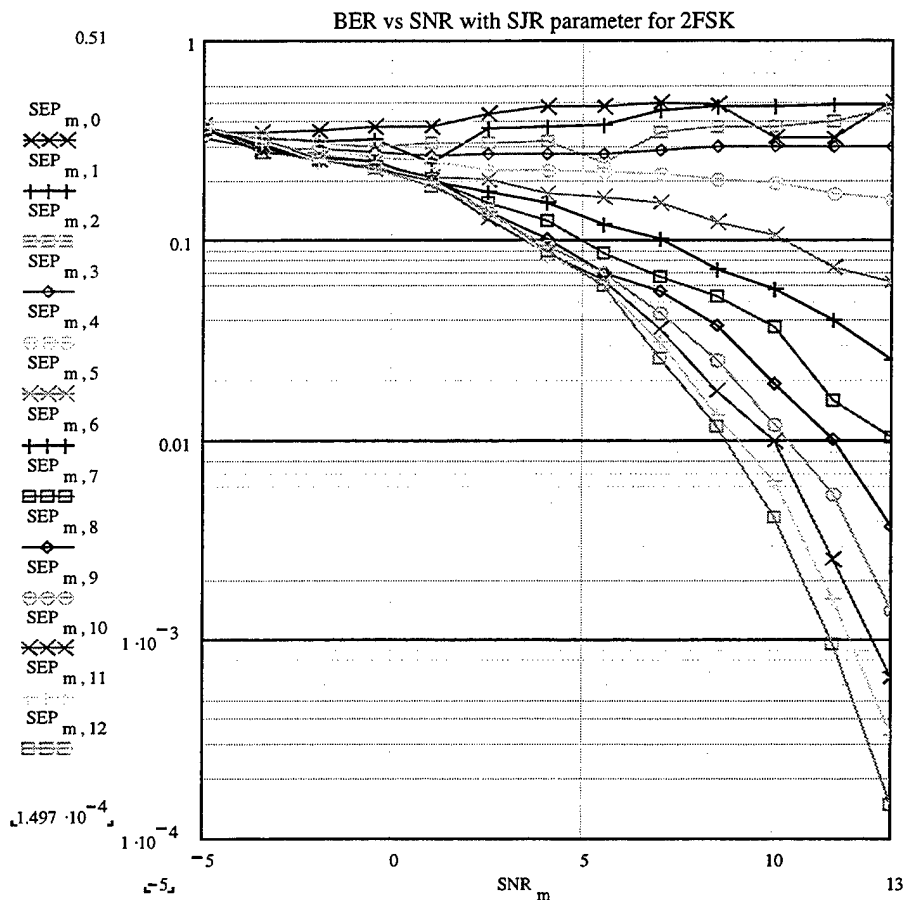
Figure 53. Simulation symbol error probability versus SNR with SJR as a parameter

for non-coherent 2FSK.

In Figure 54 and 55, we show the theoretical and the simulation results,
respectively, versus SJR with SNR as a parameter. From Figure 54, we see that as SJR
increases (that is, as the interference power decreases relative to the signal power), the
symbol error probability initially decreases but then tends to a constant value. As the
SNR increases, this constant value decreases as well.
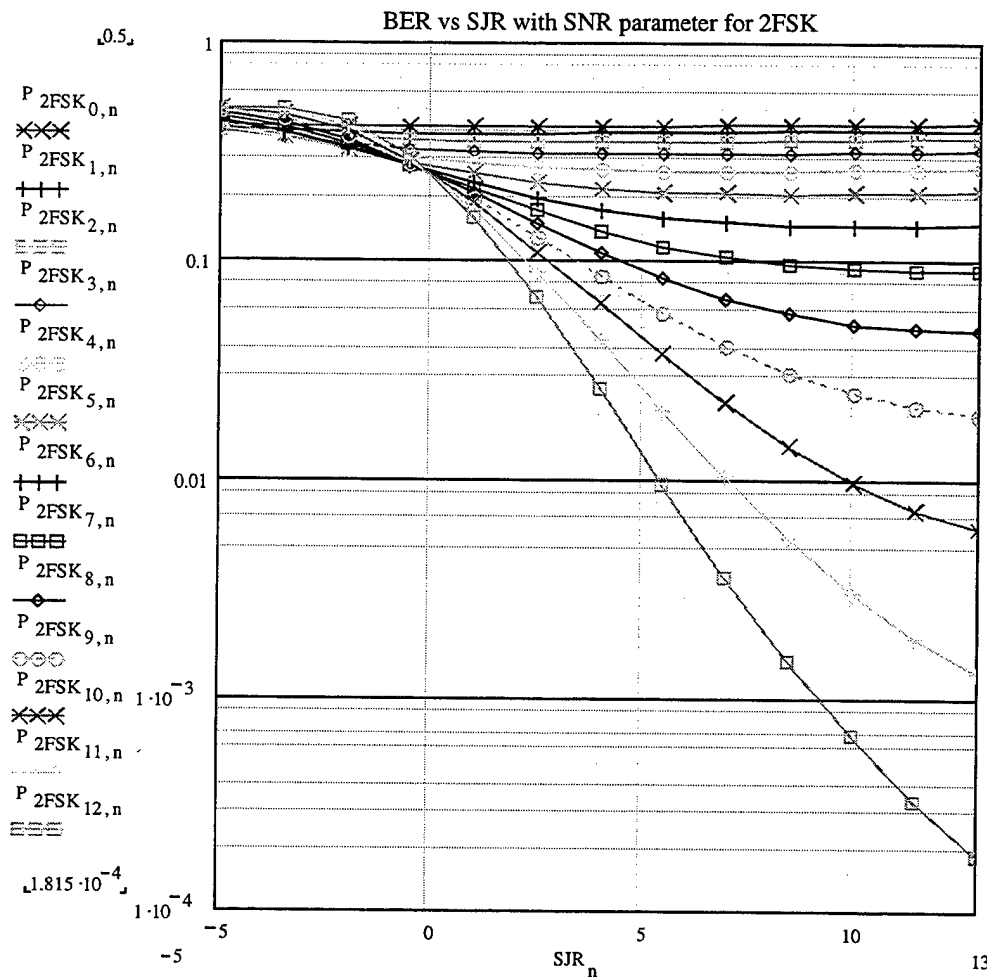
Figure 54. Theoretical symbol error probability versus SJR with SNR as a parameter for non-coherent 2FSK.

We observe again that if the signal power is larger than interference power (SJR>0) then SNR dominates performance and the curves become steeper for higher values of SNR. For low values of SJR, the symbol error probability is around 0.5, as expected, since statistically, half of the interference symbols will be opposite to the signal symbols and will be selected by the receiver due to their larger power. In Figure 55, the simulation results are presented.
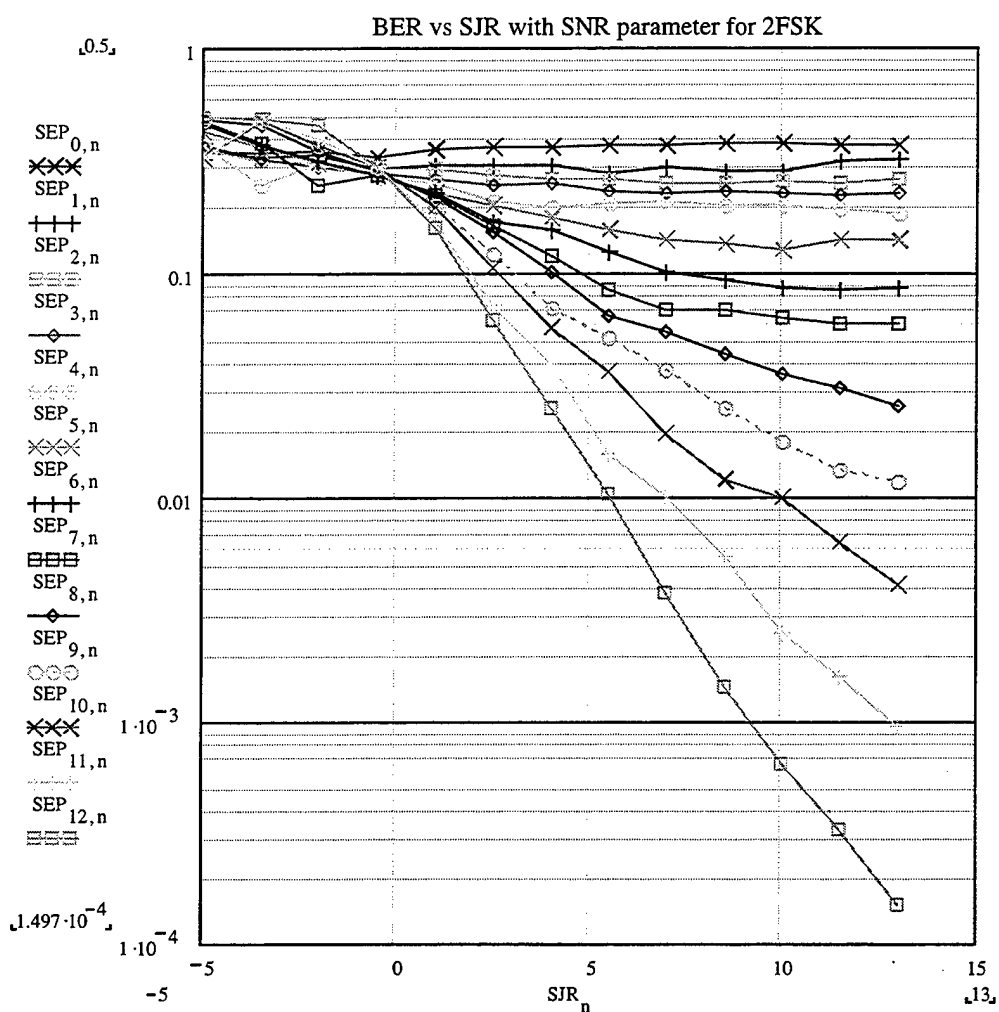
Figure 55. Simulation symbol error probability versus SJR with SNR as a parameter for non-coherent 2FSK.

The relative difference (in percent) between the theory and the simulation is presented in Table 21. In Figure 56, the average difference for each curve is plotted versus SNR and SJR for each set of 13 of the previously presented curves.
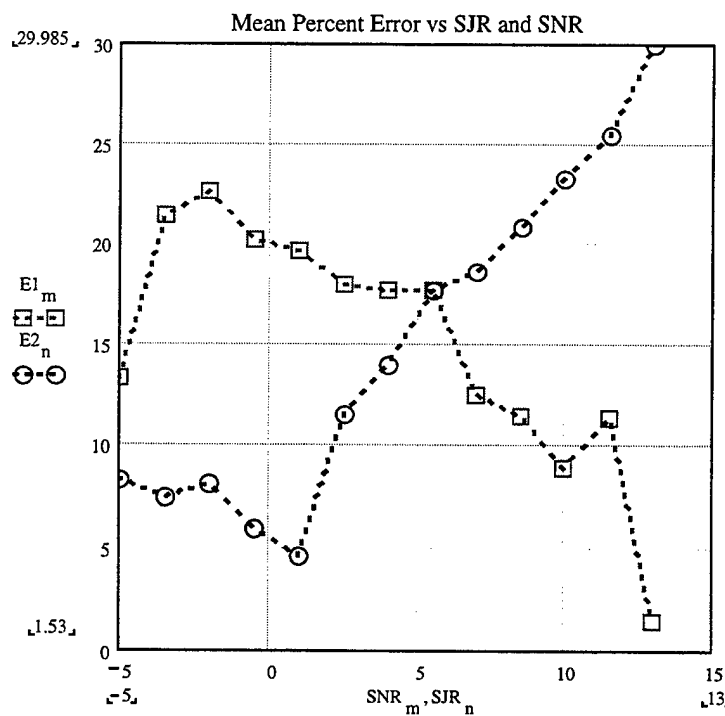
Figure 56. Mean percent difference as a function of SNR and SJR, respectively.

The two curves show how the mean difference varies with SNR and SJR, respectively. Each value of the mean difference is the average of the differences that correspond to the 13 points on each of the 13 curves for the symbol error probability as a function of SNR (with SJR as parameter) and SJR (with SNR as parameter).

	SYMBOL ERROR PROBABILITY	NON-COHERENT 2FSK
1.	Root Mean Square Difference (%)	19.823
2.	Average Mean Difference (%)	15.112
3.	Maximum Difference (%)	45.458
4.	Minimum Difference (%)	-7.939
5.	Difference Deviation (%)	12.829

Table 21. Summary of the accuracy of the simulation for non-coherent 2FSK.

3. Results For 4FSK

The probability of symbol error for non-coherent 4FSK as a function of SNR with

SJR as a parameter is shown in Figure 57.
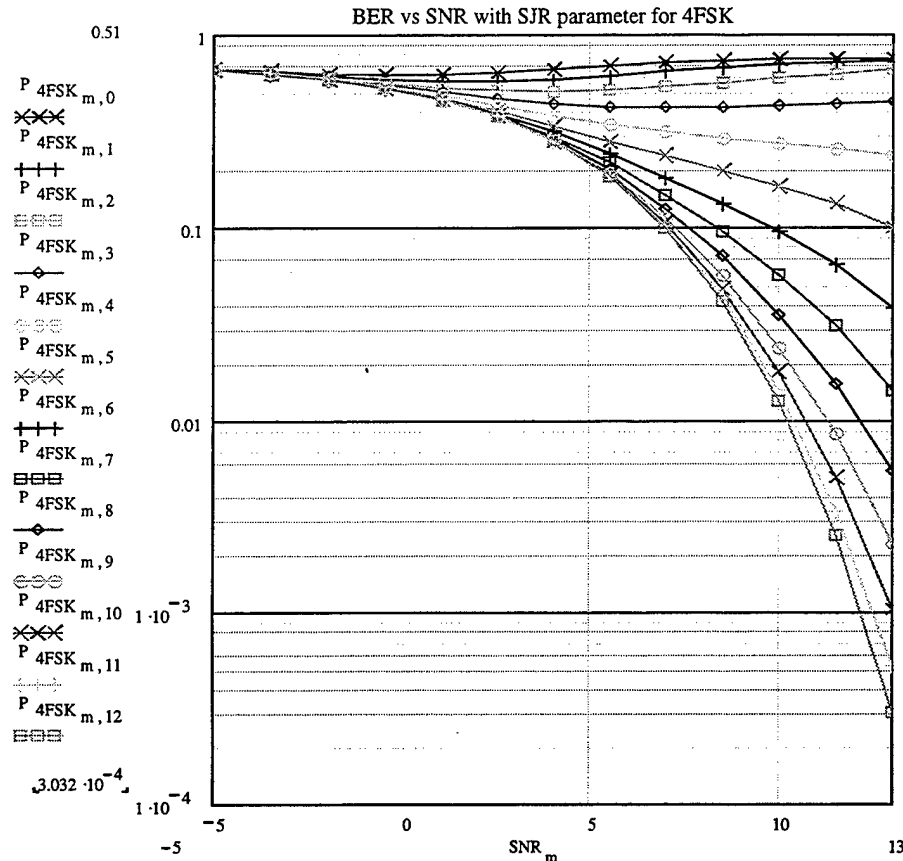
Figure 57. Theoretical symbol error probability versus SNR with SJR as a parameter for non-coherent 4FSK.

Thirteen curves for SNR values from −5 dB to +13 dB are shown in Figure 57 where the lower curve corresponds to SJR=+13 dB and the remaining curves are in increments of 1.5 dB. We observe that the symbol error probability is high for small values of SJR and is almost independent of the SNR. In Figure 58, we show the simulation results.

93
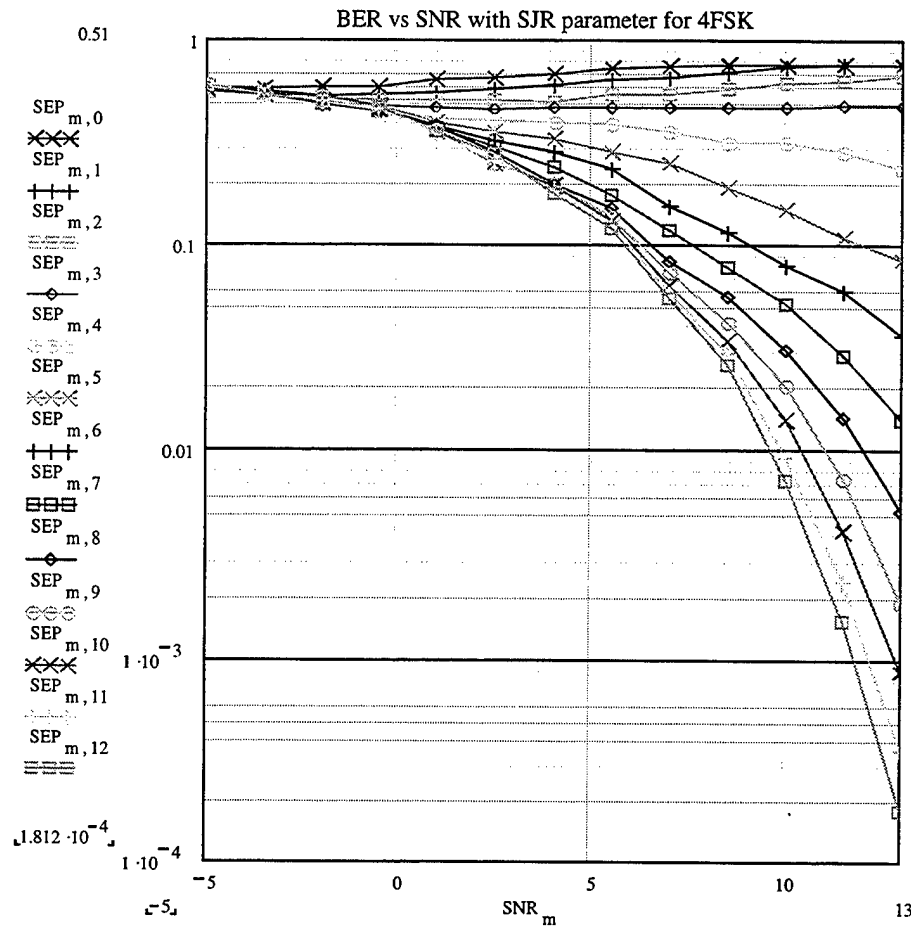
Figure 58. Simulation symbol error probability versus SNR with SJR as a parameter for non-coherent 4FSK.

In Figures 59 and 60 the theoretical and the simulation and theoretical symbol error probability are shown as functions of SJR with SNR as a parameter. It is observed from Figure 59 that as SJR increases (that is, as the interference power decreases relative to the signal power), the symbol error probability initially decreases but then tends to a constant value. This constant value also decreases as the SNR increases.

94
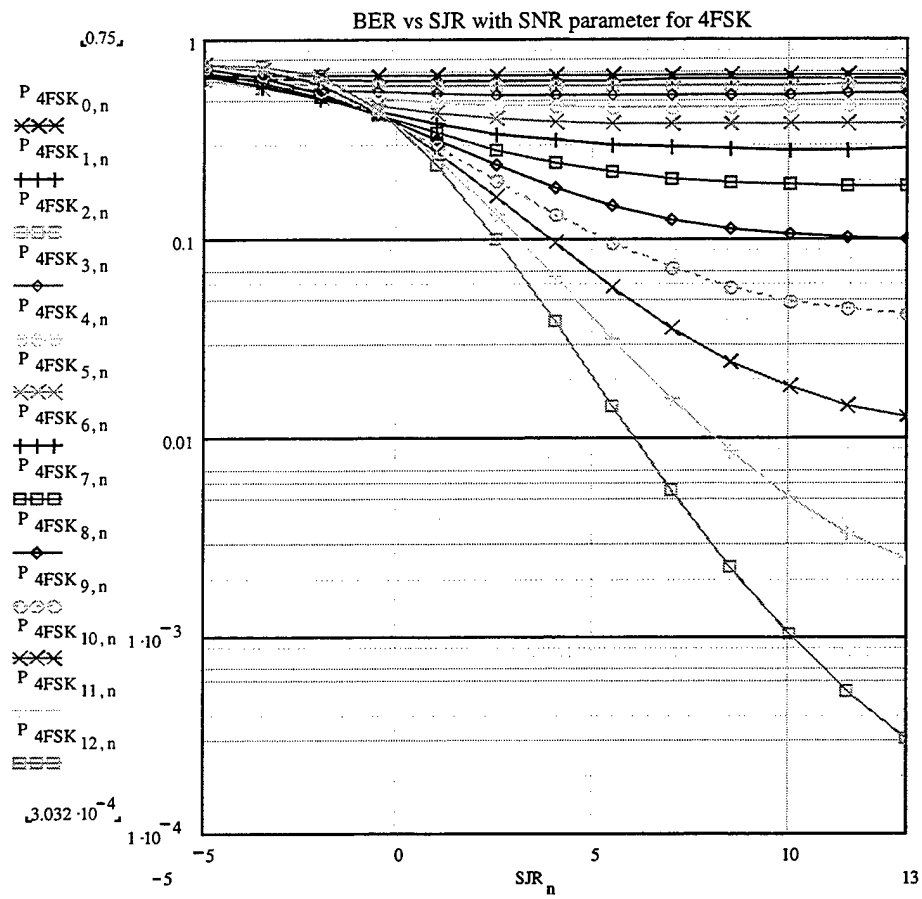
Figure 59. Theoretical symbol error probability versus SJR with SNR as a parameter for non-coherent 4FSK.

If the interference power is smaller than the signal power (SJR>0), then SNR dominates the symbol error probability and the curves are much steeper for higher values of SNR. For a low value of SJR (SJR<0) the symbol error probability tends to a high constant value. This is expected, since, statistically, almost half of the interference symbols will be opposite to the signal symbols and will be selected by the receiver due to their larger power. In Figure 60, the simulation results are presented.
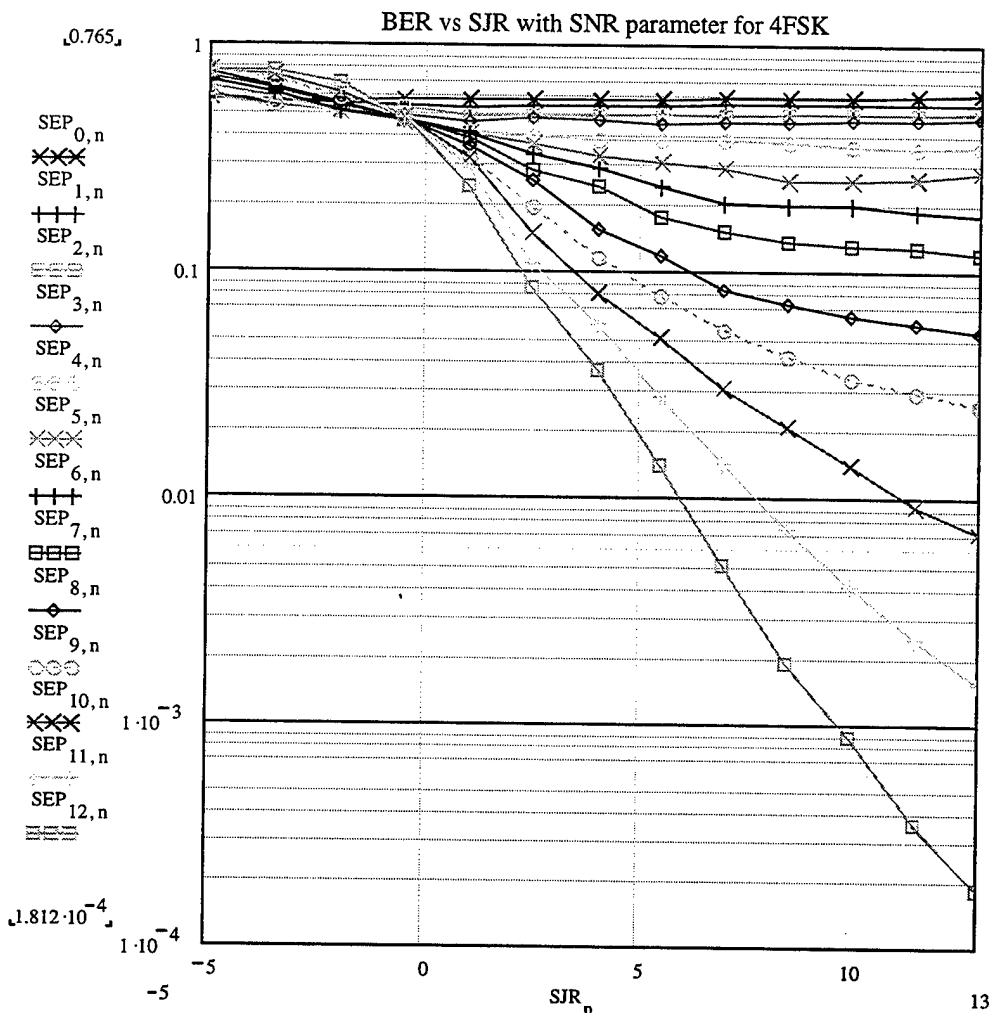
Figure 60. Simulation symbol error probability versus SJR with SNR as a parameter for non-coherent 4FSK.

The relative difference (in percent) between the theory and the simulation is presented in Table 22. In Figure 61, the average difference for each curve is plotted versus SNR and SJR for each set of 13 previously presented curves.

96
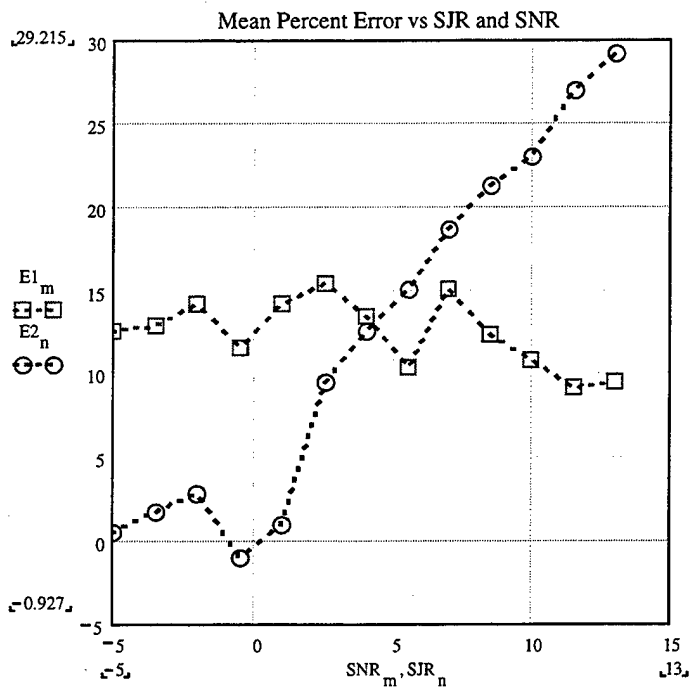
Figure 61. Mean percent difference as a function of SNR and SJR, respectively.

The two curves show how the mean difference varies with SNR and SJR, respectively. Each value of the mean difference is the average of the differences that correspond to the 13 points on each of the 13 curves for the symbol error probability as a function of SNR (with SJR as parameter) and SJR (with SNR as parameter).

	SYMBOL ERROR PROBABILITY	NON-COHERENT 4FSK
1.	Root Mean Square Difference (%)	18.298
2.	Average Mean Difference (%)	12.465
3.	Maximum Difference (%)	45.85
4.	Minimum Difference (%)	-14.319
5.	Difference Deviation (%)	13.395

Table 22. Summary of the accuracy of the simulation for non-coherent 4FSK.

4.   Results For 8FSK

The probability of symbol error for non-coherent 8FSK as a function of SNR with

SJR as a parameter is shown in Figure 62.
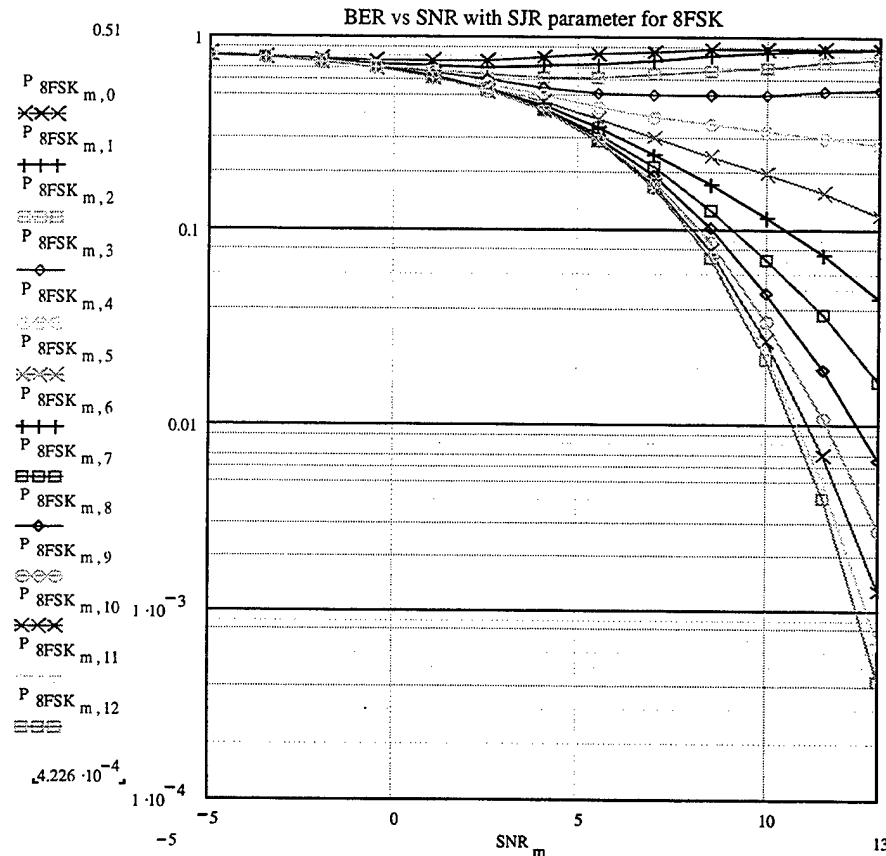
Figure 62. Theoretical symbol error probability versus SNR with SJR as a parameter
for non-coherent 8FSK.

Thirteen curves for SNR values from –5 dB to +13 dB are shown in Figure 62
where the lower curve corresponds to SJR=+13 dB and the remaining curves are in
increments of 1.5 dB. We observe that the symbol error probability is high for small
values of SJR and almost independent of the SNR. Next, in Figure 63, we show the
simulation results.

98
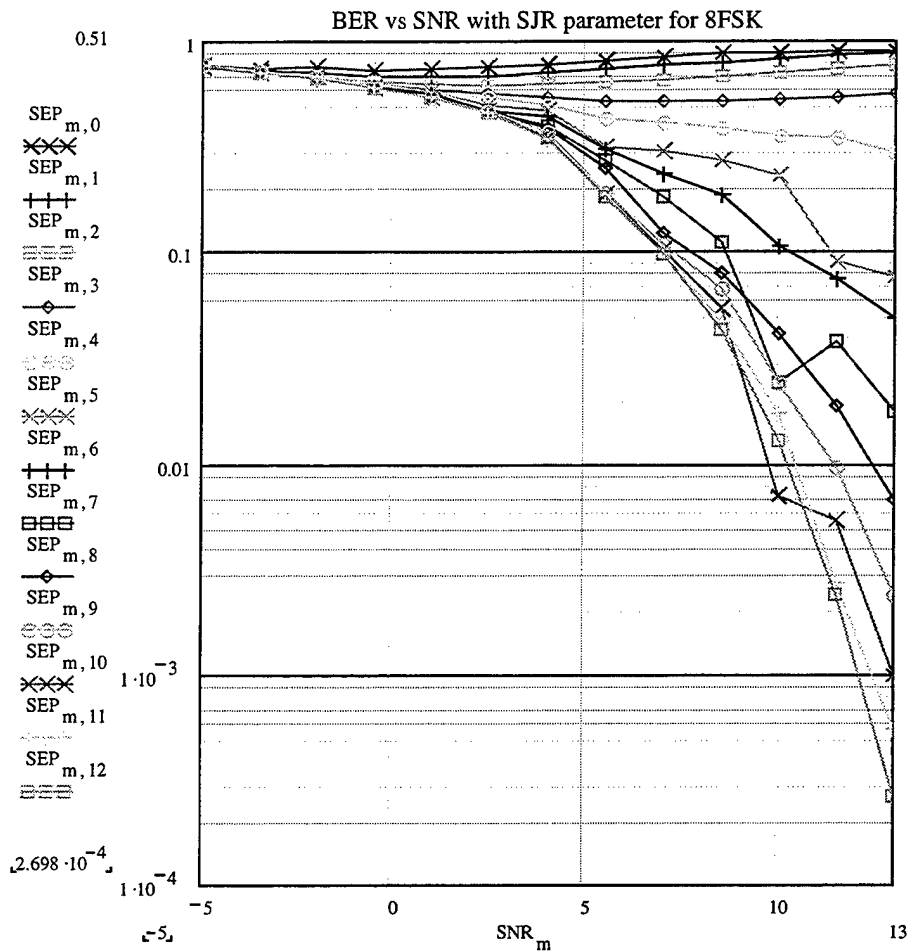
Figure 63. Simulation symbol error probability versus SNR with SJR as a parameter for non-coherent 8FSK.

In Figures 64 and 65, we show the theoretical and simulation symbol error probability as functions of SJR with SNR as a parameter. It is observed from Figure 64 that as the signal-to-interference ratio (SJR) increases (that is, as the interference power decreases relative to the signal power), the symbol error probability initially decreases but then tends to a constant value. This constant value decreases as the SNR increases.

99
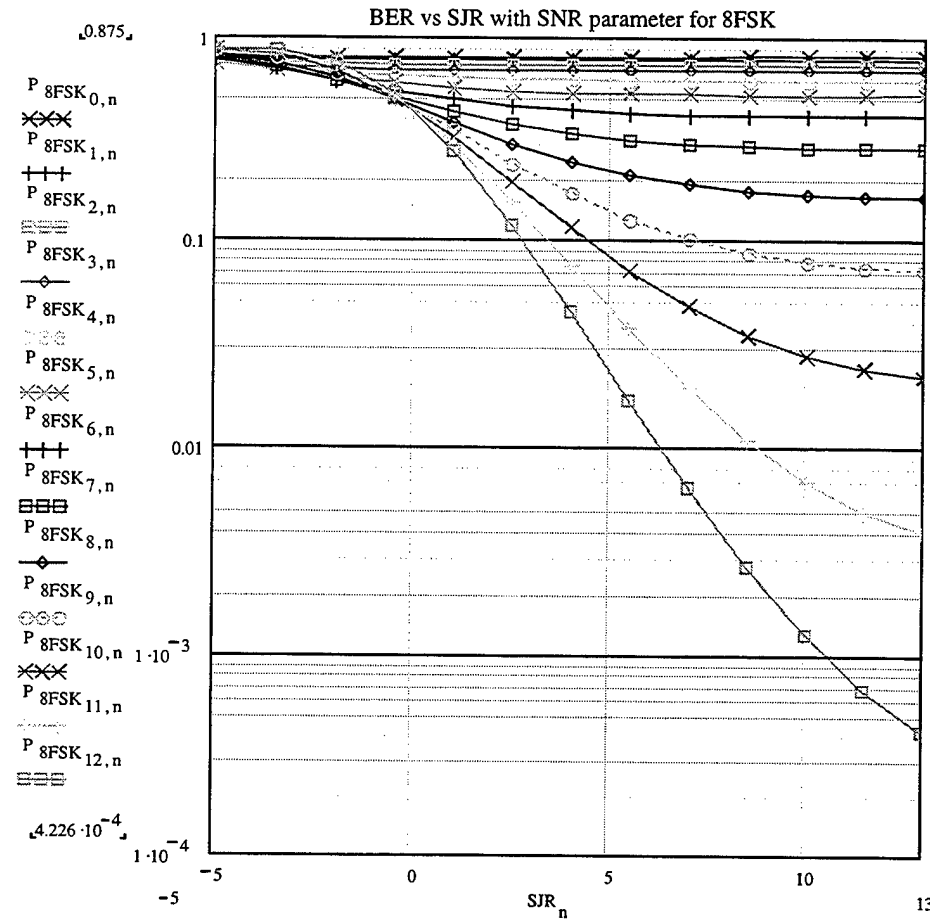
Figure 64. Theoretical symbol error probability versus SJR with SNR as a parameter for non-coherent 8FSK.

If the interference power is smaller than the signal power (SJR>0), then performance is dominated by SNR and the curves are much steeper for higher values of SNR. For a low value of SJR (SJR<0) (that is, if the interfering power is larger than the signal power), the symbol error probability tends to a high constant value. This is expected, since statistically, almost half of the interference symbols will be opposite to the signal symbols and will be selected by the receiver due to their larger power. In Figure 65, the simulation results are presented.

100
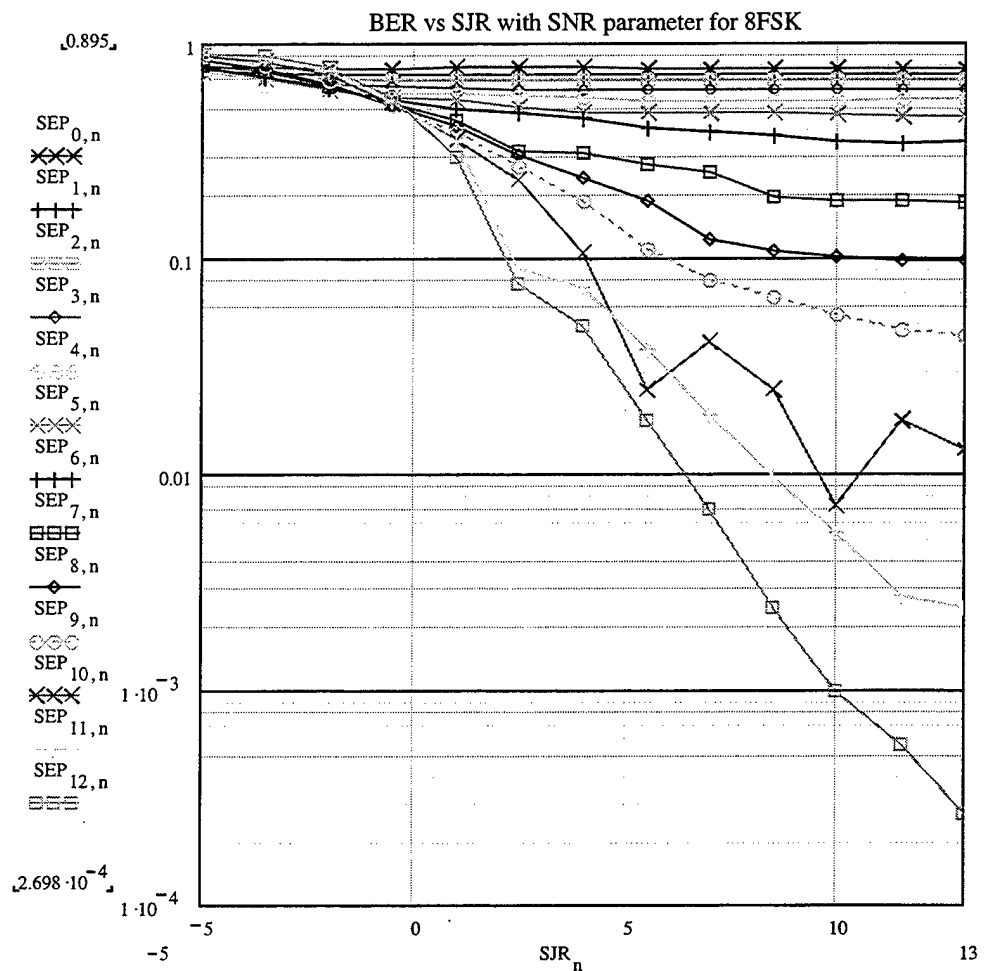
Figure 65. Simulation symbol error probability versus SJR with SNR as parameter for non-coherent 8FSK.

The relative difference (in percent) between the theory and the simulation is presented in Table 23. In Figure 66, the average difference for each curve is plotted versus SNR and SJR for each set of the 13 previously presented curves.
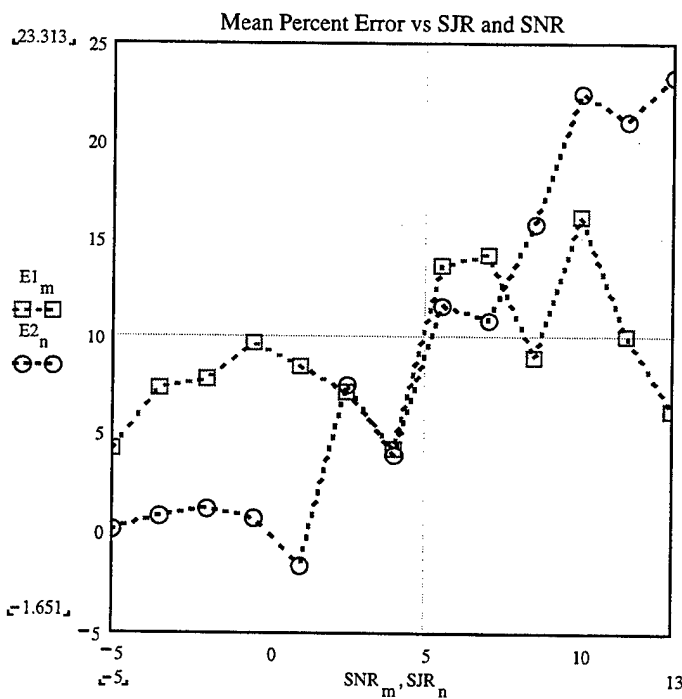
Figure 66. Mean percent difference as a function of SNR and SJR.

The two curves show how the mean difference varies with SNR and SJR. Each value of the mean difference is the average of the differences that correspond to the 13 points on each of the 13 curves for the symbol error probability as a function of SNR (with SJR as parameter) and SJR (with SNR as parameter), respectively.

	SYMBOL ERROR PROBABILITY	NON-COHERENT 8FSK
1.	Root Mean Square Difference (%)	16.868
2.	Average Mean Difference (%)	9.045
3.	Maximum Difference (%)	73.764
4.	Minimum Difference (%)	-18.69
5.	Difference Deviation (%)	14.238

Table 23. Summary of the accuracy of the simulation for non-coherent 8FSK.

Observing the results for coherent and non-coherent detection of 2, 4, and 8FSK, we note that the simulation underestimates the theory for non-coherent detection and overestimates the theory for coherent detection. The difference in percent for non-coherent detection is much greater than the difference for the coherent detection. The average results for both coherent and non-coherent detection of 2, 4, and 8FSK are presented in Table 24.

	SYMBOL ERROR PROBABILITY	AVERAGE RESULTS FOR COHERENT 2, 4, AND 8FSK	AVERAGE RESULTS FOR NON-COHERENT 2, 4, AND 8FSK
1.	Root Mean Square Difference (%)	9.38	18.33
2.	Average Mean Difference (%)	-3.77	12.207
3.	Maximum Difference (%)	25.971	55.024
4.	Minimum Difference (%)	-25.347	-13.65
5.	Difference Deviation (%)	8.42	13.487

Table 24. Average results for coherent and non-coherent detection of 2, 4, and 8FSK.

V. MFSK SIGNAL CORRUPTED BY AWGN AND CO-CHANNEL INTERFERENCE IN A FADING CHANNEL THAT AFFECTS ONLY THE DESIRABLE SIGNAL

In this chapter we derive the theoretical symbol error probability for MFSK signals affected by AWGN and co-channel interference and operating in a fading channel. The co-channel interference is represented by an additive interfering MFSK signal. We study cases of coherent and non-coherent detection for 2FSK, 4FSK, and 8FSK assuming that the fading channel affects only the desirable MFSK signal and not the interfering one. Two separate cases of channel fading are examined: the frequency-nonselective, slowly fading Rayleigh channel and the frequency-nonselective, slowly fading Rician channel.

A. RAYLEIGH FADING CHANNEL – COHERENT DETECTION

In this section, we derive the probability of symbol error for MFSK signals transmitted over a frequency-nonselective, slowly fading Rayleigh channel in the presence of AWGN and co-channel interference. The frequency-nonselective, slowly fading channel results in multiplicative distortion of the MFSK signal. The condition that the channel fades slowly implies that the multiplicative process may be considered as a constant during at least one symbol interval. Furthermore, we assume that the channel fading is sufficiently slow such that the phase shift introduced by the channel can be estimated from the received signal without error.

105

1. Theoretical Probability Of Symbol Error For Coherent Detection

The probability that an MFSK symbol will be received correctly is equal to the probability that:

- **1st case**: the signal and the interference symbols are the same and that the noise in any of the remaining M-1 branches does not exceed the sum of signal and interference symbols, and

- **2nd case**: the signal and the interference symbols are different and neither the sum of the interference and noise nor the noise in any of the remaining M-2 branches exceeds the signal.

a) The Signal And The Interference Symbols Are On The Same Branch

The conditional probability of symbol error for coherent, orthogonal MFSK signal when AWGN and co-channel interference is present, is:

$$P1(r) = 1 - \frac{1}{\sqrt{2 \cdot \pi}} \cdot \int_{-\infty}^{\infty} e^{\frac{-x^2}{2}} \cdot \left(1 - Q\left(x + \frac{r+J}{\sigma}\right)\right)^{M-1} dx \qquad (5.1)$$

where:

J is the amplitude of the interfering MFSK signal and

r is the amplitude of the desired MFSK signal.

The symbol error probability is conditioned on the amplitude r of the desired signal since the channel is modeled as a Rayleigh fading channel. The amplitude r is modeled as Rayleigh random variable with the probability density function:

106

$$f(r) = \frac{r}{P_{sig}} \cdot e^{\frac{-r^2}{2 \cdot P_{sig}}} \quad \text{for } r \geq 0 \quad \textbf{and} \quad f(r) = 0 \quad \text{for } r < 0 \tag{5.2}$$

where

P_{sig} is the average symbol power of the fading MFSK signal.

Integrating the product of the conditional probability of symbol error and the probability density function of the information signal's amplitude r over all possible values of r, we obtain the unconditional probability of symbol error for this case:

$$P1 = 1 - \frac{1}{\sqrt{2 \cdot \pi}} \cdot \int_0^\infty \int_{-\infty}^\infty e^{\frac{-x^2}{2}} \cdot \left(1 - Q\left(x + \frac{r+J}{\sqrt{P_{noise}}}\right)\right)^{M-1} \frac{r}{P_{sig}} \cdot e^{\frac{-r^2}{2 \cdot P_{sig}}} \, dx \, dr \tag{5.3}$$

Using the transformation

$$\frac{r}{\sqrt{P_{sig}}} = y \quad \text{and} \quad dr = \sqrt{P_{sig}} \cdot dy \tag{5.4}$$

we obtain:

$$P1 = 1 - \frac{1}{\sqrt{2 \cdot \pi}} \cdot \int_0^\infty \int_{-\infty}^\infty e^{\frac{-\left(x^2 + y^2\right)}{2}} \cdot \left(1 - Q\left(x + y \cdot \frac{\sqrt{P_{sig}}}{\sqrt{P_{noise}}} + \frac{J}{\sqrt{P_{noise}}}\right)\right)^{M-1} \cdot y \, dx \, dy \tag{5.5}$$

The double integral in equation (5.5) has to be evaluated numerically.

107

b)   The Signal And The Interference Symbols Are On Different Branches

The conditional probability of symbol error for this case has already been obtained in equation (4.14). This is given by:

$$P2(r)=1-\frac{1}{\sqrt{2\cdot\pi}}\cdot\int_{-\infty}^{\infty}e^{\frac{-x^2}{2}}\cdot\left(1-Q\left(x+\frac{r}{\sqrt{P_{noise}}}\right)\right)^{M-2}\cdot\left(1-Q\left(x+\frac{r-J}{\sqrt{P_{noise}}}\right)\right)dx \qquad (5.6)$$

Integrating the product of the conditional probability of symbol error and the probability density function of the information signal's amplitude r over all possible values of r, we get the unconditional probability of symbol error for the second case in the receiver:

$$P2=1-\int_{0}^{\infty}\int_{-\infty}^{\infty}\frac{1}{\sqrt{2\cdot\pi}}\cdot\left(1-Q\left(x+\frac{r}{\sqrt{P_{noise}}}\right)\right)^{M-2}\cdot\left(1-Q\left(x+\frac{r-J}{\sqrt{P_{noise}}}\right)\right)\cdot e^{\frac{-x^2}{2}}\cdot\frac{r}{P_{sig}}\cdot e^{\frac{-r^2}{2\cdot P_{sig}}}dxdr \qquad (5.7)$$

Using again the transformation of (5.4), we obtain

$$P2=1-\frac{1}{\sqrt{2\cdot\pi}}\cdot\int_{0}^{\infty}\int_{-\infty}^{\infty}e^{\frac{-(x^2+y^2)}{2}}\cdot\left(1-Q\left(x+y\frac{\sqrt{P_{sig}}}{\sqrt{P_{noise}}}\right)\right)^{M-2}\cdot\left(1-Q\left(x+y\frac{\sqrt{P_{sig}}}{\sqrt{P_{noise}}}-\frac{J}{\sqrt{P_{noise}}}\right)\right)\cdot ydxdy \qquad (5.8)$$

c)   Total Symbol Error Probability

The total symbol error probability, combining the two cases, is given by:

$$P_{total}=\frac{1}{M}\cdot P1+\frac{M-1}{M}\cdot P2 \qquad (5.9)$$

where 1/M is the probability that the transmitted and the interfering symbols are on the same branch and (M-1)/M is the probability that the transmitted and the interfering symbols are on different branches.

2.   Simulink Model and Block Analysis

The schematic diagram of the Simulink model, which has been developed for the simulation of coherent MFSK signaling affected by AWGN and co-channel interference in a Rayleigh fading channel, is shown in Figure 67.
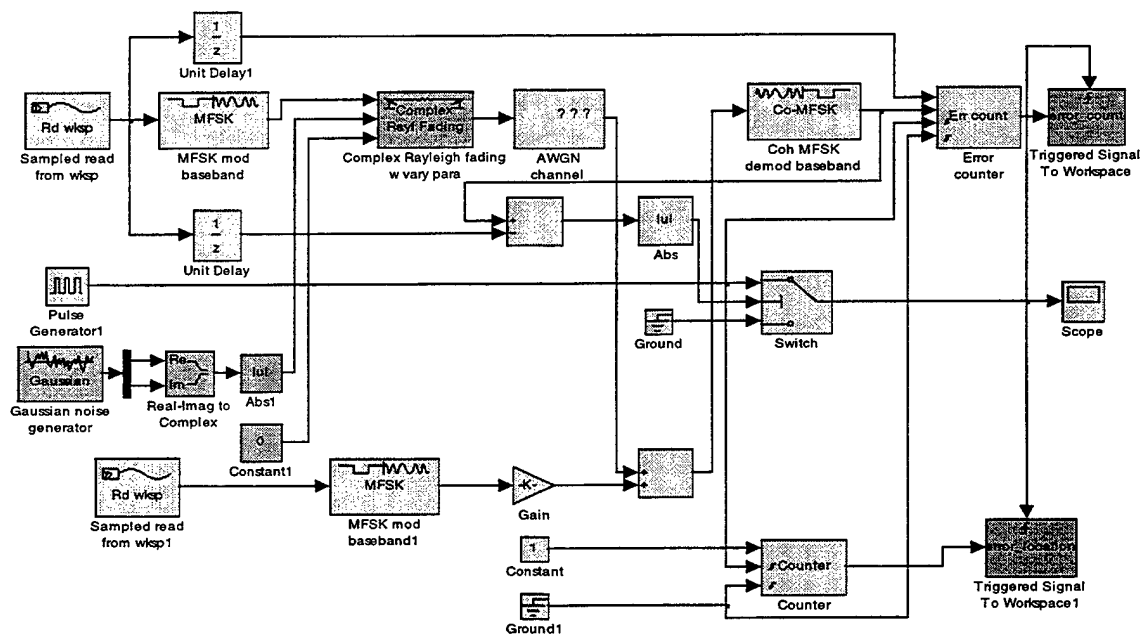

Figure 67. Model for coherent MFSK with co-channel interference in a Rayleigh fading channel.

This model is a combination of the model that was used for the coherent MFSK signal in a Rayleigh fading channel and the model that was used for coherent MFSK

signal affected by co-channel interference. These models have already been described in Chapter III.A.2 and in [Ref 1].

3. Simulation Analysis And Performance Verification

In this section, simulation results are presented in order to verify the performance of coherent detection of MFSK in a Rayleigh fading channel corrupted by AWGN and co-channel interference ("jamming"). Each simulation ran until at least 100 errors were observed. The data sequences were limited to 10^6 symbols for each simulation in order to prevent "out of memory" errors. The data sequence was repeated until a sufficient number of errors were counted.

a) Results For 2FSK

Using the relationships

$$\frac{P_{sig}}{P_{noise}} = 10^{\frac{SNR_{ave}}{10}} \quad \text{and} \quad \frac{J^2}{2 \cdot P_{noise}} = \frac{P_{interference}}{P_{noise}} = 10^{\frac{SNR_{ave} - SJR}{10}} \tag{5.10}$$

we can express the symbol error probability in terms of SNR and SJR. Evaluating and plotting the theoretical and simulation results versus SNR and SJR, as well as the difference (error) between them, we can compare the theory and the simulation.

The theoretical and the simulation symbol error probabilities for coherently detected 2FSK are presented in Figures 68 and 69, respectively, as functions of the average signal-to-noise ratio in dB with the signal-to-interference ratio as a parameter. The values for SNR and SJR are chosen from −5 dB to +30 dB in increments of 2.5 dB.

110
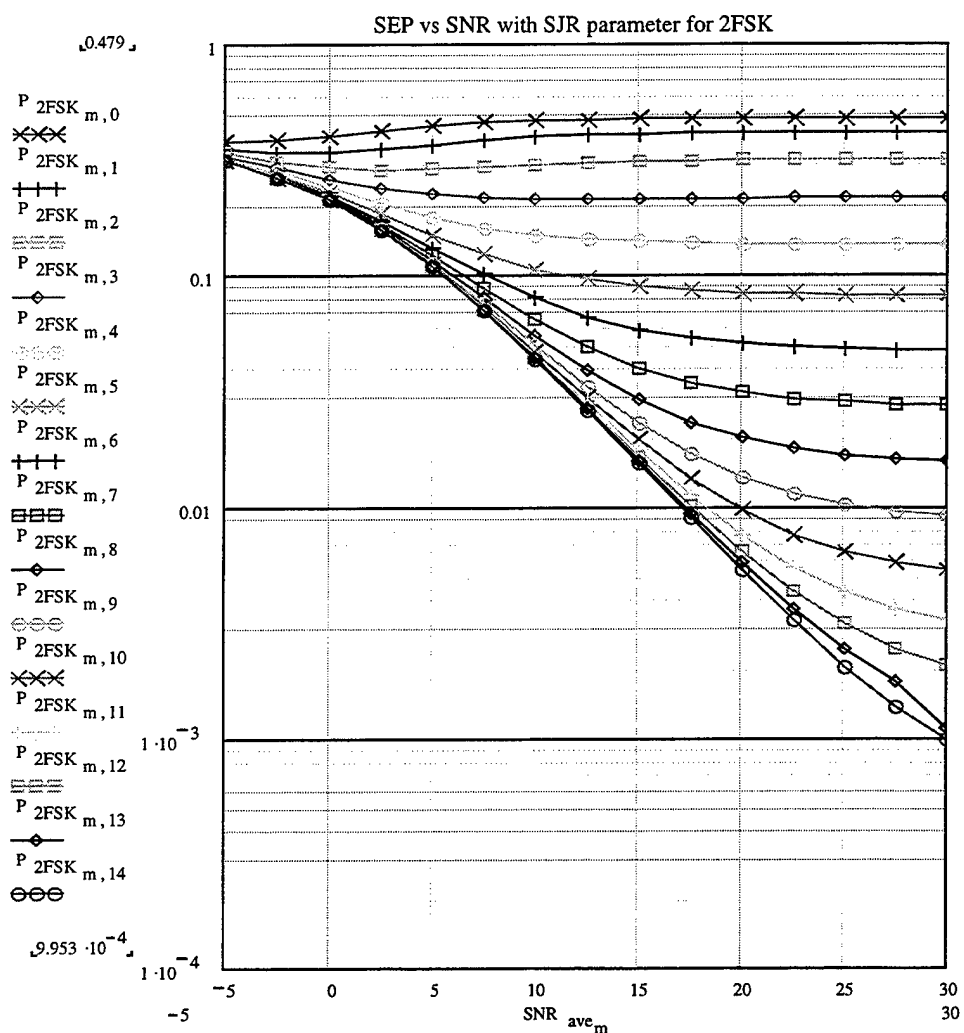
Figure 68. Theoretical symbol error probability versus SNR with SJR as a parameter

for coherent 2FSK with Rayleigh fading.

As is evident from Figure 68 and 69, the curves tend to become flat as

SNR increases; that is, they converge to a constant value determined by the value of SJR.

The consequence of signal fading is that the symbol error probability does not decrease as

fast with the increase in either SNR (along a curve) or SJR (from curve to curve) as it

does for the case of non-fading signals.

111
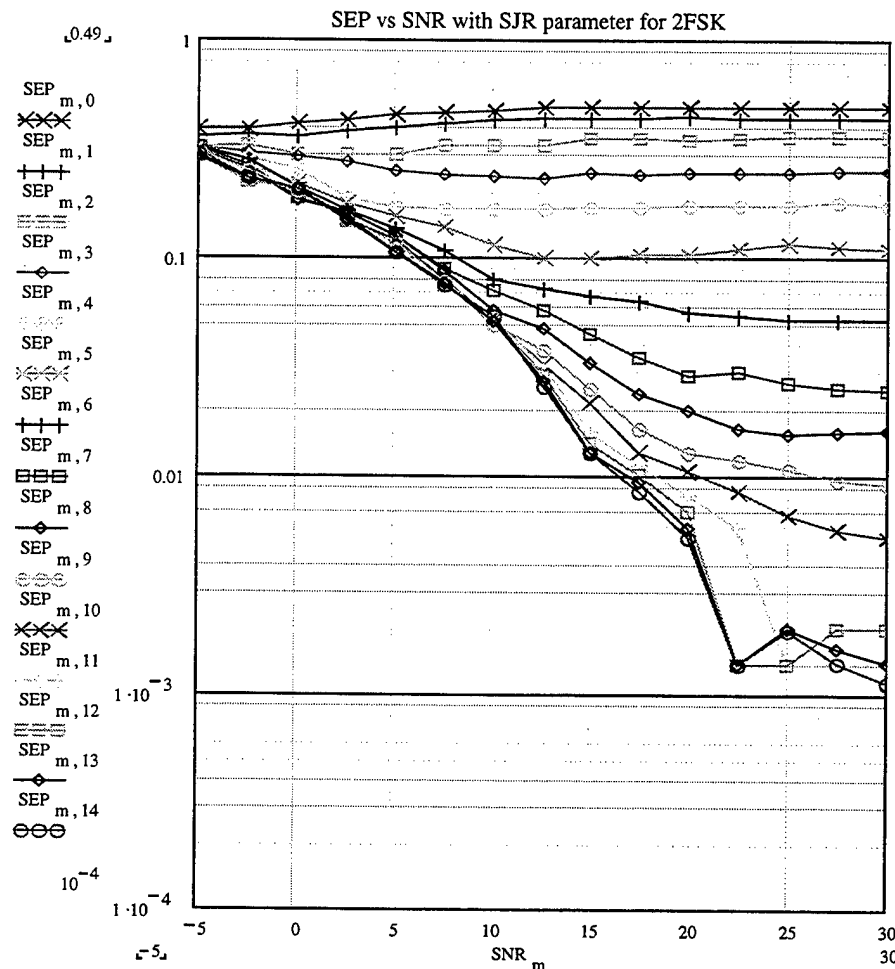
Figure 69. Simulation symbol error probability versus SNR with SJR as a parameter

for coherent 2FSK with Rayleigh fading.

In Figure 70 and 71, respectively, the theoretical and simulation results are

shown as functions of SJR with SNR as a parameter. As the SJR increases, the symbol

error probability initially decreases, but then tends to a constant value determined by the

value of the SNR. As the SNR increases, this constant value decreases, but not fast as for

the case of a non-fading channel.

112

SEP vs SJR with SNR parameter for 2FSK

Legend (left side):

$P_{2FSK_{0,n}}$
$P_{2FSK_{1,n}}$
$P_{2FSK_{2,n}}$
$P_{2FSK_{3,n}}$
$P_{2FSK_{4,n}}$
$P_{2FSK_{5,n}}$
$P_{2FSK_{6,n}}$
$P_{2FSK_{7,n}}$
$P_{2FSK_{8,n}}$
$P_{2FSK_{9,n}}$
$P_{2FSK_{10,n}}$
$P_{2FSK_{11,n}}$
$P_{2FSK_{12,n}}$
$P_{2FSK_{13,n}}$
$P_{2FSK_{14,n}}$

x-axis: SJR_n
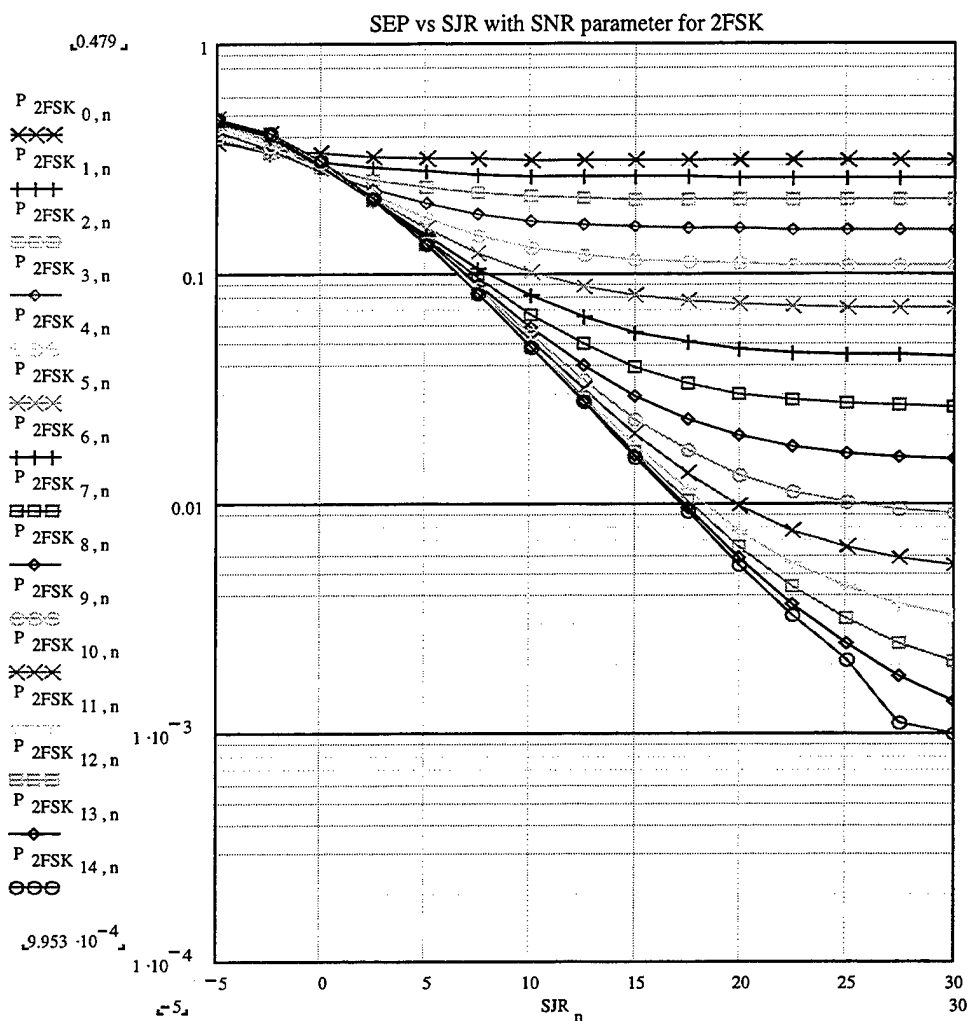
Figure 70. Theoretical symbol error probability versus SJR with SNR as a parameter for coherent 2FSK with Rayleigh fading.

We again note the dramatic increase in the symbol error probability due to Rayleigh fading and co-channel interference.
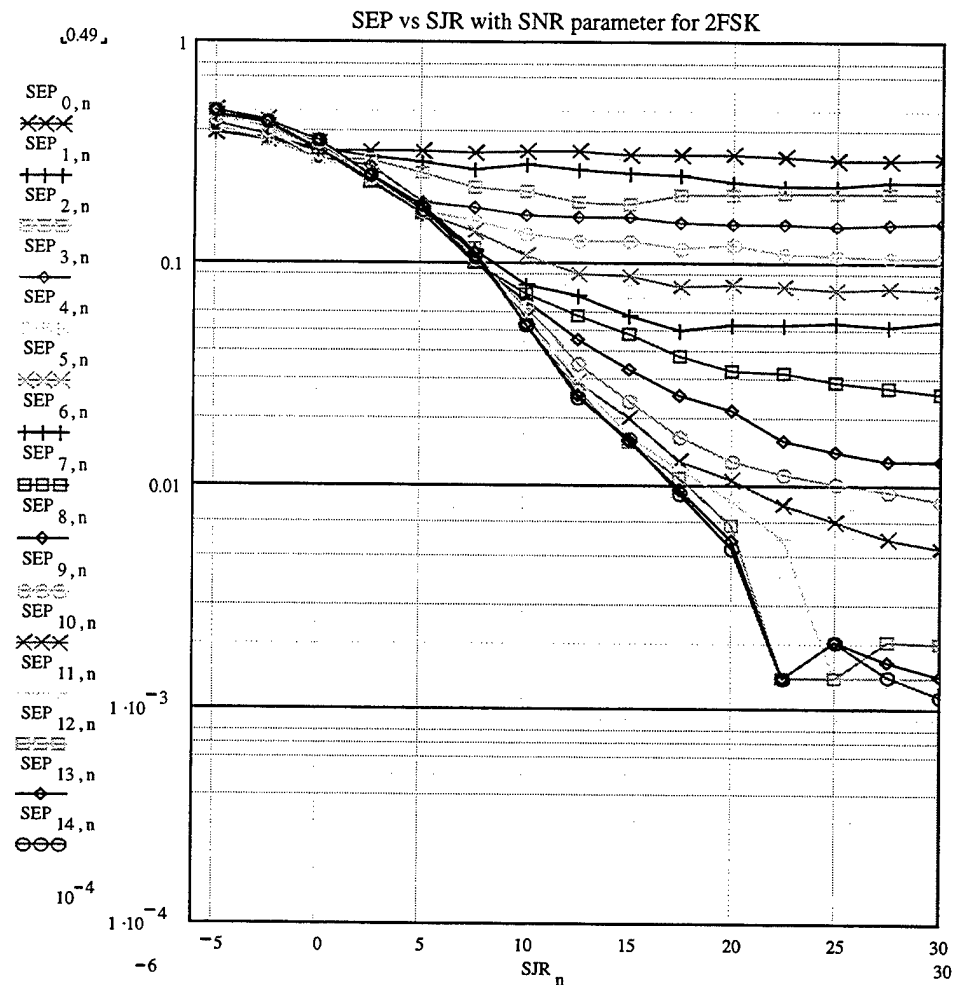
Figure 71. Simulation symbol error probability versus SJR with SNR as a parameter for coherent 2FSK with Rayleigh fading.

The relative difference (in percent) between the theoretical and simulation results is presented in Table 25. In Figure 72, the average difference for each curve is plotted versus SNR and SJR for each set of the 15 previously presented curves.

114
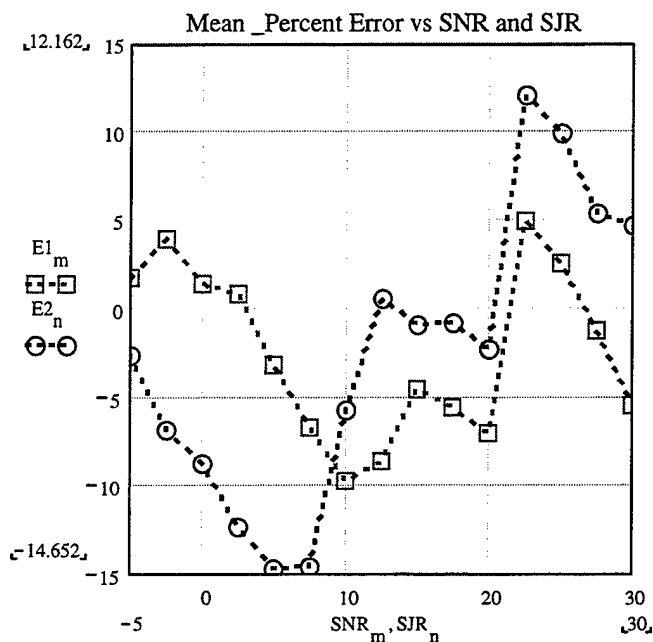
Figure 72. Mean percent difference as a function of SNR and SJR, respectively.

The two curves show how the mean difference varies with SNR and SJR. Each value of the mean difference is the average of the differences that correspond to the 15 points on each of the 15 curves for the symbol error probability as a function of SNR (with SJR as parameter) and SJR (with SNR as parameter).

	SYMBOL ERROR PROBABILITY	COHERENT 2FSK
1.	Root Mean Square Difference (%)	15.488
2.	Average Mean Difference (%)	-2.359
3.	Maximum Difference (%)	68.109
4.	Minimum Difference (%)	-42.116
5.	Difference Deviation (%)	15.307

Table 25. Summary of the accuracy of the simulation for coherent 2FSK.

115

b)   Results For 4FSK

The theoretical and the simulation symbol error probabilities for coherently detected 4FSK are presented in Figures 73 and 74, as functions of the average SNR in dB with SJR as a parameter. The values for the signal-to-noise and signal-to-interference ratios are between −5 dB and +30 dB, where the lower curve corresponds to SJR=+30 dB and the remaining curves are in increments of 2.5 dB.
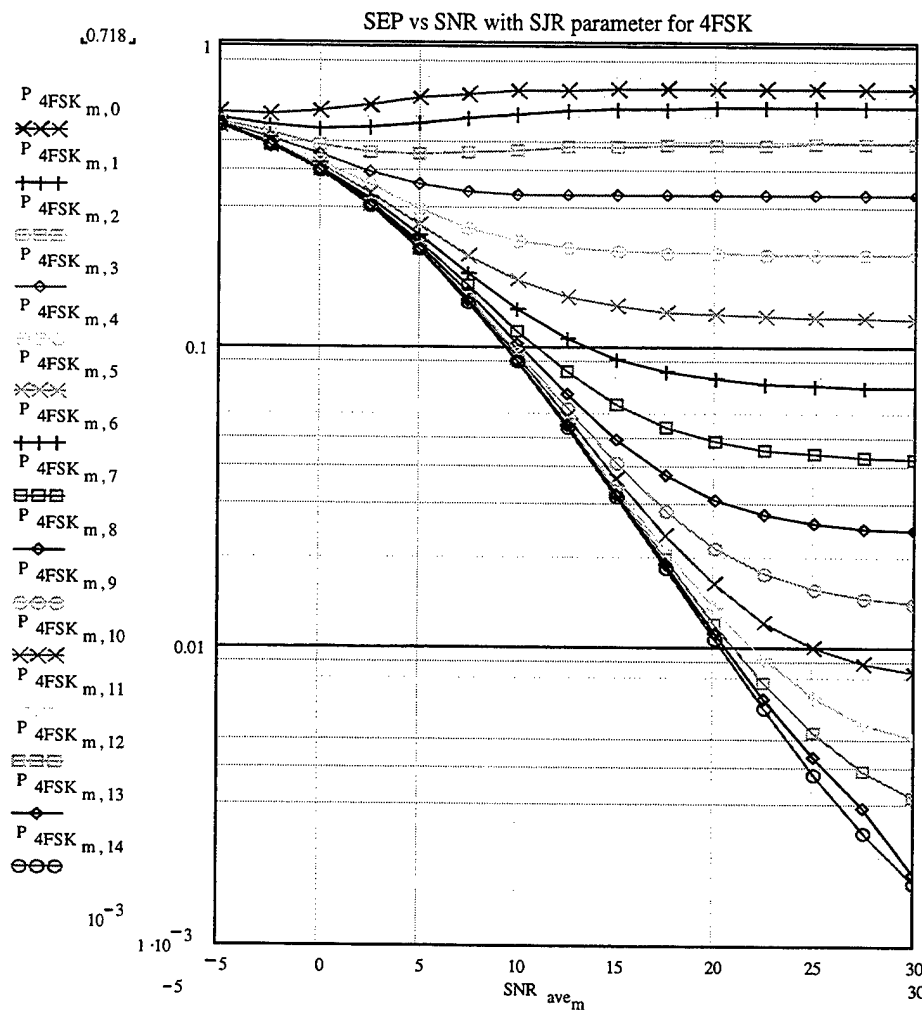

Figure 73. Theoretical symbol error probability versus SNR with SJR as a parameter for coherent 4FSK with Rayleigh fading.
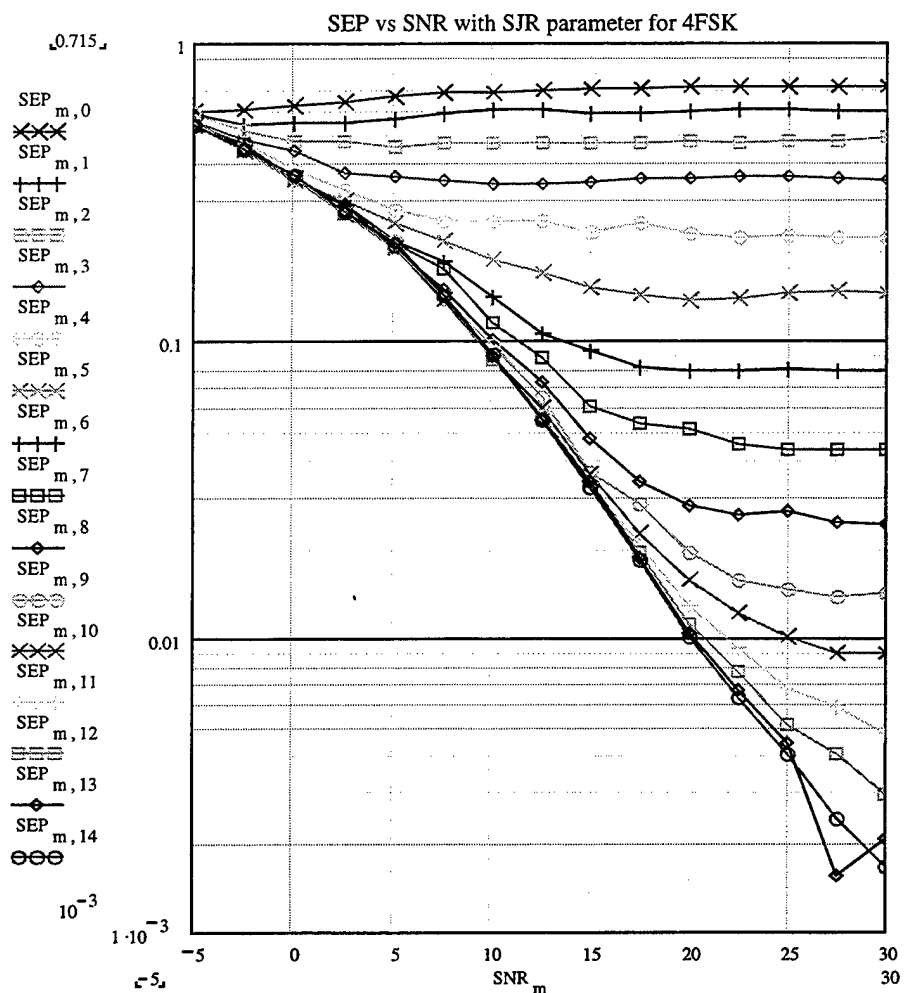
Figure 74. Simulation symbol error probability versus SNR with SJR as a parameter for coherent 4FSK with Rayleigh fading.

In Figure 75 and 76, respectively, the theoretical and simulation probabilities of symbol error are shown as functions of SJR with SNR as a parameter. The observation derived from all the graphs is that in order to achieve acceptable values for the symbol error probability for a Rayleigh fading channel (10^{-4}), SNR and SJR must be over +30 dB.
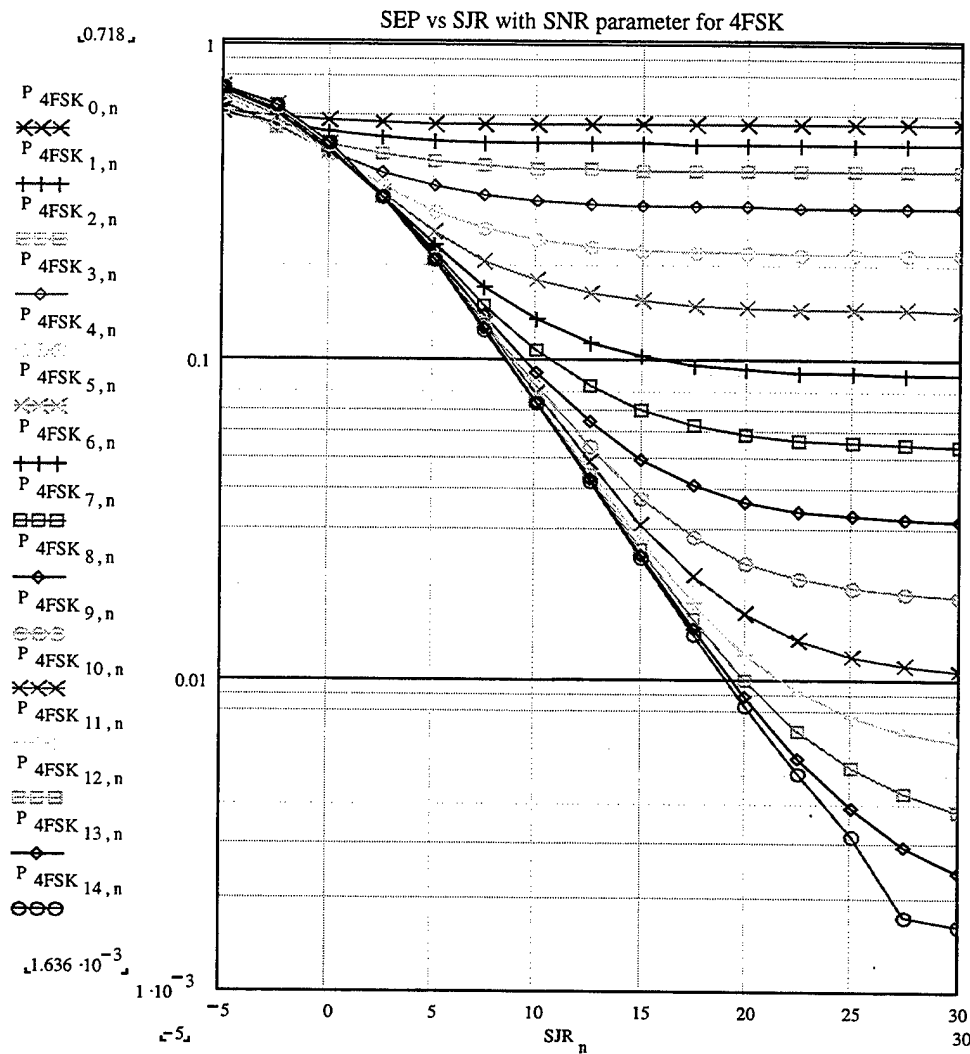
Figure 75. Theoretical symbol error probability versus SJR with SNR as a parameter for coherent 4FSK with Rayleigh fading.

The dramatic increase in the symbol error probability is due to the Rayleigh fading channel that allows low values of signal power to occur (following the Rayleigh distribution) and thus increase the number of symbol errors.

118
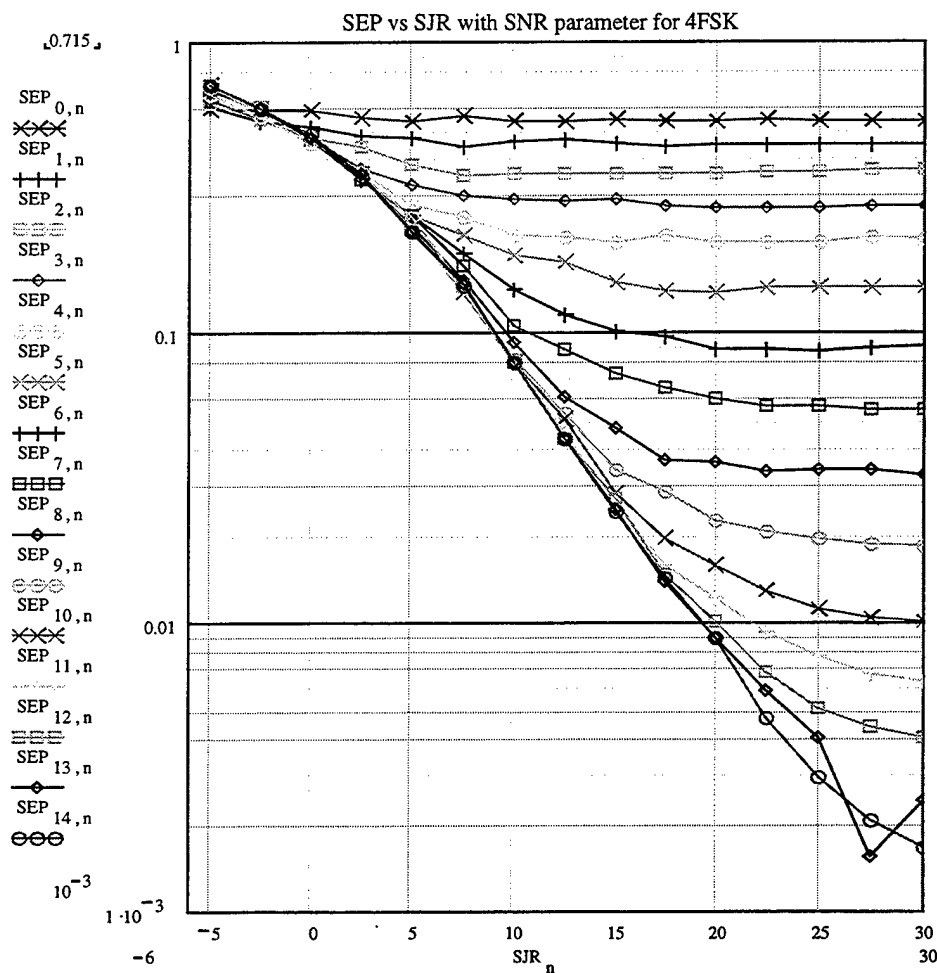
Figure 76. Simulation symbol error probability versus SJR with SNR as a parameter for coherent 4FSK with Rayleigh fading.

The relative difference (in percent) between theoretical and simulation results is presented in Table 26. In Figure 77, the average difference for each curve is plotted versus SNR and SJR for each of the 15 previously presented curves.
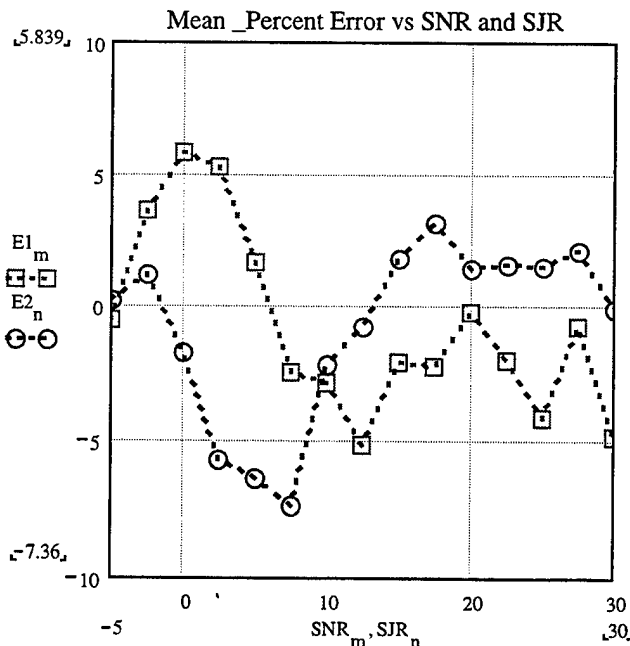
Figure 77. Mean percent difference as a function of SNR and SJR.

The two curves show how the mean difference varies with SNR and SJR. Each value of the mean difference is the average of the differences that correspond to the 15 points on each of the 15 curves for the symbol error probability as a function of SNR (with SJR as parameter) and SJR (with SNR as parameter).

	SYMBOL ERROR PROBABILITY	COHERENT 4FSK
1.	Root Mean Square Difference (%)	7.078
2.	Average Mean Difference (%)	-0.74
3.	Maximum Difference (%)	45.903
4.	Minimum Difference (%)	-20.812
5.	Difference Deviation (%)	7.039

Table 26. Summary of the accuracy of the simulation for coherent 4FSK.

120

c) Results For 8FSK

The theoretical and the simulation symbol error probabilities for coherently detected 8FSK are presented in Figures 78 and 79, respectively, as functions of the average SNR in dB with SJR as a parameter. The values for the signal-to-noise and signal-to-interference ratios are between –5 dB and +30 dB, where the lower curve corresponds to SJR=+30 dB and the remaining curves are in increments of 2.5 dB.
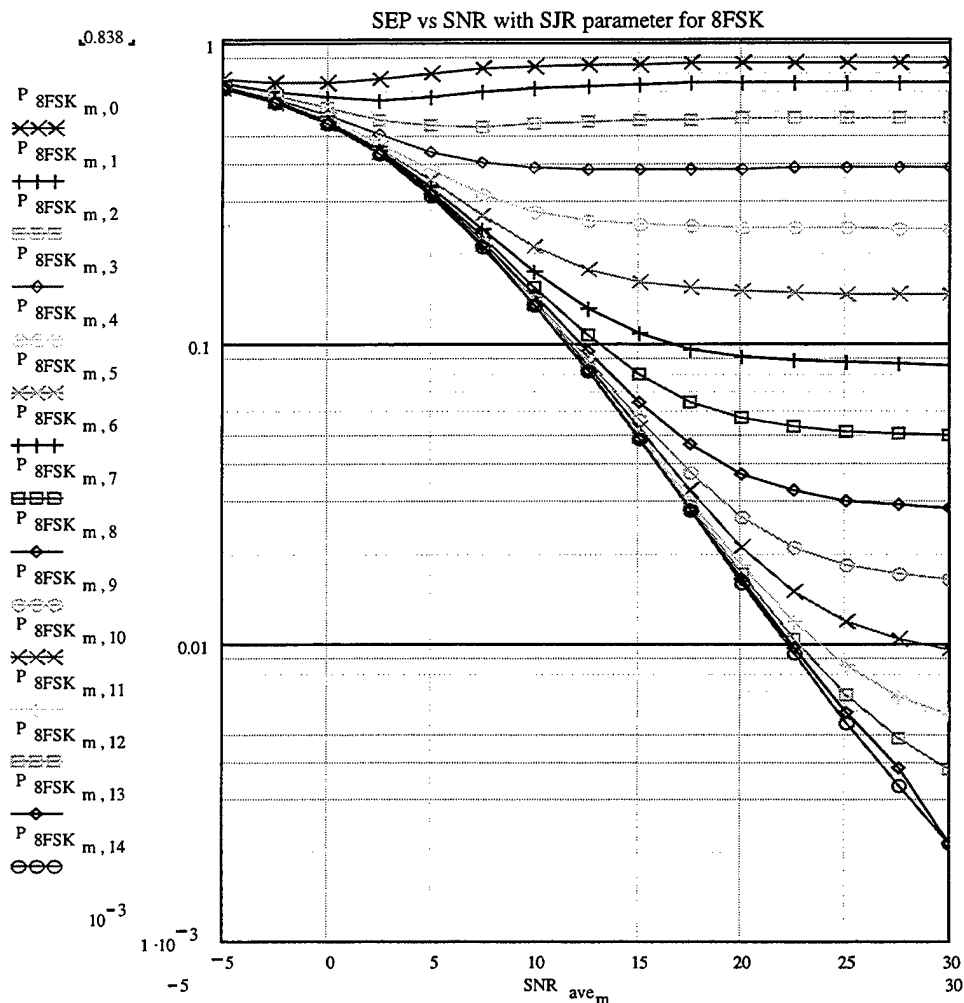

Figure 78. Theoretical symbol error probability versus SNR with SJR as a parameter for coherent 8FSK with Rayleigh fading.
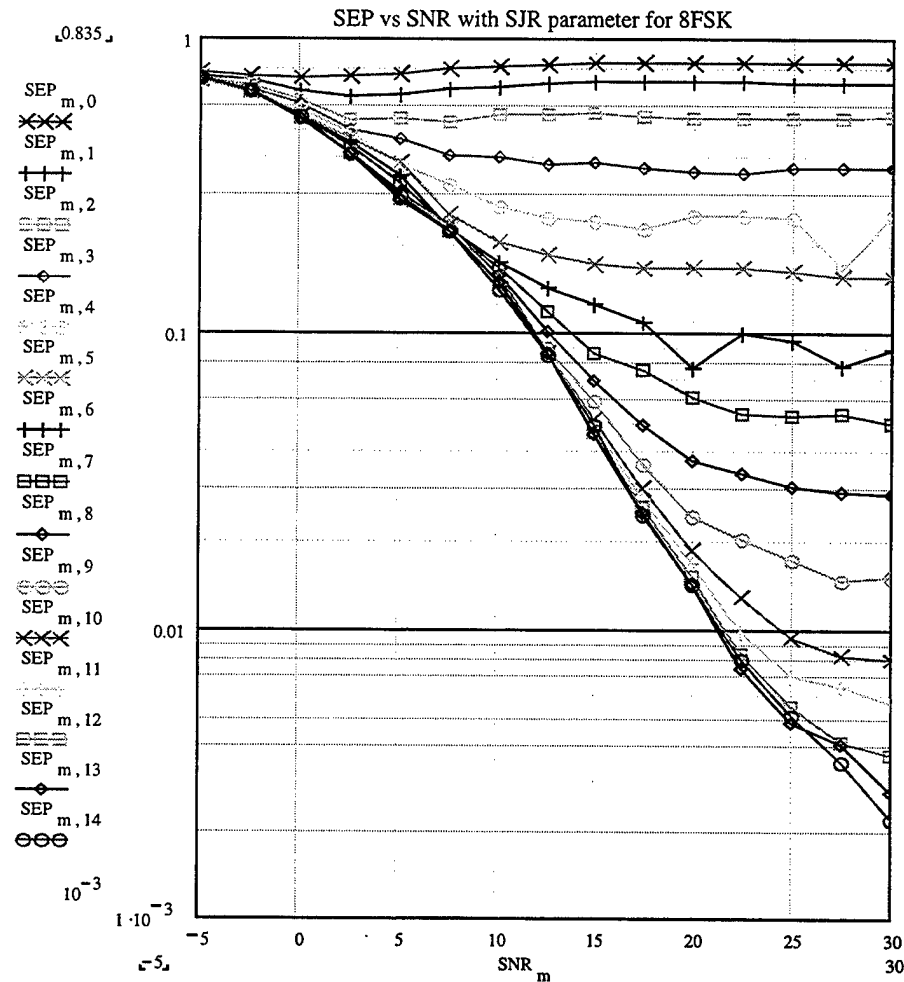
Figure 79. Simulation symbol error probability versus SNR with SJR as a parameter for coherent 8FSK with Rayleigh fading.

In Figures 81 and 82, respectively, the theoretical and simulation symbol error probability is shown as a function of SJR with SNR as a parameter. Again we observe that in order to achieve acceptable values for the symbol error probability, the SNR and SJR must be over +30 dB.

122
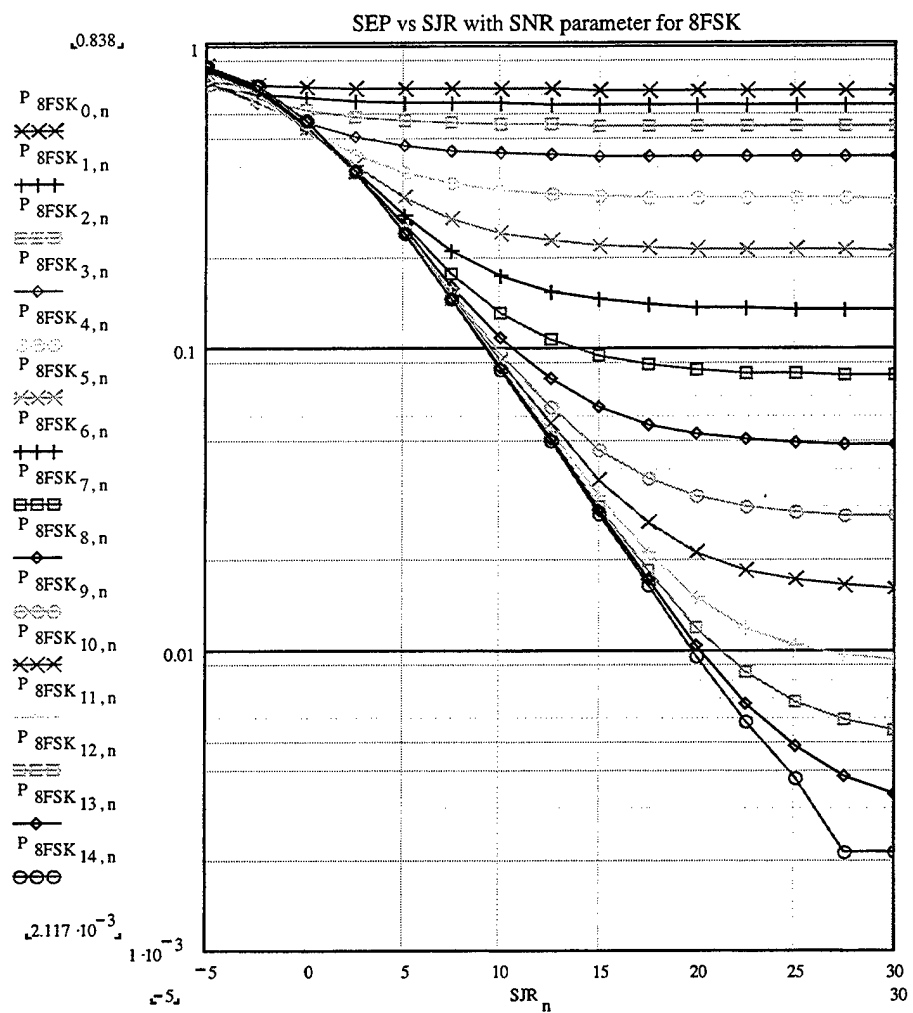
Figure 80. Theoretical symbol error probability versus SJR with SNR as a parameter

for coherent 8FSK with Rayleigh fading.

The dramatic increase in the symbol error probability is due to the

Rayleigh fading channel, as it was observed for the cases of 2FSK and 4FSK.
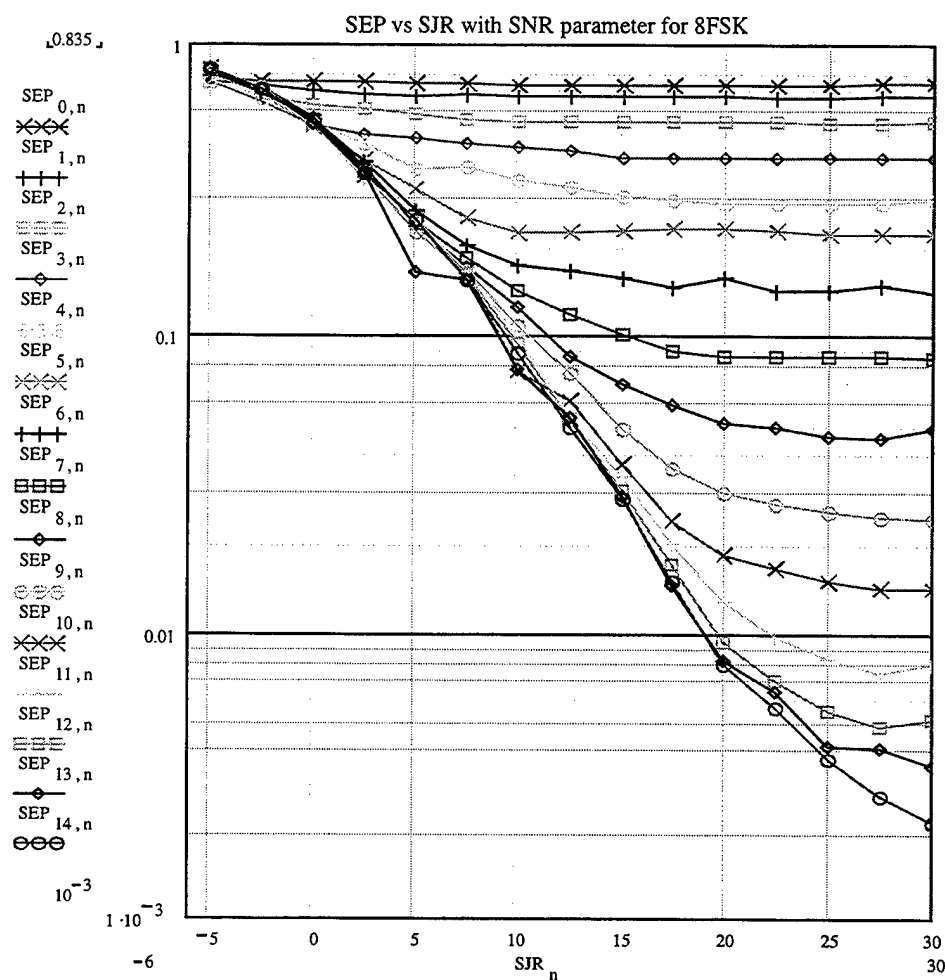
Figure 81. Simulation symbol error probability versus SJR with SNR as a parameter

for coherent 8FSK with Rayleigh fading.

The relative difference (percent "error") between the theoretical and the

simulation results is shown in Table 27. In Figure 82, the average difference for each

curve is plotted versus SNR and SJR for each of the 15 previously presented curves.

124
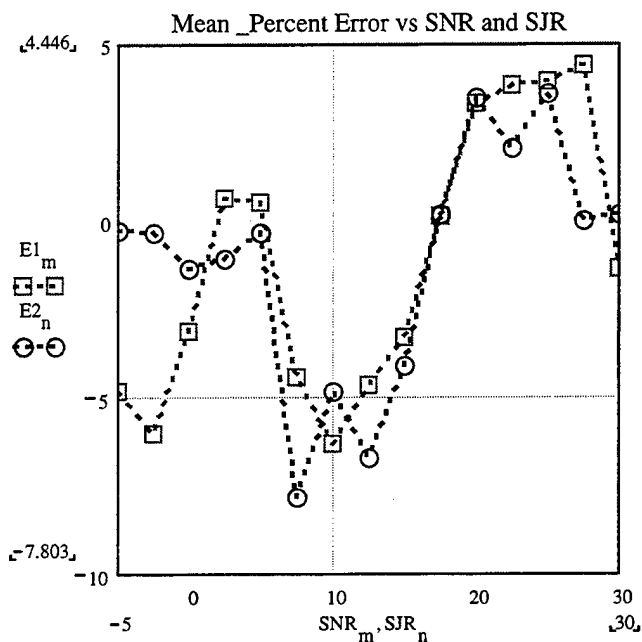
Figure 82. Mean percent difference as a function of SNR and SJR.

The two curves show how the mean difference varies with SNR and SJR. Each value of the mean difference is the average of the differences that correspond to the 15 points on each of the 15 curves for the symbol error probability as a function of SNR (with SJR as parameter) and SJR (with SNR as parameter), respectively.

	SYMBOL ERROR PROBABILITY	COHERENT 8FSK
1.	Root Mean Square Difference (%)	7.98
2.	Average Mean Difference (%)	-1.098
3.	Maximum Difference (%)	30.214
4.	Minimum Difference (%)	-30.273
5.	Difference Deviation (%)	7.904

Table 27. Summary of the accuracy of the simulation for coherent 8FSK.

125

Observing the results for coherent detection of 2, 4, and 8FSK in a Rayleigh fading channel and affected by AWGN and co-channel interference, we note that the simulation overestimates the theory for all of the cases of 2, 4, and 8FSK. The root mean square difference (in percent) is about 10% (in average) and the mean percent difference for all the cases is less than 10% (in absolute value), which suggests good accuracy.

The average results for the coherent detection of 2, 4, and 8FSK are presented in Table 28.

	SYMBOL ERROR PROBABILITY	AVERAGE RESULTS FOR COHERENT 2, 4, AND 8FSK
1.	Root Mean Square Difference (%)	10.182
2.	Average Mean Difference (%)	-1.399
3.	Maximum Difference (%)	48.075
4.	Minimum Difference (%)	-31.067
5.	Difference Deviation (%)	10.083

Table 28. Average results for the coherent detection of 2, 4, and 8FSK.

B. RAYLEIGH FADING CHANNEL – NON-COHERENT DETECTION

In this section, we derive the symbol error probability for non-coherent detection of MFSK signals transmitted over a frequency nonselective, slowly fading Rayleigh channel in the presence of AWGN and co-channel interference.

1. Theoretical Probability Of Symbol Error For Non-Coherent Detection

The probability that the signal symbol will be received correctly is evaluated, again, separately for the following two cases:

- **1st case**: the signal and the interference symbols are on the same branch.

- **2nd case**: the signal and the interference symbols are on different branches.

Then, combining the two cases, we evaluate the total symbol error probability.

a) The Signal And The Interference Symbols Are On The Same Branch

The conditional probability of symbol error for non-coherent, orthogonal MFSK signal with AWGN and co-channel interference has been already derived in Chapter IV (equation (4.30)):

$$P1_{error}(r) = \sum_{k=1}^{M-1} \frac{(M-1)!}{k! \cdot (M-1-k)!} \cdot (-1)^{k+1} \cdot \frac{1}{k+1} \cdot e^{\frac{-k \cdot (r+J)^2}{2 \cdot (k+1) \cdot \sigma^2}} \qquad (5.11)$$

where:

J is the amplitude of the interfering MFSK signal

r is the amplitude of the desired MFSK signal

The desired signal amplitude r is a Rayleigh random variable with the probability density function:

$$f(r) = \frac{r}{P_{sig}} \cdot e^{\frac{-r^2}{2 \cdot P_{sig}}} \quad \text{for} \quad r \geq 0 \quad \textbf{and} \quad f(r) = 0 \quad \text{for} \quad r < 0 \qquad (5.12)$$

where:

P_{sig} is the symbol power of the fading desired signal.

Integrating the product of the conditional probability of symbol error and the probability density function of the desired signal's amplitude r over all possible values of r, we obtain the unconditional probability of symbol error:

$$P1 = \int_0^\infty \sum_{k=1}^{M-1} \frac{(M-1)!}{k! \cdot (M-1-k)!} \cdot (-1)^{k+1} \cdot \frac{1}{k+1} \cdot e^{\frac{-k \cdot (r+J)^2}{2 \cdot (k+1) \cdot P_{noise}}} \cdot \frac{r}{P_{sig}} \cdot e^{\frac{-r^2}{2 \cdot P_{sig}}} \, dr \qquad (5.13)$$

where P_{noise} is the noise power equal to σ^2

Using the transformation:

$$\frac{r}{\sqrt{P_{sig}}} = y \quad \text{and} \quad dr = \sqrt{P_{sig}} \cdot dy \qquad (5.14)$$

we obtain:

128

$$P1 = \int_0^\infty \sum_{k=1}^{M-1} \frac{(M-1)!}{k!\cdot(M-1-k)!}\cdot\frac{(-1)^{k+1}}{k+1}\cdot e^{\frac{-k}{2\cdot(k+1)}\cdot\left(y\cdot\frac{\sqrt{P_{sig}}}{\sqrt{P_{noise}}}+\frac{J}{\sqrt{P_{noise}}}\right)^2}\cdot e^{\frac{-y^2}{2}}\cdot y\ dy \qquad (5.15)$$

The above integral must be evaluated numerically.

b)   The Signal And The Interference Symbols Are On Different Branches

The conditional probability of symbol error for coherent detection of orthogonal MFSK signal with AWGN and interference has already been obtained (equation (4.43)):

$$P2(r) = 1 - \int_0^\infty \left(1-e^{\frac{-x^2}{2}}\right)^{M-2}\cdot\left[1-e^{-\frac{1}{2}\left(x^2+\frac{J^2}{\sigma^2}\right)}\cdot\sum_{p=0}^\infty\left(\frac{J}{\sigma\cdot x}\right)^p\cdot I_p\left(\frac{J\cdot x}{\sigma}\right)\right]\cdot e^{-\frac{1}{2}\left(x^2+\frac{r^2}{\sigma^2}\right)}\cdot I0\left(\frac{r\cdot x}{\sigma}\right)\cdot x\,dx \qquad (5.16)$$

Integrating the product of the conditional probability of symbol error and the probability density function of the desired signal amplitude r over all possible values of r, we get the unconditional probability of symbol error for the second case in the receiver:

$$P2 = 1 - \int_0^\infty\int_0^\infty\left[\left(1-e^{\frac{-x^2}{2}}\right)^{M-2}\cdot\left[1-e^{-\frac{1}{2}\left(x^2+\frac{J^2}{P_{noise}}\right)}\cdot\sum_{p=0}^\infty\left(\frac{J}{\sqrt{P_{noise}}\cdot x}\right)^p\cdot I_p\left(\frac{J\cdot x}{\sqrt{P_{noise}}}\right)\right]\right.$$
$$\left. e^{-\frac{1}{2}\left(x^2+\frac{r^2}{P_{noise}}\right)}\cdot I0\left(\frac{r\cdot x}{\sqrt{P_{noise}}}\right)\cdot\frac{r}{P_{sig}}\cdot e^{\frac{-r^2}{2\cdot P_{sig}}}\cdot x\right]dx\,dr \qquad (5.17)$$

Using again the transformation of (5.14) we obtain:

$$P2 = 1 - \int_0^\infty \int_0^\infty \left[\left[\left[1 - e^{\frac{-1}{2}\cdot\left(x^2 + \frac{J^2}{P_{noise}}\right)} \cdot \sum_{p=0}^\infty \left(\frac{J}{x\cdot\sqrt{P_{noise}}}\right)^p \cdot In\left(p, x\cdot\frac{J}{\sqrt{P_{noise}}}\right) \right] \right] \left(1 - e^{\frac{-x^2}{2}}\right)^{M-2} \cdot e^{\frac{-1}{2}\cdot\left(x^2 + y^2 + y^2\cdot\frac{P_{sig}}{P_{noise}}\right)} \cdot I0\left(\sqrt{\frac{P_{sig}}{P_{noise}}}\cdot x\cdot y\right)\cdot x\cdot y \right] dxdy \quad (5.18)$$

The double integral of equation (5.18) has to be evaluated numerically. The summation that appears inside the integral has to be limited to a finite number, which sometimes causes distortion to the curves that represent the corresponding symbol error probability (c.f., Figures 83, 85, 88, 90, 93 and 95).

c)   Total Symbol Error Probability

The total symbol error probability, combining the two cases, is given by:

$$Pe\_coher = \frac{1}{M}\cdot P1 + \frac{M-1}{M}\cdot P2 \quad (5.19)$$

where 1/M is the probability that the transmitted and the interfering symbols are at the same branch and (M-1)/M is the probability that the transmitted and the interfering symbols are at different branches.

2.   Simulink Model and Block Analysis

The schematic diagram of the Simulink model for the simulation of non-coherent MFSK signal affected by AWGN and co-channel interference in a Rayleigh fading

130

channel is the same as the block diagram shown in Figure 64 for coherent detection. The only exception is that the block 'Coh MFSK demod baseband' has been displaced by the block 'Non-coherent MFSK demod baseband'.

3. Simulation Analysis And Performance Verification

In this section, simulation results are presented in order to verify the performance of MFSK with non-coherent detection of the desired signal corrupted by AWGN and co-channel interference in a Rayleigh fading channel. Each simulation ran until at least 100 errors were observed. The data sequences were limited to 10^6 symbols for each simulation to prevent 'out of memory' errors and the simulation sequence was repeated until a sufficient number of errors were counted.

a) Results For 2FSK

Using the relationships

$$\frac{P_{sig}}{P_{noise}}=10^{\frac{SNR_{ave}}{10}} \qquad \frac{J}{\sqrt{P_{noise}}}=\sqrt{2}\cdot10^{\frac{SNR_{ave}-SJR}{20}} \qquad (5.20)$$

we can express the theoretical symbol error probability in terms of SNR and SJR. The values for the SNR and SJR have been chosen from –5 dB to +16 dB in increments of 1.5 dB.
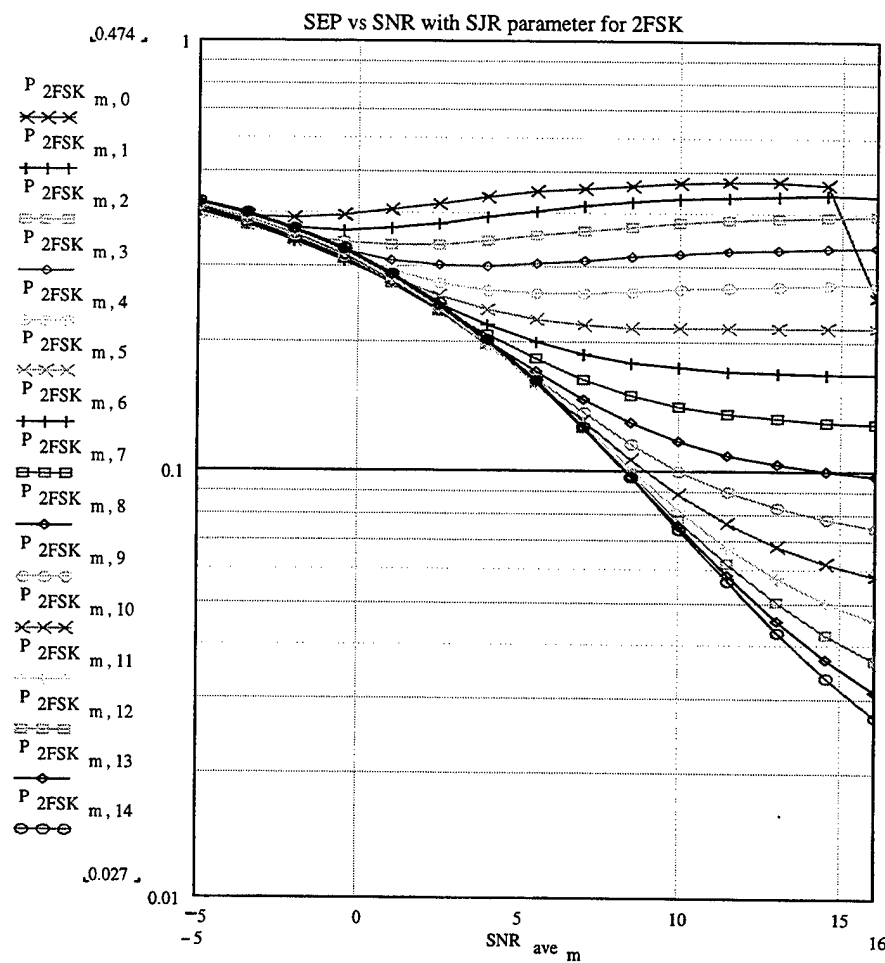
Figure 83. Theoretical symbol error probability versus SNR with SJR as a parameter

for non-coherent 2FSK with Rayleigh fading.
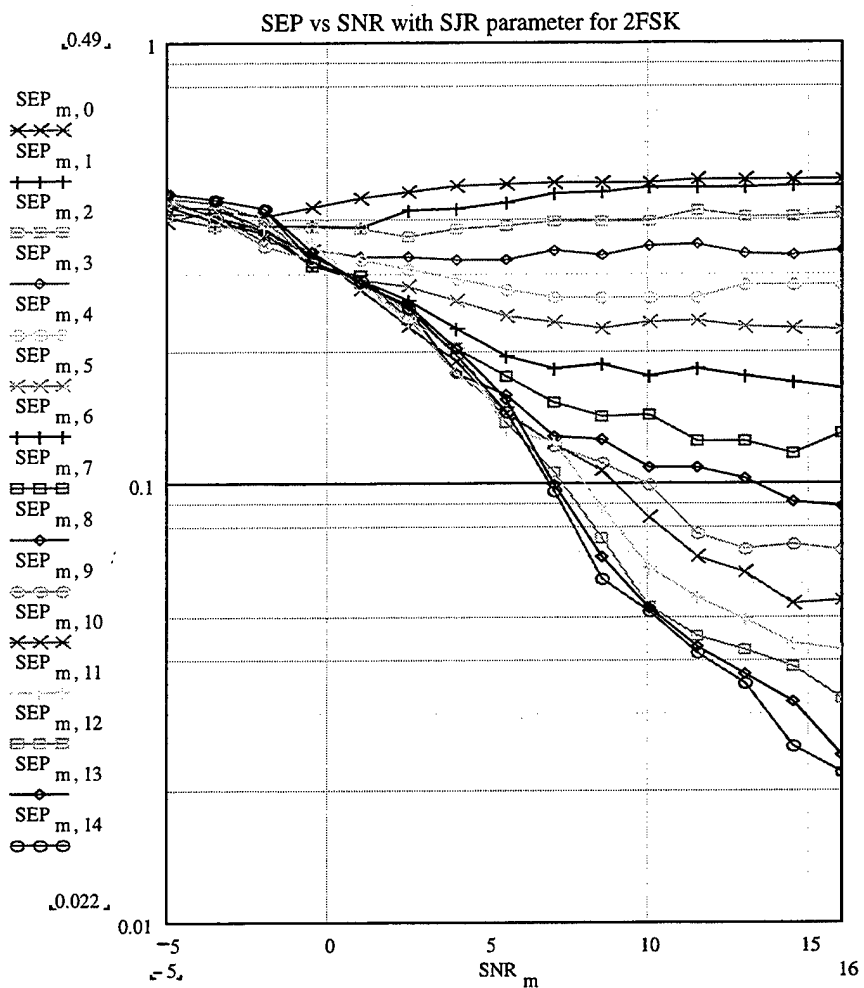
Figure 84. Simulation symbol error probability versus SNR with SJR as a parameter for non-coherent 2FSK with Rayleigh fading.

In Figure 85 and 86, respectively, the theoretical and simulation symbol error probabilities are shown as functions of SJR with SNR as a parameter.

133
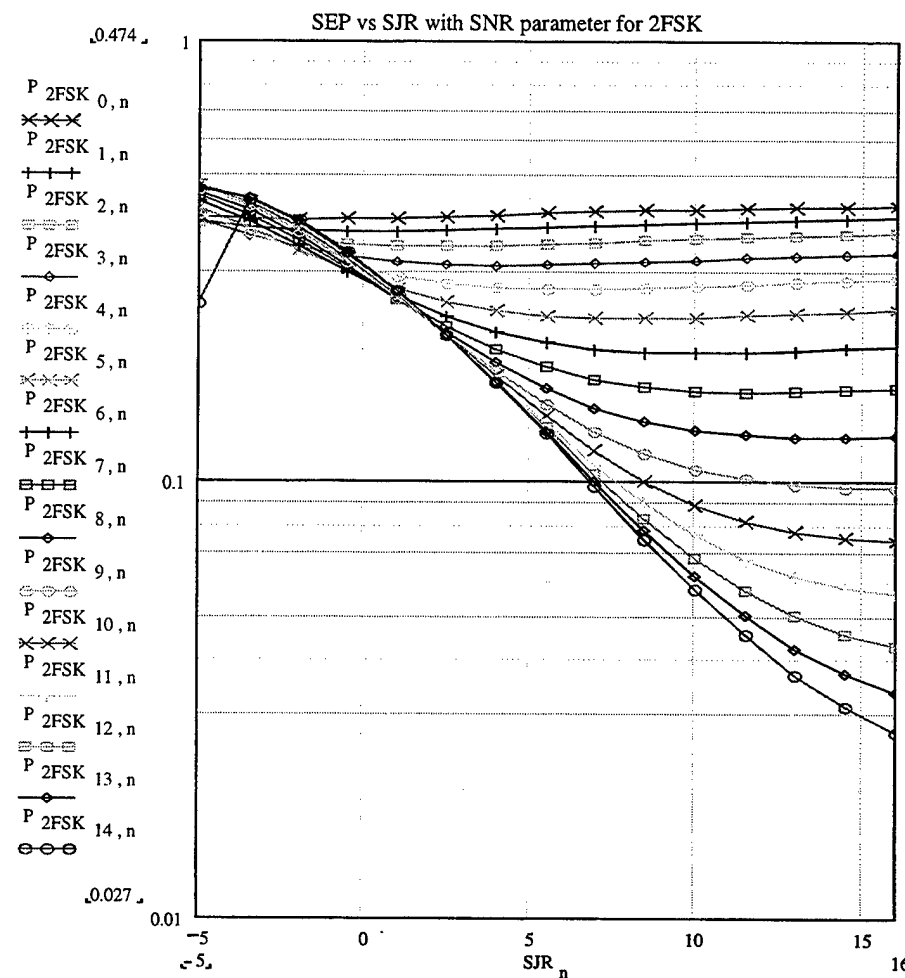
Figure 85. Theoretical symbol error probability versus SJR with SNR as a parameter

for non-coherent 2FSK with Rayleigh fading.

We again note the dramatic increase in the symbol error probability due to Rayleigh fading and co-channel interference. Furthermore, non-coherent detection also increases the number of errors in the receiver as compared to the coherent detection.
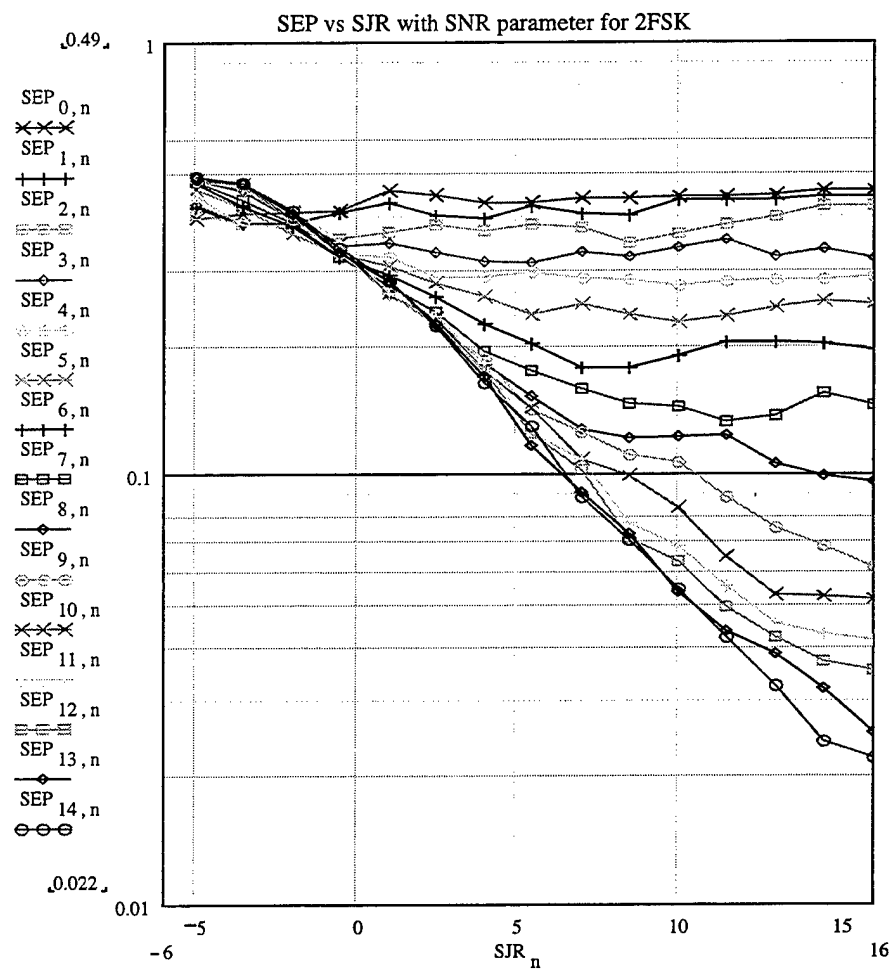
Figure 86. Simulation symbol error probability versus SJR with SNR as a parameter for non-coherent 2FSK with Rayleigh fading.

The relative difference (percent "error") between the theory and the simulation is summarized in Table 29. In Figure 87, the average difference is plotted versus SNR and SJR, respectively, for each of the 15 previously presented curves.

135
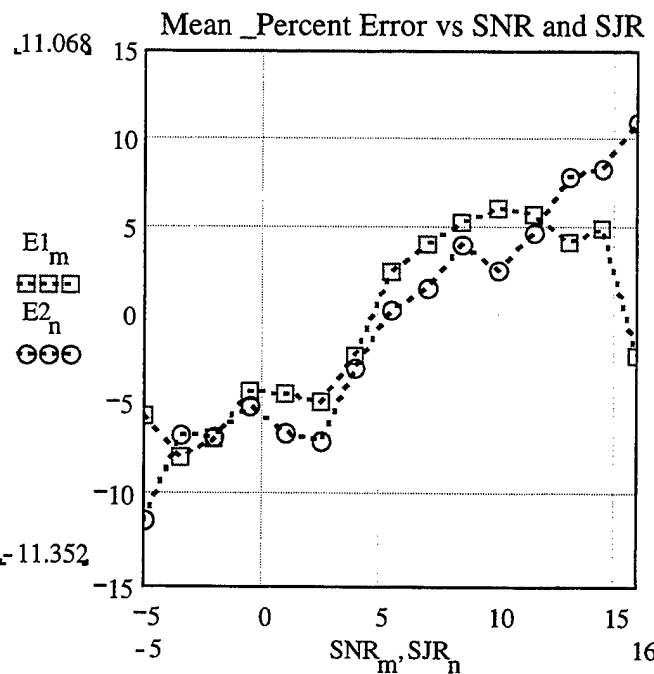
Figure 87. Mean percent difference as a function of SNR and SJR, respectively.

The two curves show how the mean difference varies with SNR and SJR. Each value of the mean difference is the average of the differences that correspond to the 15 points on each of the 15 curves for the symbol error probability as a function of SNR (with SJR as parameter) and SJR (with SNR as parameter).

	SYMBOL ERROR PROBABILITY	NON-COHERENT 2FSK
1.	Root Mean Square Difference (%)	11.852
2.	Average Mean Difference (%)	-0.376
3.	Maximum Difference (%)	37.275
4.	Minimum Difference (%)	-93.245
5.	Difference Deviation (%)	11.846

Table 29. Summary of the accuracy of the simulation for non-coherent 2FSK.

b)   Results For 4FSK

The theoretical and the simulation symbol error probabilities for non-coherently detected 4FSK are presented in Figures 88 and 89, respectively, as functions of the average SNR in dB, with SJR as a parameter. The values for the signal-to-noise and signal-to-interference ratios have been chosen from –5 dB to +16 dB, where the lower curve corresponds to SJR=+16 dB and the remaining curves are in increments of 1.5 dB.
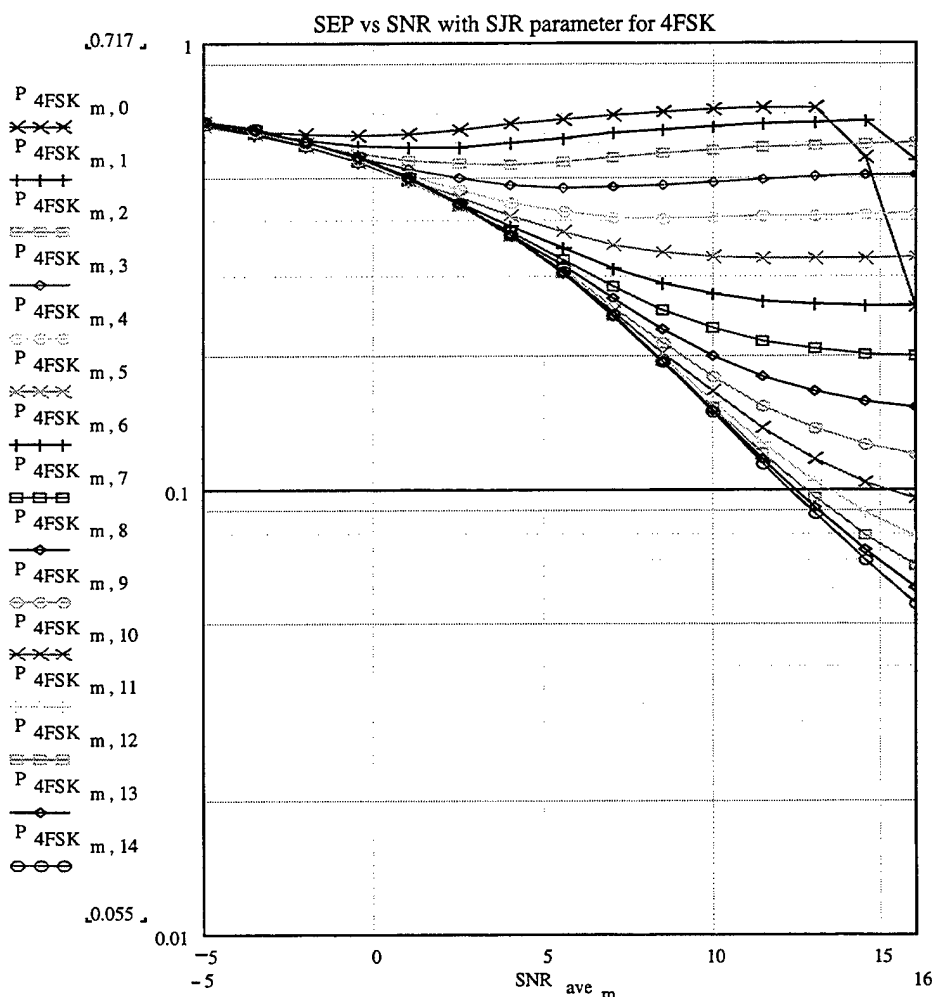
Figure 88. Theoretical symbol error probability versus SNR with SJR as a parameter for non-coherent 4FSK with Rayleigh fading.
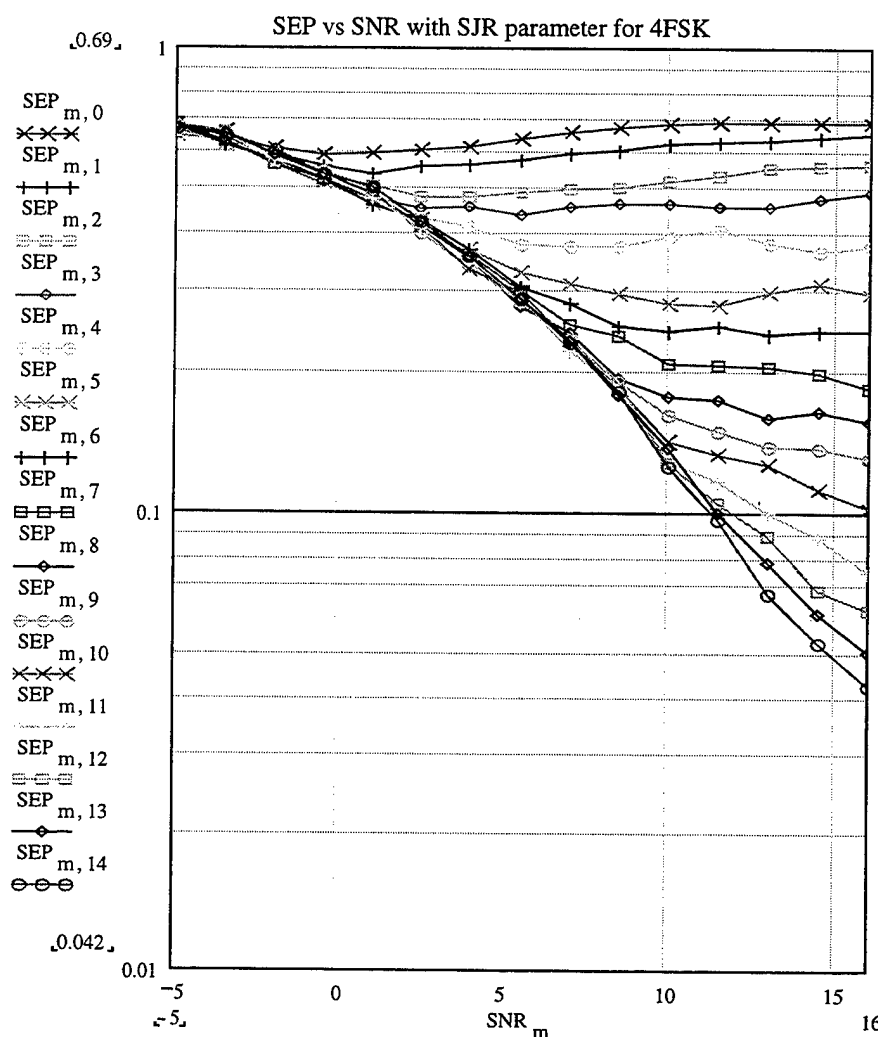
Figure 89. Experimental symbol error probability versus SNR with SJR as a parameter for non-coherent 4FSK with Rayleigh fading.

In Figures 90 and 91, respectively, the theoretical and simulation symbol error probabilities are shown as functions of SJR with SNR as a parameter.

138
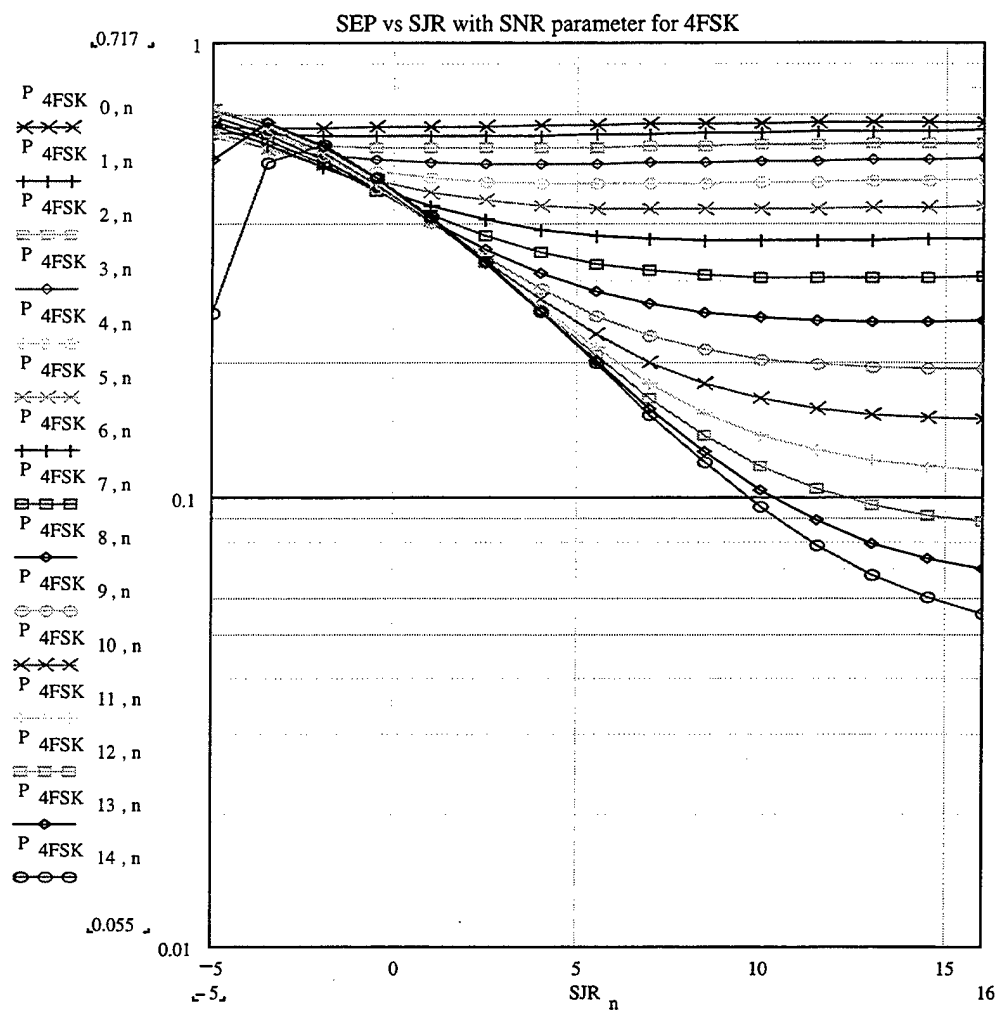
Figure 90. Theoretical symbol error probability versus SJR with SNR as a parameter for non-coherent 4FSK with Rayleigh fading.

We again note the dramatic increase in the symbol error probability due to Rayleigh fading and co-channel interference.
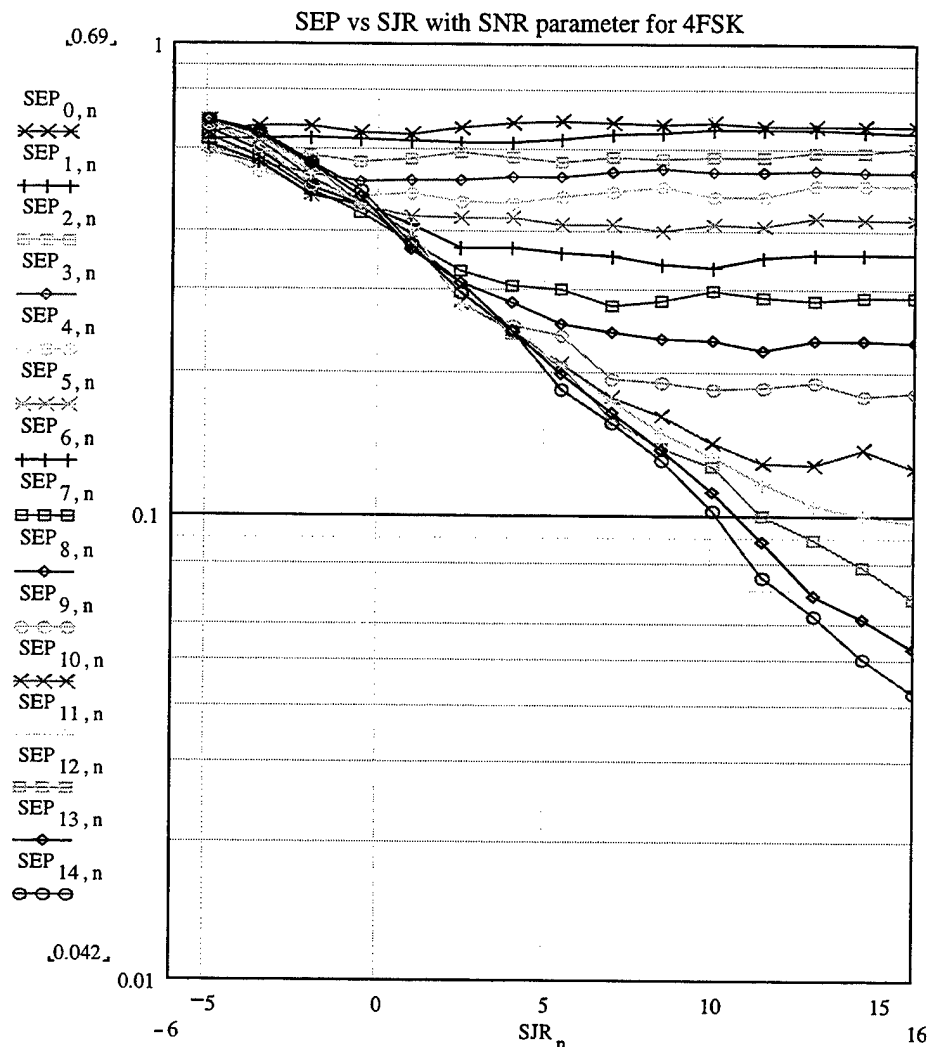
Figure 91. Simulation symbol error probability versus SJR with SNR as a parameter

for non-coherent 4FSK with Rayleigh fading.

In Figure 92, the average difference for each curve is plotted versus SNR

and SJR for each of the 15 previously presented curves. Finally, the relative difference

(percent "error") between the theory and the simulation is summarized in Table 30.

140
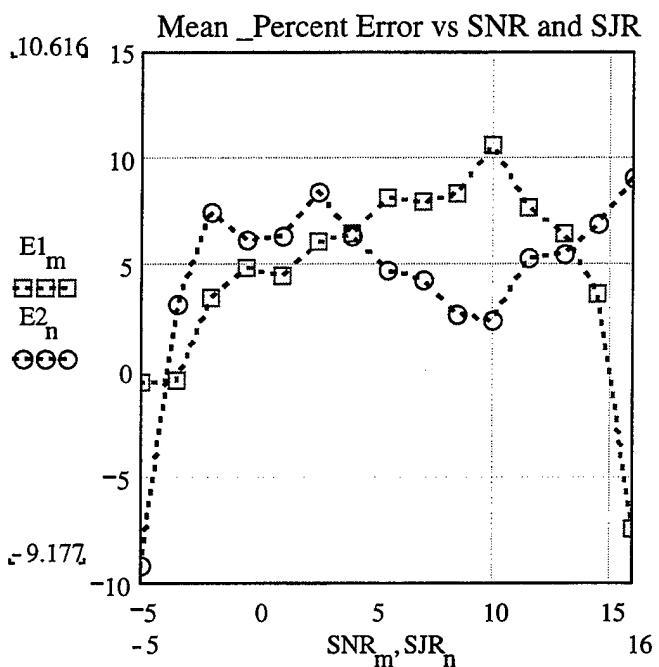
Figure 92. Mean percent difference as a function of SNR and SJR.

The two curves show how the mean difference varies with SNR and SJR. Each value of the mean difference is the average of the differences that correspond to the 15 points on each of the 15 curves for the symbol error probability as a function of SNR (with SJR as parameter) and SJR (with SNR as parameter), respectively.

	SYMBOL ERROR PROBABILITY	NON-COHERENT 4FSK
1.	Root Mean Square Difference (%)	13.913
2.	Average Mean Difference (%)	4.67
3.	Maximum Difference (%)	24.316
4.	Minimum Difference (%)	-170.45
5.	Difference Deviation (%)	13.105

Table 30. Summary of the accuracy of the simulation for non-coherent 4FSK.

c) Results For 8FSK

The theoretical and the simulation symbol error probabilities for non-coherently detected 8FSK are presented in the Figures 93 and 94, respectively, as functions of the average SNR in dB, with SJR as a parameter. The values for the signal-to-noise and signal-to-interference ratios have been chosen from –5 dB to +16 dB in increments of 1.5 dB.
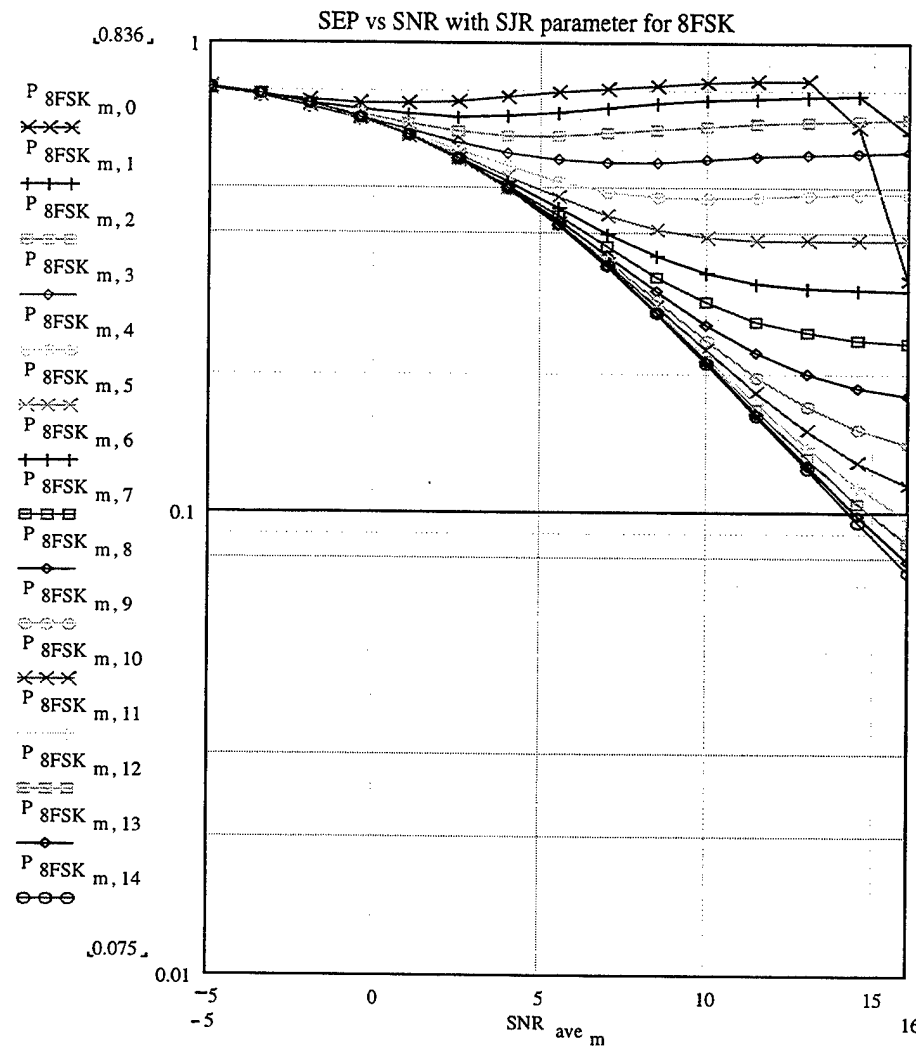
Figure 93. Theoretical symbol error probability versus SNR with SJR as a parameter for non-coherent 8FSK with Rayleigh fading.
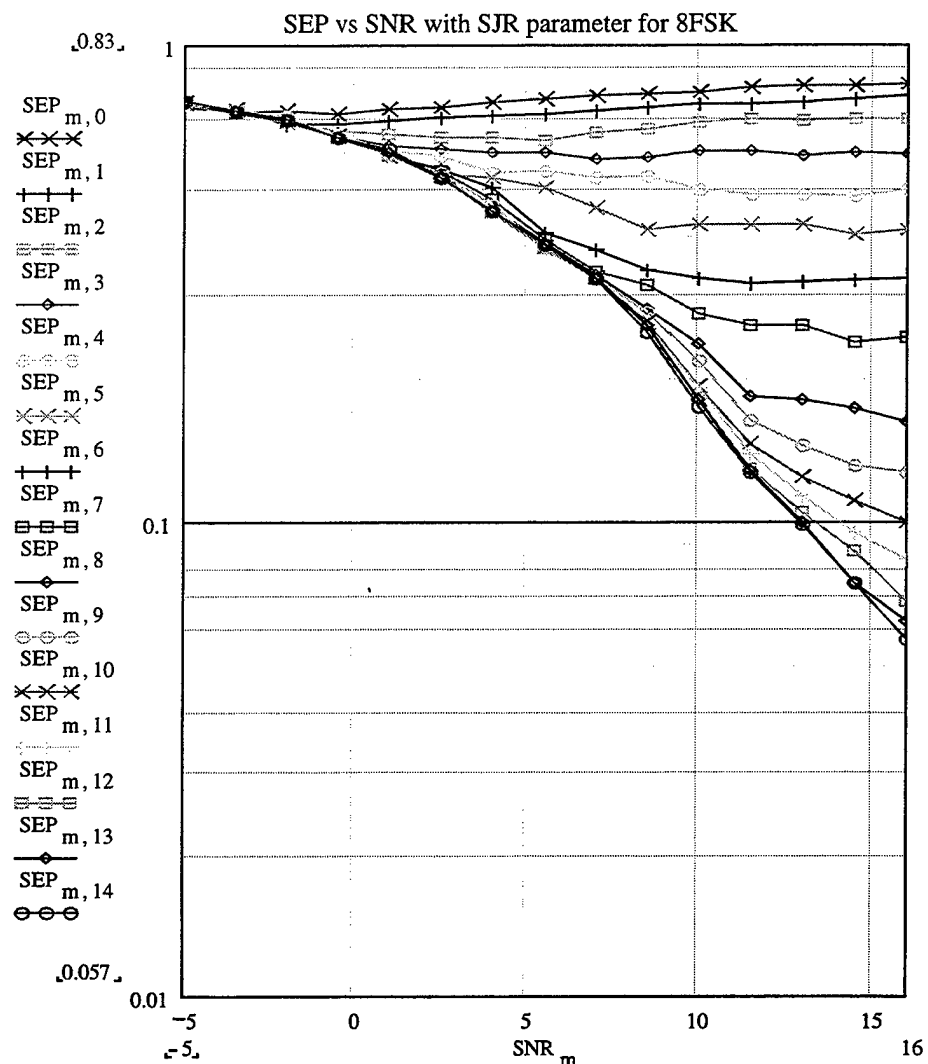
Figure 94. Simulation symbol error probability versus SNR with SJR as a parameter

for non-coherent 8FSK with Rayleigh fading.

In Figures 95 and 96, respectively, the theoretical and simulation symbol

error probabilities are shown as functions of SJR with SNR as a parameter.

143
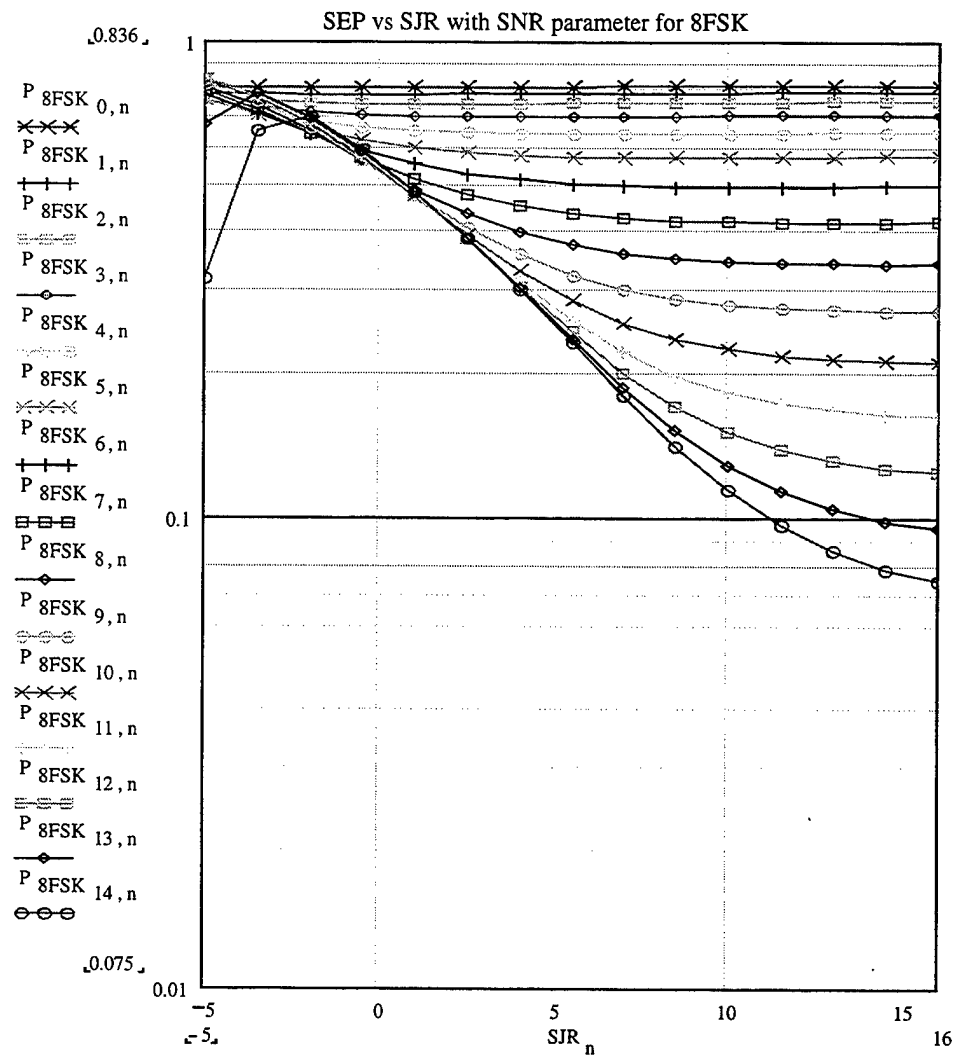
Figure 95. Theoretical symbol error probability versus SJR with SNR as a parameter

for non-coherent 8FSK with Rayleigh fading.

We again note the dramatic increase in the symbol error probability due to

Rayleigh fading and co-channel interference.

144
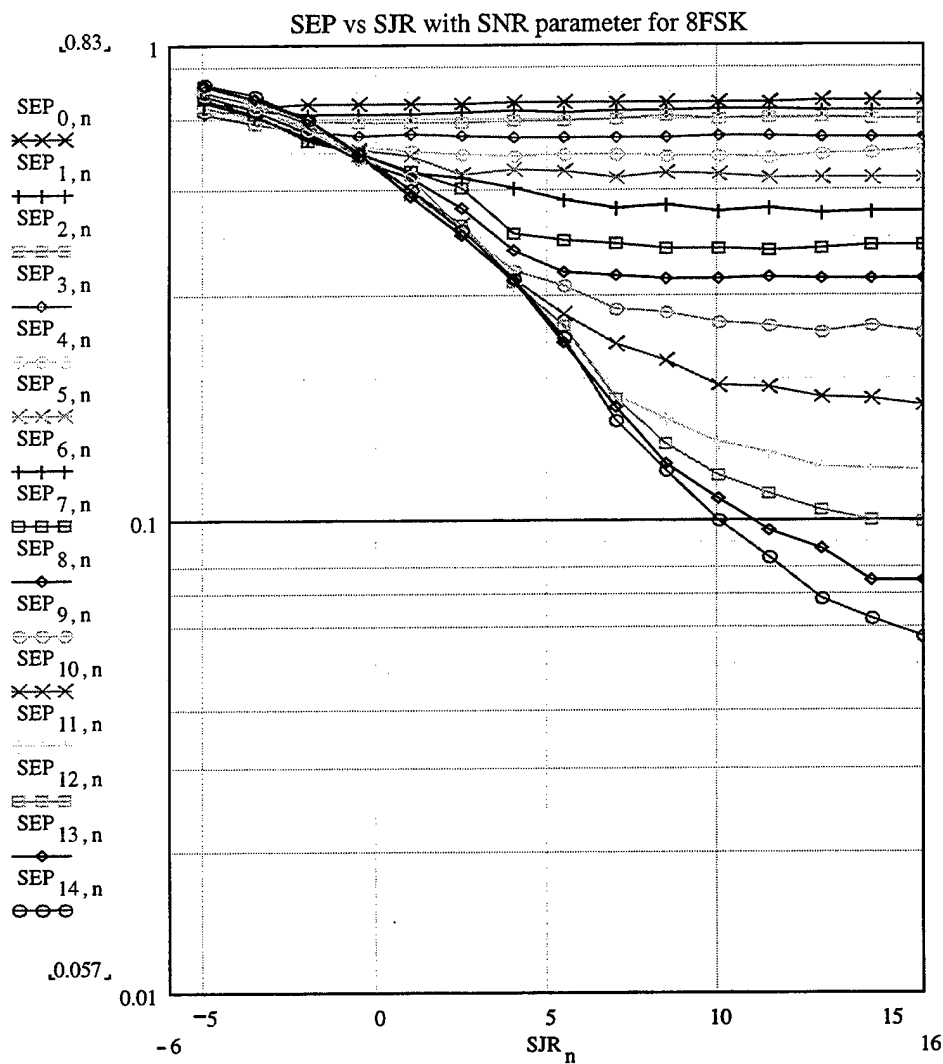
Figure 96. Simulation symbol error probability versus SJR with SNR as a parameter

for non-coherent 8FSK with Rayleigh fading.

In Figure 97, the average difference for each curve is plotted versus SNR

and SJR for each of the 15 previously presented curves. Finally, the relative difference

(percent "error") between the theory and the simulation is summarized in Table 31.
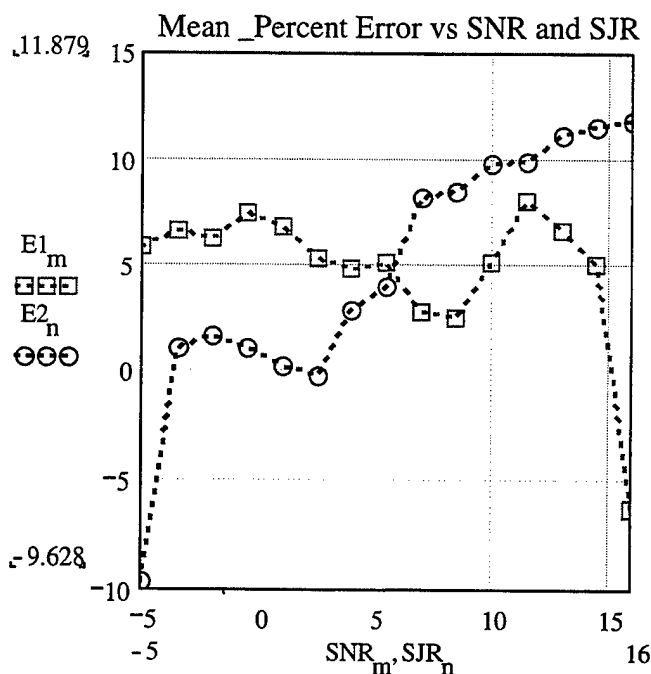
Figure 97. Mean percent difference as a function of SNR and SJR, respectively.

The two curves show how the mean difference varies with SNR and SJR. Each value of the mean difference is the average of the differences that correspond to the 15 points on each of the 15 curves for the symbol error probability as a function of SNR (with SJR as parameter) and SJR (with SNR as parameter), respectively.

	SYMBOL ERROR PROBABILITY	NON-COHERENT 8FSK
1.	Root Mean Square Difference (%)	14.029
2.	Average Mean Difference (%)	4.836
3.	Maximum Difference (%)	24.288
4.	Minimum Difference (%)	-161.825
5.	Difference Deviation (%)	13.17

Table 31. Summary of the accuracy of the simulation for non-coherent 8FSK.

146

Observing the results for non-coherent detection of 2, 4, and 8FSK in a Rayleigh fading channel and affected by AWGN and co-channel interference, we note that the simulation overestimates the theory for the case of 2FSK and underestimates the theory for the cases of 4 and 8FSK. The root mean square difference (in percent) is about 13% (in average) and the mean percent difference for all the cases is less than 5% (in absolute value), which suggests good accuracy.

The average results for the non-coherent detection of 2, 4, and 8FSK are presented in Table 32.

	SYMBOL ERROR PROBABILITY	AVERAGE RESULTS FOR NON-COHERENT 2, 4, AND 8FSK
1.	Root Mean Square Difference (%)	13.264
2.	Average Mean Difference (%)	3.043
3.	Maximum Difference (%)	28.626
4.	Minimum Difference (%)	-141.84
5.	Difference Deviation (%)	12.707

Table 32. Average results for the non-coherent detection of 2, 4, and 8FSK.

C. RICIAN FADING CHANNEL – COHERENT DETECTION

In this section, we derive the symbol error probability for MFSK signals transmitted over a frequency-nonselective, slowly fading Rician channel in the presence of AWGN and co-channel interference. The frequency-nonselective, slowly fading channel results in multiplicative distortion of the MFSK transmitted signal. The condition that the channel fades slowly implies that the multiplicative process may be considered as a constant during at least one symbol interval. Furthermore, we assume that the channel fading is sufficiently slow such that the phase shift introduced by the channel can be estimated from the received signal without error.

1. Theoretical Probability Of Symbol Error For Coherent Detection

The probability that the signal symbol will be received correctly is evaluated, again, separately for the two following cases:

- **Case 1**: the signal and the interference symbols are on the same branch of the receiver

- **Case 2**: the signal and the interference symbols are at different branches.

a) The Signal And The Interference Symbols Are On The Same Branch

The conditional probability of symbol error for coherent orthogonal MFSK with AWGN and co-channel interference has been derived in (4.7) of Chapter IV.B.1:

$$P1(r) = 1 - \frac{1}{\sqrt{2 \cdot \pi}} \cdot \int_{-\infty}^{\infty} e^{-\frac{x^2}{2}} \cdot \left(1 - Q\left(x + \frac{r+J}{\sigma}\right)\right)^{M-1} dx \qquad (5.21)$$

148

where:

J is the amplitude of the interfering MFSK signal and

r is the amplitude of the desired MFSK signal.

The above symbol error probability is conditioned on the amplitude r of the desired signal, which can be considered as a Rician random variable with the probability density function:

$$f(r) = \frac{r}{P_{dif}} \cdot e^{\frac{-\left(r^2 + 2 \cdot P_{dir}\right)}{2 \cdot P_{dif}}} \cdot I0\left(\frac{\sqrt{2 \cdot P_{dir}} \cdot r}{P_{dif}}\right) \qquad (5.22)$$

where:

P_{dir} is the power of the direct signal component

P_{dif} is the power of the diffuse signal component.

Integrating the product of the conditional probability of symbol error and the probability density function of the information signal's amplitude r over all possible values of r, we obtain the unconditional probability of symbol error for this first case:

$$P1 = 1 - \frac{1}{\sqrt{2 \cdot \pi}} \cdot \int_0^\infty \int_{-\infty}^\infty e^{\frac{-x^2}{2}} \cdot \left(1 - Q\left(x + \frac{r + J}{\sqrt{P_{noise}}}\right)\right)^{M-1} \cdot \frac{r}{P_{dif}} \cdot e^{\frac{-\left(r^2 + 2 \cdot P_{dir}\right)}{2 \cdot P_{dif}}} \cdot I0\left(\frac{\sqrt{2 \cdot P_{dir}} \cdot r}{P_{dif}}\right) dx dr \quad (5.23)$$

Using the transformation:

$$\frac{r}{\sqrt{P_{dif}}} = y \qquad dr = \sqrt{P_{dif}} dy \qquad (5.24)$$

149

we obtain:

$$P1 = 1 - \frac{1}{\sqrt{2 \cdot \pi}} \cdot \int_0^\infty \int_{-\infty}^\infty e^{\frac{-x^2}{2}} \cdot \left(1 - Q\left(x + \frac{y \cdot \sqrt{P_{dif}} + J}{\sqrt{P_{noise}}}\right)\right)^{M-1} \cdot e^{\frac{-1}{2}\left(y^2 + 2\frac{P_{dir}}{P_{dif}}\right)} \cdot I0\left(\frac{\sqrt{2 \cdot P_{dir}} \cdot y}{\sqrt{P_{dif}}}\right) \cdot y \, dx \, dy \quad (5.25)$$

The above double integral has to be evaluated numerically.

b)   The Signal And The Interference Symbols Are On Different Branches

The conditional probability of symbol error for this case has been derived in (4.14) of Chapter IV.B.1:

$$P2(r) = 1 - \frac{1}{\sqrt{2 \cdot \pi}} \cdot \int_{-\infty}^\infty \left(1 - Q\left(x + \frac{r}{\sigma}\right)\right)^{M-2} \cdot \left(1 - Q\left(x + \frac{r-J}{\sigma}\right)\right) \cdot e^{\frac{-x^2}{2}} \, dx \quad (5.26)$$

Integrating the product of the conditional probability of symbol error and the probability density function of the desired signal's amplitude r over all possible values of r, we get the unconditional probability of symbol error:

$$P2 = 1 - \frac{1}{\sqrt{2 \cdot \pi}} \cdot \int_0^\infty \int_{-\infty}^\infty \left[\begin{array}{c} \left(1 - Q\left(x + \frac{r}{\sqrt{P_{noise}}}\right)\right)^{M-2} \cdot \left(1 - Q\left(x + \frac{r-J}{\sqrt{P_{noise}}}\right)\right) \\ e^{\frac{-x^2}{2}} \cdot \frac{r}{P_{dif}} \cdot e^{\frac{-\left(r^2 + 2 \cdot P_{dir}\right)}{2 \cdot P_{dif}}} \cdot I0\left(\frac{\sqrt{2 \cdot P_{dir}} \cdot r}{P_{dif}}\right) \end{array} \right] dx \, dr \quad (5.27)$$

Using again the transformation of equation (5.24), we obtain:

150

$$P2 = 1 - \frac{1}{\sqrt{2 \cdot \pi}} \cdot \int_0^\infty \int_{-\infty}^\infty \left[\left(1 - Q\left(x + \frac{y \cdot \sqrt{P_{dif}}}{\sqrt{P_{noise}}} \right) \right)^{M-2} \cdot \left(1 - Q\left(x + \frac{y \cdot \sqrt{P_{dif}} - J}{\sqrt{P_{noise}}} \right) \right) \cdot e^{\frac{-1}{2} \cdot \left(x^2 + y^2 + 2 \cdot \frac{P_{dir}}{P_{dif}} \right)} \cdot I0\left(\frac{\sqrt{2 \cdot P_{dir}} \cdot y}{\sqrt{P_{dif}}} \right) \cdot y \right] dx\, dy \quad (5.28)$$

The above integral must be evaluated numerically.

c)   Total Symbol Error Probability

The total symbol error probability, combining the two cases, is given by:

$$P_{total} = \frac{1}{M} \cdot P1 + \frac{M-1}{M} \cdot P2 \quad (5.29)$$

where 1/M is the probability that the desired and the interfering symbols are at the same branch and (M-1)/M is the probability that the desired and the interfering symbols are at different branches.

It is convenient to define the ratio of the powers of direct and diffuse components as:

$$R = \frac{P_{dir}}{P_{dif}} \quad (5.30)$$

For a given value of total signal power, we have:

$$Power_{dir} + Power_{dif} = Power_{signal\_total} \quad (5.31)$$

Next, we will express the last relationship in terms of the ratio of the two powers of direct and diffuse components as:

$$\frac{Power_{signal\_total}}{Power_{dif}} = 1 + R \quad (5.32)$$

151

The SNR is defined as the ratio of the total signal power to the noise power:

$$SNR = \frac{P_{dir} + P_{dif}}{P_{noise}} = \frac{P_{dif}}{P_{noise}} \cdot (1 + R)$$ (5.33)

Equivalently, we obtain:

$$\sqrt{\frac{P_{dif}}{P_{noise}}} = \sqrt{\frac{SNR}{1+R}} = \frac{10^{\frac{SNR_{dB}}{20}}}{\sqrt{1+R}}$$ (5.34)

Substituting equation (5.30) and (5.34) into equations (5.25) and (5.28), we get the following expressions for the symbol error probability:

$$P1 = 1 - \frac{1}{\sqrt{2 \cdot \pi}} \cdot \int_0^\infty \int_{-\infty}^\infty \left[\left(1 - Q\left(x + y \cdot \sqrt{\frac{1}{1+R}} \cdot 10^{\frac{SNR}{20}} + \sqrt{2} \cdot 10^{\frac{SNR-SJR}{20}} \right) \right)^{M-1} \cdot e^{\frac{-1}{2} \cdot (x^2 + y^2 + 2 \cdot R)} \cdot I0\left(\sqrt{2 \cdot R} \cdot y \right) \cdot y \right] dxdy$$ (5.35)

$$P2 = 1 - \frac{1}{\sqrt{2 \cdot \pi}} \cdot \int_0^\infty \int_{-\infty}^\infty \left[e^{\frac{-1}{2} \cdot (x^2 + y^2 + 2 \cdot R)} \cdot \left(1 - Q\left(x + y \cdot \sqrt{\frac{1}{1+R}} \cdot 10^{\frac{SNR}{20}} \right) \right)^{M-2} \cdot \left(1 - Q\left(x + y \cdot \sqrt{\frac{1}{1+R}} \cdot 10^{\frac{SNR}{20}} - \sqrt{2} \cdot 10^{\frac{SNR-SJR}{20}} \right) \right) \cdot I0\left(\sqrt{2 \cdot R} \cdot y \right) \cdot y \right] dxdy$$ (5.36)

Now, we are able to evaluate and plot the theoretical symbol error probability as a function of the ratio of the powers of the direct and diffuse signal components.

2.   Simulink Model and Block Analysis

The block diagram of the Simulink model for coherent MFSK with AWGN and co-channel interference in a Rician fading channel is shown on Figure 98. This model is a combination of the model that was used for coherent MFSK in a Rician fading channel and the model that was used for coherent MFSK signal with co-channel interference.
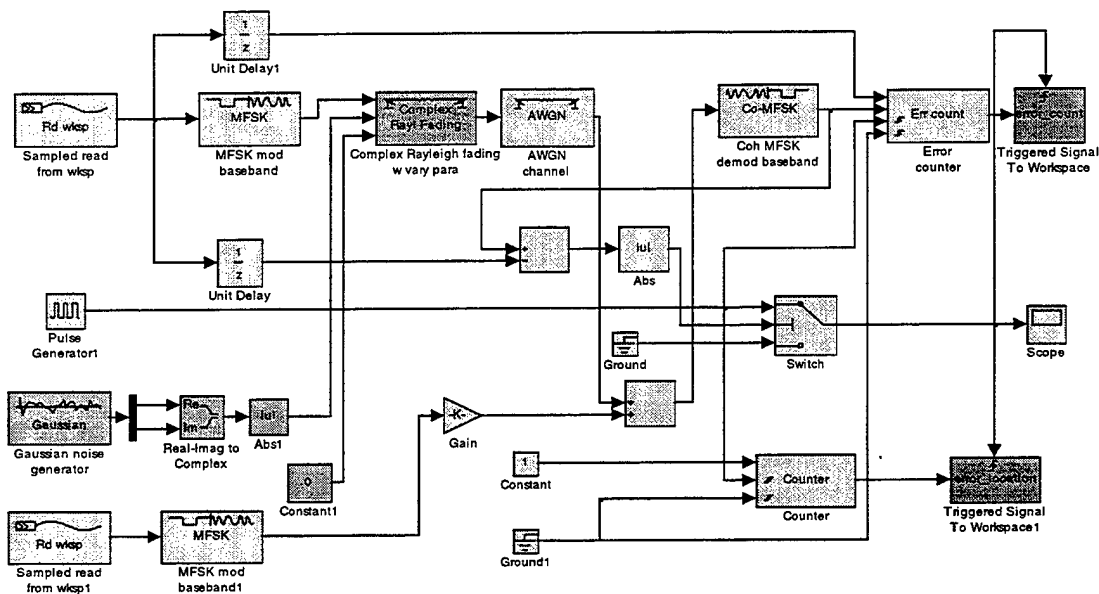
Figure 98. Model for coherent MFSK with AWGN and co-channel interference in a Rician fading channel.

3.   Simulation Analysis And Performance Verification

In this section, simulation results are presented in order to verify the performance of coherent detection of MFSK corrupted by AWGN and co-channel interference in a Rician fading channel. Each simulation ran until at least 100 errors were observed. The data sequences were limited to 10^6 symbols for each simulation in order to prevent "out of memory" errors. The simulation sequence was repeated until a sufficient number of errors were counted.

a)   Results For 2FSK

The theoretical and the simulation symbol error probabilities for coherently detected 2FSK are presented in the Figures 99 and 100, respectively, as functions of the average SNR in dB, with SJR as a parameter. The values for the signal-to-noise and signal-to-interference ratios were chosen from −5 dB to +30 dB in increments of 2.5 dB.
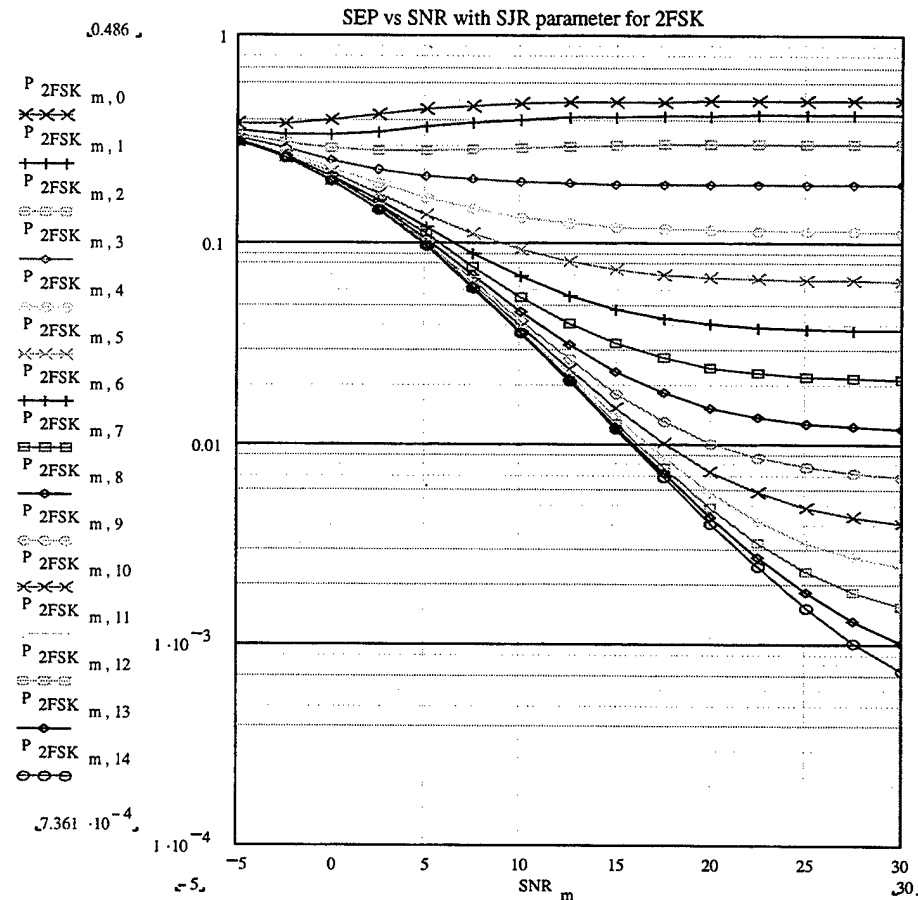
Figure 99. Theoretical symbol error probability versus SNR with SJR as a parameter for coherent 2FSK, with Rician fading and R=1.

154
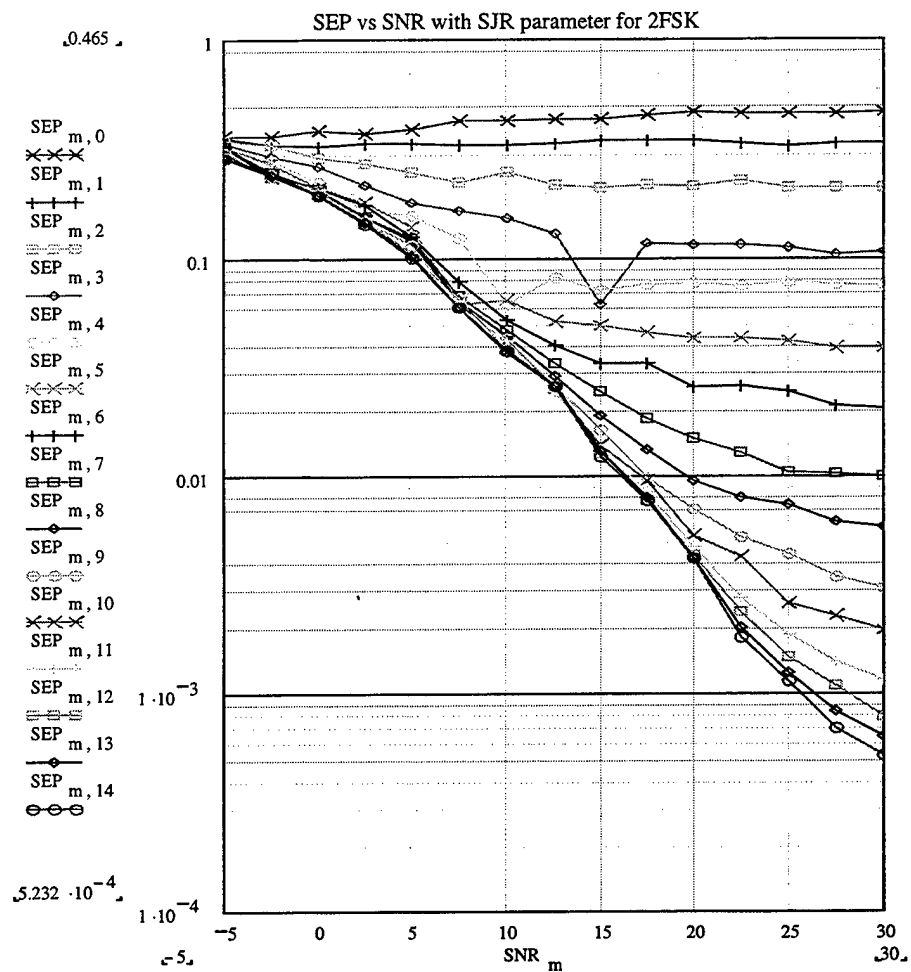
Figure 100. Simulation symbol error probability versus SNR with SJR as a parameter for coherent 2FSK with Rician fading and R=1.

In Figure 101 and 102, respectively, the theoretical and simulation results for the symbol error probability are presented as functions of SJR with SNR as a parameter.
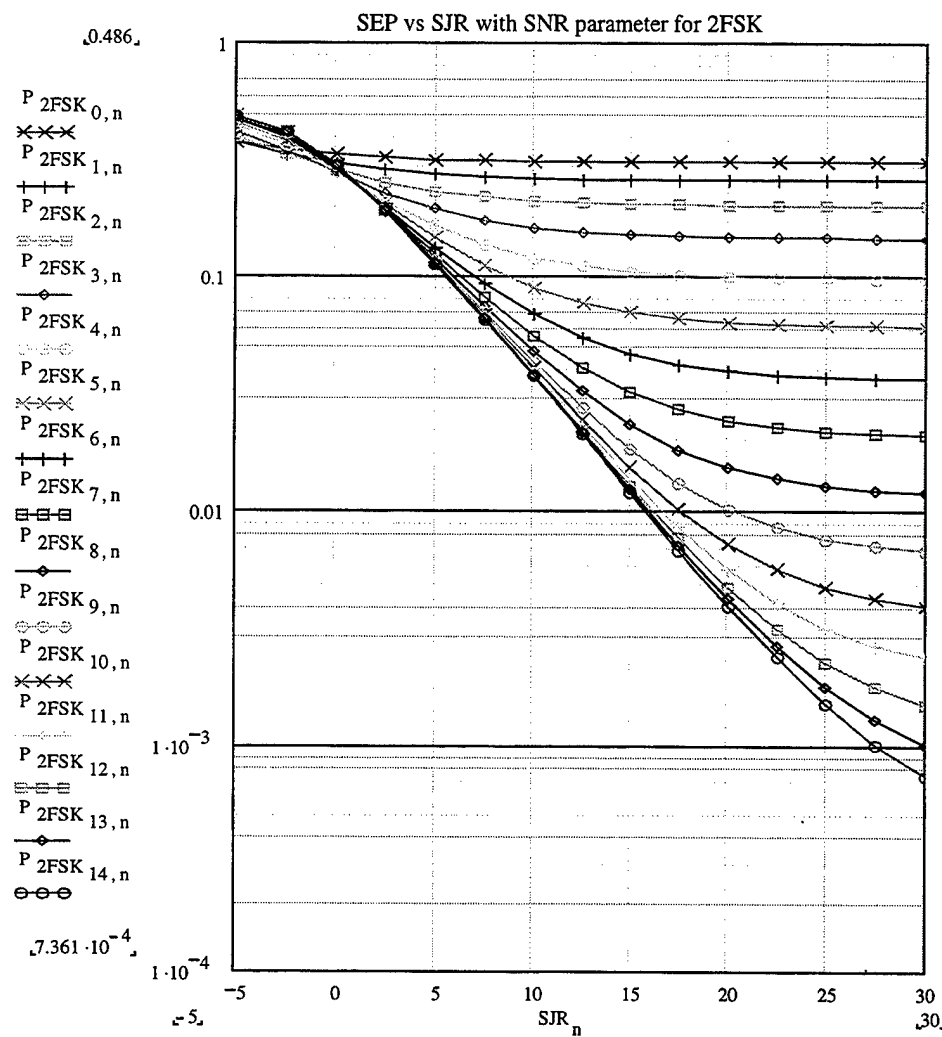
Figure 101. Theoretical symbol error probability versus SJR with SNR as a parameter for coherent 2FSK, with Rician fading and R=1.

We note again the dramatic increase in the symbol error probability due to Rician fading and co-channel interference.

156
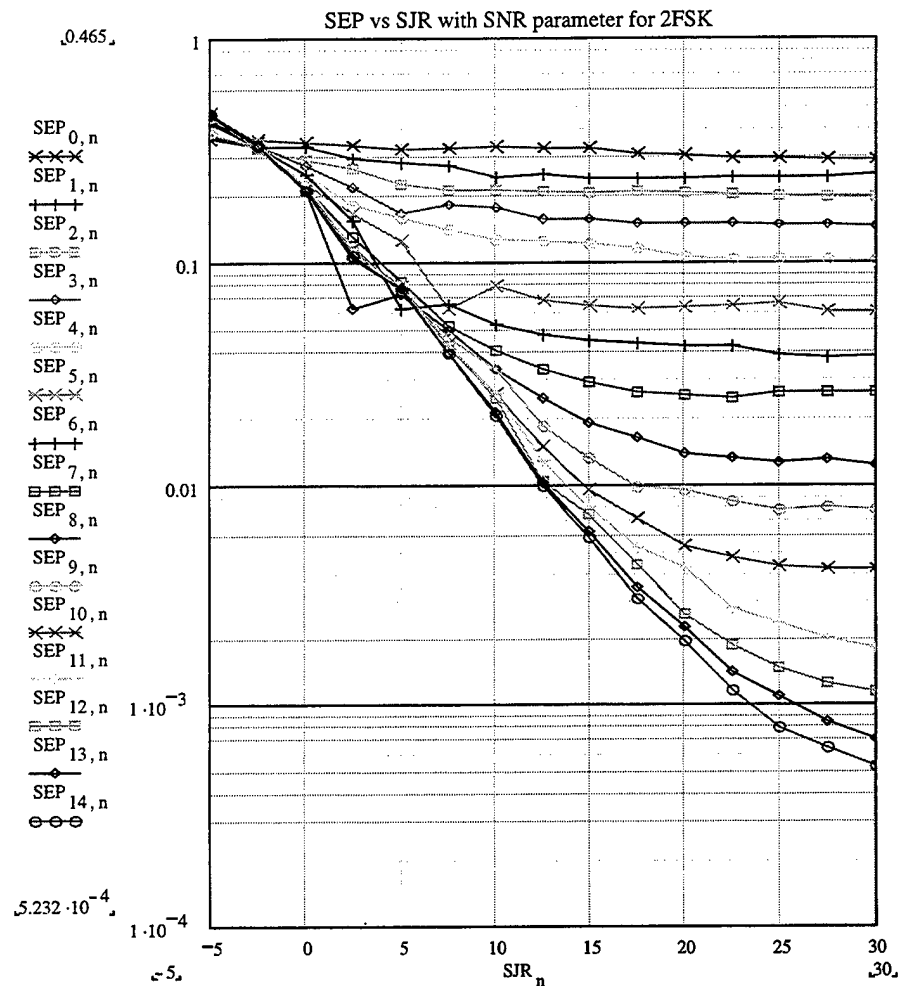
Figure 102. Simulation symbol error probability versus SJR with SNR as a parameter

for coherent 2FSK, with Rician fading and R=1.

To avoid any by chance distortion on the curves of the simulation results,

we have to run the same pattern many times and average the results. The relative

difference (percent "error") between the theory and the simulation is presented in Table

33. In Figure 103, the average difference for each curve is plotted versus SNR and SJR

for each of the 15 previously presented curves.
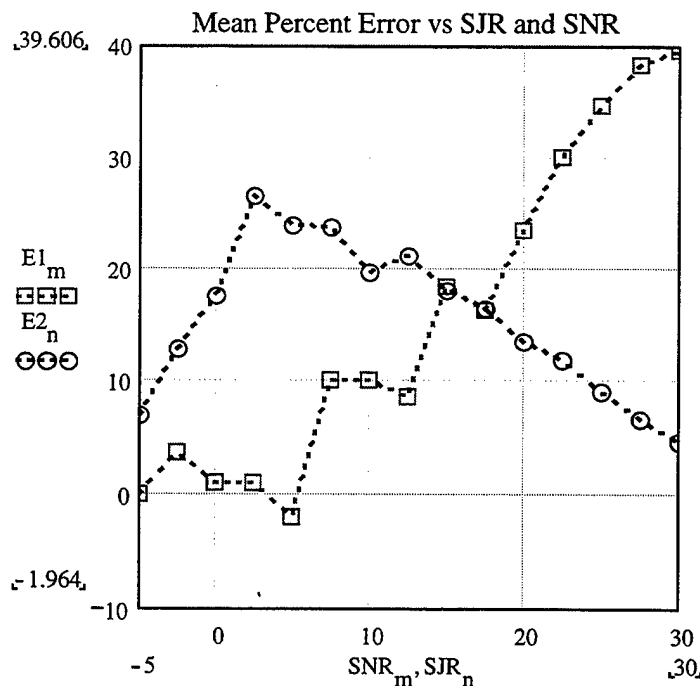
Figure 103. Mean percent difference as a function of SNR and SJR, respectively.

The two curves show how the mean difference varies with SNR and SJR. Each value of the mean difference is the average of the differences that correspond to the 15 points on each of the 15 curves for the symbol error probability as a function of SNR (with SJR as parameter) and SJR (with SNR as parameter), respectively.

	SYMBOL ERROR PROBABILITY	COHERENT 2FSK
1.	Root Mean Square Difference (%)	24.529
2.	Average Mean Difference (%)	15.583
3.	Maximum Difference (%)	68.105
4.	Minimum Difference (%)	-26.173
5.	Difference Deviation (%)	18.943

Table 33. Summary of the accuracy of the simulation for coherent 2FSK.

158

b)   Results For 4FSK

The theoretical and the simulation symbol error probabilities for coherently detected 4FSK are presented in the Figures 104 and 105, respectively, as functions of the average SNR in dB, with SJR as a parameter. The values for the signal-to-noise and signal-to-interference ratios were chosen from –5 dB to +30 dB in increments of 2.5 dB.
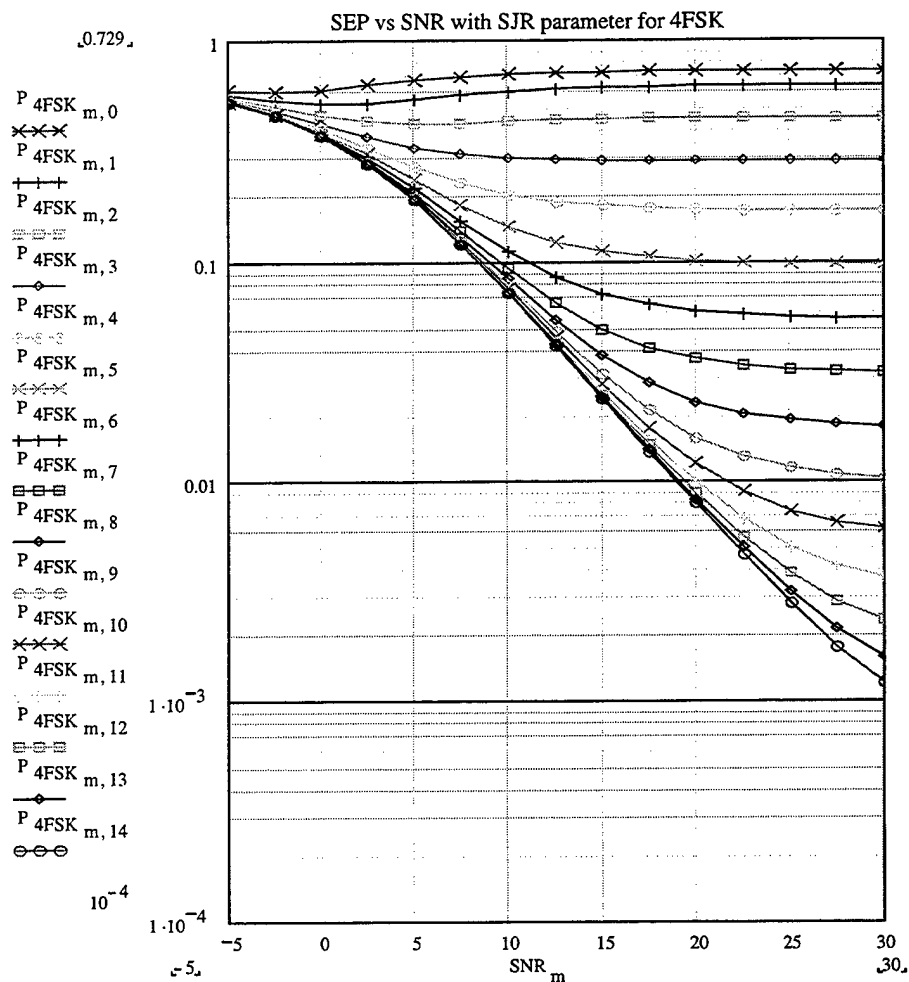

Figure 104. Theoretical symbol error probability versus SNR with SJR as a parameter for coherent 4FSK, with Rician fading and R=1.

159
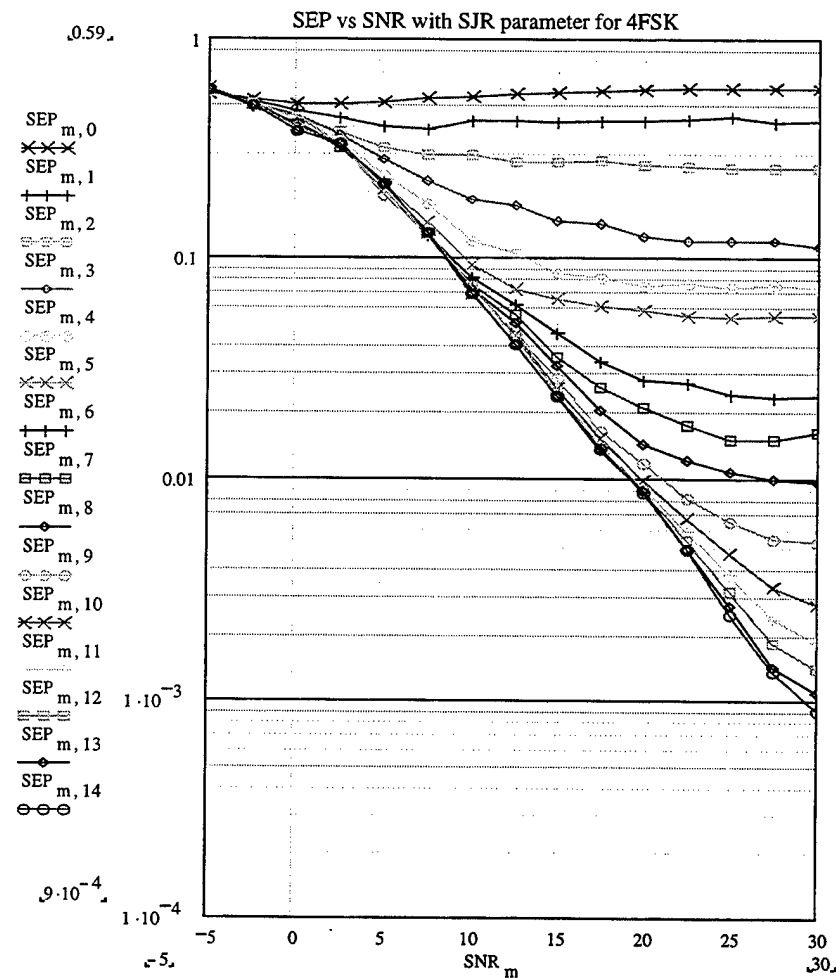
Figure 105. Simulation symbol error probability versus SNR with SJR as a parameter for coherent 4FSK, with Rician fading and R=1.

In Figure 106 and 107, respectively, the theoretical and simulation results for the symbol error probability are presented as functions of SJR with SNR as a parameter.
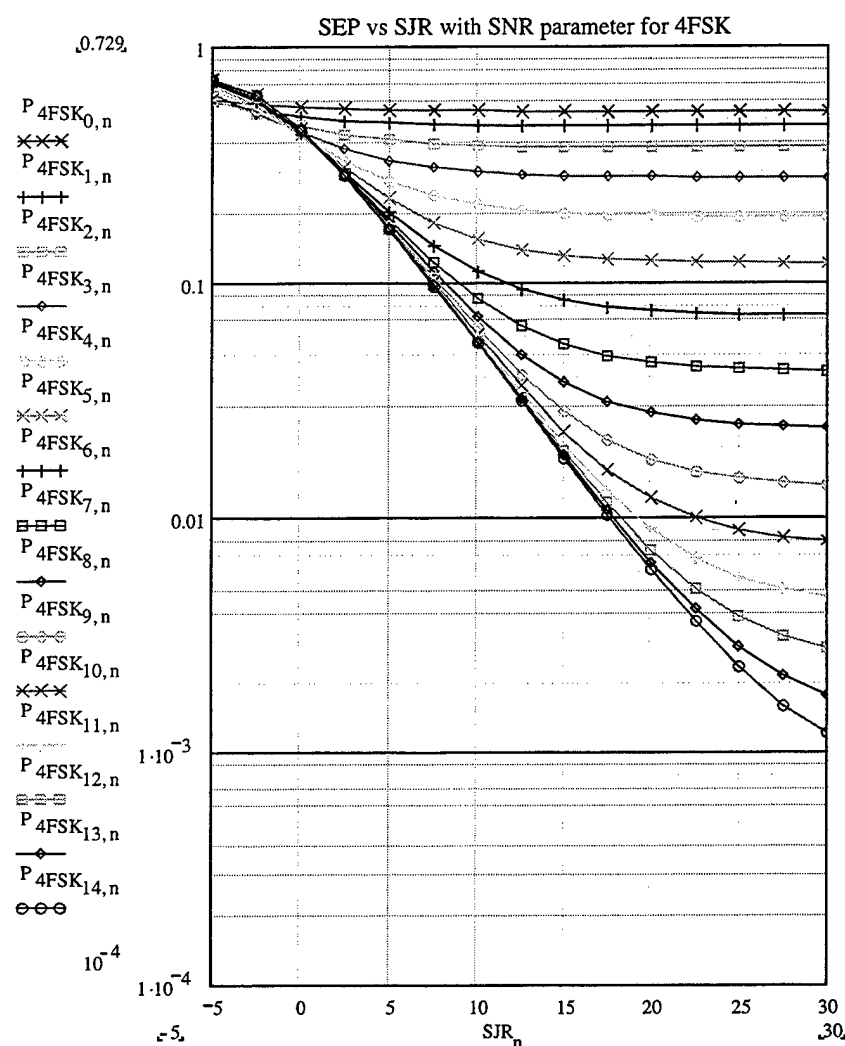
Figure 106. Theoretical symbol error probability versus SJR with SNR as a parameter

for coherent 4FSK, with Rician fading and R=1.

We note again the dramatic increase in the symbol error probability due to

Rician fading and co-channel interference.

161
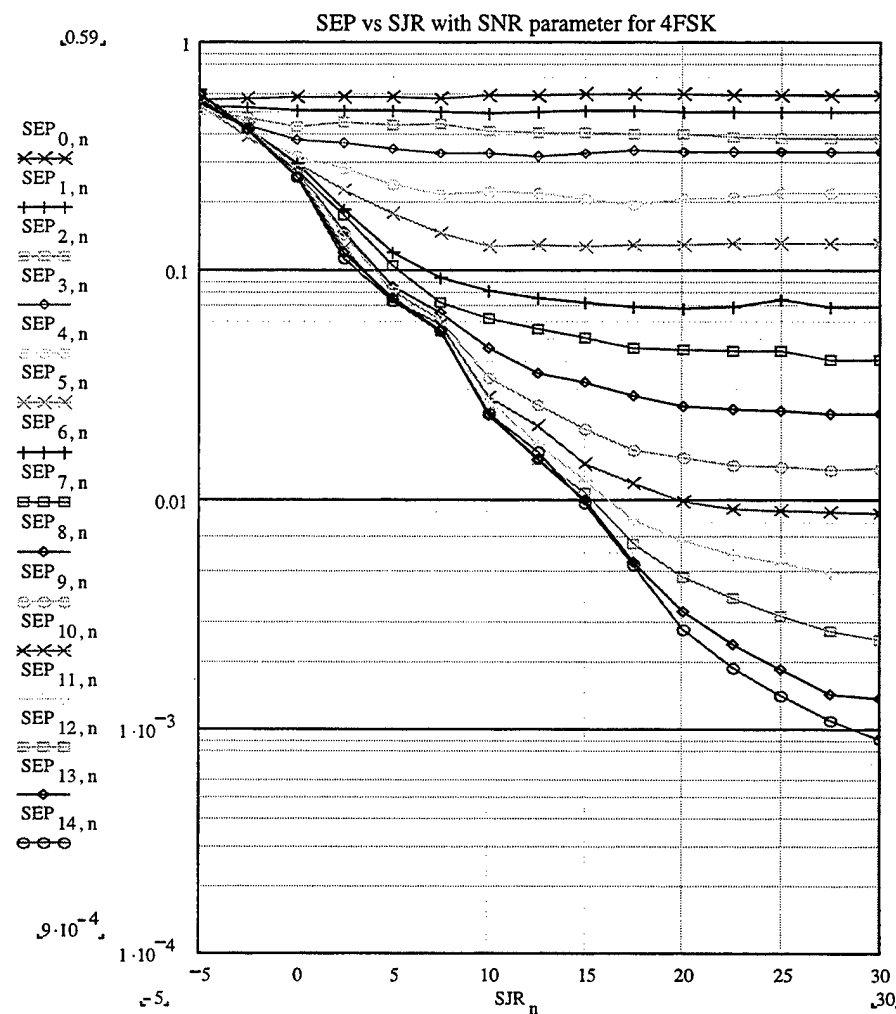
Figure 107. Simulation symbol error probability versus SJR with SNR as a parameter for coherent 4FSK, with Rician fading and R=1.

The relative difference (percent "error") between the theory and the simulation is presented in Table 34. In Figure 108, the average difference for each curve is plotted versus SNR and SJR for each of the 15 previously presented curves.

162
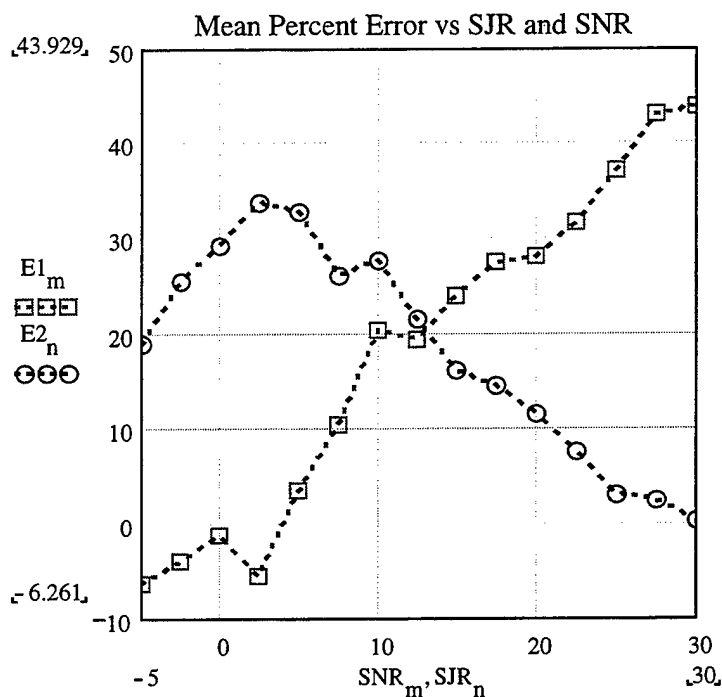
Figure 108. Mean percent difference as a function of SNR and SJR, respectively.

The two curves show how the mean difference varies with SNR and SJR. Each value of the mean difference is the average of the differences that correspond to the 15 points on each of the 15 curves for the symbol error probability as a function of SNR (with SJR as parameter) and SJR (with SNR as parameter), respectively.

	SYMBOL ERROR PROBABILITY	COHERENT 4FSK
1.	Root Mean Square Difference (%)	28.765
2.	Average Mean Difference (%)	18.161
3.	Maximum Difference (%)	60.64
4.	Minimum Difference (%)	-17.322
5.	Difference Deviation (%)	22.307

Table 34. Summary of the accuracy of the simulation for coherent 4FSK.

c) Results For 8FSK

The theoretical and the simulation symbol error probabilities for coherently detected 8FSK are presented in the Figures 109 and 110, respectively, as functions of the average SNR in dB with SJR as a parameter. The values for the signal-to-noise and signal-to-interference ratios were chosen from –5 dB to +30 dB in increments of 2.5 dB.
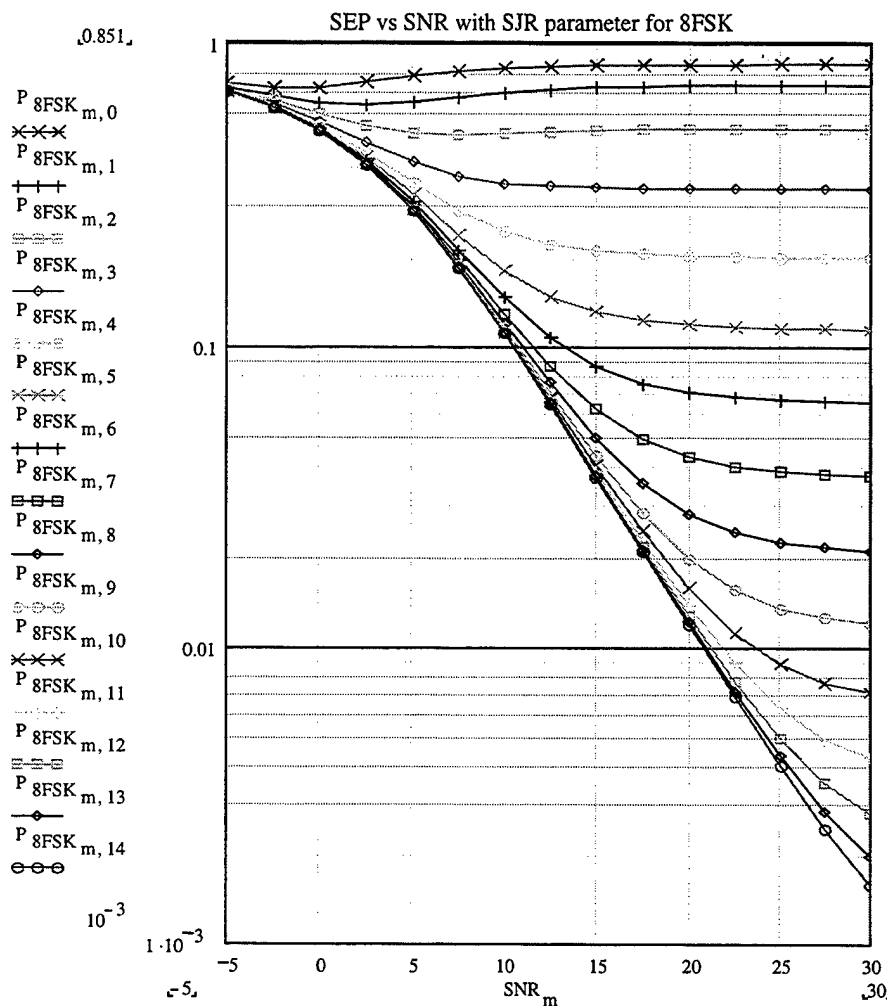

Figure 109. Theoretical symbol error probability versus SNR with SJR as a parameter, for coherent 8FSK, with Rician fading and R=1.
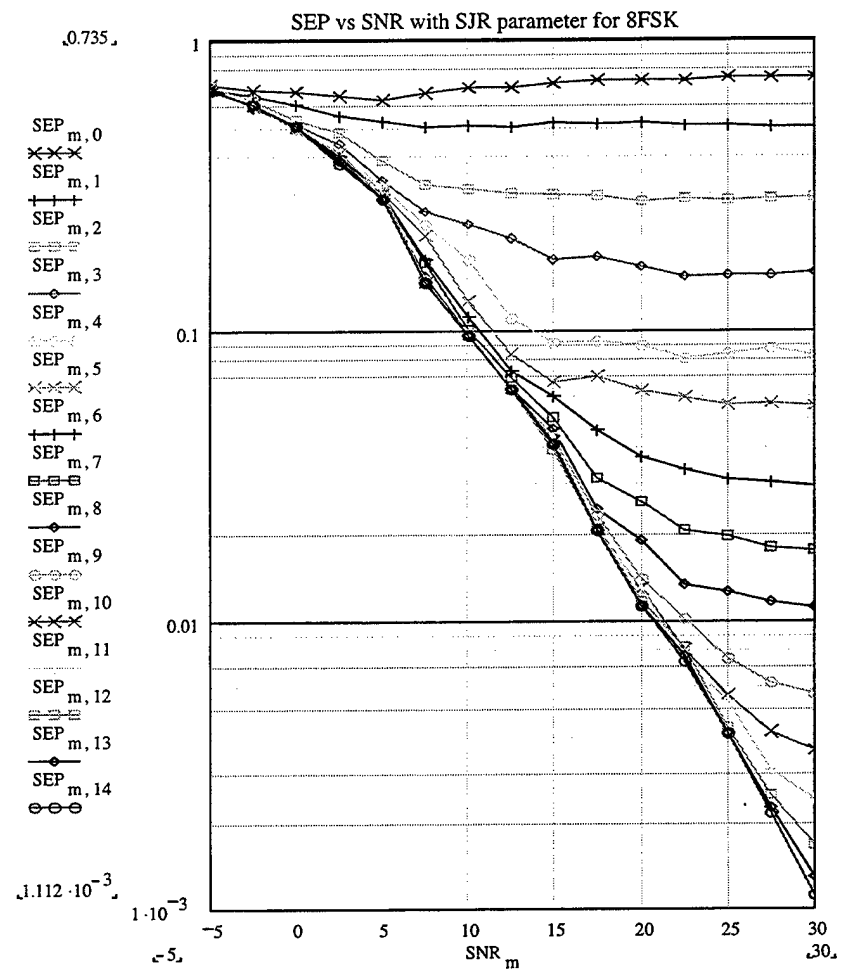
Figure 110. Simulation symbol error probability versus SNR with SJR as parameter

for coherent 8FSK, with Rician fading and R=1.

In Figures 111 and 112, respectively, the theoretical and simulation results

for the symbol error probability are presented as functions of SJR with SNR as a
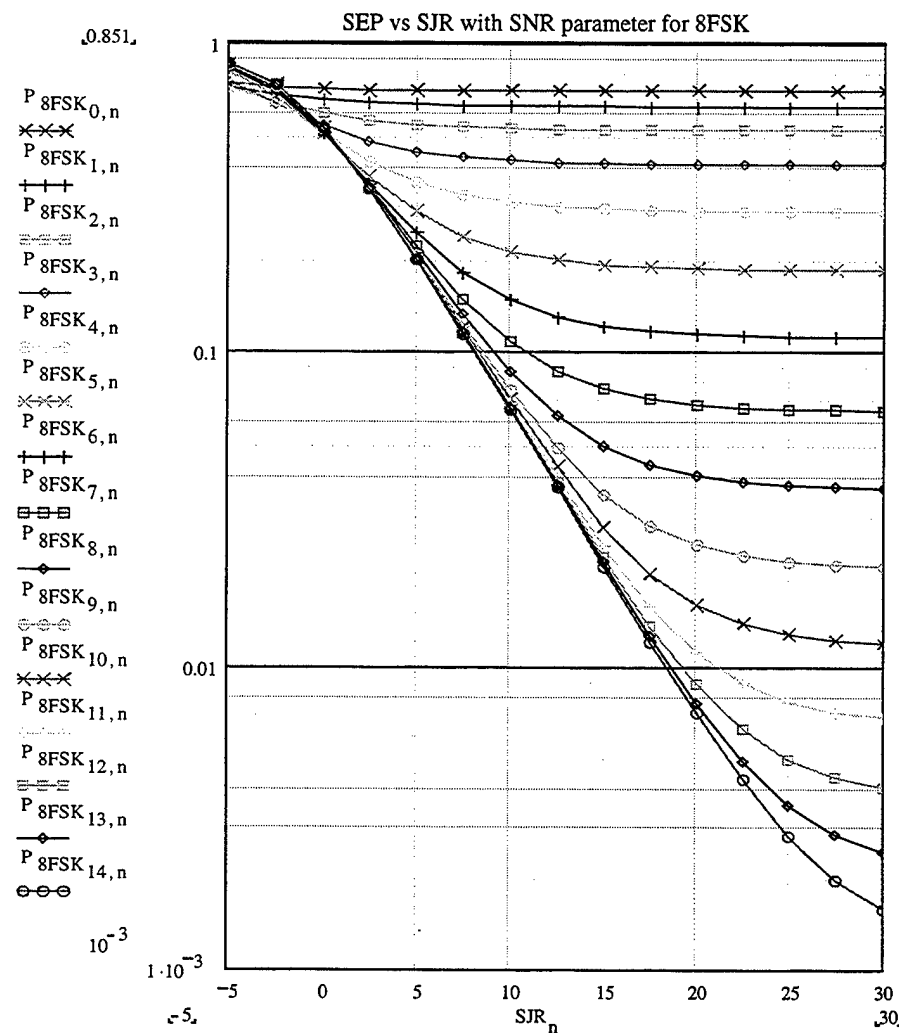
parameter.

Figure 111. Theoretical symbol error probability versus SJR with SNR as a parameter

for coherent 8FSK, with Rician fading and R=1.

We note again the dramatic increase in the symbol error probability due to

Rician fading and co-channel interference.
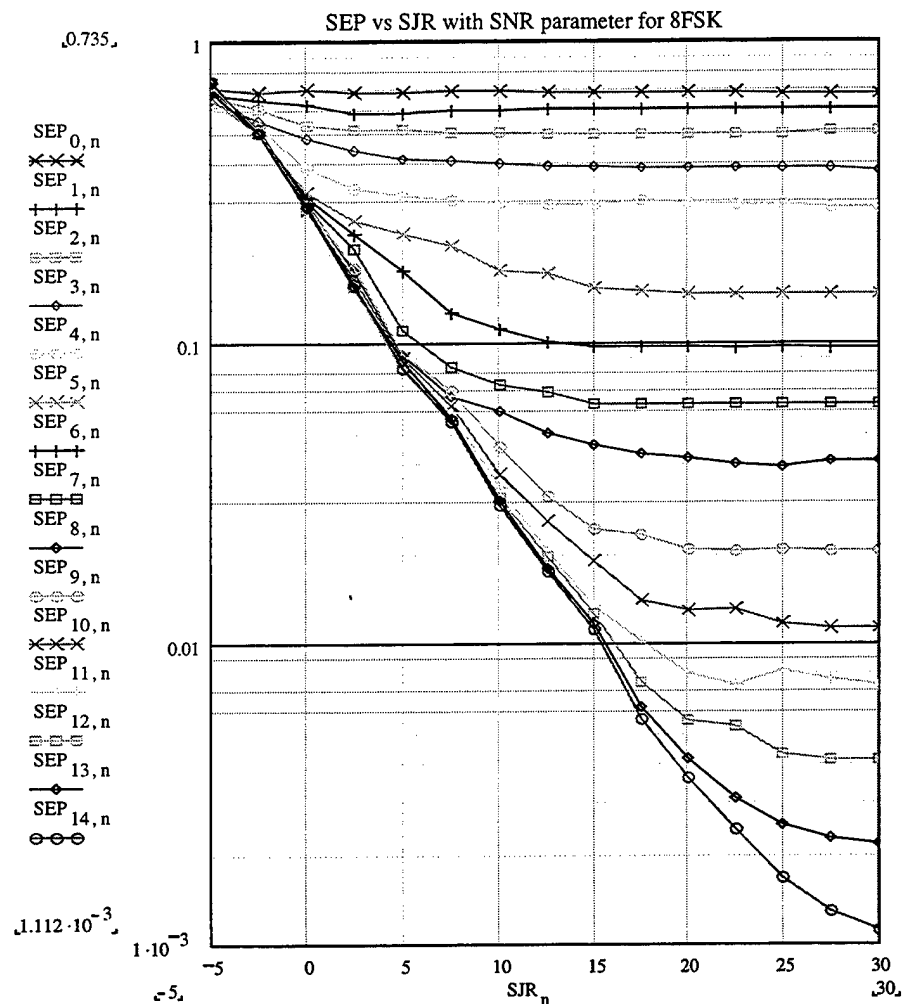
Figure 112. Simulation symbol error probability versus SJR with SNR as parameter

for coherent 8FSK, with Rician fading and R=1.

The relative difference (percent "error") between the theory and the

simulation is presented in Table 35. In Figure 113, the average difference for each curve

is plotted versus SNR and SJR for each of the 15 previously presented curves.

167
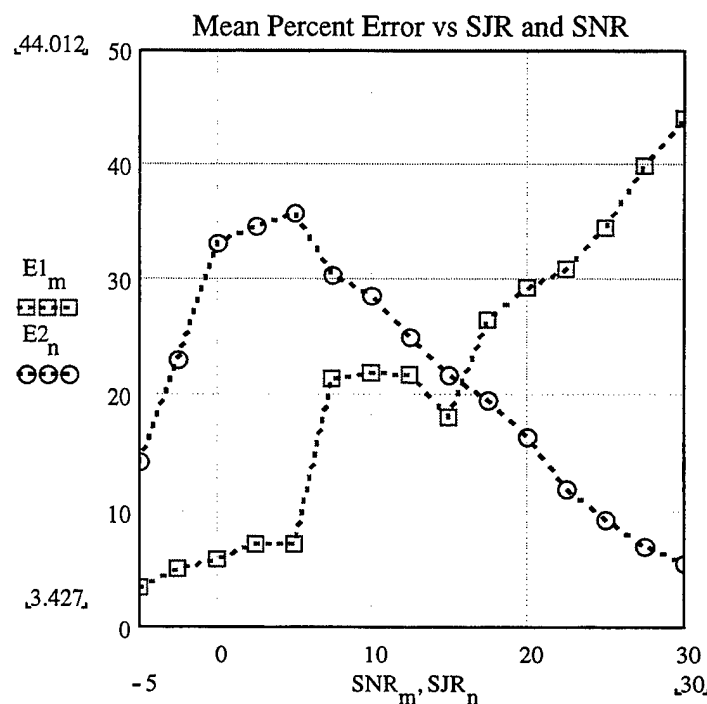
Figure 113. Mean percent difference as a function of SNR and SJR, respectively.

The two curves show how the mean difference varies with SNR and SJR. Each value of the mean difference is the average of the differences that correspond to the 15 points on each of the 15 curves for the symbol error probability as a function of SNR (with SJR as parameter) and SJR (with SNR as parameter), respectively.

	SYMBOL ERROR PROBABILITY	COHERENT 8FSK
1.	Root Mean Square Difference (%)	28.276
2.	Average Mean Difference (%)	21.138
3.	Maximum Difference (%)	60.009
4.	Minimum Difference (%)	-9.858
5.	Difference Deviation (%)	18.781

Table 35. Summary of the accuracy of the simulation for coherent 8FSK.

Observing the results for coherent detection of 2, 4, and 8FSK in a Rician

fading channel and affected by AWGN and co-channel interference, we note that the

simulation underestimates the theory for all of the cases of 2, 4 and 8FSK. The root mean

square difference (in percent) is about 27% (in average) and the mean percent difference

for all the cases is about 18%.

The average results for the coherent detection of 2, 4, and 8FSK are

presented in Table 36.

	SYMBOL ERROR PROBABILITY	AVERAGE RESULTS FOR COHERENT 2, 4, AND 8FSK
1.	Root Mean Square Difference (%)	27.19
2.	Average Mean Difference (%)	18.294
3.	Maximum Difference (%)	62.918
4.	Minimum Difference (%)	-17.784
5.	Difference Deviation (%)	20.01

Table 36. Average results for the coherent detection of 2, 4, and 8FSK.

D. RICIAN FADING CHANNEL – NON-COHERENT DETECTION

In this section, we derive the symbol error probability for non-coherent detection of MFSK signals transmitted over a frequency-nonselective, slowly fading Rician channel with AWGN and co-channel interference.

1. Theoretical Probability Of Symbol Error For Coherent Detection

The probability that the signal symbol will be received correctly is evaluated, again, separately for the two cases:

- **1st case**: the signal and the interference symbols are on the same branch.

- **2nd case**: the signal and the interference symbols are on different branches.

Then, combining the two cases, we evaluate the total symbol error probability.

a) The Signal And The Interference Symbols Are On The Same Branch

The conditional probability of symbol error for non-coherent, orthogonal MFSK with AWGN and co-channel interference has already been derived in (4.30) of Chapter IV.C:

$$P1(r) = \sum_{k=1}^{M-1} \frac{(M-1)!}{k! \cdot (M-1-k)!} \cdot (-1)^{k+1} \cdot \frac{1}{k+1} \cdot e^{\frac{-k \cdot (r+J)^2}{2 \cdot (k+1) \cdot \sigma^2}} \quad (5.37)$$

where:

J is the amplitude of the interfering MFSK signal and

r is the amplitude of the desired MFSK signal.

170

The above symbol error probability is conditioned on the amplitude r of the desired signal since the channel is modeled as a Rician fading channel. The amplitude r is a Rician random variable with the probability density function:

$$f(r) = \frac{r}{P_{dif}} \cdot e^{\frac{-\left(r^2 + 2 \cdot P_{dir}\right)}{2 \cdot P_{dif}}} \cdot I0\left(\frac{\sqrt{2 \cdot P_{dir}} \cdot r}{P_{dif}}\right) \tag{5.38}$$

where:

P_{dir} is the power of the direct signal component

P_{dif} is the power of the diffuse signal component.

Integrating the product of the conditional probability and the probability density function of the desired signal's amplitude r over all possible values of r, we obtain the unconditional probability of symbol error for this case:

$$P1 = \int_0^\infty \sum_{k=1}^{M-1} \frac{(M-1)!}{k! \cdot (M-1-k)!} \cdot (-1)^{k+1} \frac{1}{k+1} \cdot e^{\frac{-k \cdot (r+J)^2}{2 \cdot (k+1) \cdot P_{noise}}} \frac{r}{P_{dif}} \cdot e^{\frac{-\left(r^2 + 2 \cdot P_{dir}\right)}{2 \cdot P_{dif}}} \cdot I0\left(\frac{\sqrt{2 \cdot P_{dir}} \cdot r}{P_{dif}}\right) dr \tag{5.39}$$

Using the transformation:

$$\frac{r}{\sqrt{P_{dif}}} = y \tag{5.40}$$

we obtain (see also the closed form solution in Appendix 2):

$$P1 = \int_0^\infty \sum_{k=1}^{M-1} \frac{(M-1)!}{k! \cdot (M-1-k)!} \cdot \frac{(-1)^{k+1}}{(k+1)} \cdot e^{\frac{-k}{2 \cdot (k+1)} \cdot \left(\frac{\sqrt{P_{dif}} \cdot y + J}{\sqrt{P_{noise}}}\right)^2} \cdot e^{\frac{-1}{2}\left(y^2 + 2 \cdot \frac{P_{dir}}{P_{dif}}\right)} \cdot I0\left(2 \cdot \sqrt{\frac{P_{dir}}{P_{dif}}} \cdot y\right) \cdot y \, dy \tag{5.41}$$

171

The last integral must be evaluated numerically.

b)   The Signal And The Interference Symbols Are At Different Branches

The conditional probability of symbol error for this case has already been derived in (4.43) of Chapter IV.C:

$$P2(r)=1-\int_0^\infty \left(1-e^{-\frac{x^2}{2}}\right)^{M-2}\left[1-e^{-\frac{1}{2}\left(x^2+\frac{r^2}{\sigma^2}\right)}\cdot\sum_{p=0}^\infty \left(\frac{J}{\sigma\cdot x}\right)^p\cdot I_p\left(\frac{J\cdot x}{\sigma}\right)\right]e^{-\frac{1}{2}\left(x^2+\frac{r^2}{\sigma^2}\right)}\cdot I0\left(\frac{r\cdot x}{\sigma}\right)\cdot x\,dx \quad (5.42)$$

Integrating the product of the conditional probability of symbol error and the probability density function of the desired signal's amplitude r over all possible values of r, we get the unconditional probability of symbol error which, applying the transformation of (5.40), is given by:

$$P2=1-\frac{1}{\sqrt{2\cdot\pi}}\cdot\int_0^\infty\int_{-\infty}^\infty\left[\left[\left(1-e^{-\frac{x^2}{2}}\right)^{M-2}\left[1-e^{-\frac{1}{2}\left(x^2+\frac{J^2}{P_{noise}}\right)}\cdot\sum_{p=0}^\infty\left(\frac{J}{\sqrt{P_{noise}}\cdot x}\right)^p\cdot In\left(p,\frac{J}{\sqrt{P_{noise}}}\cdot x\right)\right]\right.\right.\left.\left.e^{-\frac{1}{2}\left(x^2+\frac{P_{dif}}{P_{noise}}\cdot y^2+y^2+2\frac{P_{dir}}{P_{dif}}\right)}\cdot I0\left(\sqrt{\frac{P_{dif}}{P_{noise}}}\cdot y\cdot x\right)\cdot I0\left(\sqrt{2\cdot\frac{P_{dir}}{P_{dif}}}\cdot y\right)\cdot x\cdot y\right]\right]dxdy(5.43)$$

The integral above must be evaluated numerically.

c)   Total Symbol Error Probability

The total symbol error probability, combining the two cases is given by:

$$P_{total}=\frac{1}{M}\cdot P1+\frac{M-1}{M}\cdot P2 \quad (5.44)$$

172

where 1/M is the probability that the transmitted and the interfering symbols are at the same branch and (M-1)/M is the probability that the transmitted and the interfering symbols are at different branches.

Substituting equation (5.30) and (5.34) into the equation (5.41) and (5.43), we get for the symbol error probability the following expressions:

$$P1=\int_0^\infty \left[\sum_{k=1}^{M-1} \frac{(M-1)!}{k!\cdot(M-1-k)!}\cdot\frac{(-1)^{k+1}}{(k+1)} \cdot e^{\frac{-k}{2\cdot(k+1)}\left[\frac{1}{\sqrt{1+R}}\cdot10^{\frac{SNR}{20}}\cdot y+\sqrt{2}\cdot10^{\frac{SNR-SJR}{20}}\right]^2} \cdot e^{\frac{-1}{2}\left(y^2+2\cdot R\right)}\cdot I0\left(\sqrt{2\cdot R}\cdot y\right)\cdot y \right] dy \quad (5.45)$$

$$P2=1-\int_0^\infty\int_0^\infty \left[\left(1-e^{\frac{-x^2}{2}}\right)^{M-2} \left[1-e^{\frac{-1}{2}\left(x^2+2\cdot10^{\frac{SNR-SJR}{10}}\right)}\cdot\sum_{p=0}^\infty 10^{\frac{(SNR-SJR)\cdot p}{20}}\frac{\left(\sqrt{2}\right)^p}{x^p}\cdot I n\left(p,\sqrt{2}\cdot10^{\frac{SNR-SJR}{20}}\cdot x\right)\right] \right. \\ \left. e^{\frac{-1}{2}\left(x^2+\frac{1}{1+R}\cdot10^{\frac{SNR}{10}}\cdot y^2\right)}\cdot I0\left(\frac{1}{\sqrt{1+R}}\cdot10^{\frac{SNR}{20}}\cdot y\cdot x\right)\cdot e^{\frac{-1}{2}\left(y^2+2\cdot R\right)}\cdot I0\left(\sqrt{2\cdot R}\cdot y\right)\cdot x\cdot y \right] dxdy (5.46)$$

The above integrals have to be evaluated numerically.

2. Simulink Model and Block Analysis

The schematic diagram of the Simulink model, which has been developed for the simulation of non-coherent MFSK with AWGN and co-channel interference in a Rician fading channel, is the same as the block diagram shown in Figure 95 for coherent detection except that the block 'Coh MFSK demod baseband' has been replaced by the block 'Non-coherent MFSK demod baseband'.

3. Simulation Analysis And Performance Verification

In this section, simulation results are presented in order to verify the performance of non-coherent detection of MFSK corrupted by AWGN and co-channel interference in a Rician fading channel. Each simulation ran until at least 100 errors were observed. The data sequences were limited to 10^6 symbols for each simulation in order to prevent "out of memory" errors. The simulation sequence was repeated until a sufficient number of errors were counted.

a) Results For 2FSK

The theoretical and the simulation symbol error probabilities for non-coherently detected 2FSK are presented in Figures 114 and 115, respectively, as functions of average SNR in dB with SJR as a parameter. The values for the signal-to-noise and signal-to-interference ratios were chosen from −5 dB to +16 dB in increments of 1.5 dB.
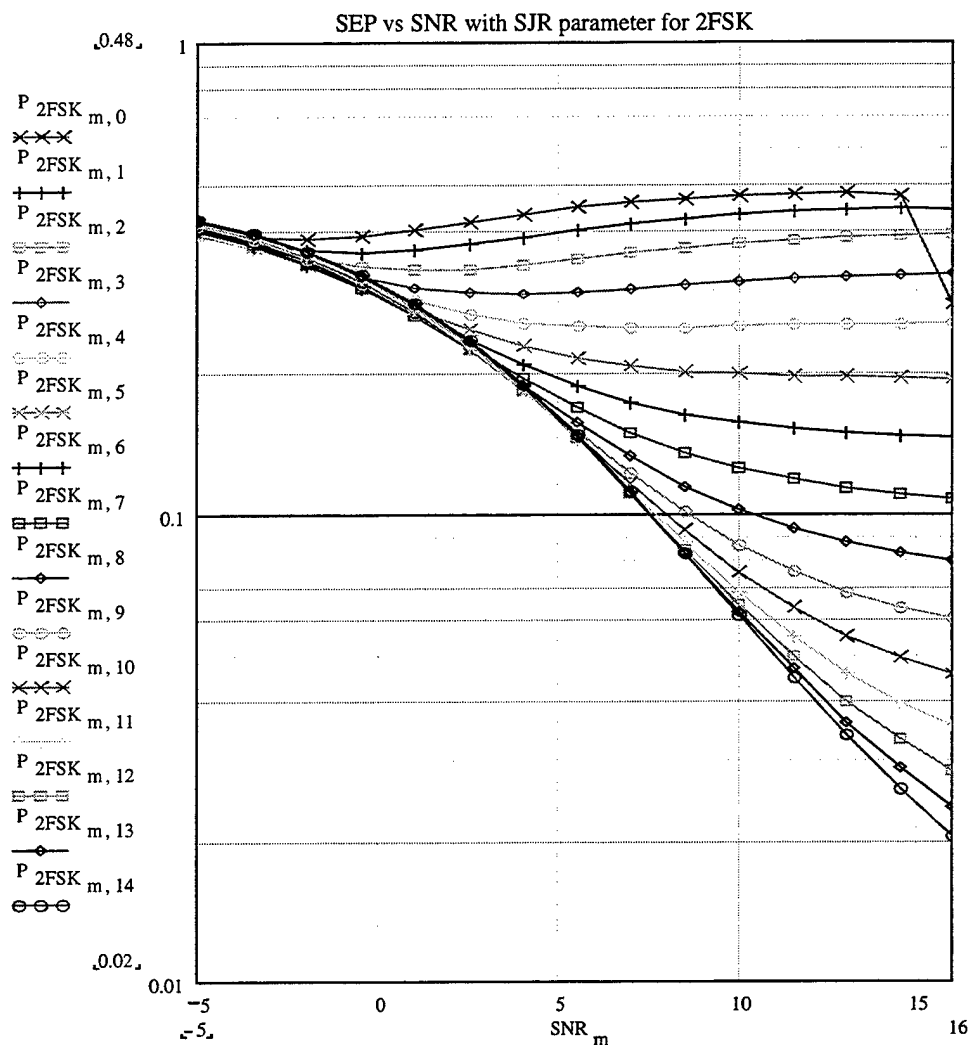
Figure 114. Theoretical symbol error probability versus SNR with SJR as a parameter

for non-coherent 2FSK, with Rician fading and R=1.

As evident from Figure 114 and 115, the curves tend to become flat as

SNR increases; that is, they converge to a constant value determined by the value of SJR.

The consequence of the signal fading is that the symbol error probability does not

decrease as fast with the increase in either SNR (along a curve) or SJR (from curve to

curve) as it does for the case of non-fading signals.

175
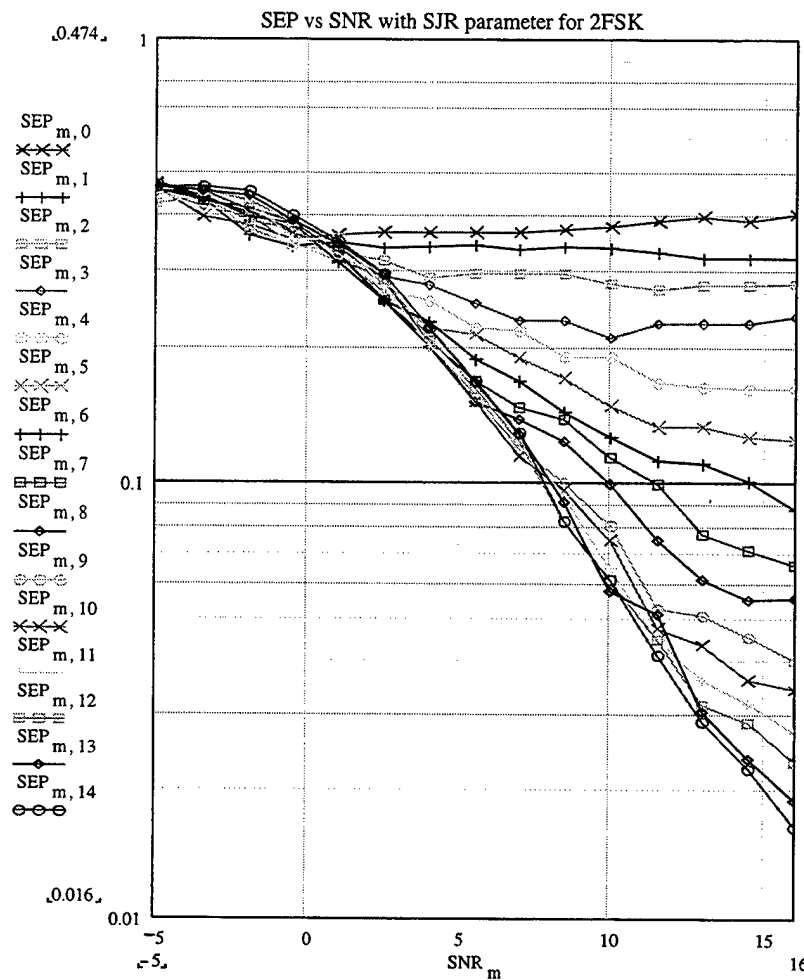
Figure 115. Simulation symbol error probability versus SNR with SJR as a parameter for non-coherent 2FSK, with Rician fading and R=1.

In Figures 116 and 117, respectively, the theoretical and simulation results for the symbol error probability are presented as functions of SJR with SNR as a parameter.
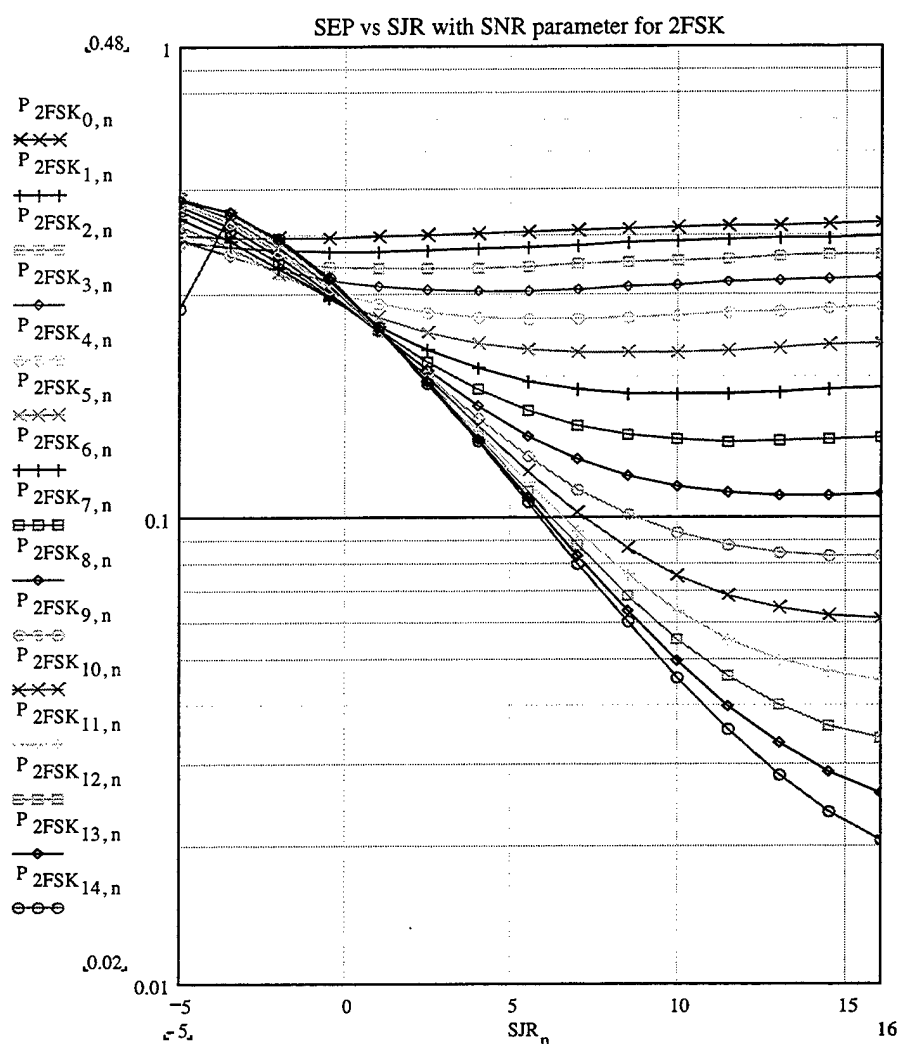
Figure 116. Theoretical symbol error probability versus SJR with SNR as a parameter for non-coherent 2FSK, with Rician fading and R=1.

We note again the dramatic increase in the symbol error probability due to Rician fading and co-channel interference.
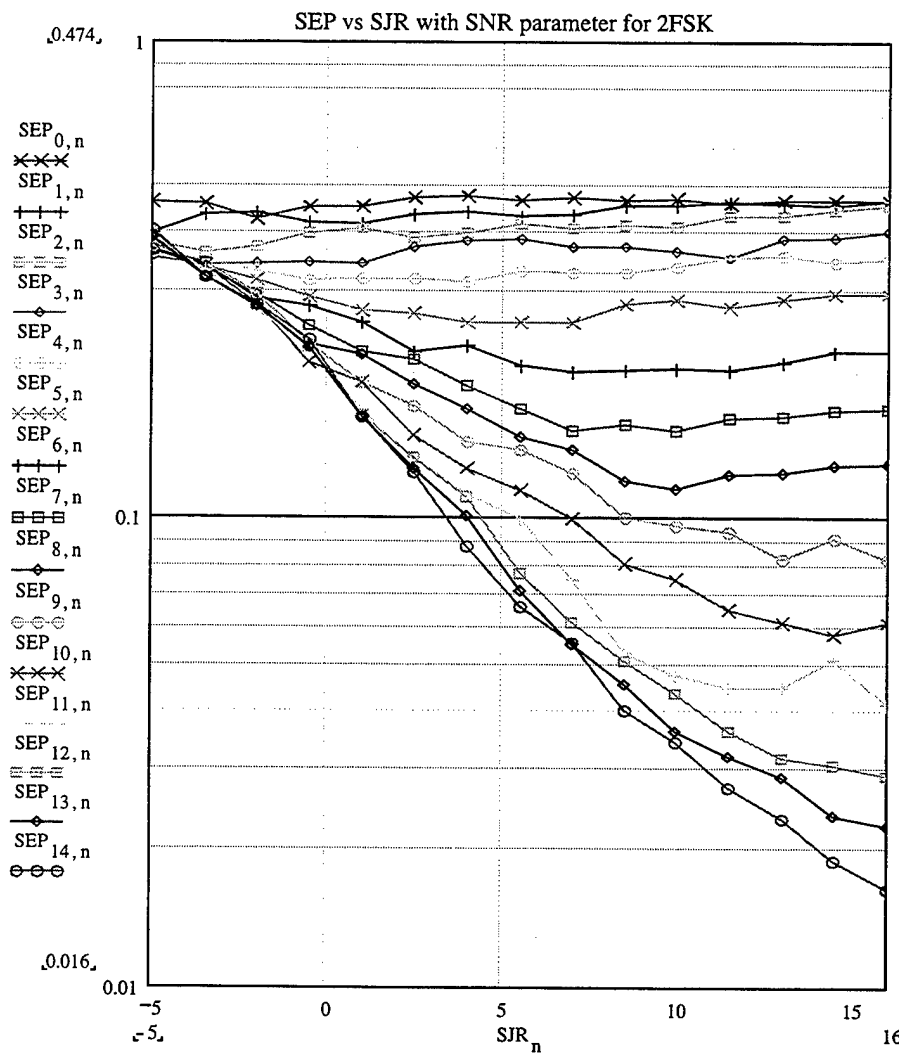
Figure 117. Simulation symbol error probability versus SJR with SNR as a parameter

for non-coherent 2FSK, with Rician fading and R=1.

The relative difference (percent "error") between the theory and the

simulation is presented in Table 37. In Figure 118, the average difference for each curve

is plotted versus SNR and SJR for each of the 15 previously presented curves.

178
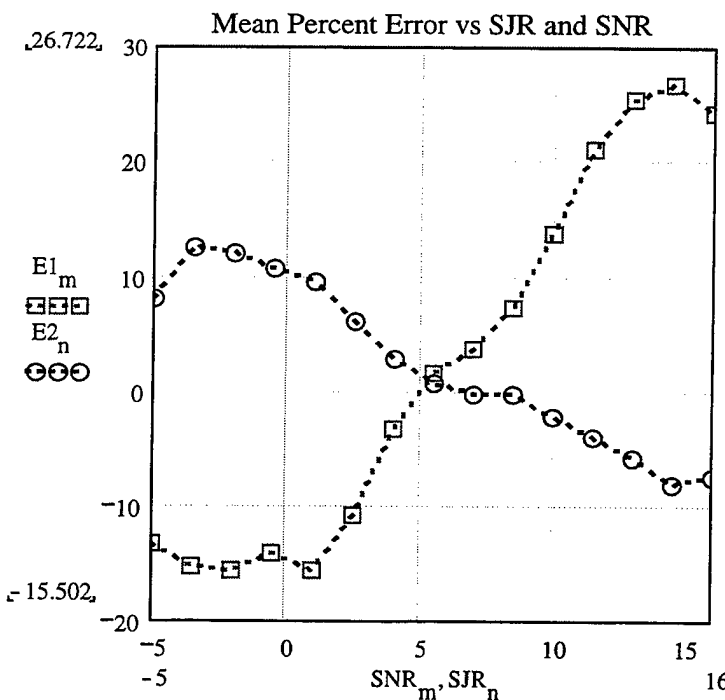
Figure 118. Mean percent difference as a function of SNR and SJR, respectively.

The two curves show how the mean difference varies with SNR and SJR. Each value of the mean difference is the average of the differences that correspond to the 15 points on each of the 15 curves for the symbol error probability as a function of SNR (with SJR as parameter) and SJR (with SNR as parameter), respectively.

	SYMBOL ERROR PROBABILITY	NON-COHERENT 2FSK
1.	Root Mean Square Difference (%)	19.441
2.	Average Mean Difference (%)	2.461
3.	Maximum Difference (%)	39.575
4.	Minimum Difference (%)	-45.235
5.	Difference Deviation (%)	19.285

Table 37. Summary of the accuracy of the simulation for non-coherent 2FSK.

b) Results For 4FSK

The theoretical and the simulation symbol error probabilities for non-coherently detected 4FSK are presented in the Figures 119 and 120, respectively, as functions of average SNR in dB with SJR as parameter. The values for the signal-to-noise and signal-to-interference ratios were chosen from −5 dB to +16 dB in increments of 1.5 dB.
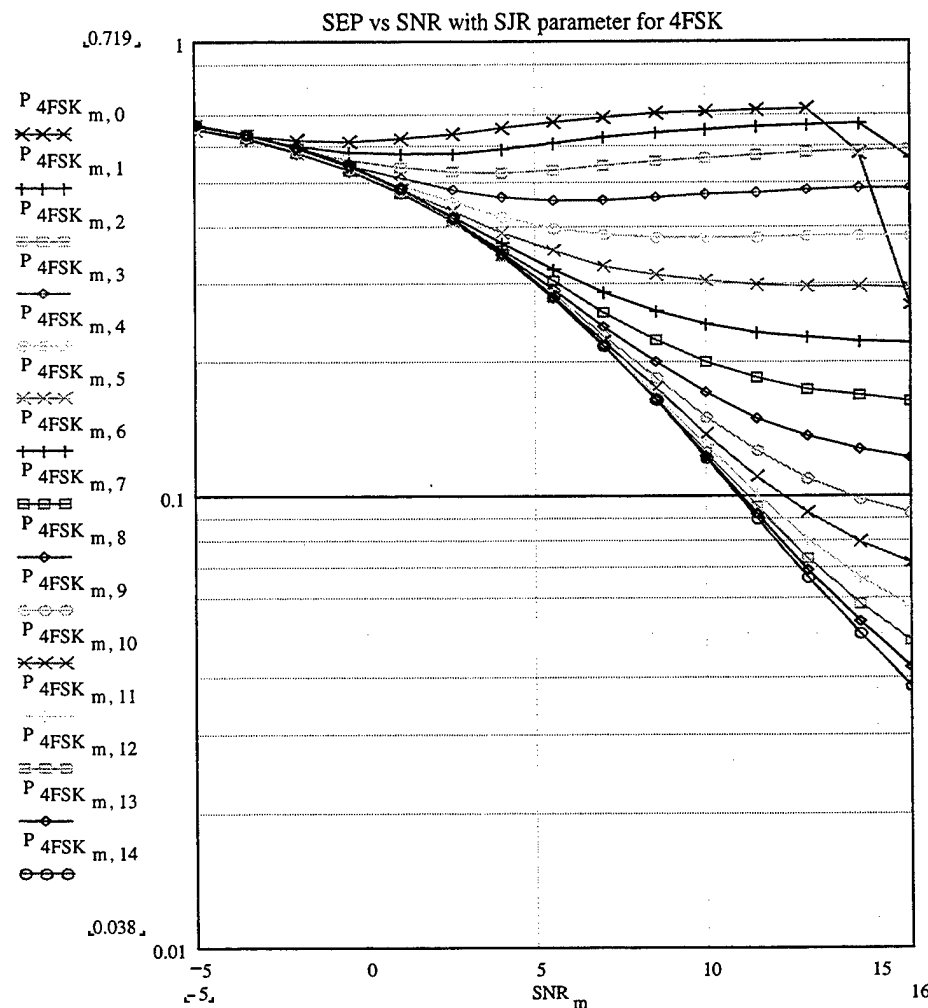

Figure 119. Theoretical symbol error probability versus SNR with SJR as a parameter for non-coherent 4FSK, with Rician fading and R=1.
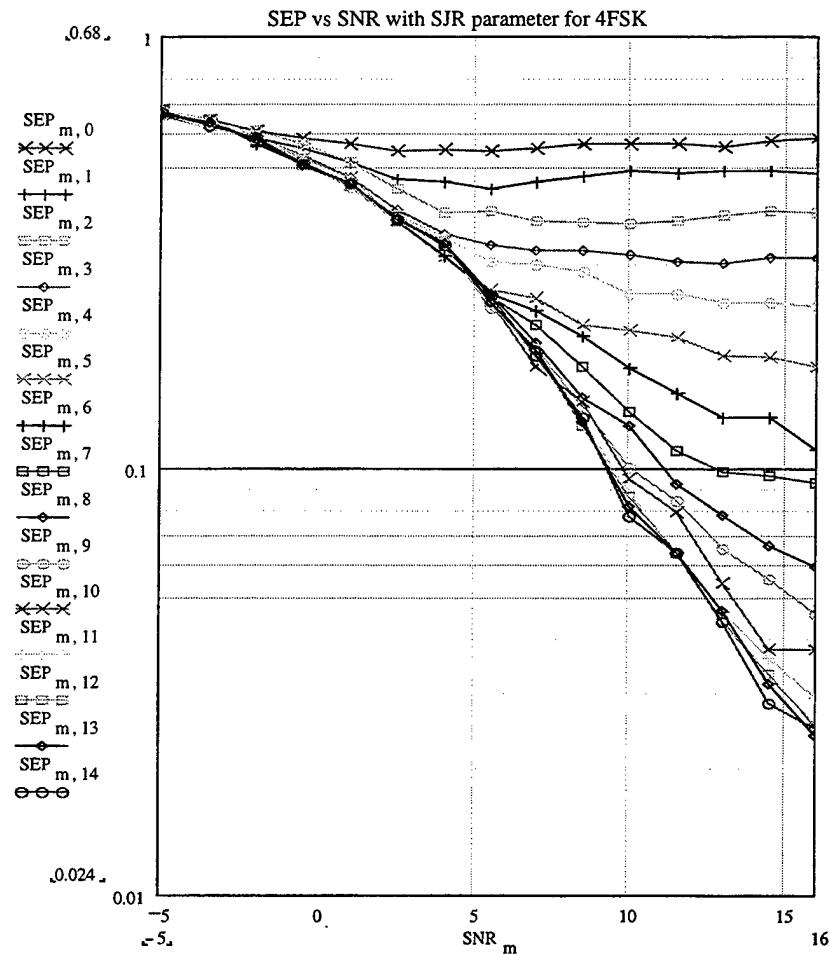
Figure 120. Simulation symbol error probability versus SNR with SJR as parameter for non-coherent 4FSK, with Rician fading and R=1.

In Figures 121 and 122, respectively, the theoretical and simulation results for the symbol error probability are presented as functions of SJR with SNR as a parameter.

181
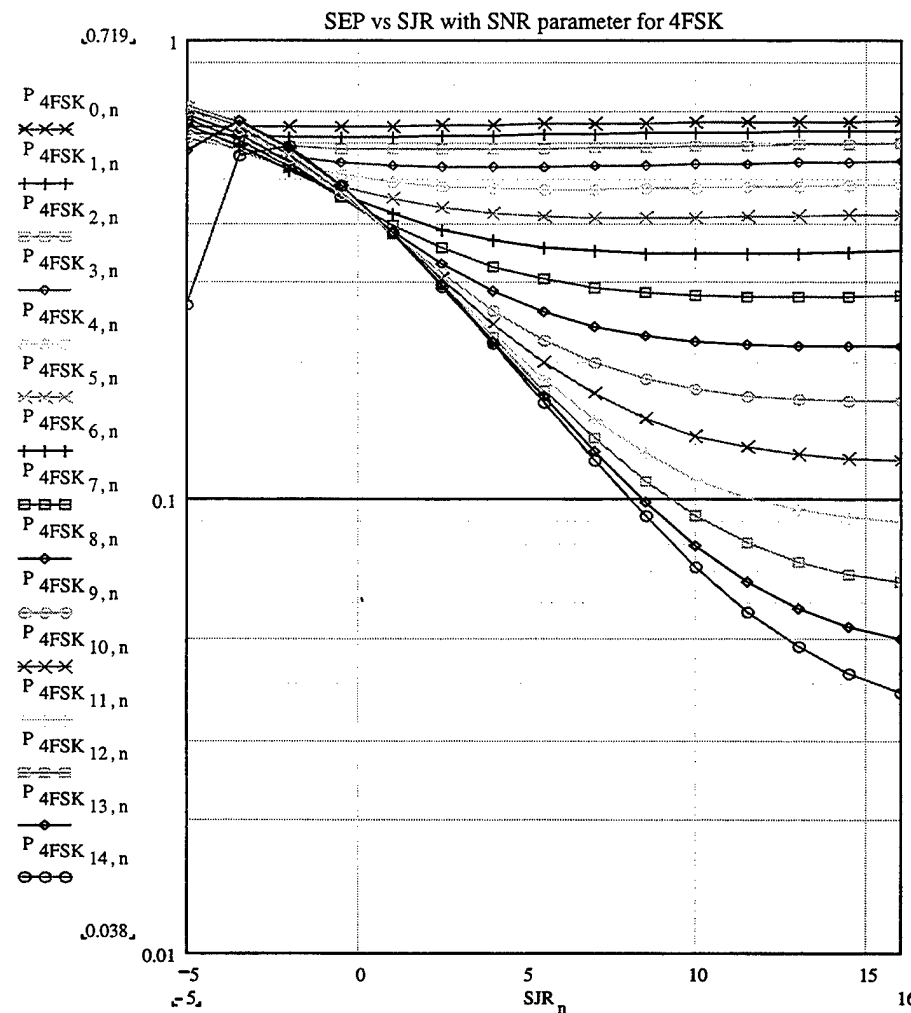
Figure 121. Theoretical symbol error probability versus SJR with SNR as a parameter for non-coherent 4FSK, with Rician fading and R=1.

We note again the dramatic increase in the symbol error probability due to Rician fading and co-channel interference.
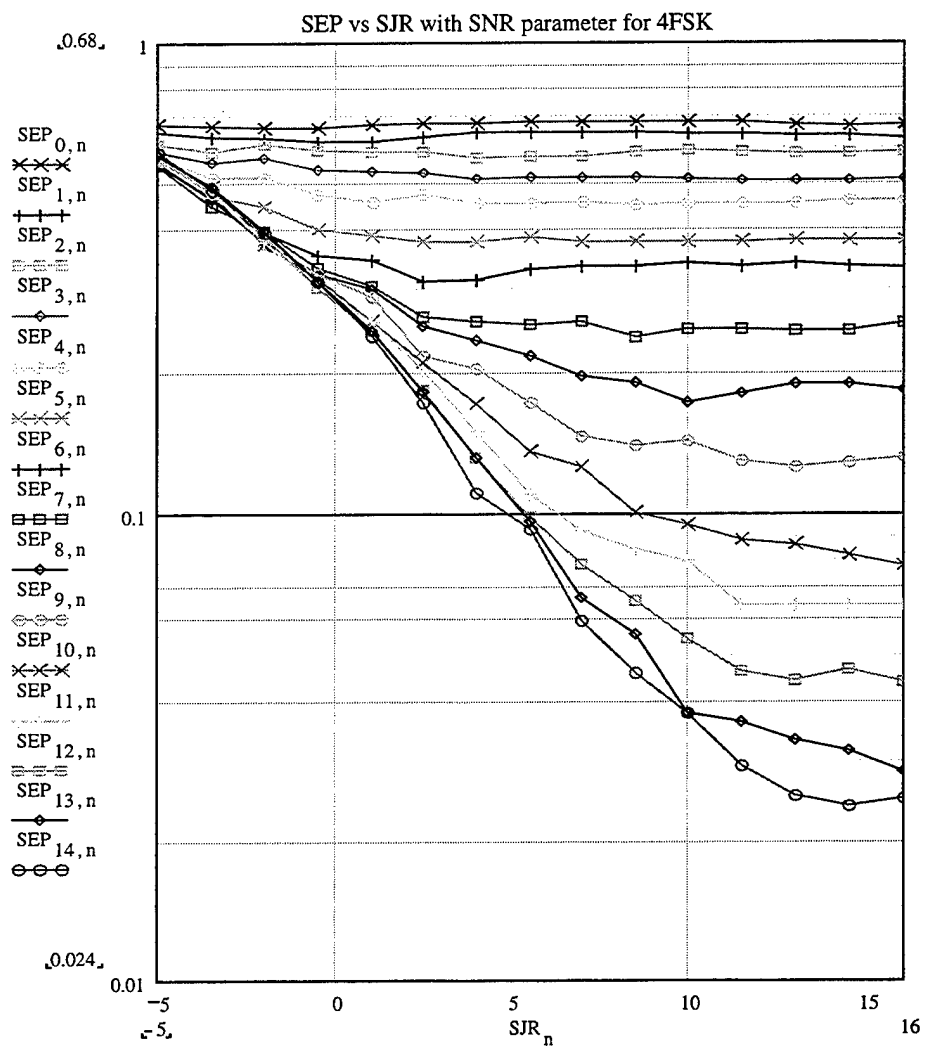
Figure 122. Simulation symbol error probability versus SJR with SNR as a parameter for non-coherent 4FSK, with Rician fading and R=1.

The relative difference (percent "error") between the theory and the simulation is presented in Table 38. In Figure 123, the average difference for each curve is plotted versus SNR and SJR for each of the 15 previously presented curves.
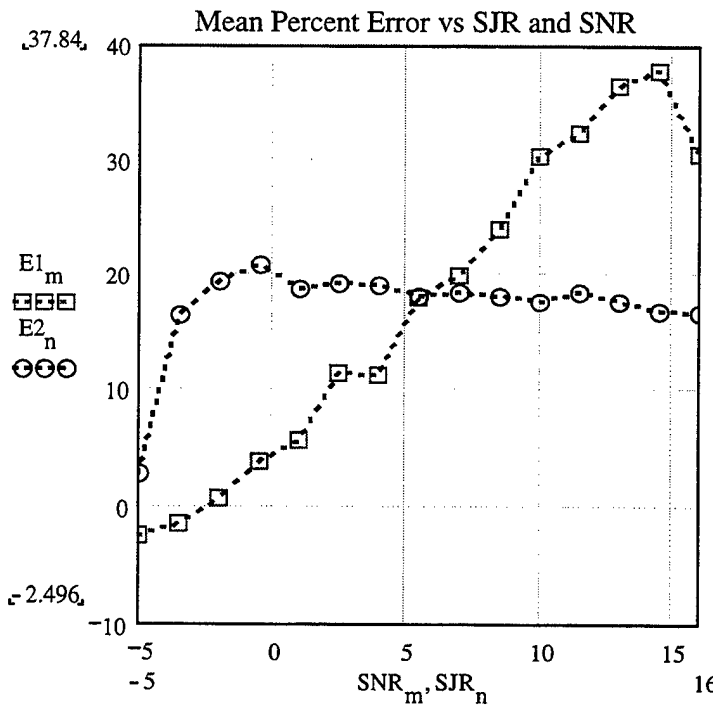
Figure 123. Mean percent difference as a function of SNR and SJR, respectively.

The two curves show how the mean difference varies with SNR and SJR. Each value of the mean difference is the average of the differences that correspond to the 15 points on each of the 15 curves for the symbol error probability as a function of SNR (with SJR as parameter) and SJR (with SNR as parameter), respectively.

	SYMBOL ERROR PROBABILITY	NON-COHERENT 4FSK
1.	Root Mean Square Difference (%)	25.018
2.	Average Mean Difference (%)	17.252
3.	Maximum Difference (%)	52.157
4.	Minimum Difference (%)	-119.047
5.	Difference Deviation (%)	18.119

Table 38. Summary of the accuracy of the simulation for non-coherent 4FSK.

184

c) Results For 8FSK

The theoretical and the simulation symbol error probabilities for non-coherently detected 8FSK are presented in the Figures 124 and 125, respectively, as functions of average SNR in dB with SJR as a parameter. The values for the signal-to-noise and signal-to-interference ratios were chosen from –5 dB to +16 dB in increments of 1.5 dB.
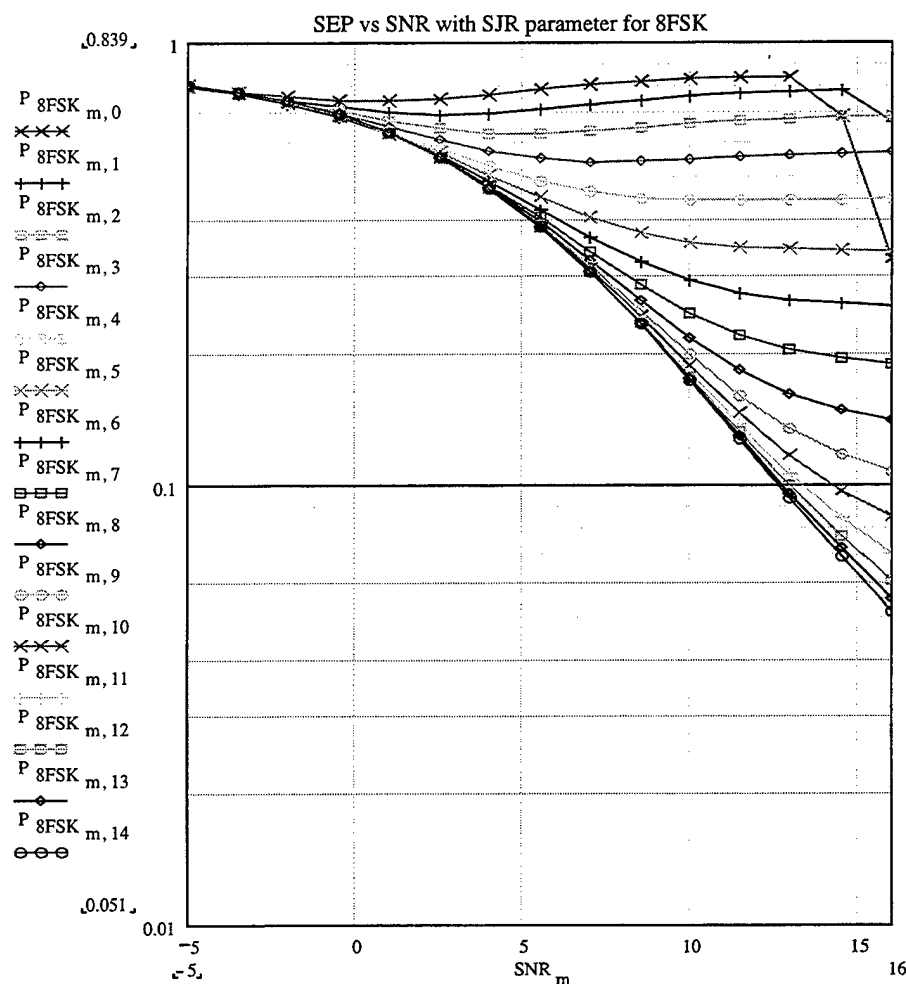

Figure 124. Theoretical symbol error probability versus SNR with SJR as a parameter for non-coherent 8FSK, with Rician fading and R=1.
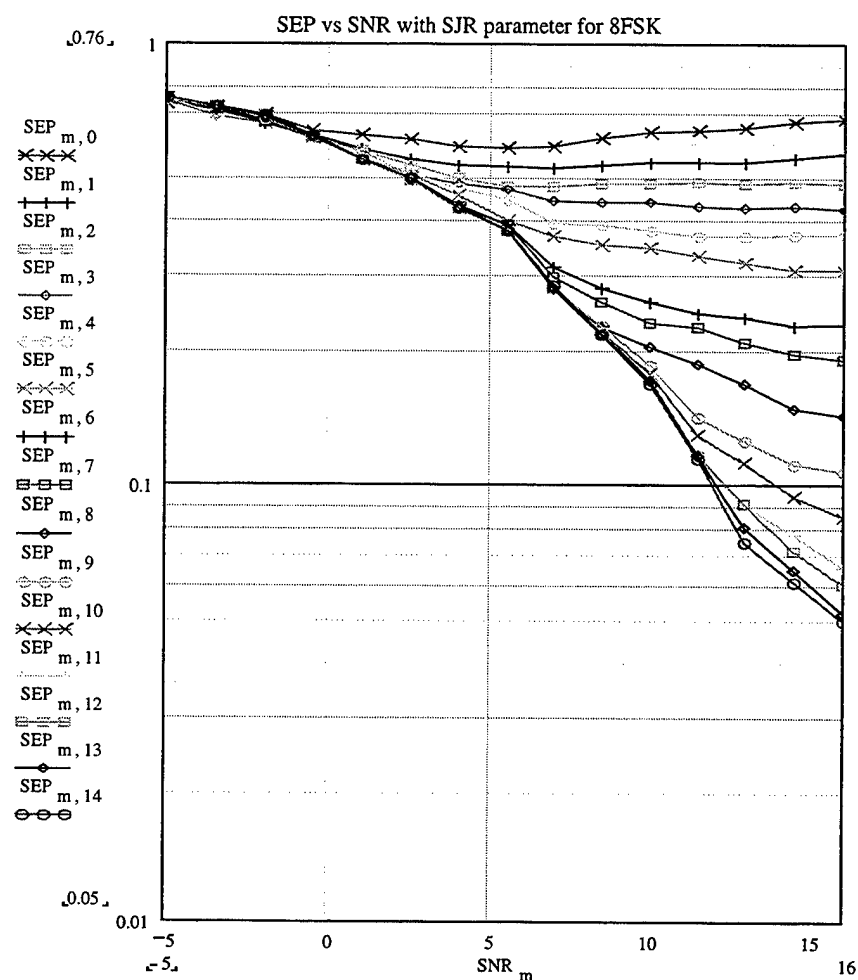
Figure 125. Simulation symbol error probability versus SNR with SJR as a parameter

for non-coherent 8FSK, with Rician fading and R=1.

In Figures 126 and 127, respectively, the theoretical and simulation results

for the symbol error probability are presented as functions of SJR with SNR as a

parameter.

186
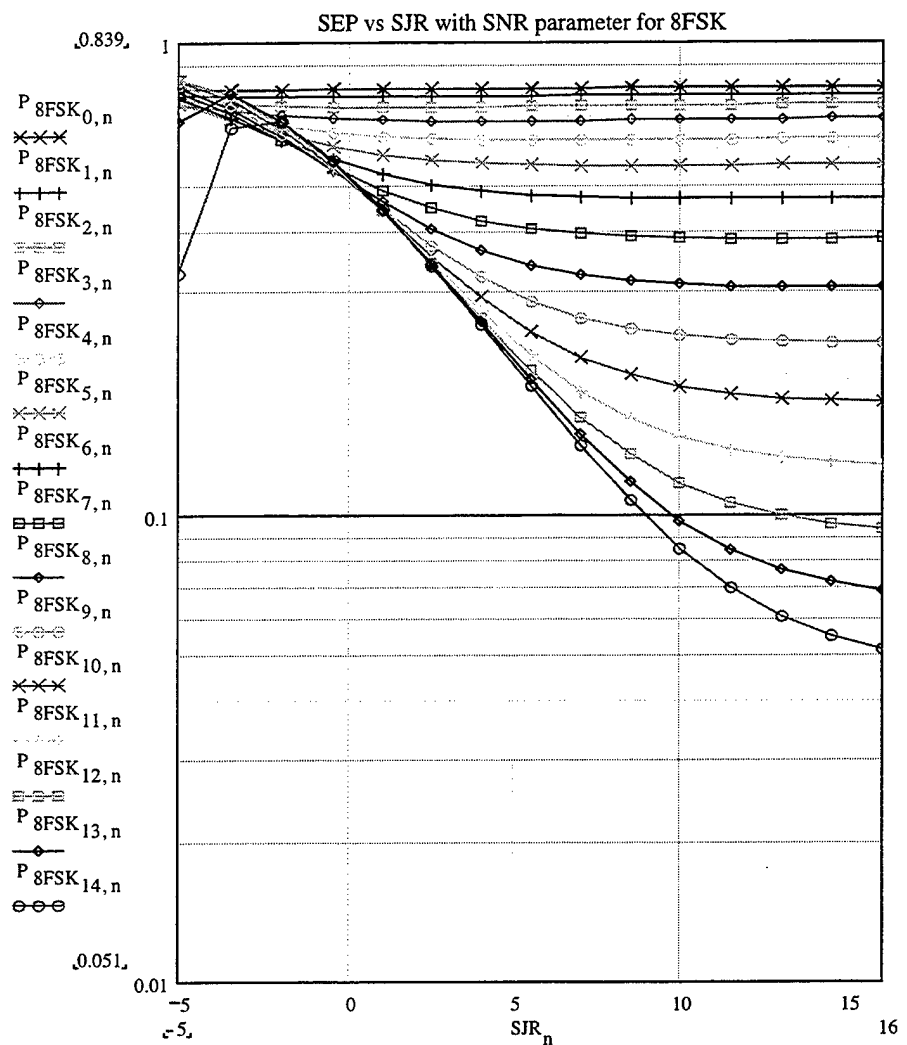
Figure 126. Theoretical symbol error probability versus SJR with SNR as a parameter for non-coherent 8FSK, with Rician fading and R=1.

We note again the dramatic increase in the symbol error probability due to Rician fading and co-channel interference.
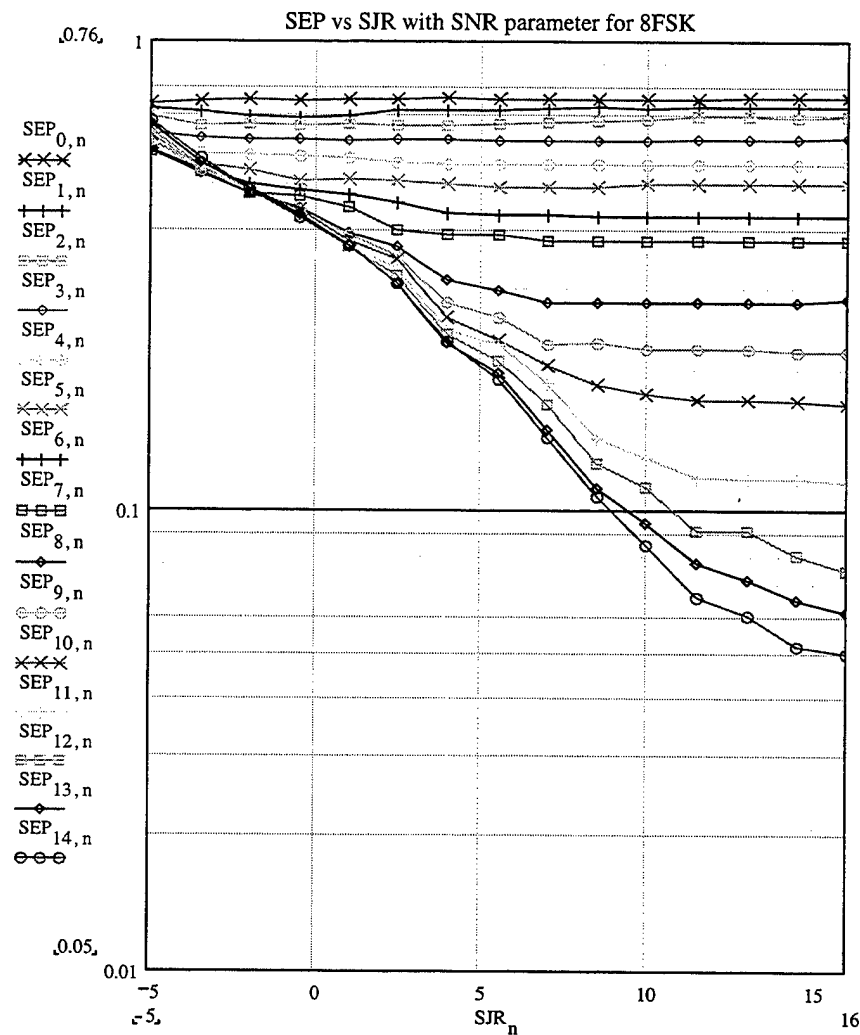
Figure 127. Simulation symbol error probability versus SJR with SNR as a parameter for non-coherent 8FSK, with Rician fading and R=1.

The relative difference (percent "error") between the theory and the simulation is presented in Table 39. In Figure 128, the average difference for each curve is plotted versus SNR and SJR for each of the 15 previously presented curves.

188
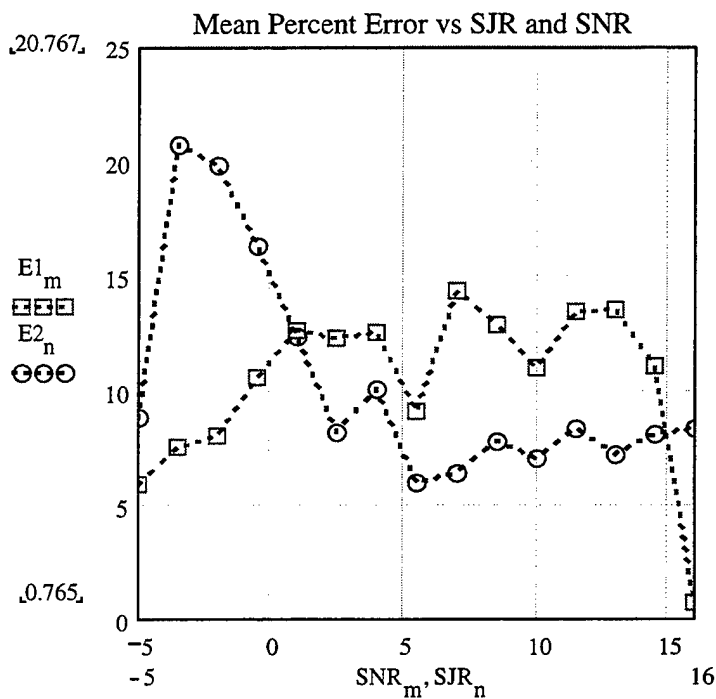
Figure 128. Mean percent difference as a function of SNR and SJR, respectively.

The two curves show how the mean difference varies with SNR and SJR. Each value of the mean difference is the average of the differences that correspond to the 15 points on each of the 15 curves for the symbol error probability as a function of SNR (with SJR as parameter) and SJR (with SNR as parameter), respectively.

	SYMBOL ERROR PROBABILITY	NON-COHERENT 8FSK
1.	Root Mean Square Difference (%)	14.848
2.	Average Mean Difference (%)	10.402
3.	Maximum Difference (%)	30.315
4.	Minimum Difference (%)	-108.758
5.	Difference Deviation (%)	10.596

Table 39. Summary of the accuracy of the simulation for non-coherent 8FSK.

189

Observing the results for non-coherent detection of 2, 4, and 8FSK in a Rician fading channel and affected by AWGN and co-channel interference, we note that the simulation underestimates the theory for all of the cases of 2, 4, and 8FSK. The root mean square difference (in percent) is about 27% (in average) and the mean percent difference for all the cases is about 18%.

The average results for the non-coherent detection of 2, 4, and 8FSK are presented in Table 40.

	SYMBOL ERROR PROBABILITY	AVERAGE RESULTS FOR NON-COHERENT 2, 4, AND 8FSK
1.	Root Mean Square Difference (%)	19.769
2.	Average Mean Difference (%)	10.038
3.	Maximum Difference (%)	40.682
4.	Minimum Difference (%)	-91.013
5.	Difference Deviation (%)	16

Table 40. Average results for the non-coherent detection of 2, 4, and 8FSK.

VI. MFSK SIGNAL CORRUPTED BY AWGN AND CO-CHANNEL INTERFERENCE IN A FADING CHANNEL THAT AFFECTS BOTH THE DESIRED AND THE INTERFERING SIGNAL

In this chapter we derive the theoretical symbol error probability for MFSK with AWGN and co-channel interference and operating in a fading channel. The co-channel interference is represented by another MFSK signal added to the desired MFSK signal. We study cases of both coherent and non-coherent detection for 2FSK, 4FSK, and 8FSK and assume that the fading channel affects both the desirable MFSK signal and the interfering one. Two separate cases of channel fading are examined; a frequency-nonselective, slowly fading Rayleigh channel and a frequency-nonselective, slowly fading Rician channel.

A. RAYLEIGH FADING CHANNEL – COHERENT DETECTION

In this section, we derive the symbol error rate for MFSK signals transmitted over a frequency-nonselective, slowly fading Rayleigh channel in the presence of AWGN and co-channel interference. The frequency-nonselective, slowly fading channel results in multiplicative distortion of the MFSK transmitted signal and also of the MFSK interfering signal. The condition that the channel fades slowly implies that the multiplicative process may be considered as a constant during at least one symbol time interval. Furthermore, we assume that the channel fading is sufficiently slow such that the phase shift introduced by the channel can be estimated from the received signal without error.

191

1.   Theoretical Probability Of Symbol Error For Coherent Detection

The probability that the signal symbol will be received correctly is equal to the probability that:

- **1st case**: the signal and the interference symbols are on the same branch and that the noise in any of the remaining M-1 branches does not exceed the sum of signal and interference symbols, and

- **2nd case**: the signal and the interference symbols are on different branches and neither the sum of the interference and noise nor the noise in any of the remaining M-2 branches exceeds the signal.

a)   The Signal And The Interference Symbols Are On The Same Branch

The conditional probability of symbol error for coherent, orthogonal MFSK Rayleigh fading signal when AWGN and co-channel interference are present has been determined in the preceding Chapter V.A, equation (5.5):

$$P1 = 1 - \frac{1}{\sqrt{2 \cdot \pi}} \cdot \int_0^\infty \int_{-\infty}^\infty e^{-\frac{\left(x^2 + y^2\right)}{2}} \cdot \left(1 - Q\left(x + y \cdot \frac{\sqrt{P_{sig}}}{\sqrt{P_{noise}}} + \frac{r_j}{\sqrt{P_{noise}}}\right)\right)^{M-1} \cdot y \, dx \, dy \qquad (6.1)$$

where:

r_j is the amplitude of the interfering MFSK signal.

This symbol error probability is conditioned on the amplitude r_j of the interfering signal, since the interfering signal is affected by the Rayleigh fading channel.

The amplitude r_j of the interfering signal is a Rayleigh random variable with the probability density function:

$$f\left(r_j, P_{jam}\right) = \frac{r_j}{P_{jam}} \cdot e^{\frac{-r_j^2}{2 \cdot P_{jam}}} \tag{6.2}$$

where P_{jam} is the symbol power of the fading interfering signal.

Integrating the product of the conditional probability of symbol error and the probability density function of the interfering signal's amplitude r_j over all possible values of r_j, we obtain the unconditional probability of symbol error for this case:

$$P_1 = 1 - \int_0^\infty \int_0^\infty \int_{-\infty}^\infty \frac{1}{\sqrt{2 \cdot \pi}} \cdot e^{\frac{-(x^2+y^2)}{2}} \cdot \left(1 - Q\left(x + \frac{\sqrt{P_{sig}}}{\sqrt{P_{noise}}} \cdot y + \frac{r_j}{\sqrt{P_{noise}}}\right)\right)^{M-1} \frac{r_j}{P_{jam}} \cdot e^{\frac{-r_j^2}{2 \cdot P_{jam}}} \cdot y \, dx \, dy \, dr_j \tag{6.3}$$

Using the transformation:

$$\frac{r_j}{\sqrt{P_{jam}}} = z \tag{6.4}$$

we obtain:

$$P_1 = 1 - \int_0^\infty \int_0^\infty \int_{-\infty}^\infty \frac{1}{\sqrt{2 \cdot \pi}} \cdot e^{\frac{-(x^2+y^2+z^2)}{2}} \cdot \left(1 - Q\left(x + \frac{\sqrt{P_{sig}}}{\sqrt{P_{noise}}} \cdot y + \frac{\sqrt{P_{jam}}}{\sqrt{P_{noise}}} \cdot z\right)\right)^{M-1} \cdot y \cdot z \, dx \, dy \, dz \tag{6.5}$$

This triple integral has to be evaluated numerically.

193

b) The Signal And The Interference Symbols Are On Different Branches

The conditional probability of symbol error for this case has already been obtained in equation (5.8) of Chapter V.A:

$$P2\left(r_j\right) = 1 - \frac{1}{\sqrt{2\cdot\pi}} \cdot \int_0^\infty \int_{-\infty}^\infty \left(1 - Q\left(x + y\cdot\frac{\sqrt{P_{sig}}}{\sqrt{P_{noise}}}\right)\right)^{M-2} \cdot \left(1 - Q\left(x + \frac{y\cdot\sqrt{P_{sig}} - r_j}{\sqrt{P_{noise}}}\right)\right) \cdot e^{\frac{-\left(x^2+y^2\right)}{2}} \cdot y\, dx\, dy \quad (6.6)$$

Integrating the product of the conditional probability of symbol error and the probability density function of the interfering signal's amplitude r_j over all possible values of r_j, we get the unconditional probability of symbol error:

$$P2 = 1 - \int_0^\infty \int_0^\infty \int_{-\infty}^\infty \left[\frac{1}{\sqrt{2\cdot\pi}} \cdot \left(1 - Q\left(x + y\cdot\frac{\sqrt{P_{sig}}}{\sqrt{P_{noise}}}\right)\right)^{M-2} \cdot \left(1 - Q\left(x + \frac{y\cdot\sqrt{P_{sig}} - r_j}{\sqrt{P_{noise}}}\right)\right) \cdot e^{\frac{-\left(x^2+y^2\right)}{2}} \cdot y \cdot \frac{r_j}{P_{jam}} \cdot e^{\frac{-r_j^2}{2\cdot P_{jam}}} \right] dx\, dy\, dr_j \quad (6.7)$$

Using the transformation of (6.4), we obtain:

$$P2 = 1 - \int_0^\infty \int_0^\infty \int_{-\infty}^\infty \left[\frac{1}{\sqrt{2\cdot\pi}} \cdot e^{\frac{-\left(x^2+y^2+z^2\right)}{2}} \cdot \left(1 - Q\left(x + \sqrt{\frac{P_{sig}}{P_{noise}}}\cdot y\right)\right)^{M-2} \cdot \left(1 - Q\left(x + \sqrt{\frac{P_{sig}}{P_{noise}}}\cdot y - \sqrt{\frac{P_{jam}}{P_{noise}}}\cdot z\right)\right) \cdot y\cdot z \right] dx\, dy\, dz \quad (6.8)$$

The above integral must be evaluated numerically.

194

c) Total Symbol Error Probability

The total symbol error probability, obtained by combining the two cases, is given by:

$$P_{total} = \frac{1}{M} \cdot P1 + \frac{M-1}{M} \cdot P2 \qquad (6.9)$$

where 1/M is the probability that the transmitted and the interfering symbols are on the same branch and (M-1)/M is the probability that the transmitted and the interfering symbols are on different branches.

2. Simulink Model and Block Analysis

The schematic diagram of the Simulink model, developed for the simulation of coherent MFSK with AWGN and co-channel interference in a Rayleigh fading channel, is shown in Figure 129.
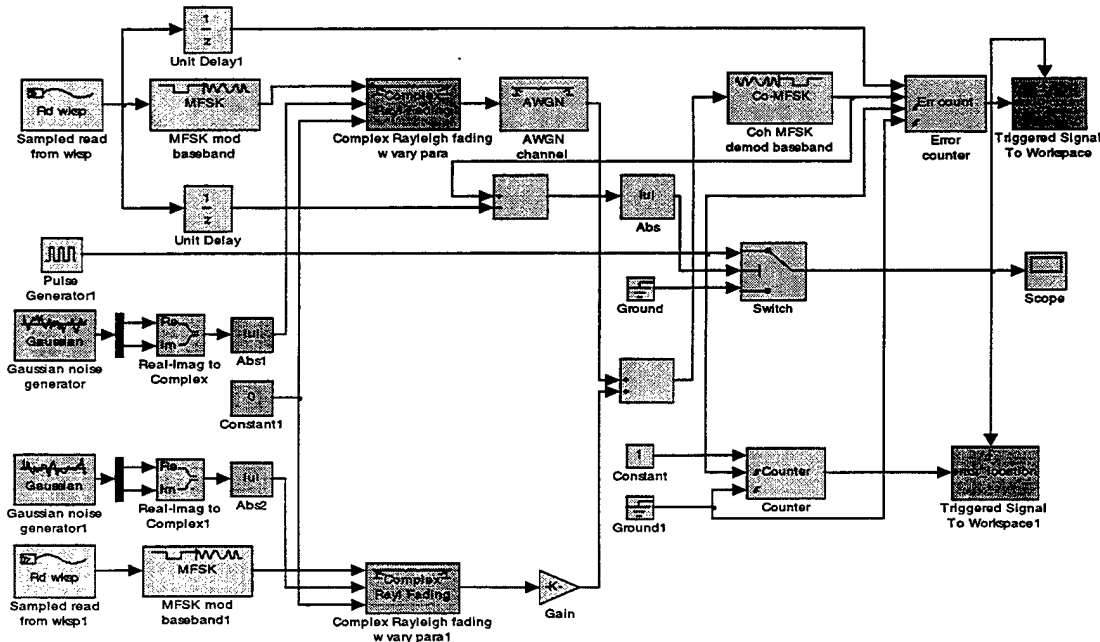
Figure 129. Model for coherent MFSK with co-channel interference in a Rayleigh fading channel.

195

This model is the combination of the model that was used for the coherent MFSK signal in a Rayleigh fading channel and the model that was used for coherent MFSK signal affected by co-channel interference. Note that the desired MFSK signal and the interfering one fade independently.

3. Simulation Analysis And Performance Verification

In this section, simulation results are presented in order to verify the performance of coherent MFSK system with AWGN and co-channel interference in a Rayleigh fading channel. Each simulation ran until at least 100 errors were observed. The data sequences were limited to 10^6 symbols for each simulation in order to prevent "out of memory" errors. The data sequence was repeated until a sufficient number of errors were counted.

a) Results For 2FSK

Using the relationships

$$\frac{P_{sig}}{P_{noise}} = 10^{\frac{SNR}{10}} \qquad \frac{P_{jam}}{P_{noise}} = 10^{\frac{SNR-SJR}{10}} \qquad (6.10)$$

we can express the symbol error probability in terms of SNR and SJR. Evaluating and plotting the theoretical and simulation results versus SNR and SJR, as well as the difference (error) between them, we can compare the theory and the simulation.

The theoretical and the simulation symbol error probabilities for coherently detected 2FSK are presented in Figures 130 and 131, respectively, as functions of average SNR in dB with SJR as a parameter. The values for the signal-to-

196

noise and signal-to-interference ratios are chosen from −5 dB to +30 dB in increments of

2.5 dB.
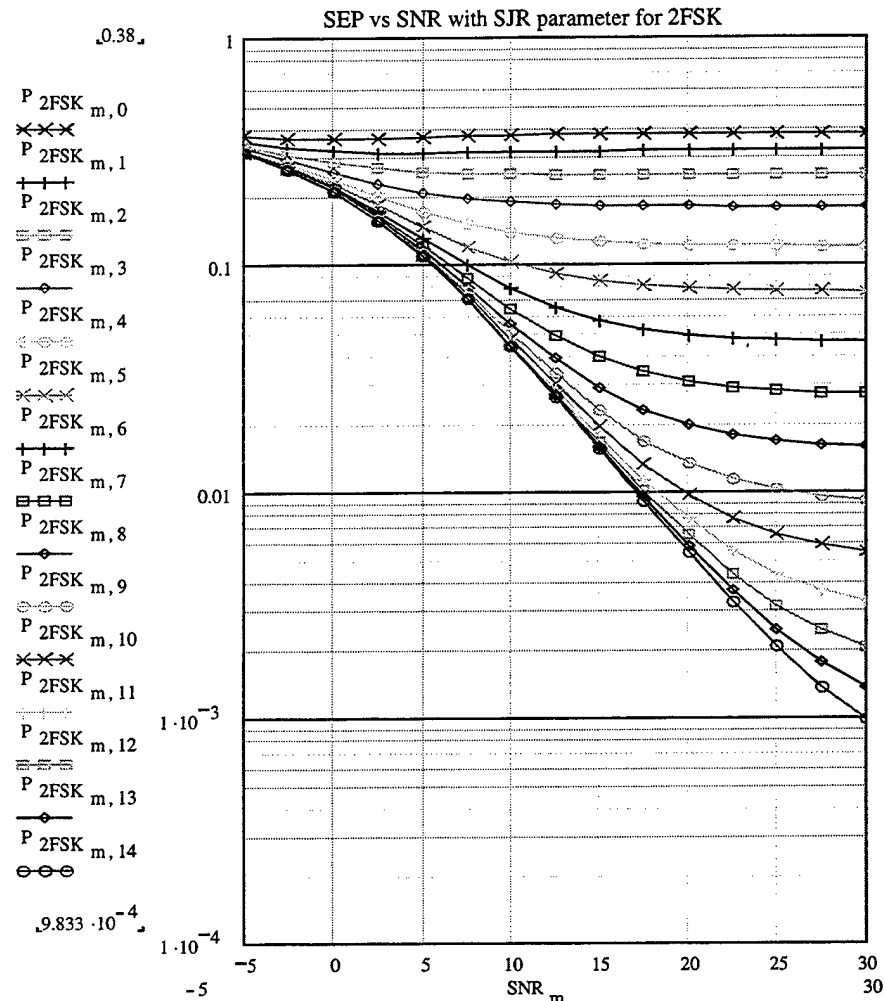
Figure 130. Theoretical symbol error probability versus SNR with SJR as a parameter for coherent 2FSK with Rayleigh fading.

As evident from Figures 129 and 130, the curves tend to become flat as the SNR increases; that is, they converge to a constant value determined by the value of the SJR. The consequence of signal fading is that the symbol error probability does not

197

decrease as rapidly with the increase in either SNR (along a curve) or SJR (from curve to curve) as it does for cases of non-fading signals.
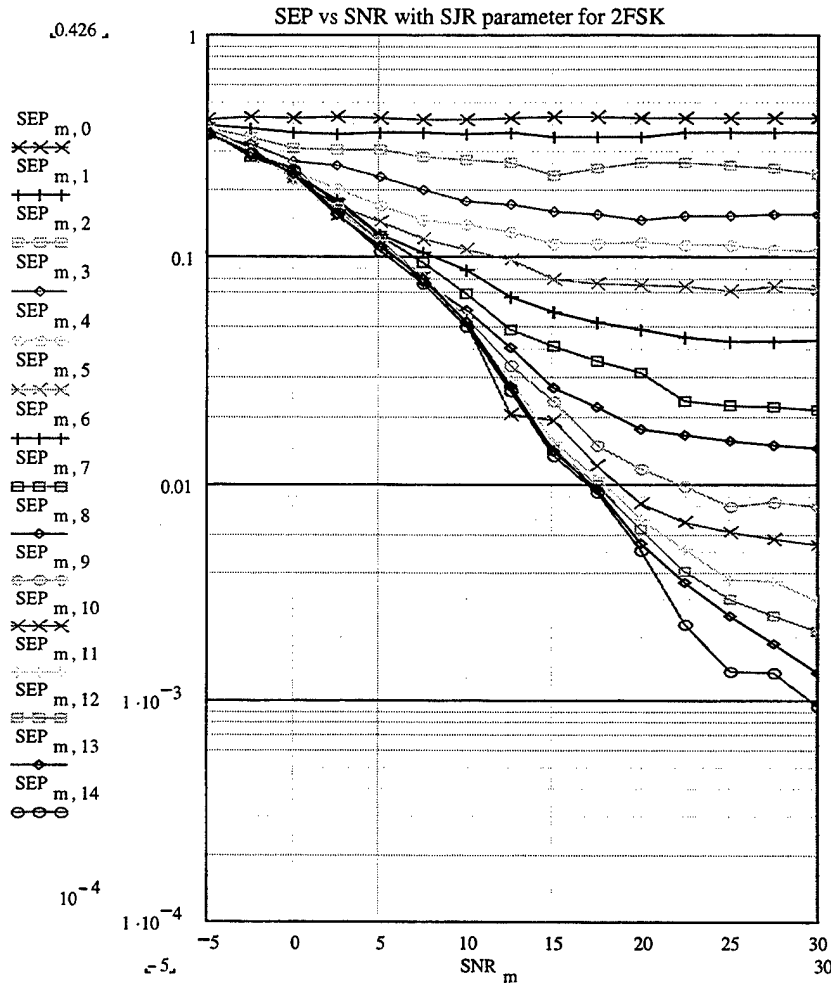
Figure 131. Simulation symbol error probability versus SNR with SJR as a parameter for coherent 2FSK with Rayleigh fading.

In Figures 132 and 133, respectively, the theoretical and simulation results are shown as functions of SJR with SNR as a parameter. As SJR increases, the symbol error probability initially decreases but then tends to a constant value determined by the

value of the SNR. As the SNR increases this constant value decreases but not rapidly as

for the case of a non-fading channel.
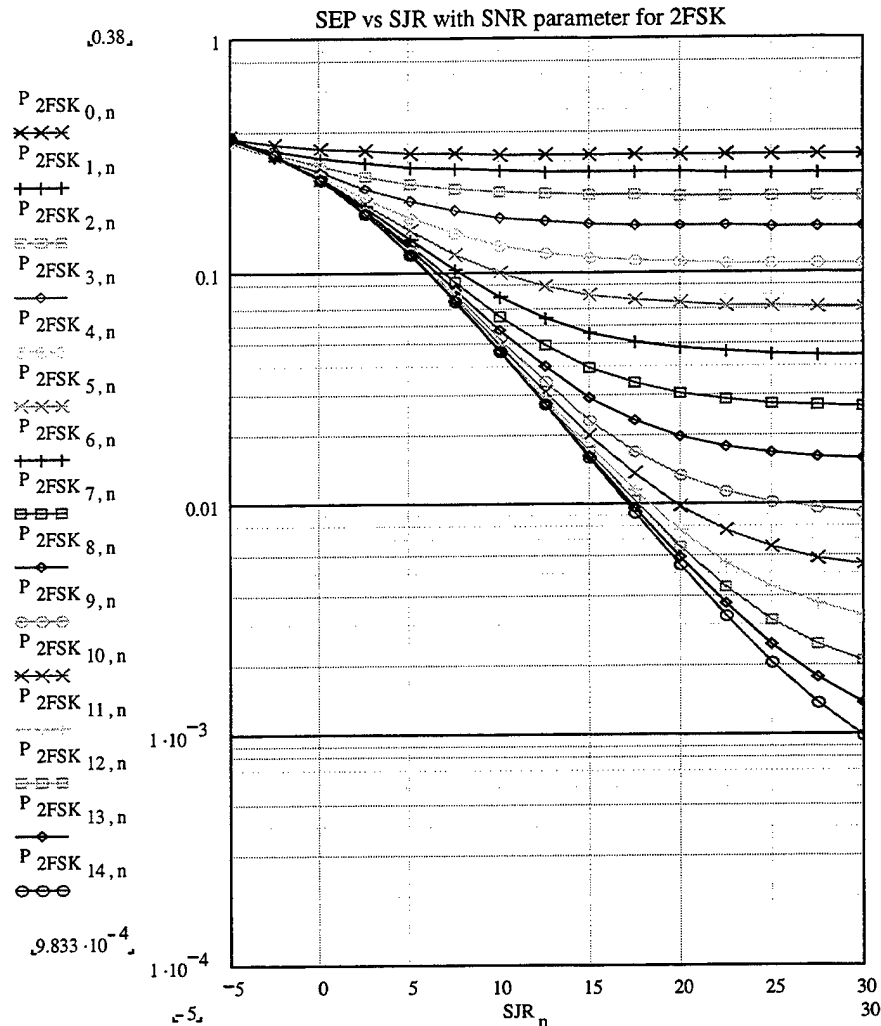
Figure 132. Theoretical symbol error probability versus SJR with SNR as a parameter

for coherent 2FSK with Rayleigh fading.

We again note the dramatic increase in the symbol error probability due to

Rayleigh fading and co-channel interference.
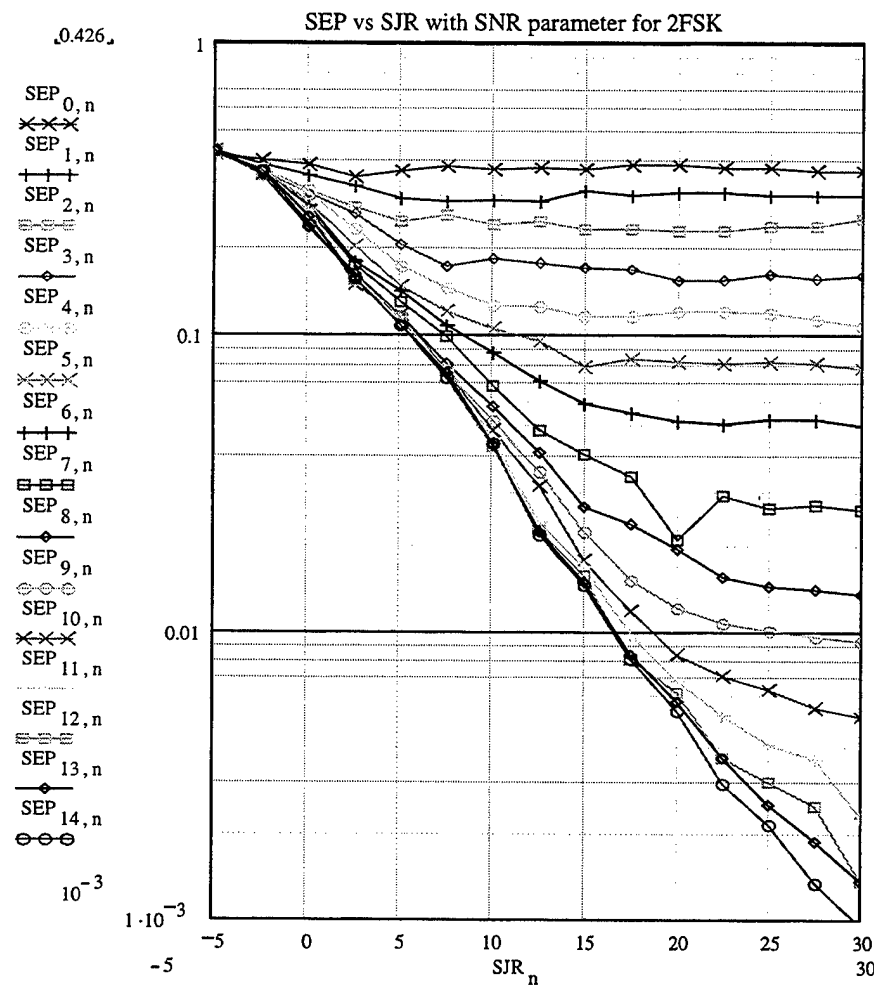
Figure 133. Simulation symbol error probability versus SJR with SNR as a parameter for coherent 2FSK with Rayleigh fading.

The relative difference (in percent) between the theoretical and simulation results is presented in Table 41. In Figure 134, the average difference for each curve is plotted versus SNR and SJR for each set of the 15 previously presented curves.

200
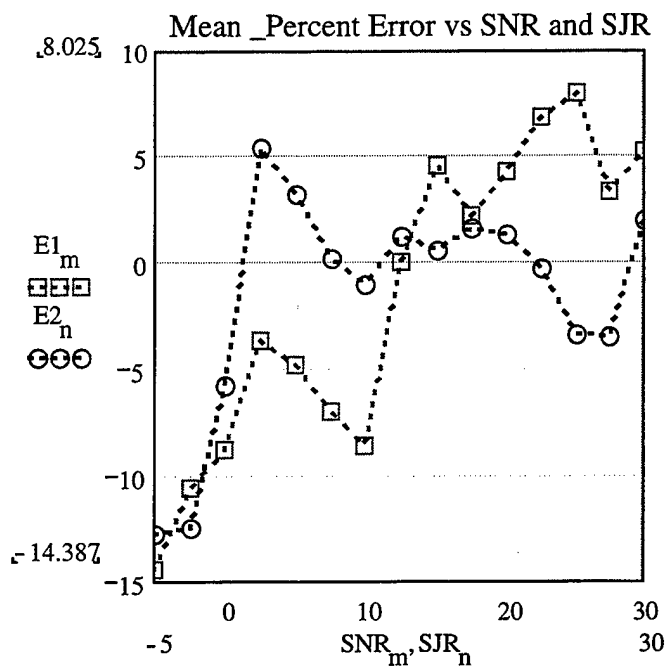
Figure 134. Mean percent difference as a function of SNR and SJR, respectively.

The two curves show how the mean difference varies with SNR and SJR. Each value of the mean difference is the average of the differences that correspond to the 15 points on each of the 15 curves for the symbol error probability as a function of SNR (with SJR as parameter) and SJR (with SNR as parameter).

	SYMBOL ERROR PROBABILITY	COHERENT 2FSK
1.	Root Mean Square Difference (%)	10.524
2.	Average Mean Difference (%)	-1.52
3.	Maximum Difference (%)	34.107
4.	Minimum Difference (%)	-19.562
5.	Difference Deviation (%)	10.414

Table 41. Summary of the accuracy of the simulation for coherent 2FSK.

b)   Results For 4FSK

The theoretical and the simulation symbol error probabilities for coherently detected 4FSK are presented in Figures 135 and 136, respectively, as functions of average SNR in dB with SJR as a parameter. The values for SNR and SJR are between −5 dB and +30 dB in increments of 2.5 dB.
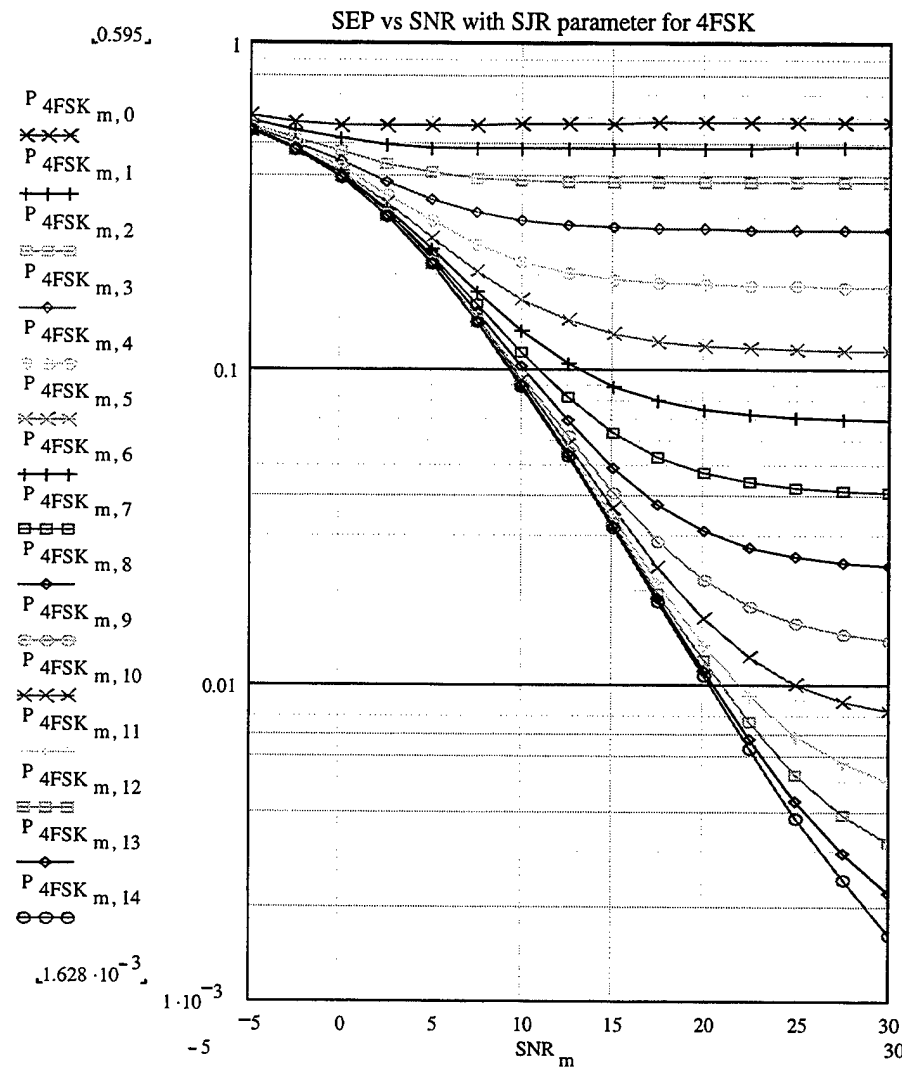

Figure 135. Theoretical symbol error probability versus SNR with SJR as a parameter for coherent 4FSK with Rayleigh fading.

202
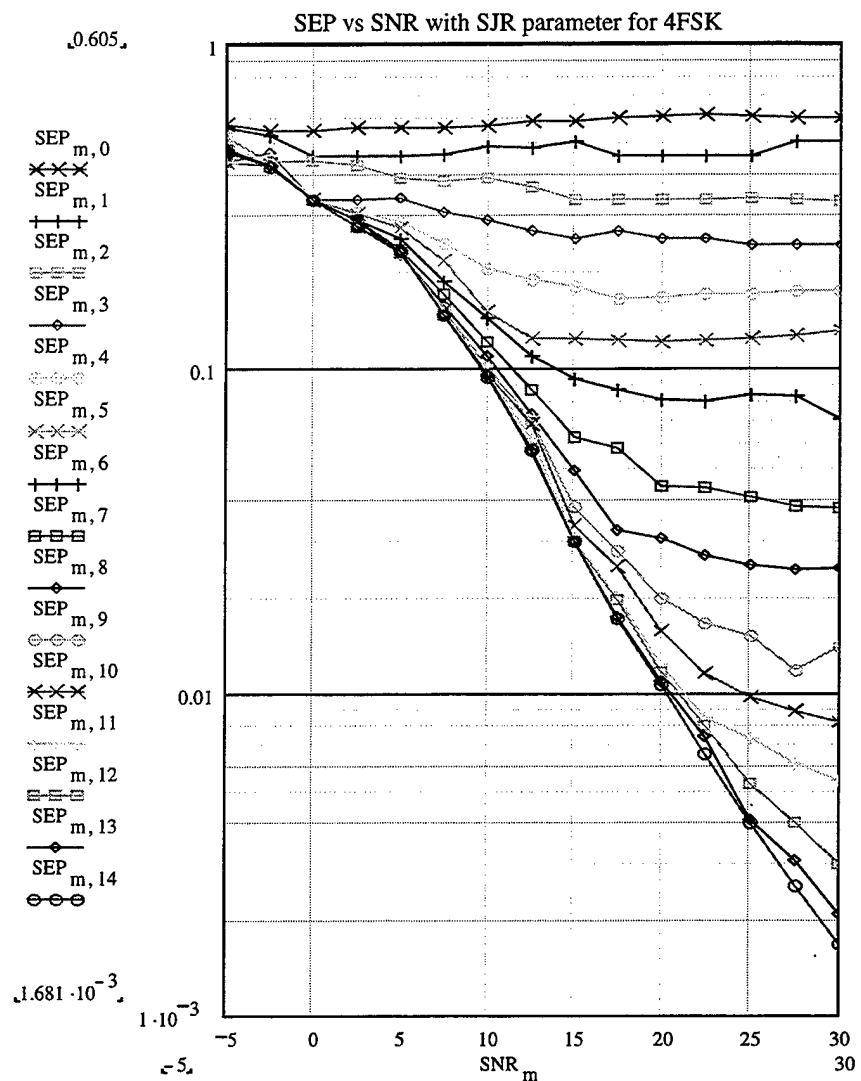
Figure 136. Simulation symbol error probability versus signal-to-noise ratio (SNR), with the signal-to-interference ratio (SJR) as parameter, for coherent 4FSK.

In Figures 137 and 138, respectively, the theoretical and simulation probabilities of symbol error are shown as functions of SJR with SNR as a parameter. The observation derived from all the graphs is that in order to achieve acceptable values for the symbol error probability (10^{-4}) for a Rayleigh fading channel, SNR and SJR must both be over +30 dB.

203
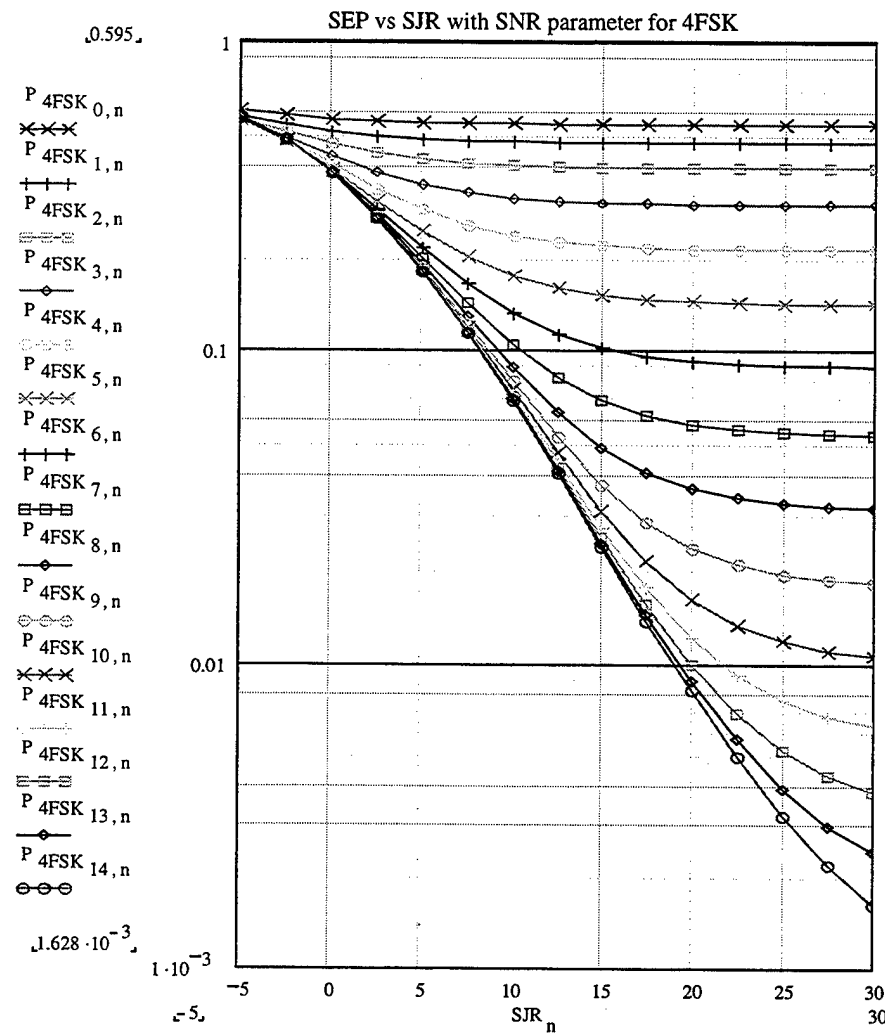
Figure 137. Theoretical symbol error probability versus SJR with SNR as a parameter for coherent 4FSK with Rayleigh fading.

The dramatic increase in the symbol error probability is due to the Rayleigh fading channel that allows low values of signal power to occur (following the Rayleigh distribution) and this case increase in the number of symbol errors.
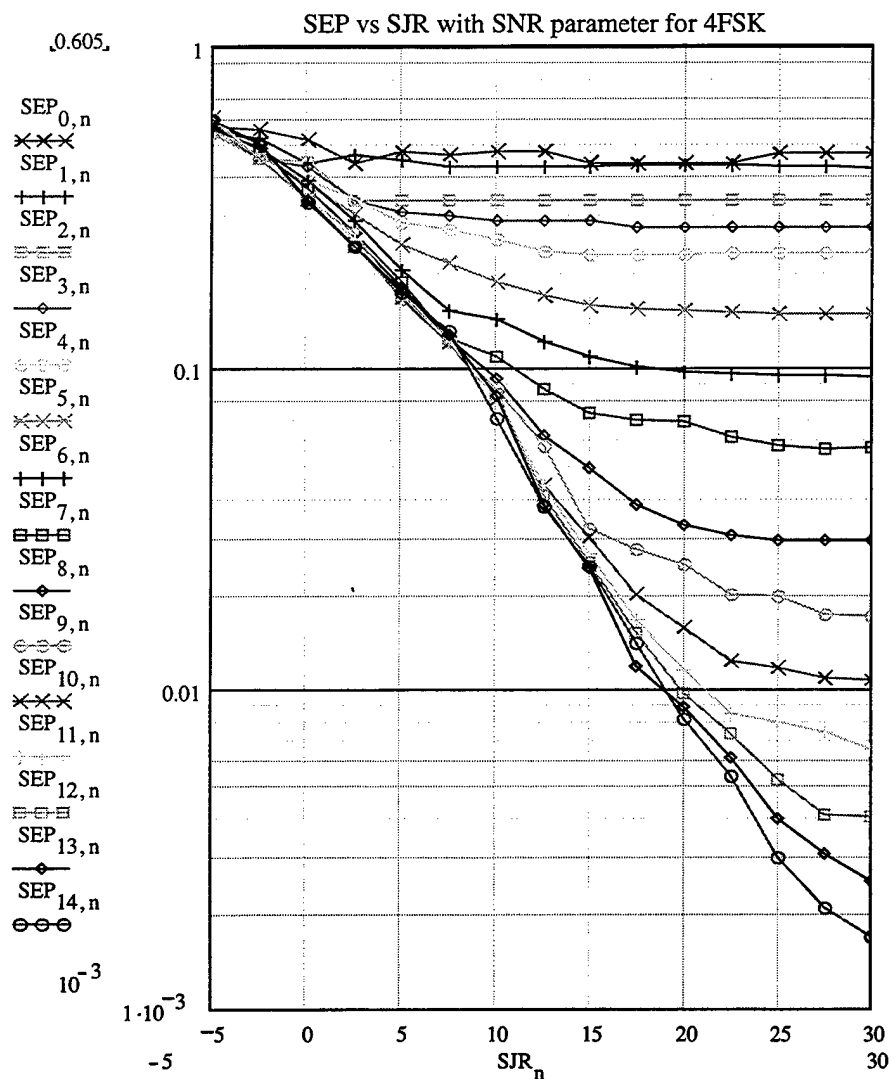
Figure 138. Simulation symbol error probability versus SJR with SNR as a parameter for coherent 4FSK with Rayleigh fading.

The relative difference (percent "error") between the theoretical and simulation results is presented in Table 42. In Figure 139, the average difference for each curve is plotted versus SNR and SJR for each of the 15 previously presented curves.

205
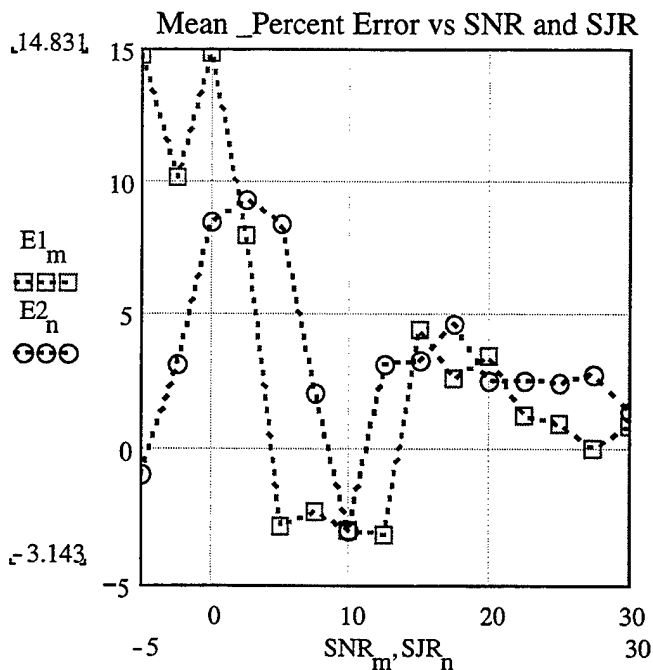
Figure 139. Mean percent difference as a function of SNR and SJR, respectively.

The two curves show how the mean difference varies with SNR and SJR. Each value of the mean difference is the average of the differences that correspond to the 15 points on each of the 15 curves for the symbol error probability as a function of SNR (with SJR as parameter) and SJR (with SNR as parameter).

	SYMBOL ERROR PROBABILITY	COHERENT 4FSK
1.	Root Mean Square Difference (%)	9.02
2.	Average Mean Difference (%)	3.327
3.	Maximum Difference (%)	24.071
4.	Minimum Difference (%)	-18.58
5.	Difference Deviation (%)	8.384

Table 42. Summary of the accuracy of the simulation for coherent 4FSK.

c)   Results For 8FSK

The theoretical and the simulation symbol error probabilities for coherently detected 8FSK are presented in Figures 140 and 141, respectively, as functions of average SNR in dB with SJR as a parameter. The values for SNR and SJR are between –5 dB and +30 dB in increments of 2.5 dB.
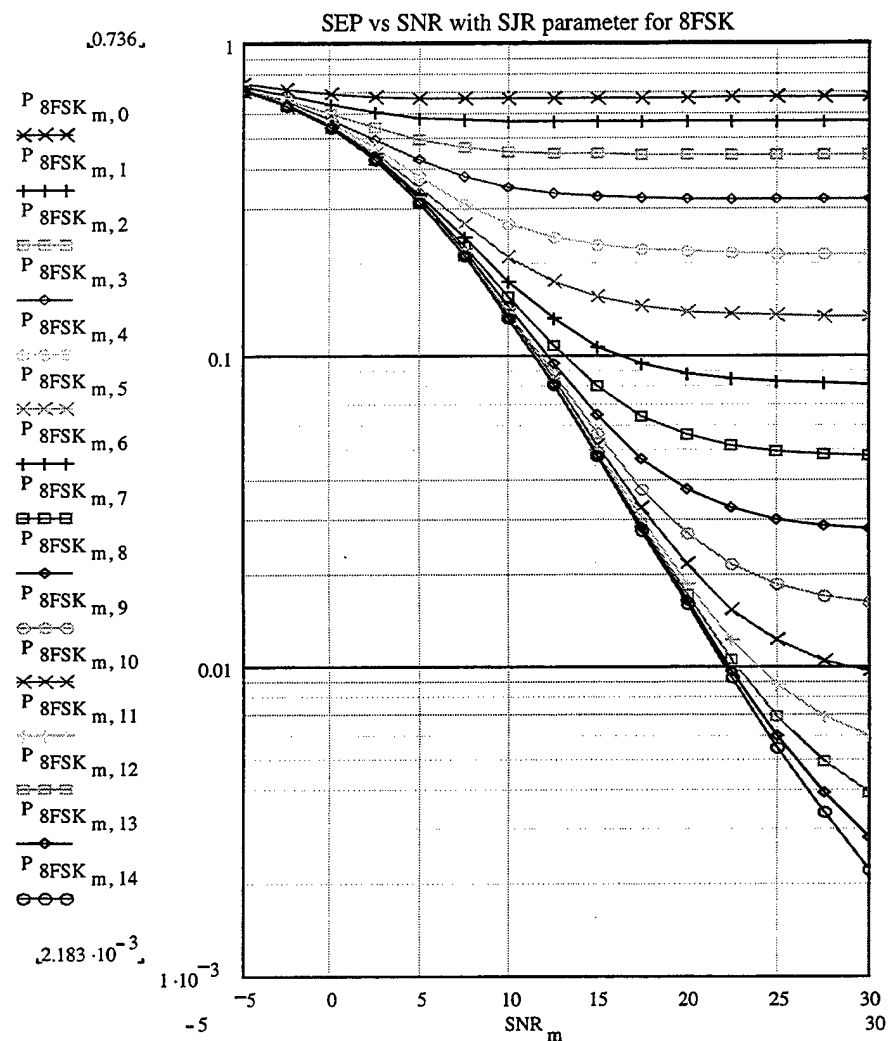

Figure 140. Theoretical symbol error probability versus SNR with SJR as a parameter for coherent 8FSK with Rayleigh fading.

207
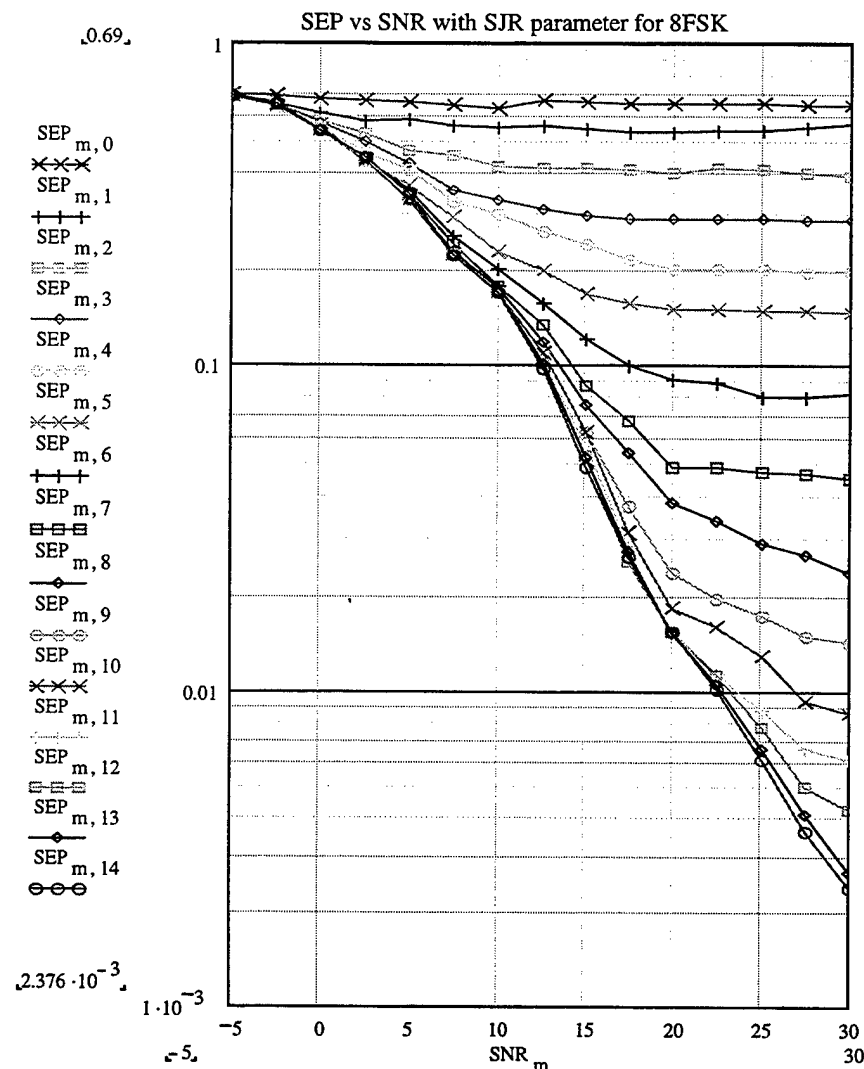
Figure 141. Simulation symbol error probability versus SNR with SJR as a parameter

for coherent 8FSK with Rayleigh fading.

In Figures 142 and 143, respectively, the theoretical and simulation

symbol error probabilities are shown as functions of SJR with SNR as a parameter. Again

we observe that in order to achieve acceptable values for the symbol error probability,

SNR and SJR must both be over +30 dB.
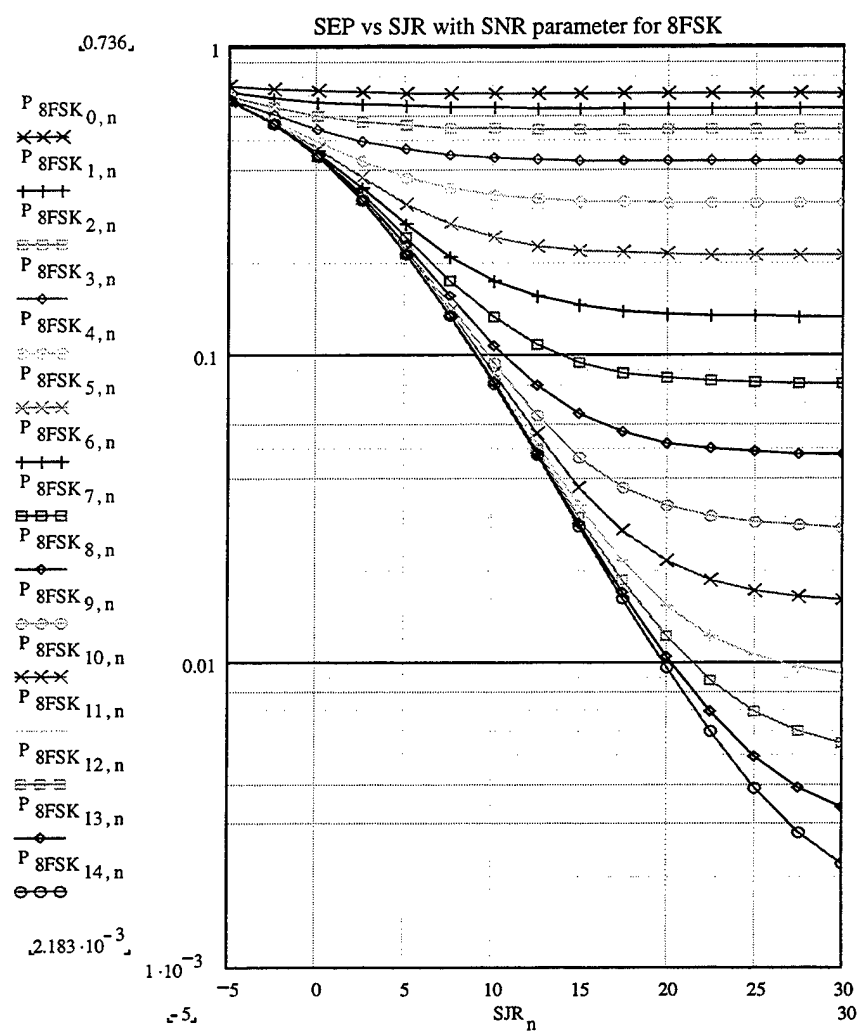
Figure 142. Theoretical symbol error probability versus SJR with SNR as a parameter

for coherent 8FSK with Rayleigh fading.

The dramatic increase in the symbol error probability is due to the

Rayleigh fading channel, as was observed for the cases of 2FSK and 4FSK.
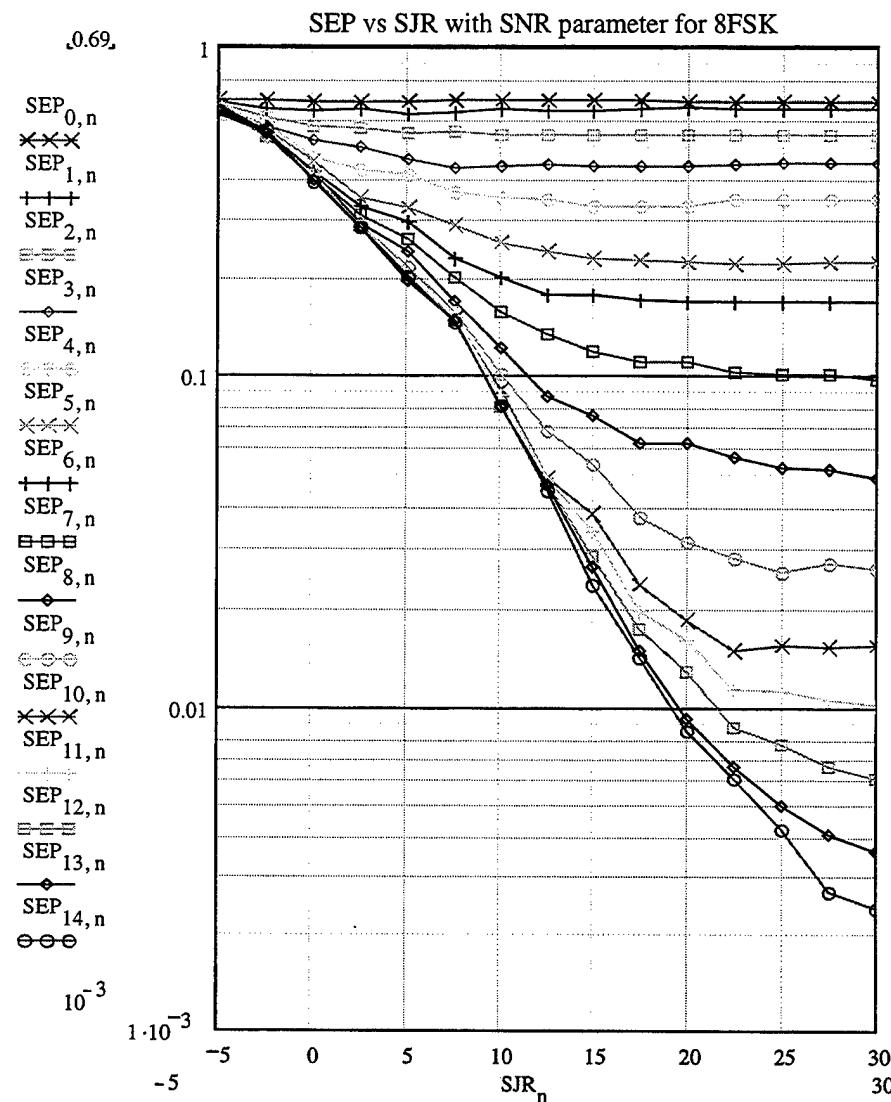
Figure 143. Simulation symbol error probability versus SJR with SNR as a parameter for coherent 8FSK with Rayleigh fading.

The relative difference (percent "error") between the theoretical and the simulation results is shown in Table 43. In Figure 144, the average difference for each curve is plotted versus SNR and SJR for each of the 15 previously presented curves.
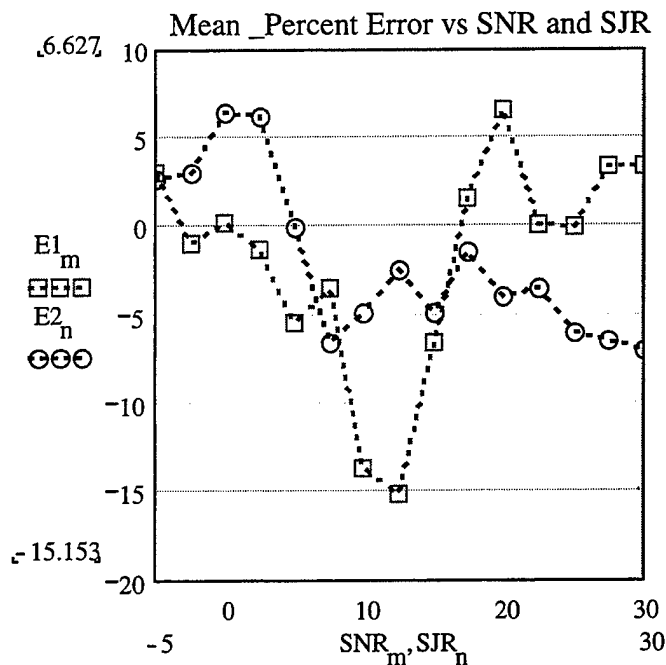
Figure 144. Mean percent difference as a function of SNR and SJR, respectively.

The two curves show how the mean difference varies with SNR and SJR. Each value of the mean difference is the average of the differences that correspond to the 15 points on each of the 15 curves for the symbol error probability as a function of SNR (with SJR as parameter) and SJR (with SNR as parameter), respectively.

	SYMBOL ERROR PROBABILITY	COHERENT 8FSK
1.	Root Mean Square Difference (%)	9.446
2.	Average Mean Difference (%)	-1.851
3.	Maximum Difference (%)	19.206
4.	Minimum Difference (%)	-30.409
5.	Difference Deviation (%)	9.263

Table 43. Summary of the accuracy of the simulation for coherent 8FSK.

211

Observing the results for coherent detection of 2, 4, and 8FSK with AWGN and co-channel interference in a Rayleigh fading channel, we note that the simulation overestimates the theory for the cases of 2 and 8FSK and underestimates the theory for the cases of 4FSK. The root mean square difference (in percent) is about 10% (in average) and the mean percent difference for all the cases is much less than 10% (about -0.015%), which suggests good accuracy.

The average results for the coherent detection of 2, 4, and 8FSK are presented in Table 44.

	SYMBOL ERROR PROBABILITY	AVERAGE RESULTS FOR COHERENT 2, 4, AND 8FSK
1.	Root Mean Square Difference (%)	9.663
2.	Average Mean Difference (%)	-0.015
3.	Maximum Difference (%)	25.795
4.	Minimum Difference (%)	-22.85
5.	Difference Deviation (%)	9.354

Table 44. Average results for the coherent detection of 2, 4, and 8FSK.

B.   RAYLEIGH FADING CHANNEL – NON-COHERENT DETECTION

In this section, we derive the symbol error probability for non-coherent MFSK transmitted over a frequency-nonselective, slowly fading Rayleigh channel in the presence of AWGN and co-channel interference.

1.   Theoretical Probability Of Symbol Error For Coherent Detection

The probability that the desired symbol will be received correctly is evaluated separately for the following two cases:

- **1st case:** the signal and the interference symbols are on the same branch.

- **2nd case:** the signal and the interference symbols are on different branches.

a)   The Signal And The Interference Symbols Are On The Same Branch

The conditional probability of symbol error for non-coherent, orthogonal MFSK Rayleigh fading signal with AWGN and co-channel interference has been already derived in Chapter V (equation (5.15)):

$$P1(r_j) = \int_0^\infty \sum_{k=1}^{M-1} \frac{(M-1)!}{k! \cdot (M-1-k)!} \cdot \frac{(-1)^{k+1}}{k+1} \cdot e^{\frac{-k}{2 \cdot (k+1)} \cdot \left(y \cdot \frac{\sqrt{P_{sig}}}{\sqrt{P_{noise}}} + \frac{r_j}{\sqrt{P_{noise}}} \right)^2} \cdot e^{\frac{-y^2}{2}} \cdot y \, dy \quad (6.11)$$

where:

r_j is the amplitude of the interfering MFSK signal.

The above symbol error probability is conditioned on the amplitude r_j of the interfering signal since the channel is modeled as a Rayleigh fading channel. The amplitude r_j of the interference is modeled as Rayleigh random variable with the probability density function:

$$f\left(r_j, P_{jam}\right) = \frac{r_j}{P_{jam}} \cdot e^{\frac{-r_j^2}{2 \cdot P_{jam}}} \tag{6.12}$$

where P_{jam} is the symbol power of the fading interfering signal.

Integrating the product of the conditional probability of symbol error and the probability density function of the interfering signal's amplitude r_j over all possible values of r_j, we obtain the unconditional probability of symbol error for this case:

$$P_1 = \int_0^\infty \int_0^\infty \sum_{k=1}^{M-1} \frac{(M-1)!}{k! \cdot (M-1-k)!} \cdot \frac{(-1)^{k+1}}{k+1} \cdot e^{\frac{-k}{2 \cdot (k+1)} \cdot \left(y \cdot \frac{\sqrt{P_{sig}}}{\sqrt{P_{noise}}} + \frac{r_j}{\sqrt{P_{noise}}} \right)^2} \cdot e^{\frac{-y^2}{2}} \cdot y \cdot \frac{r_j}{P_{jam}} \cdot e^{\frac{-r_j^2}{2 P_{jam}}} \, dy \, dr_j \tag{6.13}$$

Using the transformation

$$\frac{r_j}{\sqrt{P_{jam}}} = z \tag{6.14}$$

we obtain the following expression which must be evaluated numerically:

$$P_1 = \int_0^\infty \int_0^\infty \sum_{k=1}^{M-1} \frac{(M-1)!}{k! \cdot (M-1-k)!} \cdot \frac{(-1)^{k+1}}{k+1} \cdot e^{\frac{-k}{2 \cdot (k+1)} \cdot \left(y \cdot \frac{\sqrt{P_{sig}}}{\sqrt{P_{noise}}} + z \cdot \frac{\sqrt{P_{jam}}}{\sqrt{P_{noise}}} \right)^2} \cdot e^{\frac{-\left(y^2 + z^2 \right)}{2}} \cdot y \cdot z \, dy \, dz \tag{6.15}$$

214

b) The Signal And The Interference Symbols Are On Different Branches

The conditional probability of symbol error for this case of non-coherent, orthogonal MFSK Rayleigh fading signal with AWGN and interference has been derived in Chapter V (equation (5.18)):

$$P2\left(r_j\right) = 1 - \int_0^\infty \int_0^\infty \left[\left[\left[1 - e^{-\frac{1}{2}\cdot\left(x^2 + \frac{r_j^2}{P_{noise}}\right)} \cdot \sum_{p=0}^\infty \left(\frac{r_j}{x\cdot\sqrt{P_{noise}}}\right)^p \cdot In\left(p, x\cdot\frac{r_j}{\sqrt{P_{noise}}}\right)\right]\right] \left(1 - e^{-\frac{x^2}{2}}\right)^{M-2} \cdot e^{-\frac{1}{2}\left(x^2 + y^2 + y^2\frac{P_{sig}}{P_{noise}}\right)} \cdot I0\left(\sqrt{\frac{P_{sig}}{P_{noise}}}\cdot x\cdot y\right)\cdot x\cdot y\right] dxdy \quad (6.16)$$

Integrating the product of the conditional probability of symbol error and the probability density function of the interfering signal's amplitude r_j over all possible values of r_j, we get the unconditional probability of symbol error. Using (6.14) we obtain:

$$P2 = 1 - \int_0^\infty \int_0^\infty \int_0^\infty \left[\left[\left[1 - e^{-\frac{1}{2}\cdot\left(x^2 + z^2\frac{P_{jam}}{P_{noise}}\right)} \cdot \sum_{p=0}^\infty \left(\sqrt{\frac{P_{jam}}{P_{noise}}}\right)^p \frac{z^p}{x^p}\cdot In\left(p, x\cdot z\cdot\sqrt{\frac{P_{jam}}{P_{noise}}}\right)\right]\right] \left(1 - e^{-\frac{x^2}{2}}\right)^{M-2}\cdot e^{-\frac{1}{2}\left(x^2 + y^2\frac{P_{sig}}{P_{noise}} + y^2 + z^2\right)}\cdot I0\left(\sqrt{\frac{P_{sig}}{P_{noise}}}\cdot x\cdot y\right)\cdot x\cdot y\cdot z\right] dxdydz \quad (6.17)$$

The triple integral of equation (6.17) has to be evaluated numerically. The summation that appears inside the integral has to be limited to a finite number, which sometimes causes distortion to the curves that represent the corresponding symbol error probability.

c) Total Symbol Error Probability

The total symbol error probability, obtained by combining the two cases is given by:

$$Pe\_ncoh = \frac{1}{M} \cdot P1 + \frac{M-1}{M} \cdot P2 \qquad (6.18)$$

where 1/M is the probability that the transmitted and the interfering symbols are at the same branch and (M-1)/M is the probability that the transmitted and the interfering symbols are at different branches.

2. Simulink Model and Block Analysis

The schematic diagram of the Simulink model which has been developed for the simulation of non-coherent MFSK with AWGN and co-channel interference in a Rayleigh fading channel, is the same as the block diagram shown in Figure 129 for coherent detection, except that the block 'Coh MFSK demod baseband' has been replaced by the block 'Non-coherent MFSK demod baseband'.

3. Simulation Analysis And Performance Verification

In this section, simulation results are presented in order to verify the performance of MFSK with non-coherent detection of the desired signal corrupted by AWGN and co-channel interference in a Rayleigh fading channel. Each simulation ran until at least 100 errors were observed. The data sequences were limited to 10^6 symbols for each simulation, to prevent "out of memory" errors and the simulation sequence was repeated until a sufficient number of errors were counted.

216

a) Results For 2FSK

Using the relationships

$$\frac{P_{sig}}{P_{noise}} = 10^{\frac{SNR}{10}} \qquad\qquad \frac{P_{jam}}{P_{noise}} = 10^{\frac{SNR-SJR}{10}} \qquad (6.19)$$

we express the theoretical symbol error probability in terms of SNR and SJR. The values for the signal-to-noise and signal-to-interference ratios were chosen from –5 dB to +16 dB in increments of 1.5 dB.
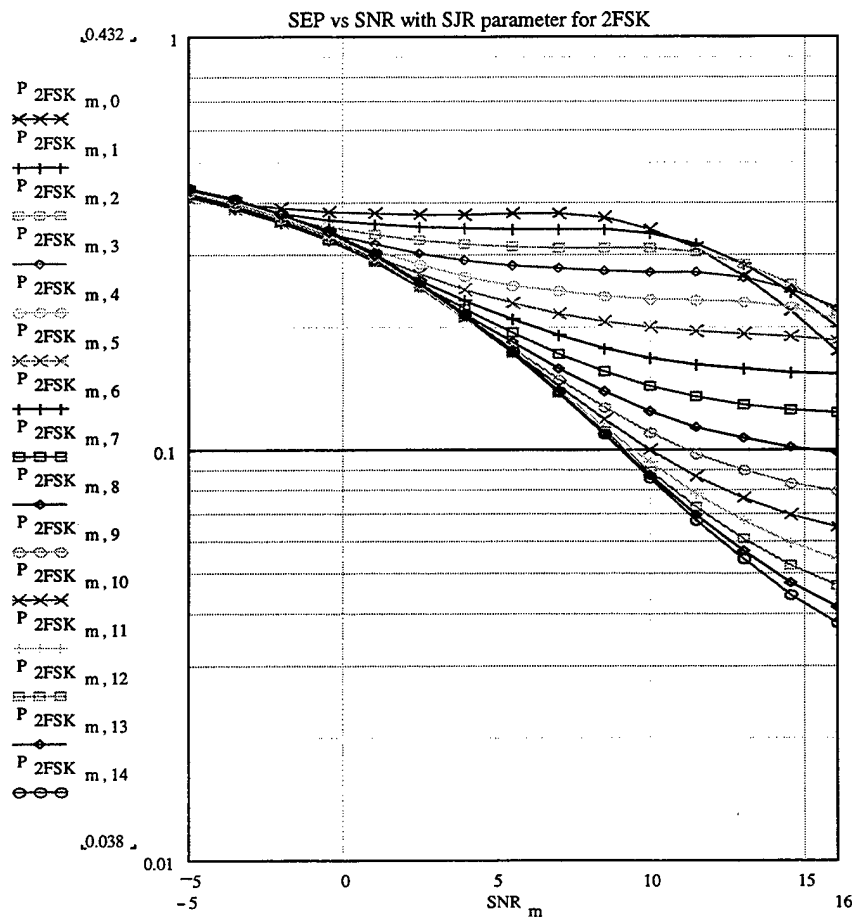
Figure 145. Theoretical symbol error probability versus SNR, with SJR as a parameter for non-coherent 2FSK with Rayleigh fading.

217
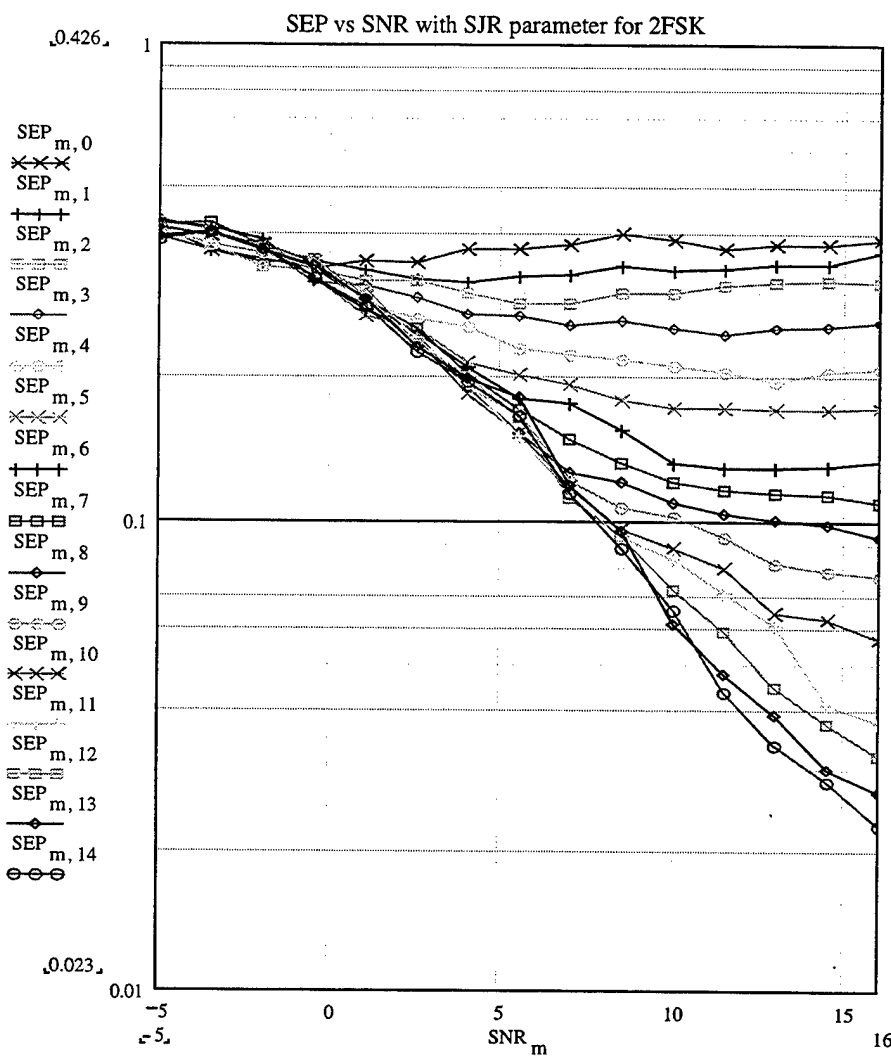
Figure 146. Simulation symbol error probability versus SNR with SJR as a parameter

for non-coherent 2FSK with Rayleigh fading.

In Figures 147 and 148, respectively, the theoretical and simulation

symbol error probability are shown as functions of SJR with SNR as a parameter.

218
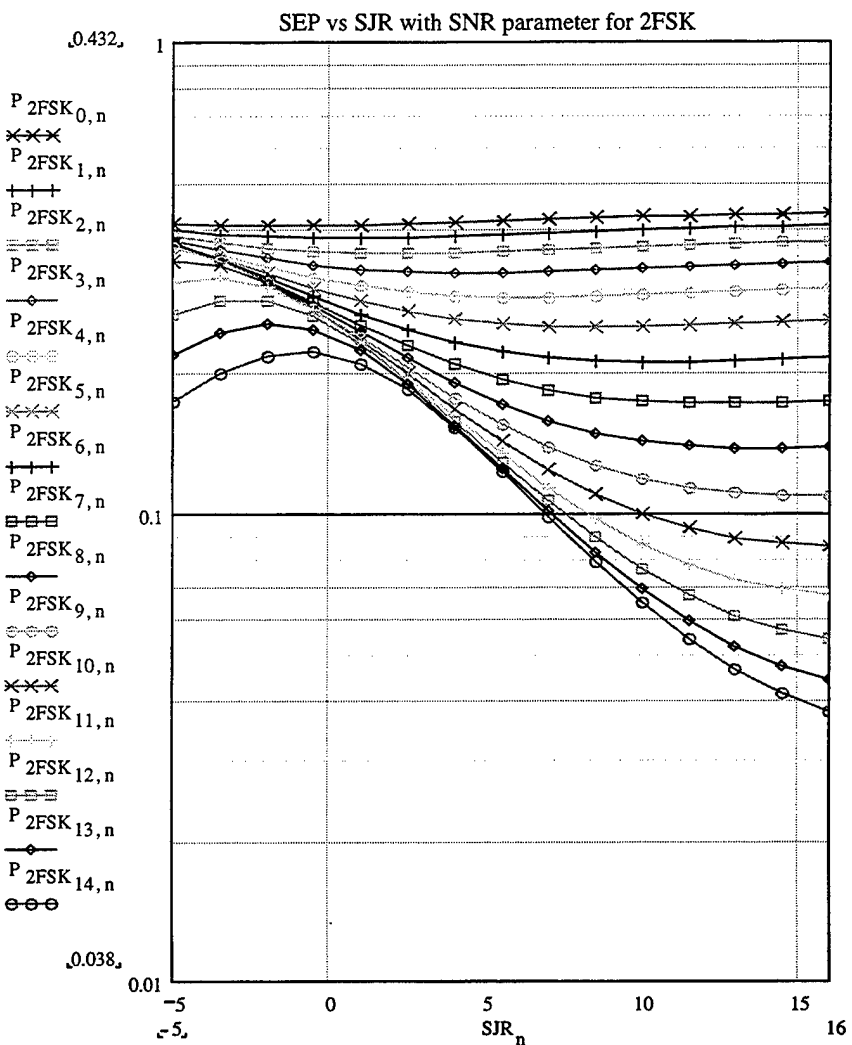
Figure 147. Theoretical symbol error probability versus SJR with SNR as a parameter

for non-coherent 2FSK with Rayleigh fading.

We again note the dramatic increase in the symbol error probability due to Rayleigh fading and co-channel interference. Furthermore, non-coherent detection also increases the number of errors in the receiver as compared to the coherent detection.

219
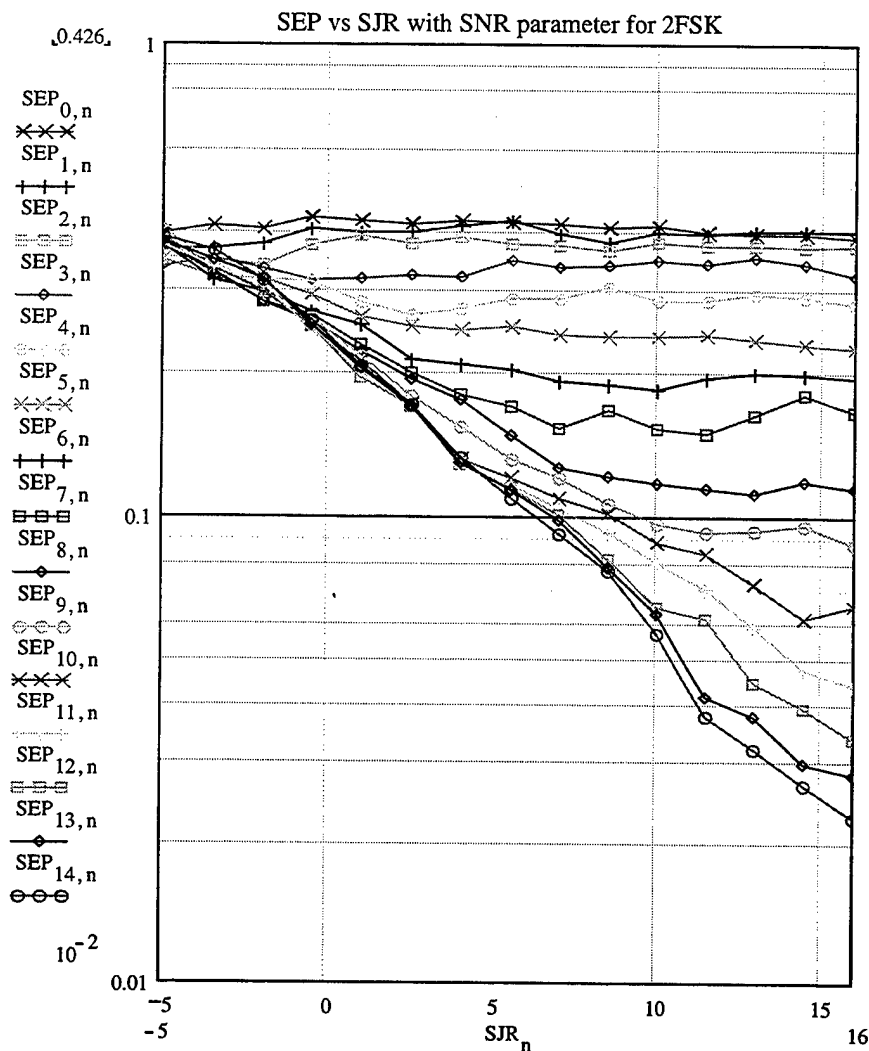
Figure 148. Simulation symbol error probability versus SJR with SNR as a parameter

for non-coherent 2FSK with Rayleigh fading.

The relative difference (percent "error") between the theory and the simulation is summarized in Table 45. In Figure 149, the average difference is plotted versus SNR and SJR respectively for each of the 15 previously presented curves.

220
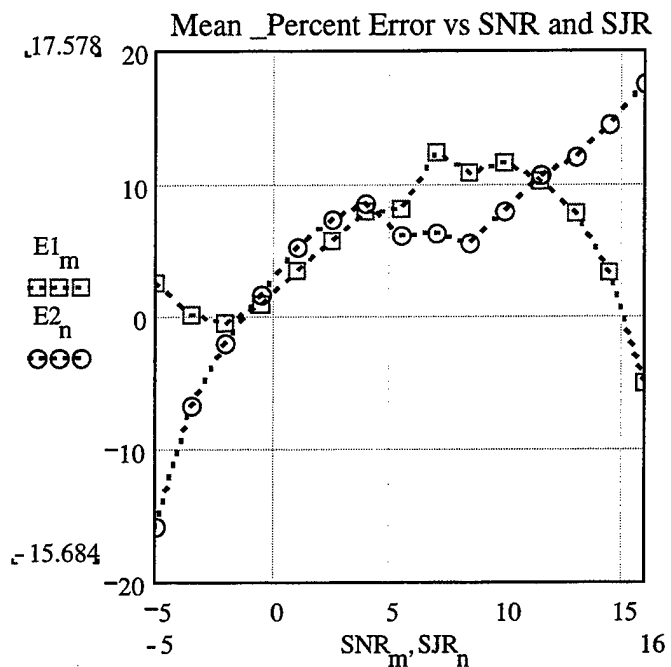
Figure 149. Mean percent difference as a function of SNR and SJR, respectively.

The two curves show how the mean difference varies with SNR and SJR. Each value of the mean difference is the average of the differences that correspond to the 15 points on each of the 15 curves for the symbol error probability as a function of SNR (with SJR as parameter) and SJR (with SNR as parameter).

	SYMBOL ERROR PROBABILITY	NON-COHERENT 2FSK
1.	Root Mean Square Difference (%)	17.385
2.	Average Mean Difference (%)	5.34
3.	Maximum Difference (%)	40.188
4.	Minimum Difference (%)	-123.22
5.	Difference Deviation (%)	16.544

Table 45. Summary of the accuracy of the simulation for non-coherent 2FSK.

221

b)   Results For 4FSK

The theoretical and the simulation symbol error probabilities for non-coherently detected 4FSK are presented in Figures 150 and 151, respectively, as functions of average SNR in dB with SJR as a parameter. The values for SNR and SJR have been chosen from –5 dB to +16 dB in increments of 1.5 dB.
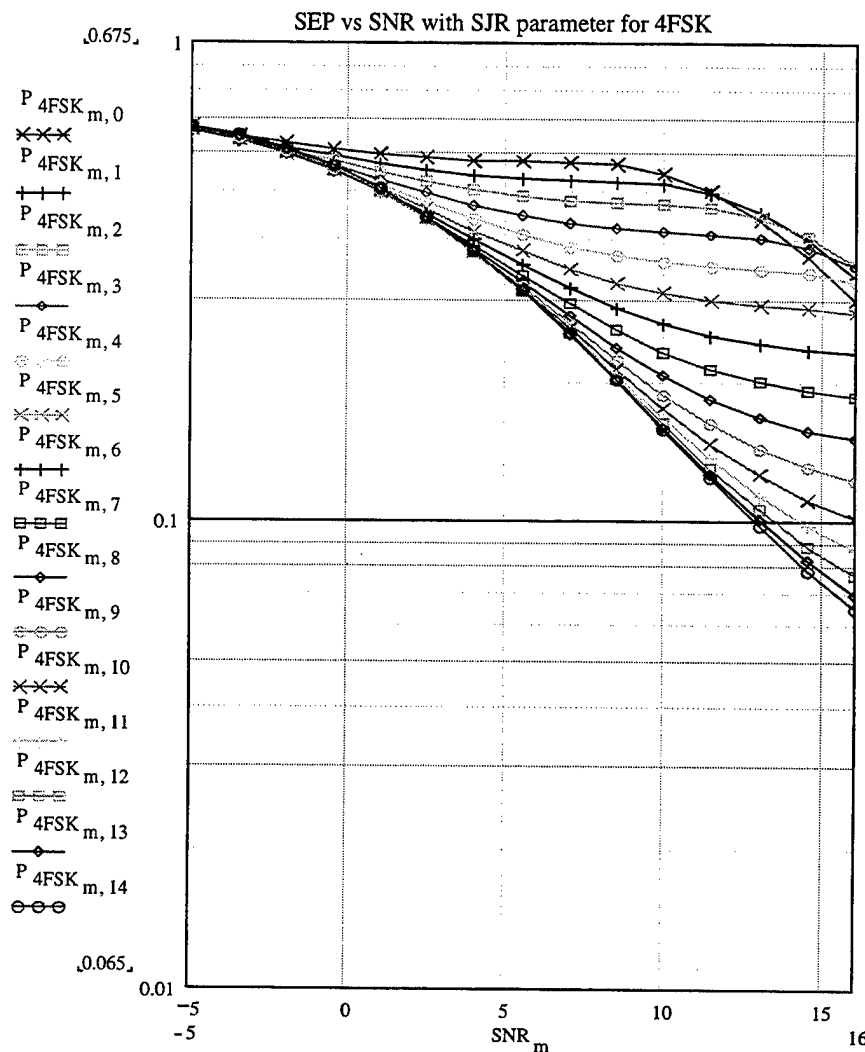

Figure 150. Theoretical symbol error probability versus SNR with SJR as a parameter for non-coherent 4FSK with Rayleigh fading.

222
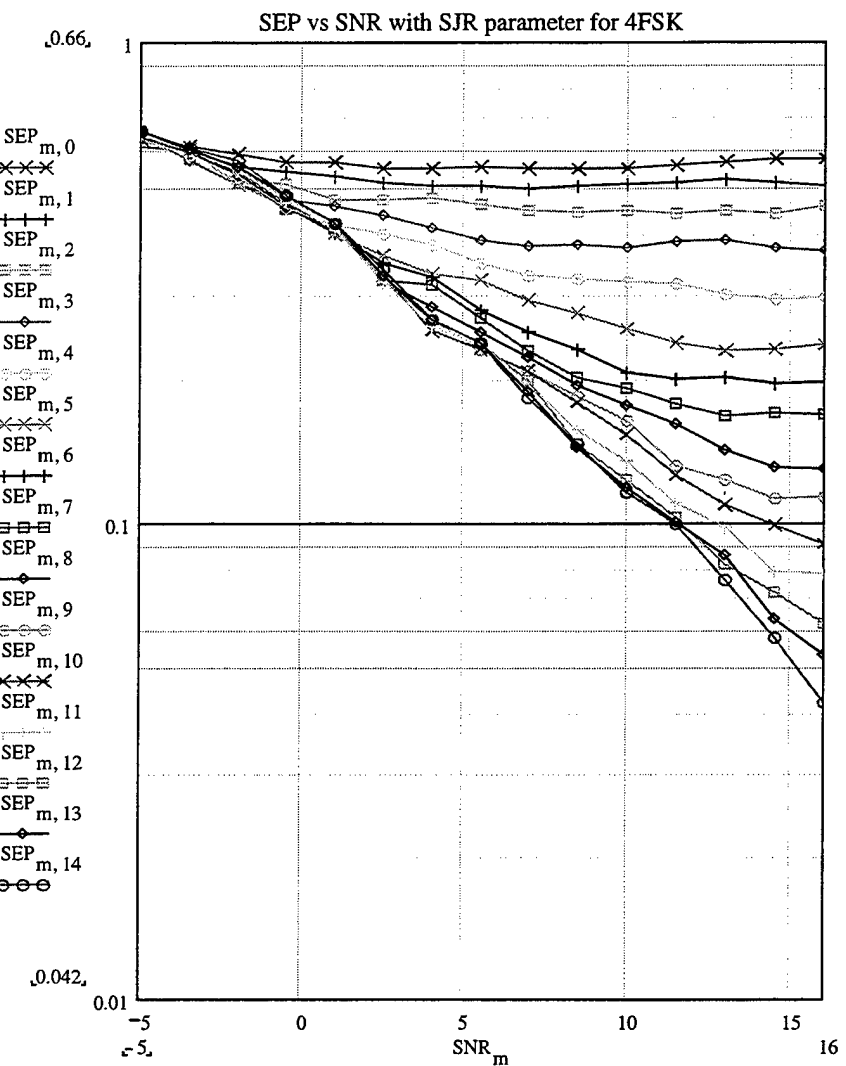
Figure 151. Simulation symbol error probability versus SNR with SJR as a parameter

for non-coherent 4FSK with Rayleigh fading.

In Figures 152 and 153, respectively, the theoretical and simulation

symbol error probabilities are shown as functions of SJR with SNR as a parameter.

223
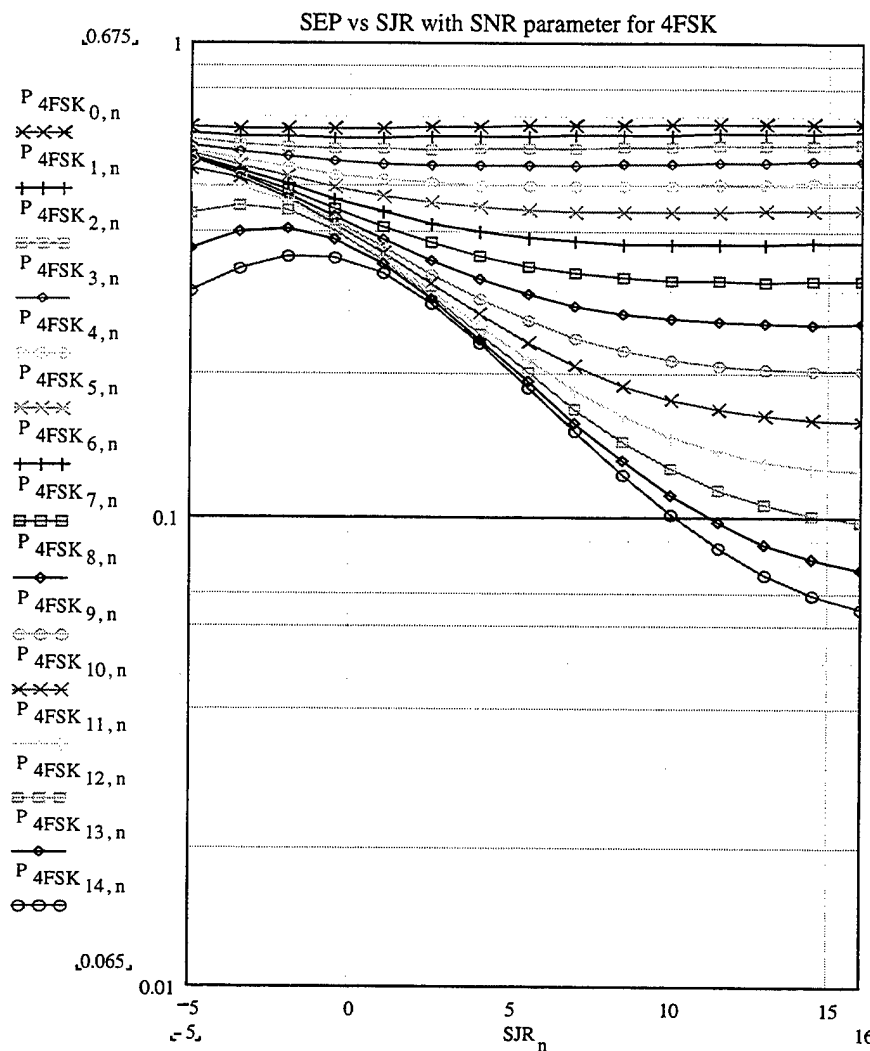
Figure 152. Theoretical symbol error probability versus SJR with SNR as a parameter

for non-coherent 4FSK with Rayleigh fading.

We again note the dramatic increase in the symbol error probability due to

Rayleigh fading and co-channel interference.
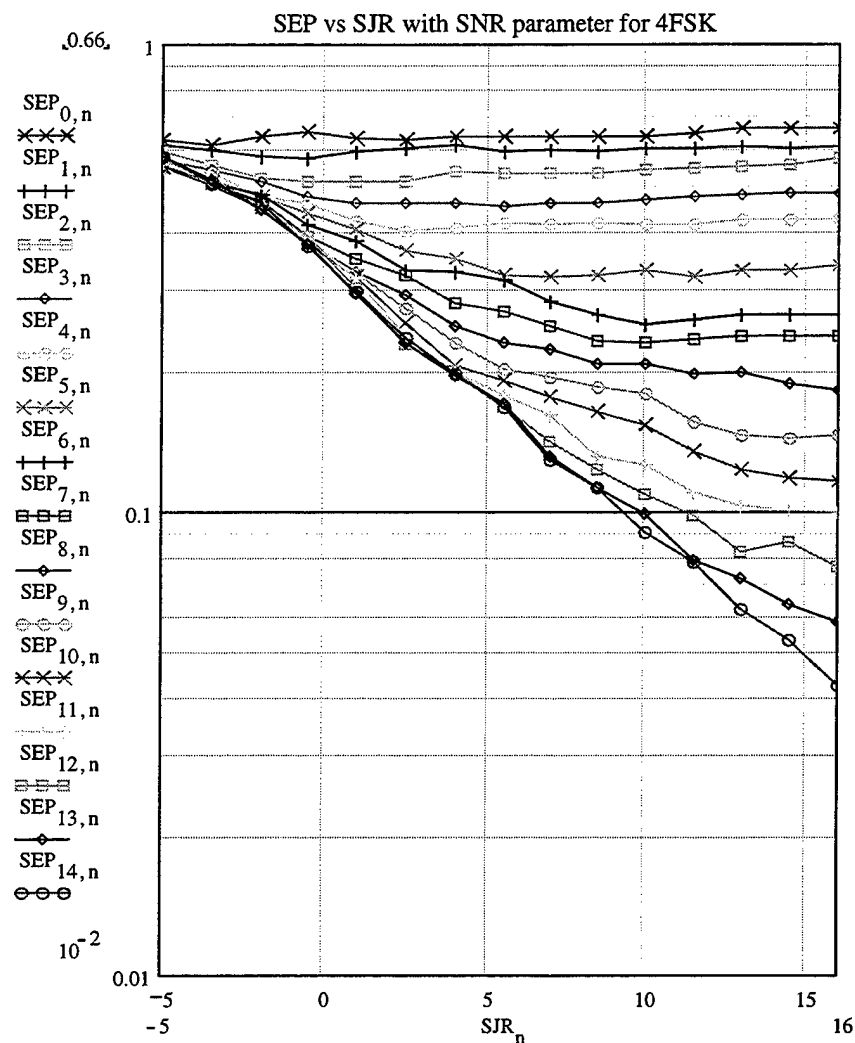
Figure 153. Simulation symbol error probability versus SJR with SNR as a parameter

for non-coherent 4FSK with Rayleigh fading.

In Figure 154, the average difference for each curve is plotted versus SNR

and SJR for each of the 15 previously presented curves. Finally, the relative difference

(percent "error") between the theory and the simulation is summarized in Table 46.


225
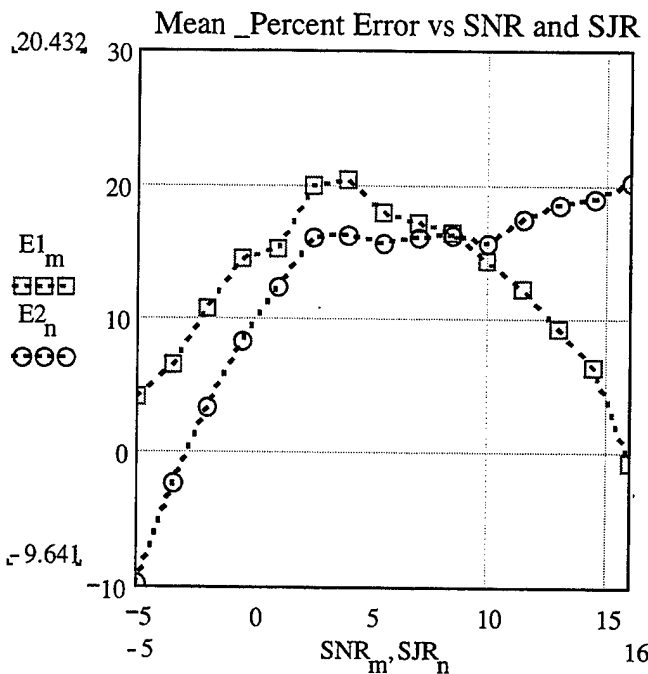
Figure 154. Mean percent difference as a function of SNR and SJR, respectively.

The two curves show how the mean difference varies with SNR and SJR. Each value of the mean difference is the average of the differences that correspond to the 15 points on each of the 15 curves for the symbol error probability as a function of SNR (with SJR as parameter) and SJR (with SNR as parameter), respectively.

	SYMBOL ERROR PROBABILITY	NON-COHERENT 4FSK
1.	Root Mean Square Difference (%)	18.335
2.	Average Mean Difference (%)	12.331
3.	Maximum Difference (%)	34.441
4.	Minimum Difference (%)	-92.531
5.	Difference Deviation (%)	13.568

Table 46. Summary of the accuracy of the simulation for non-coherent 4FSK.

c) Results For 8FSK

The theoretical and the simulation symbol error probabilities for non-coherently detected 8FSK are presented in the Figures 155 and 156, respectively, as functions of average SNR in dB with SJR as a parameter. The values for the signal-to-noise and signal-to-interference ratios have been chosen from -5 dB to $+16$ dB in increments of 1.5 dB.
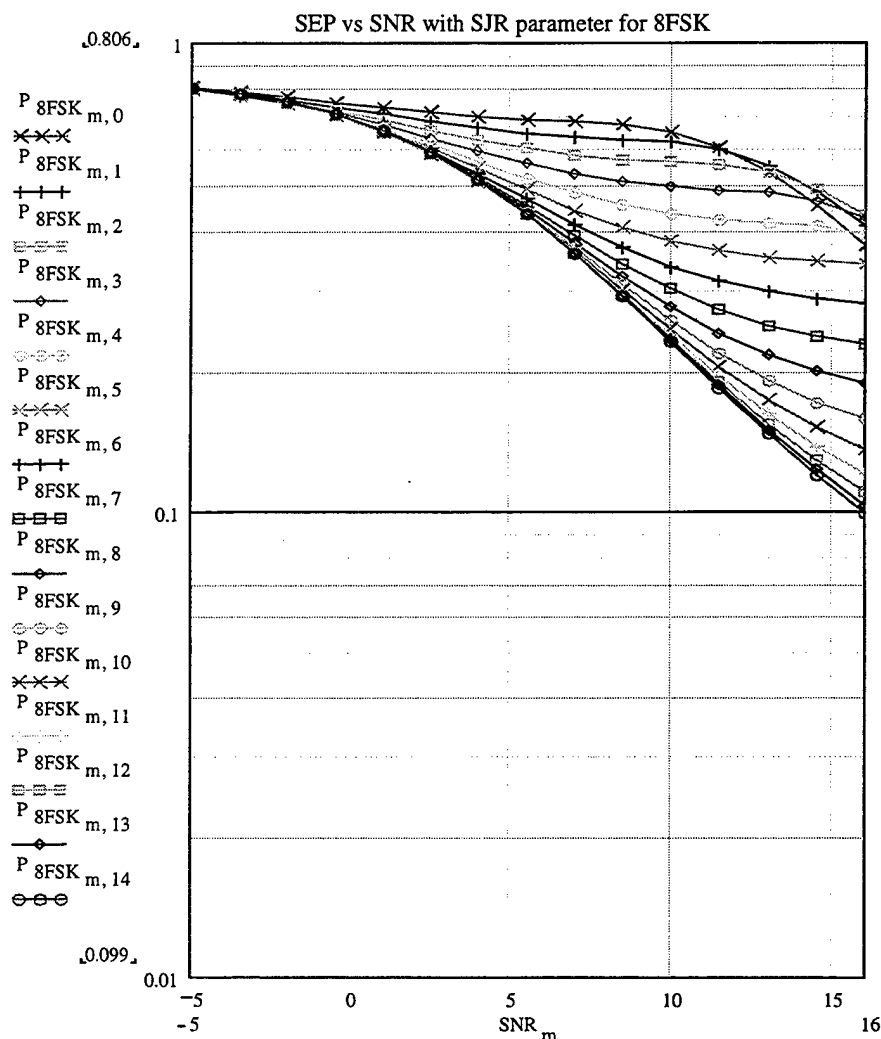

Figure 155. Theoretical symbol error probability versus SNR with SJR as a parameter for non-coherent 8FSK with Rayleigh fading.
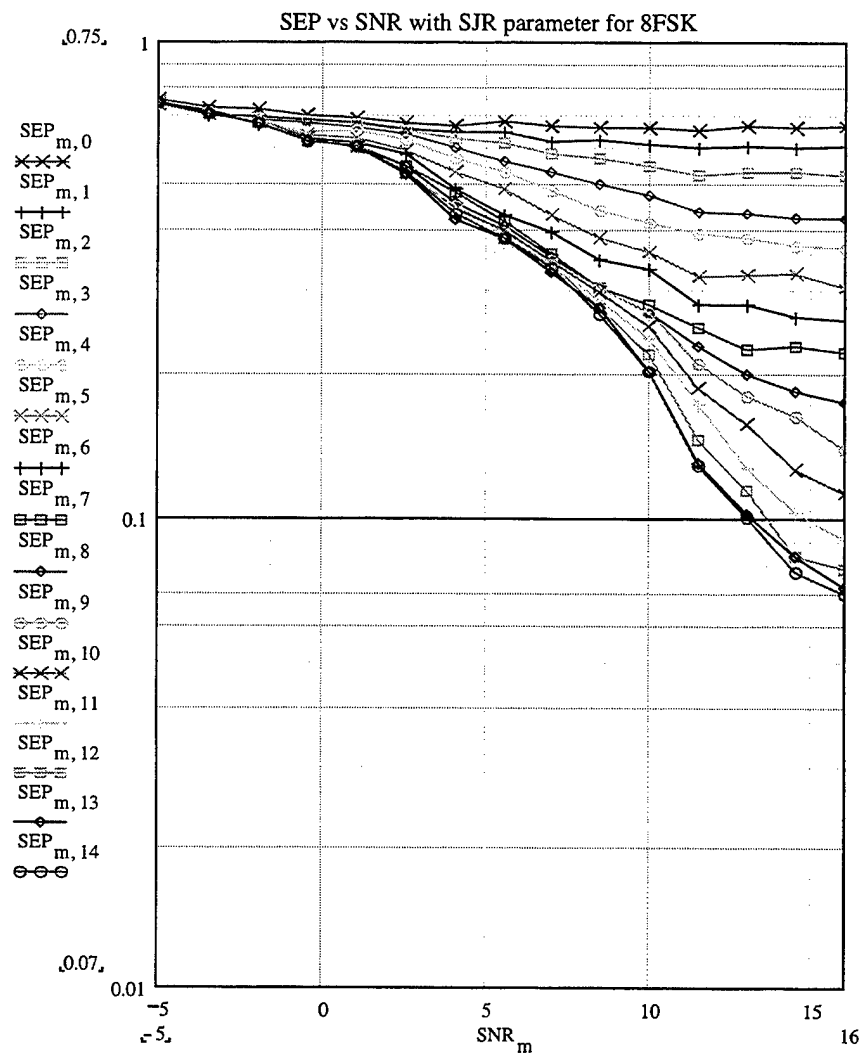
Figure 156. Simulation symbol error probability versus SNR with SJR as a parameter

for non-coherent 8FSK with Rayleigh fading.

In Figures 157 and 158, respectively, the theoretical and simulation

symbol error probabilities are shown as functions of SJR with SNR as a parameter.
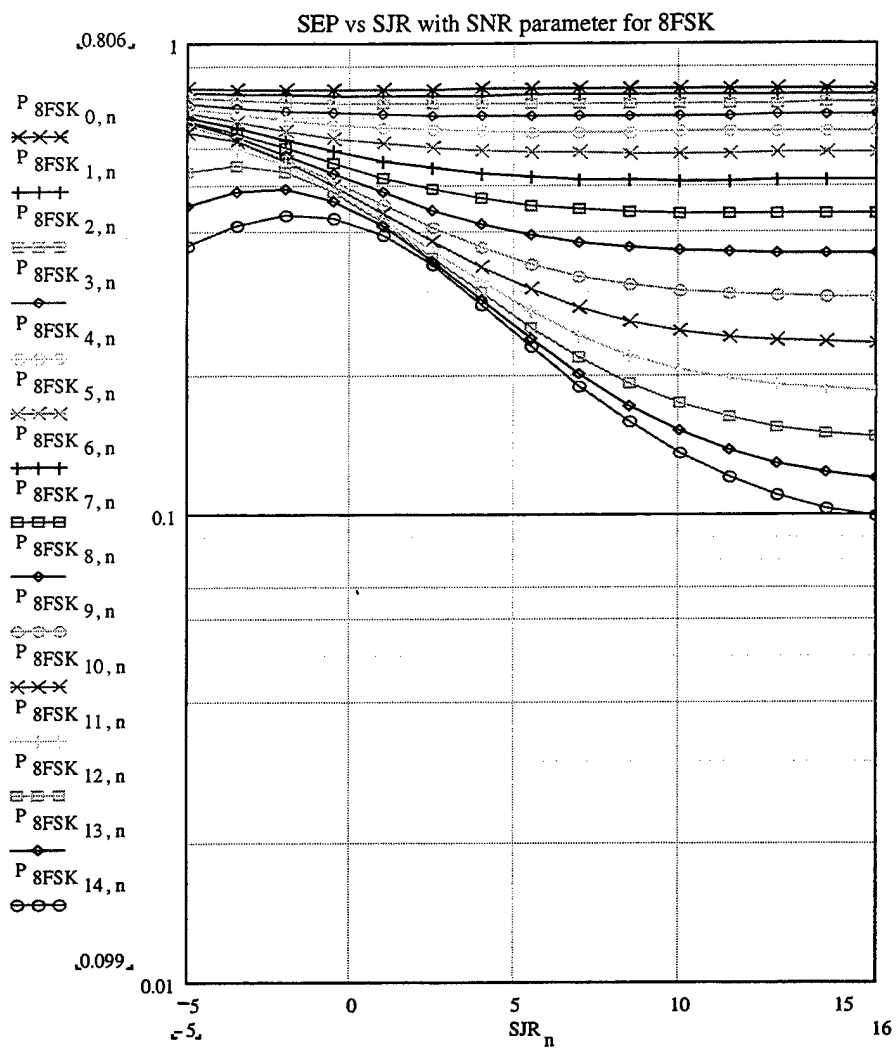
Figure 157. Theoretical symbol error probability versus SJR with SNR as a parameter

for non-coherent 8FSK with Rayleigh fading.

We again note the dramatic increase in the symbol error probability due to

Rayleigh fading and co-channel interference.
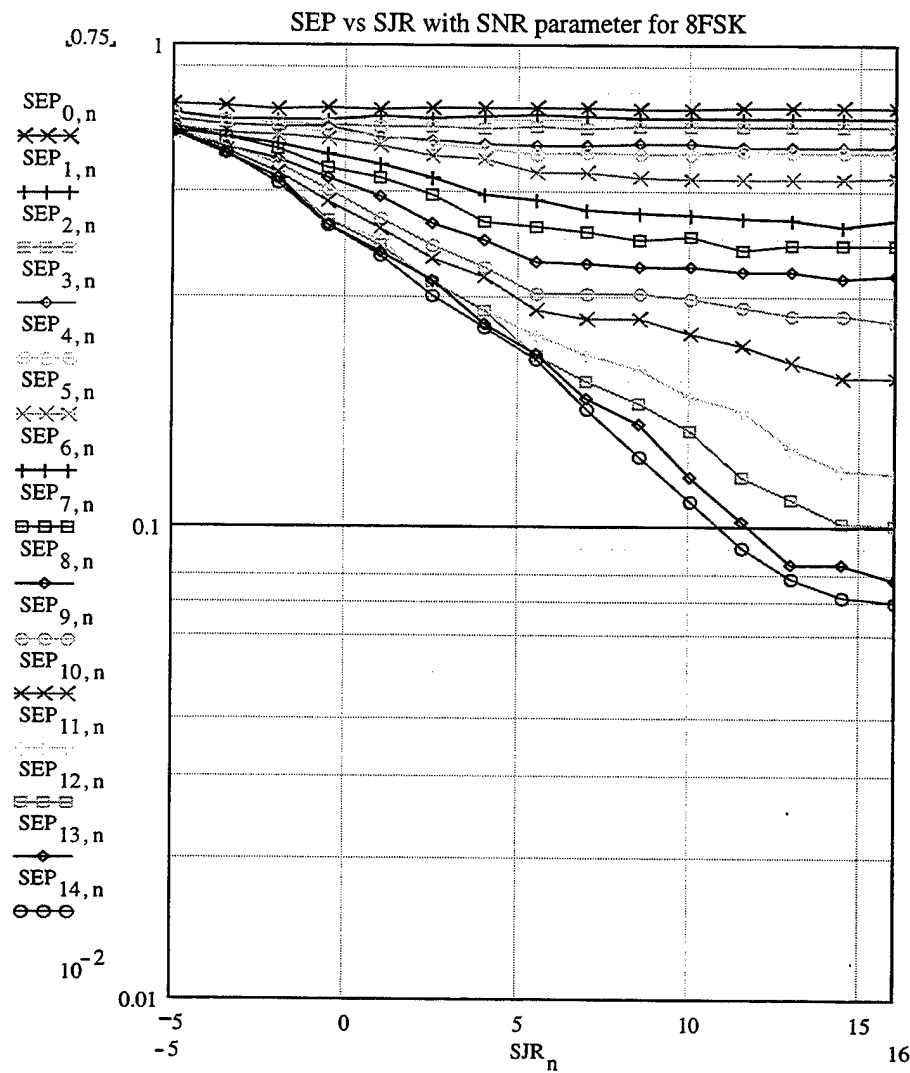
Figure 158. Experimental symbol error probability versus SJR with SNR as a parameter for non-coherent 8FSK with Rayleigh fading.

In Figure 159, the average difference for each curve is plotted versus SNR and SJR for each of the 15 previously presented curves. Finally, the relative difference (percent "error") between the theory and the simulation is summarized in Table 47.
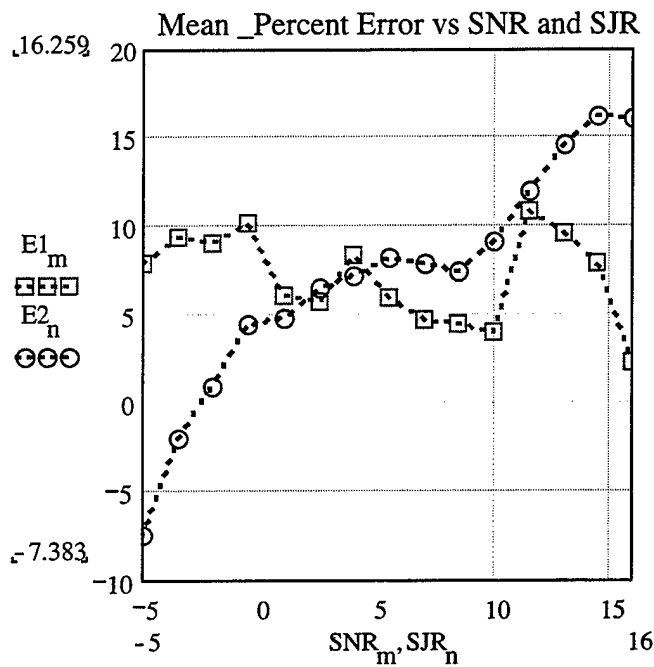
Figure 159. Mean percent difference as a function of SNR and SJR, respectively.

The two curves show how the mean difference varies with SNR and SJR. Each value of the mean difference is the average of the differences that correspond to the 15 points on each of the 15 curves for the symbol error probability as a function of SNR (with SJR as parameter) and SJR (with SNR as parameter).

	SYMBOL ERROR PROBABILITY	NON-COHERENT 8FSK
1.	Root Mean Square Difference (%)	13.126
2.	Average Mean Difference (%)	7.145
3.	Maximum Difference (%)	35.017
4.	Minimum Difference (%)	-78.858
5.	Difference Deviation (%)	11.011

Table 47. Summary of the accuracy of the simulation for non-coherent 8FSK.

231

Observing the results for non-coherent detection of 2, 4, and 8FSK in a Rayleigh fading channel with AWGN and co-channel interference, we note that the simulation underestimates the theory for all of the cases of 2, 4 and 8FSK. The root mean square difference (in percent) is about 16% (in average) and the mean percent difference in average is about 8%, which suggests good accuracy.

The average results for the non-coherent detection of 2, 4, and 8FSK are presented in Table 48.

	SYMBOL ERROR PROBABILITY	AVERAGE RESULTS FOR NON-COHERENT 2, 4, AND 8FSK
1.	Root Mean Square Difference (%)	16.282
2.	Average Mean Difference (%)	8.272
3.	Maximum Difference (%)	36.548
4.	Minimum Difference (%)	-98.203
5.	Difference Deviation (%)	13.708

Table 48. Average results for the non-coherent detection of 2, 4, and 8FSK.

C. RICIAN FADING CHANNEL – COHERENT DETECTION

In this section, we derive the symbol error probability for MFSK signals transmitted over a frequency-nonselective, slowly fading Rician channel with AWGN and co-channel interference. The frequency-nonselective, slowly fading channel results in multiplicative distortion of both the MFSK transmitted signal and the interfering MFSK signal. The condition that the channel fades slowly implies that the multiplicative process may be considered as a constant during at least one symbol time interval. Furthermore, we assume that the channel fading is sufficiently slow that the phase shift introduced by the channel can be estimated from the received signal without error.

1. Theoretical Probability Of Symbol Error For Coherent Detection

The probability that the signal symbol will be received correctly is evaluated, again, separately for the two following cases:

- **1st case**: the signal and the interference symbols are on the same branch.

- **2nd case**: the signal and the interference symbols are on different branches.

  #### a) The Signal And The Interference Symbols Are On The Same Branch

  The conditional probability of symbol error for coherent, orthogonal MFSK Rician fading signal with AWGN and co-channel interference has been derived in Chapter V (equation (5.25)):

$$P1(r_j) = 1 - \int_0^\infty \int_{-\infty}^\infty \frac{1}{\sqrt{2\cdot\pi}} \cdot \left(1 - Q\left(x + y\cdot\frac{\sqrt{P_{dif}}}{\sqrt{P_{noise}}} + \frac{r_j}{\sqrt{P_{noise}}}\right)\right)^{M-1} \cdot e^{-\frac{1}{2}\left(x^2 + y^2 + 2\cdot R\right)} \cdot I0\left(\sqrt{2\cdot R}\cdot y\right)\cdot y\, dx\, dy \quad (6.20)$$

where r_j is the amplitude of the interfering MFSK signal.

The above symbol error probability is conditioned on the amplitude r_j of the interfering signal, with r_j considered as a Rician random variable with the pdf:

$$f\left(r_j\right)=\frac{r_j}{P_{j\_dif}}\cdot e^{\dfrac{-\left(r_j^2+2\cdot P_{j\_dir}\right)}{2\cdot P_{j\_dif}}}\cdot I0\left(\frac{\sqrt{2\cdot P_{j\_dir}}\cdot r_j}{P_{j\_dif}}\right) \qquad (6.21)$$

where:

P_{j_dir} is the power of the direct interfering signal component

P_{j_dif} is the power of the diffuse interfering signal component.

Integrating the product of the conditional probability of symbol error and the probability density function of the interfering signal's amplitude r_j over all possible values of r_j, we obtain the unconditional probability of symbol error for this case. Using the transformation:

$$\frac{r_j}{\sqrt{P_{j\_dif}}}=z \qquad (6.22)$$

we obtain:

$$P1=1-\int_0^\infty\int_0^\infty\int_{-\infty}^\infty\left[\frac{1}{\sqrt{2\cdot\pi}}\cdot\left(1-Q\left(x+y\cdot\sqrt{\frac{P_{dif}}{P_{noise}}}+z\cdot\sqrt{\frac{P_{j\_dif}}{P_{noise}}}\right)\right)^{M-1}\right.$$
$$\left. e^{\dfrac{-1}{2}\cdot\left(x^2+y^2+z^2+2\frac{P_{dir}}{P_{dif}}+2\frac{P_{j\_dir}}{P_{j\_dif}}\right)}\cdot I0\left(\sqrt{2\cdot\frac{P_{dir}}{P_{dif}}}\cdot y\right)\cdot I0\left(\sqrt{2\cdot\frac{P_{j\_dir}}{P_{j\_dif}}}\cdot z\right)\cdot y\cdot z\right]dxdydz \quad (6.23)$$

This integral has to be evaluated numerically.

234

b) The Signal And The Interference Symbols Are On Different Branches

The conditional probability of symbol error for this case has already been derived in Chapter V (equation (5.28)):

$$P2\left(r_j\right) = 1 - \frac{1}{\sqrt{2 \cdot \pi}} \cdot \int_0^\infty \int_{-\infty}^\infty \left[\left(1 - Q\left(x + y \cdot \frac{\sqrt{P_{dif}}}{\sqrt{P_{noise}}}\right)\right)^{M-2} \cdot \left(1 - Q\left(x + \frac{y \cdot \sqrt{P_{dif}} - r_j}{\sqrt{P_{noise}}}\right)\right) \right. \\ \left. e^{\frac{-1}{2} \cdot \left(x^2 + y^2 + 2 \cdot R\right)} \cdot I0\left(\sqrt{2 \cdot R \cdot y}\right) \cdot y \right] dx\,dy \quad (6.24)$$

Integrating the product of the conditional probability of symbol error and the probability density function of the interfering signal's amplitude r_j over all possible values of r_j, and using the transformation of equation (6.22) we get the unconditional probability of symbol error for this case:

$$P2 = 1 - \int_0^\infty \int_0^\infty \int_{-\infty}^\infty \left[\frac{1}{\sqrt{2 \cdot \pi}} \cdot \left(1 - Q\left(x + y \cdot \sqrt{\frac{P_{dif}}{P_{noise}}} - z \cdot \sqrt{\frac{P_{j\_dif}}{P_{noise}}}\right)\right) \right. \\ \left(1 - Q\left(x + y \cdot \sqrt{\frac{P_{dif}}{P_{noise}}}\right)\right)^{M-2} \cdot e^{\frac{-1}{2} \cdot \left(x^2 + y^2 + z^2 + 2 \cdot R + 2 \frac{P_{j\_dir}}{P_{j\_dif}}\right)} \\ \left. I0\left(\sqrt{2 \cdot R \cdot y}\right) \cdot y \cdot z \cdot I0\left(2 \cdot \sqrt{\frac{P_{j\_dir}}{P_{j\_dif}}} \cdot z\right) \right] dx\,dy\,dz \quad (6.25)$$

This triple integral has to be evaluated numerically.

c) Total Symbol Error Probability

The total symbol error probability, combining the two cases is given by:

$$P_{total} = \frac{1}{M} \cdot P1 + \frac{M-1}{M} \cdot P2 \qquad (6.26)$$

where 1/M is the probability that the desired and the interfering symbols are on the same branch and (M-1)/M is the probability that the desired and the interfering symbols are on different branches.

It is convenient to define the ratio of the powers of direct and diffuse components of the interfering signal, as:

$$R_{jam} = \frac{P_{j\_dir}}{P_{j\_dif}} \qquad (6.27)$$

For a given value of total signal power, we have:

$$Power_{j\_dir} + Power_{j\_dif} = Power_{jam\_signal\_total} \qquad (6.28)$$

Next, we will express the last relationship in terms of the ratio of the powers of direct and diffuse components of the interfering signal, as:

$$\frac{Power_{jam\_signal\_total}}{Power_{j\_dif}} = 1 + R_{jam} \qquad (6.29)$$

We can easily obtain the relationships:

$$\frac{P_{j\_dir}}{P_{noise}} = \frac{R_{jam}}{1+R_{jam}} \cdot 10^{\frac{SNR-SJR}{10}} \qquad \frac{P_{j\_dif}}{P_{noise}} = \frac{1}{1+R_{jam}} \cdot 10^{\frac{SNR-SJR}{10}} \qquad (6.30)$$

Substituting equations (6.27) and (6.30) into equations (6.23) and (6.25), we are able to evaluate and plot the theoretical symbol error probability as a function of the ratio of the powers of the direct and diffuse signal components.

2. Simulink Model and Block Analysis

The block diagram of the Simulink model, developed for the simulation of coherent MFSK with AWGN and co-channel interference in a Rician fading channel, is shown on Figure 160. This model is the combination of the model that was used for the coherent MFSK in a Rician fading channel and the model that was used for coherent MFSK signal affected by co-channel interference. (The block parameters were retained).
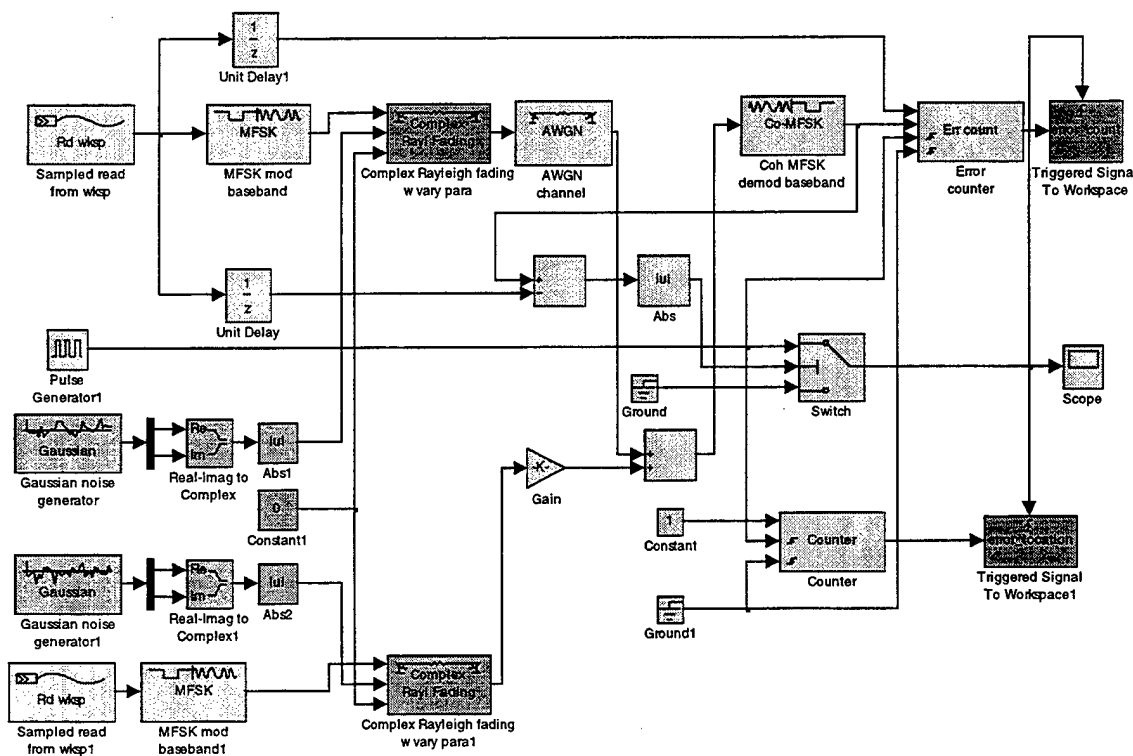
Figure 160. Model for coherent MFSK with AWGN and co-channel interference in a Rician fading channel.

3.   Simulation Analysis And Performance Verification

In this section, simulation results are presented in order to verify the performance

of coherent MFSK.

a)   Results For 2FSK

The theoretical and the simulation symbol error probabilities for

coherently detected 2FSK are presented in the Figures 161 and 162, respectively, as

functions of average SNR in dB with SJR as a parameter. The values for the SNR and

SJR were chosen from –5 dB to +30 dB in increments of 2.5 dB.
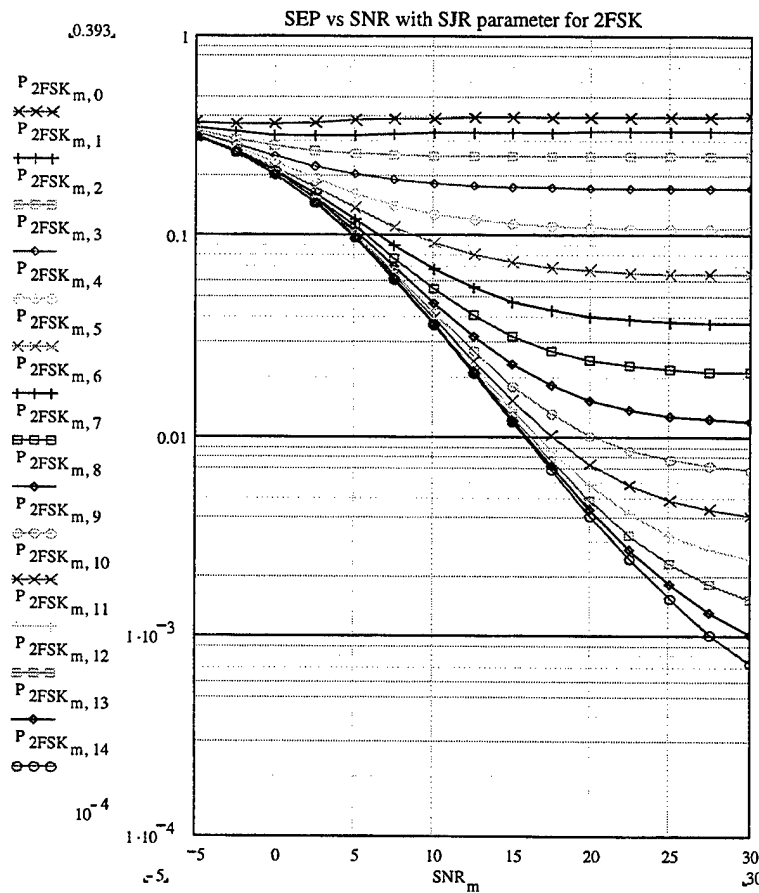
Figure 161. Theoretical symbol error probability versus SNR with SJR as a parameter

238

for coherent 2FSK, with Rician fading and R=1 for both MFSK signals (desirable and interfering).
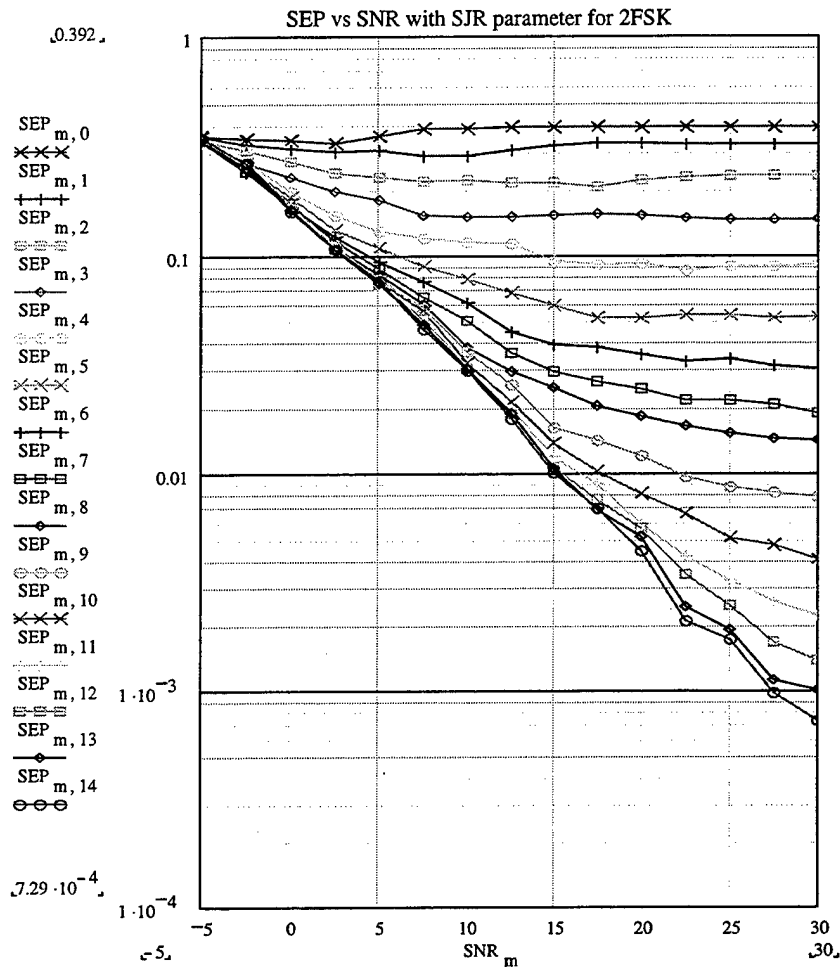
Figure 162. Simulation symbol error probability versus SNR with SJR as a parameter for coherent 2FSK, with Rician fading and R=1 for both MFSK signals (desirable and interfering).

In Figure 163 and 164, respectively, the theoretical and simulation results for the symbol error probability are presented as functions of SJR with SNR as a parameter.

239

SEP vs SJR with SNR parameter for 2FSK

Legend (left side):

$P_{2FSK_{0,n}}$
✕✕✕
$P_{2FSK_{1,n}}$
+ + +
$P_{2FSK_{2,n}}$
▣▣▣
$P_{2FSK_{3,n}}$
—◇—
$P_{2FSK_{4,n}}$
···
$P_{2FSK_{5,n}}$
✕✕✕
$P_{2FSK_{6,n}}$
+ + +
$P_{2FSK_{7,n}}$
▣▣▣
$P_{2FSK_{8,n}}$
—◇—
$P_{2FSK_{9,n}}$
⊖⊖⊖
$P_{2FSK_{10,n}}$
✕✕✕
$P_{2FSK_{11,n}}$
···
$P_{2FSK_{12,n}}$
▣▣▣
$P_{2FSK_{13,n}}$
—◇—
$P_{2FSK_{14,n}}$
⊖⊖⊖

$.0.393.$

10^{-4}

X-axis: SJR_n from -5 to 30
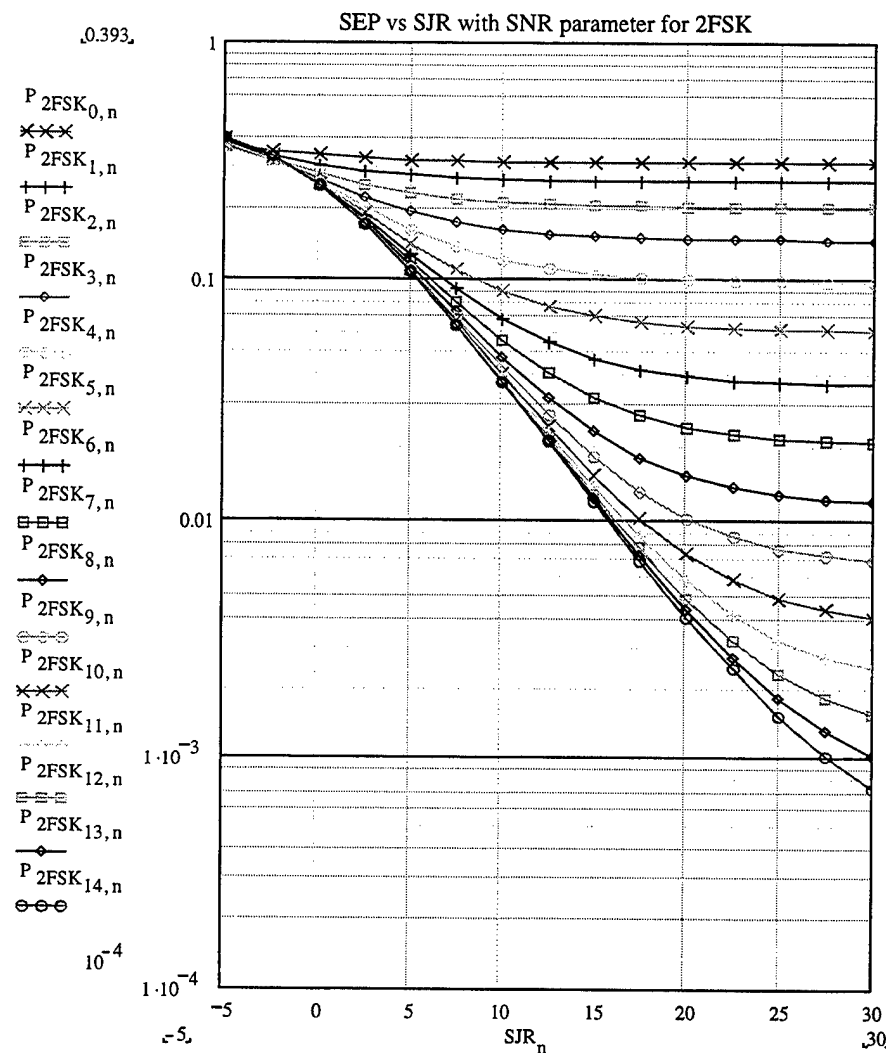
Figure 163. Theoretical symbol error probability versus SJR with SNR as a parameter for coherent 2FSK, with Rician fading and R=1 for both MFSK signals (desirable and interfering).

We note again the dramatic increase in the symbol error probability due to Rician fading and co-channel interference.

240
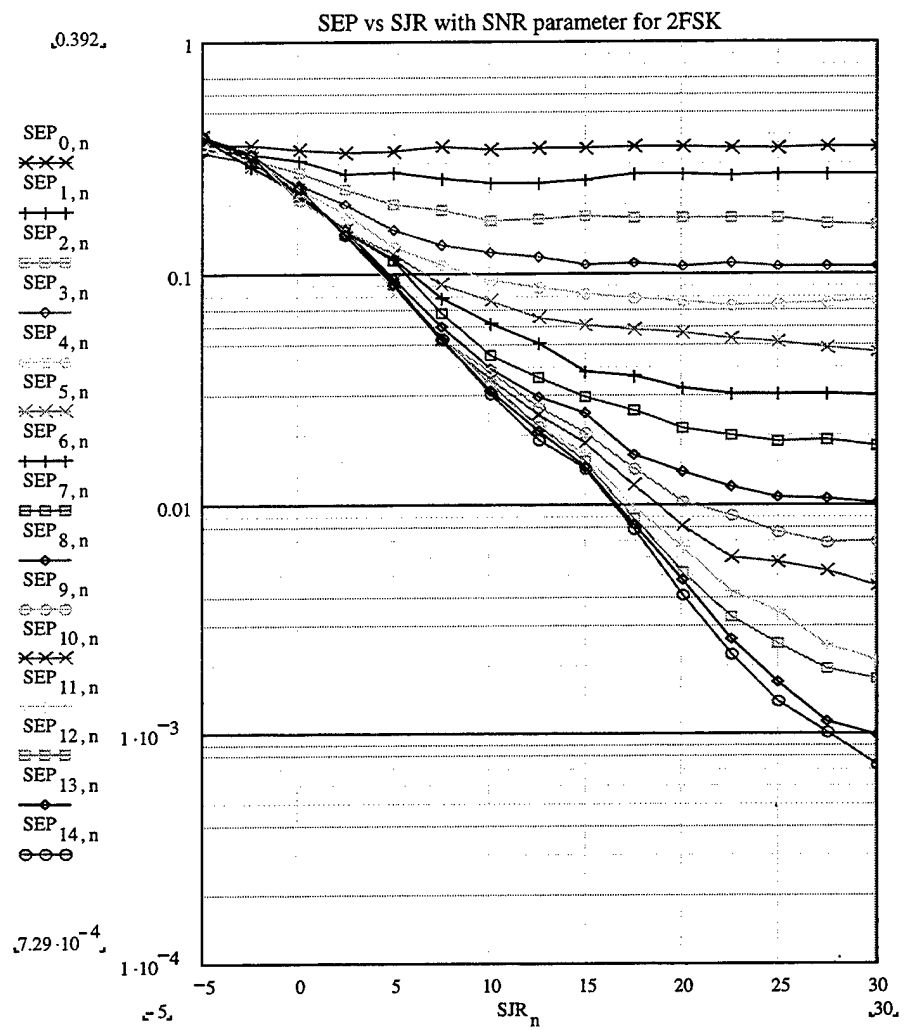
Figure 164. Simulation symbol error probability versus SJR with SNR as a parameter for coherent 2FSK, with Rician fading and R=1 for both MFSK signals (desirable and interfering).

The relative difference (percent "error") between the theory and the simulation is presented in Table 49. In Figure 165, the average difference for each curve is plotted versus SNR and SJR for each of the 15 previously presented curves.
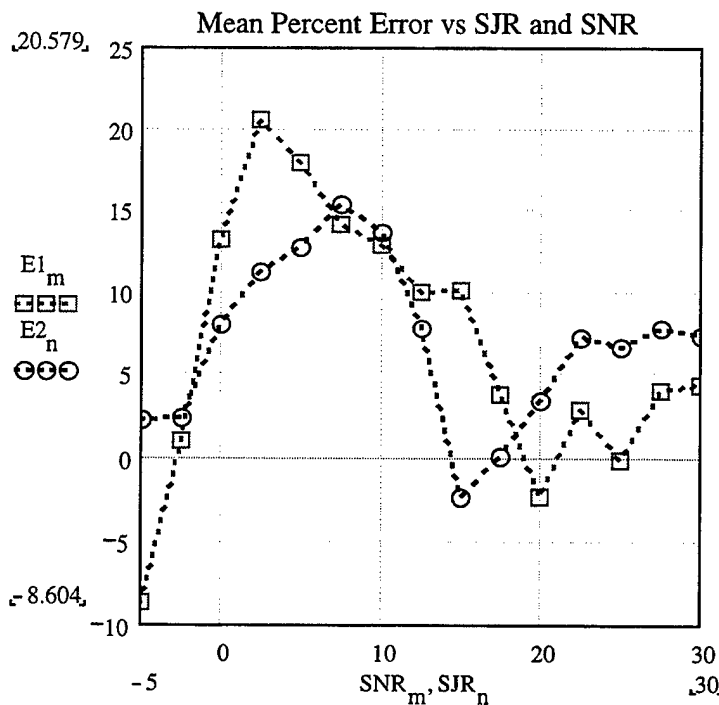
Figure 165. Mean percent difference as a function of SNR and SJR, respectively.

The two curves show how the mean difference varies with SNR and SJR. Each value of the mean difference is the average of the differences that correspond to the 15 points on each of the 15 curves for the symbol error probability as a function of SNR (with SJR as parameter) and SJR (with SNR as parameter), respectively.

	SYMBOL ERROR PROBABILITY	COHERENT 2FSK
1.	Root Mean Square Difference (%)	13.486
2.	Average Mean Difference (%)	6.962
3.	Maximum Difference (%)	27.207
4.	Minimum Difference (%)	-22.565
5.	Difference Deviation (%)	11.55

Table 49. Summary of the accuracy of the simulation for coherent 2FSK.

b)   Results For 4FSK

The theoretical and the simulation symbol error probabilities for coherently detected 4FSK are presented in the Figures 166 and 167, respectively, as functions of average SNR in dB with SJR as a parameter. The values for the signal-to-noise and signal-to-interference ratios were chosen from –5 dB to +30 dB in increments of 2.5 dB.
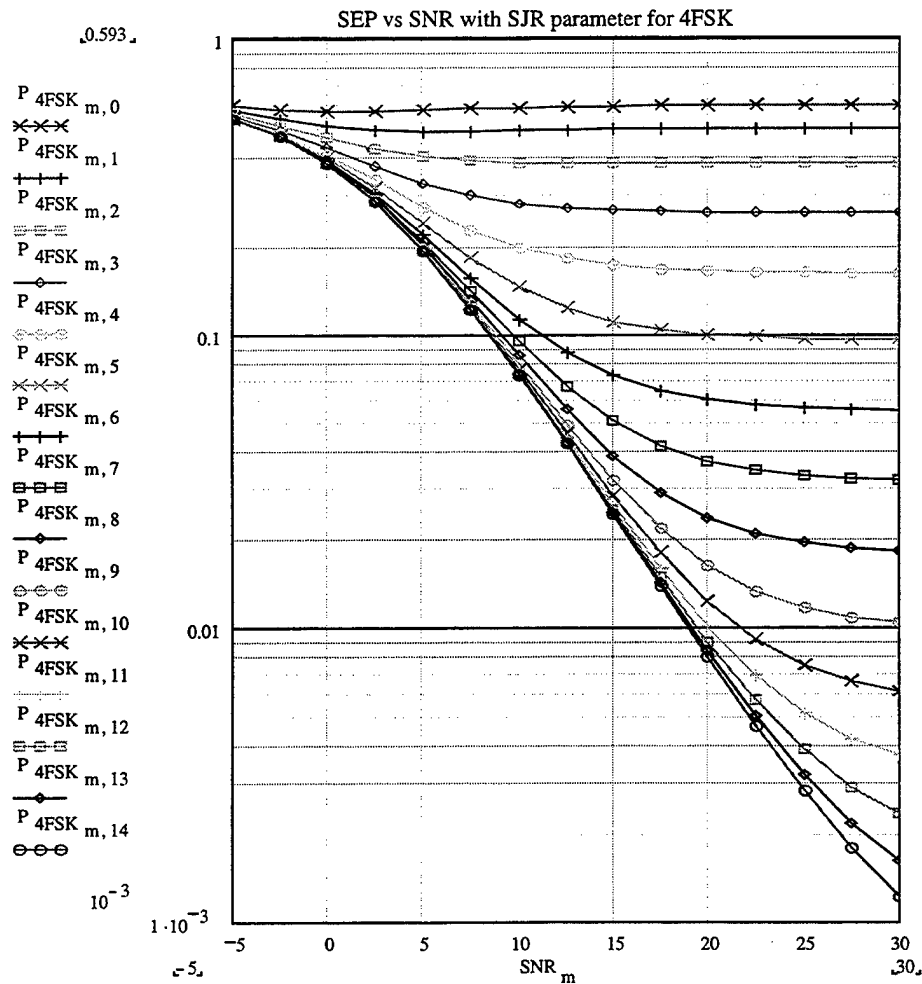
Figure 166. Theoretical symbol error probability versus SNR with SJR as a parameter for coherent 4FSK, with Rician fading and R=1 for both MFSK signals (desirable and interfering).

243
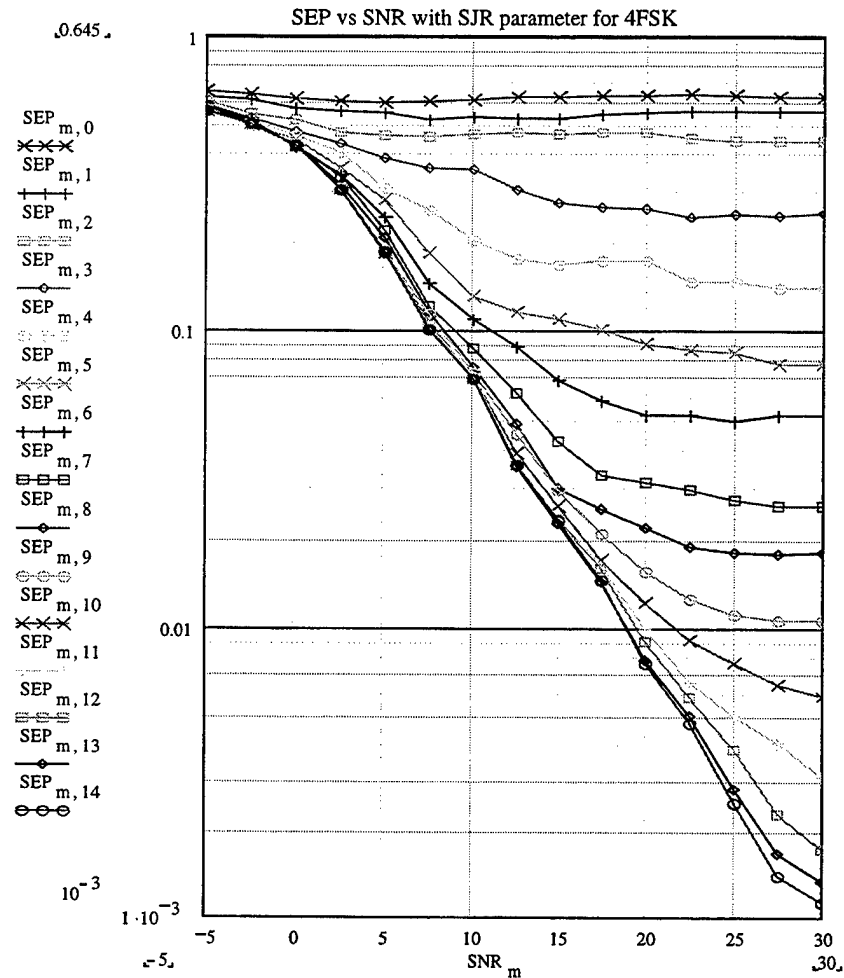
Figure 167. Simulation symbol error probability versus SNR with SJR as a parameter for coherent 4FSK, with Rician fading and R=1 for both MFSK signals (desirable and interfering).

In Figures 168 and 169, respectively, the theoretical and simulation results for the symbol error probability are presented as functions of SJR with SNR as a parameter.

244
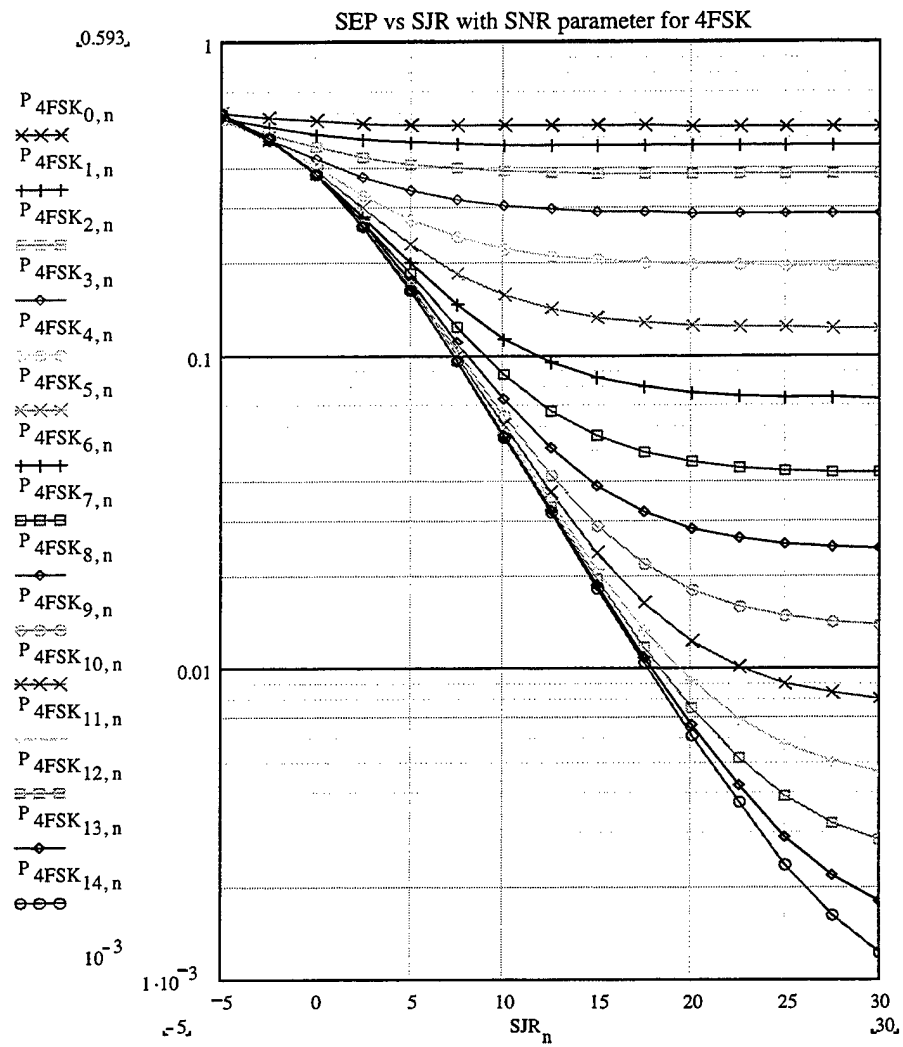
Figure 168. Theoretical symbol error probability versus SJR with SNR as a parameter

for coherent 4FSK, with Rician fading and R=1 for both MFSK signals (desirable and

interfering).

We note again the dramatic increase in the symbol error probability due to

Rician fading and co-channel interference.
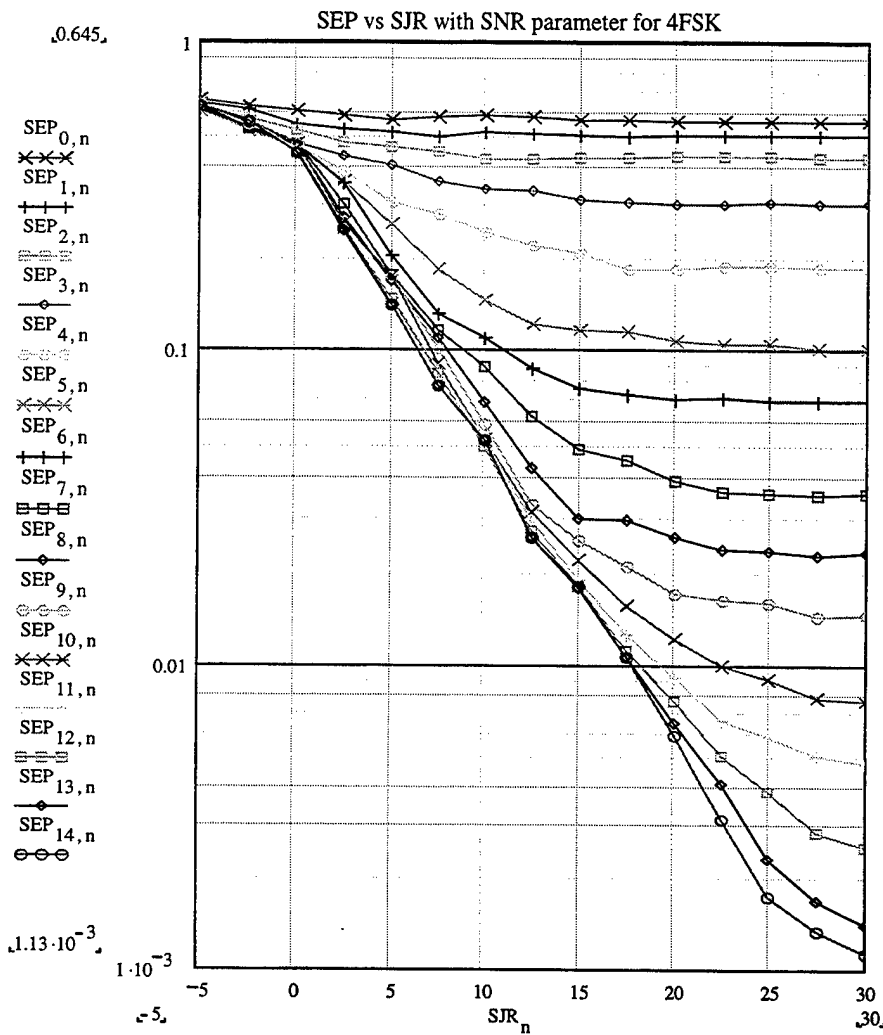
Figure 169. Simulation symbol error probability versus SJR with SNR as a parameter for coherent 4FSK, with Rician fading and R=1 for both MFSK signals (desirable and interfering).

The relative difference (percent "error") between the theory and the simulation is presented in Table 50. In Figure 170, the average error for each curve is plotted versus SNR and SJR for each of the 15 previously presented curves.
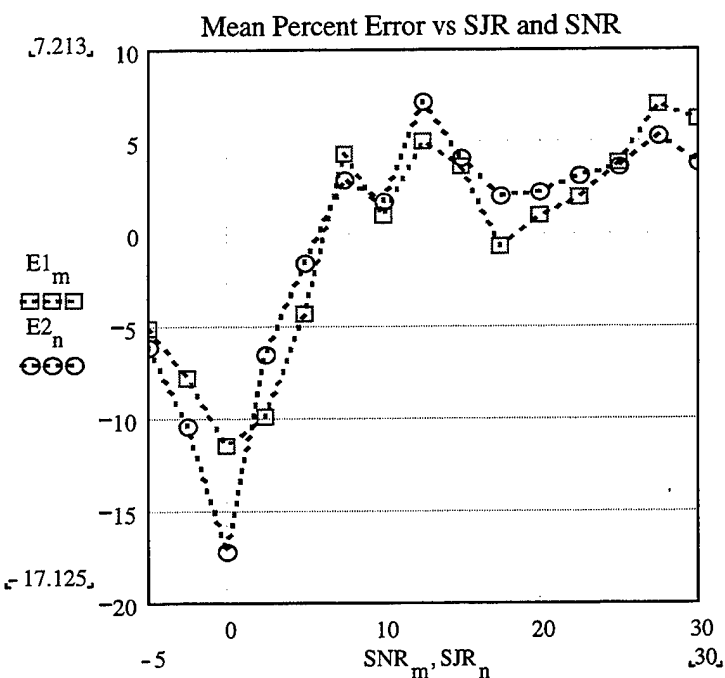
Figure 170. Mean percent difference as a function of SNR and SJR, respectively.

The two curves show how the mean difference varies with SNR and SJR. Each value of the mean difference is the average of the differences that correspond to the 15 points on each of the 15 curves for the symbol error probability as a function of SNR (with SJR as parameter) and SJR (with SNR as parameter), respectively.

	SYMBOL ERROR PROBABILITY	COHERENT 4FSK
1.	Root Mean Square Difference (%)	10.995
2.	Average Mean Difference (%)	-0.322
3.	Maximum Difference (%)	26.542
4.	Minimum Difference (%)	-25.95
5.	Difference Deviation (%)	10.99

Table 50. Summary of the accuracy of the simulation for coherent 4FSK.

247

c)   Results For 8FSK

The theoretical and the simulation symbol error probabilities for coherently detected 8FSK are presented in the Figures 171 and 172, respectively, as functions of average SNR in dB with SJR as a parameter. The values for the signal-to-noise and signal-to-interference ratios were chosen from −5 dB to +30 dB in increments of 2.5 dB.
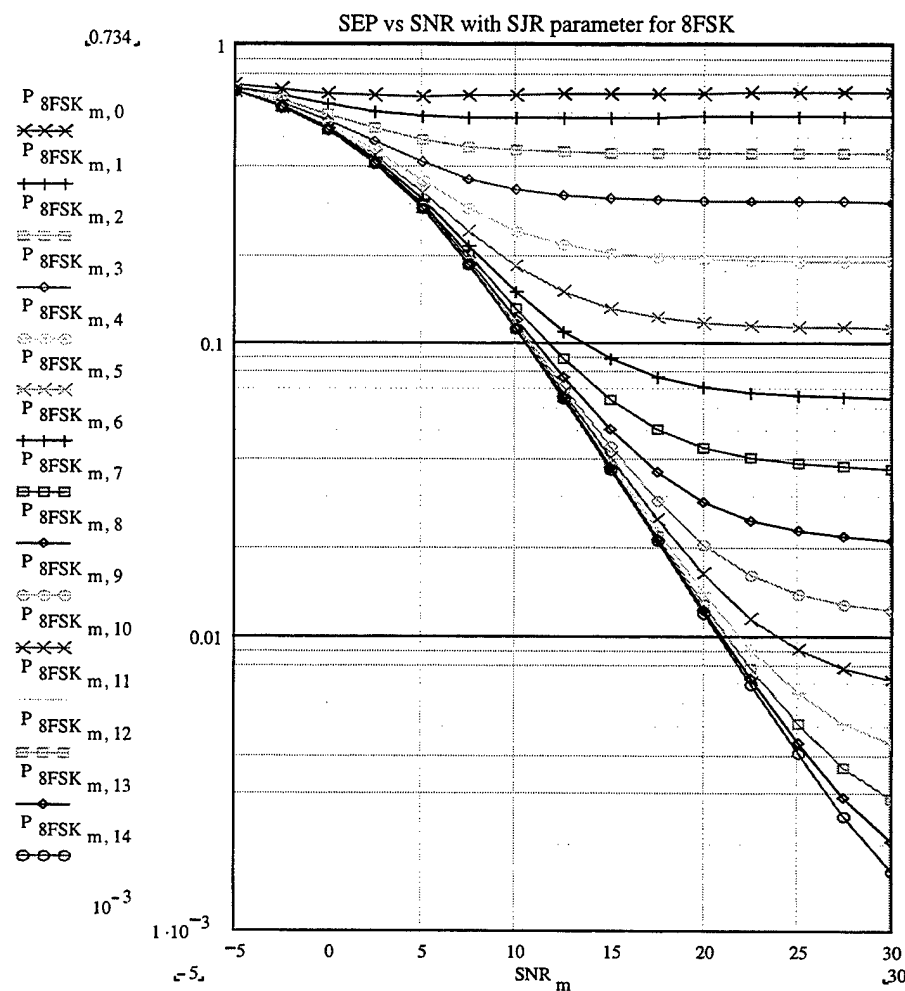

Figure 171. Theoretical symbol error probability versus SNR with SJR as a parameter for coherent 8FSK, with Rician fading and R=1 for both MFSK signals (desirable and interfering).

248
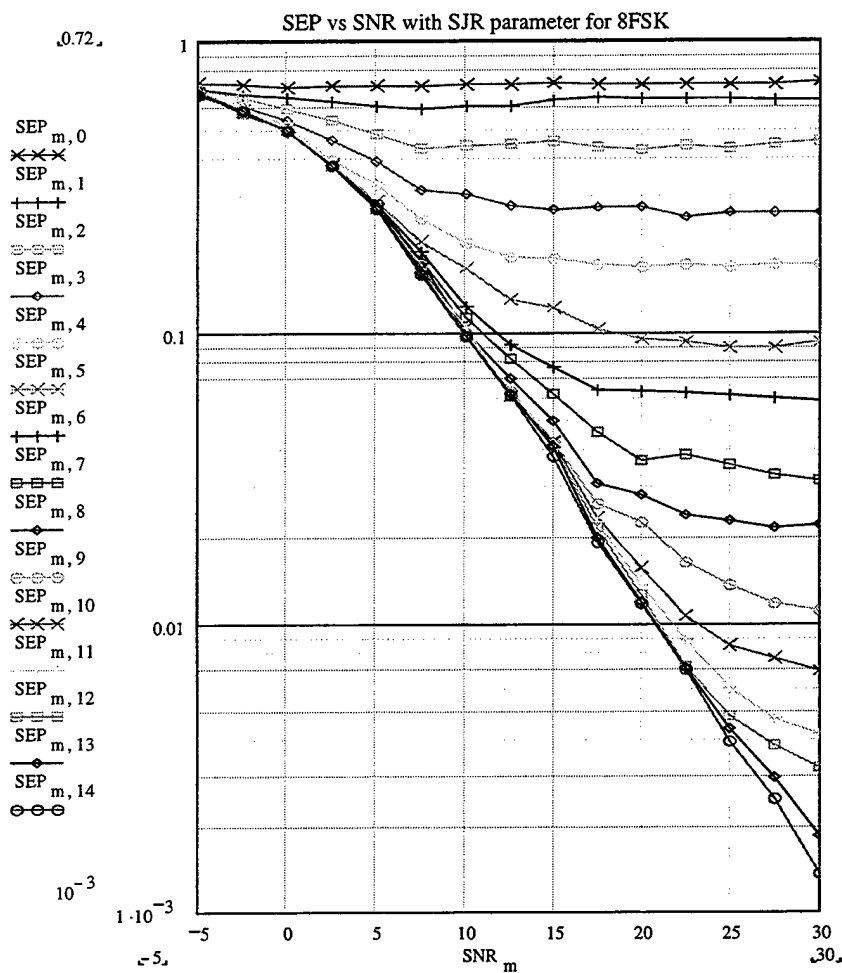
Figure 172. Simulation symbol error probability versus SNR with SJR as a parameter for coherent 8FSK, with Rician fading and R=1 for both MFSK signals (desirable and interfering).

In Figures 173 and 174, respectively, the theoretical and simulation results for the symbol error probability are presented as functions of SJR with SNR as a parameter.

249
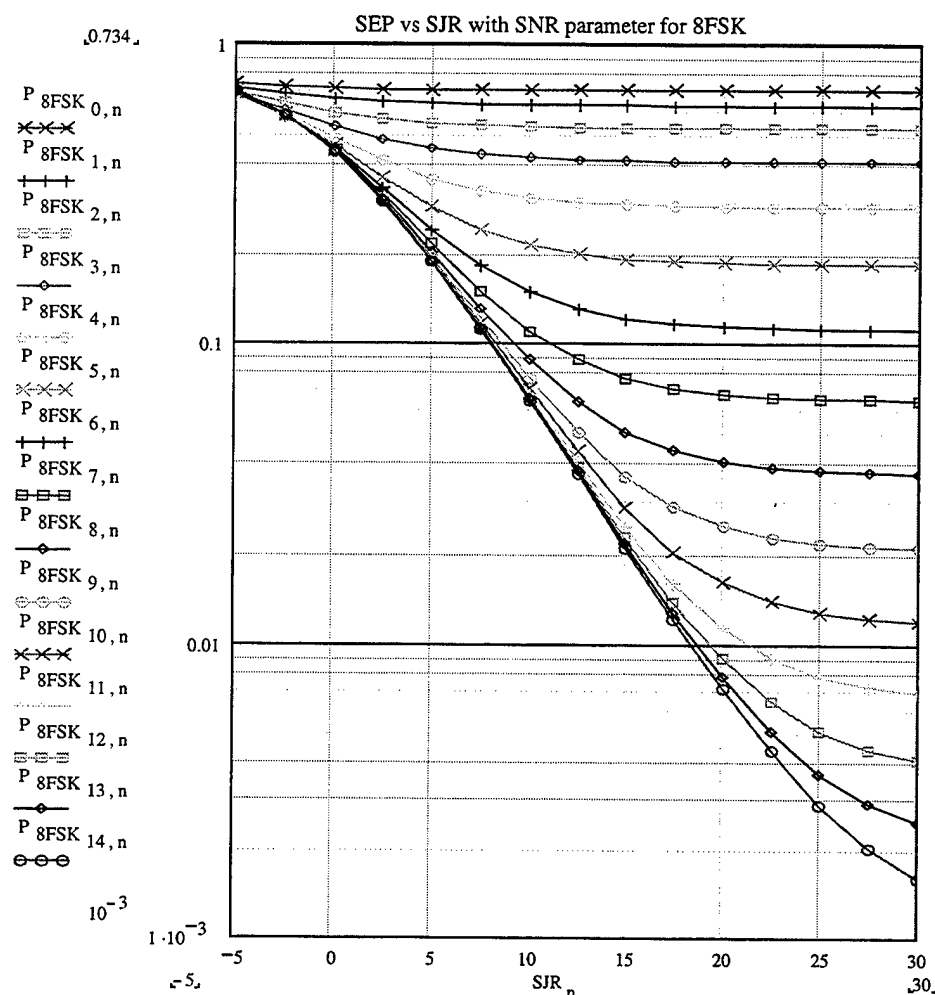
Figure 173. Theoretical symbol error probability versus SJR with SNR as a parameter for coherent 8FSK, with Rician fading and R=1 for both MFSK signals (desirable and interfering).

We note again the dramatic increase in the symbol error probability due to Rician fading and co-channel interference.
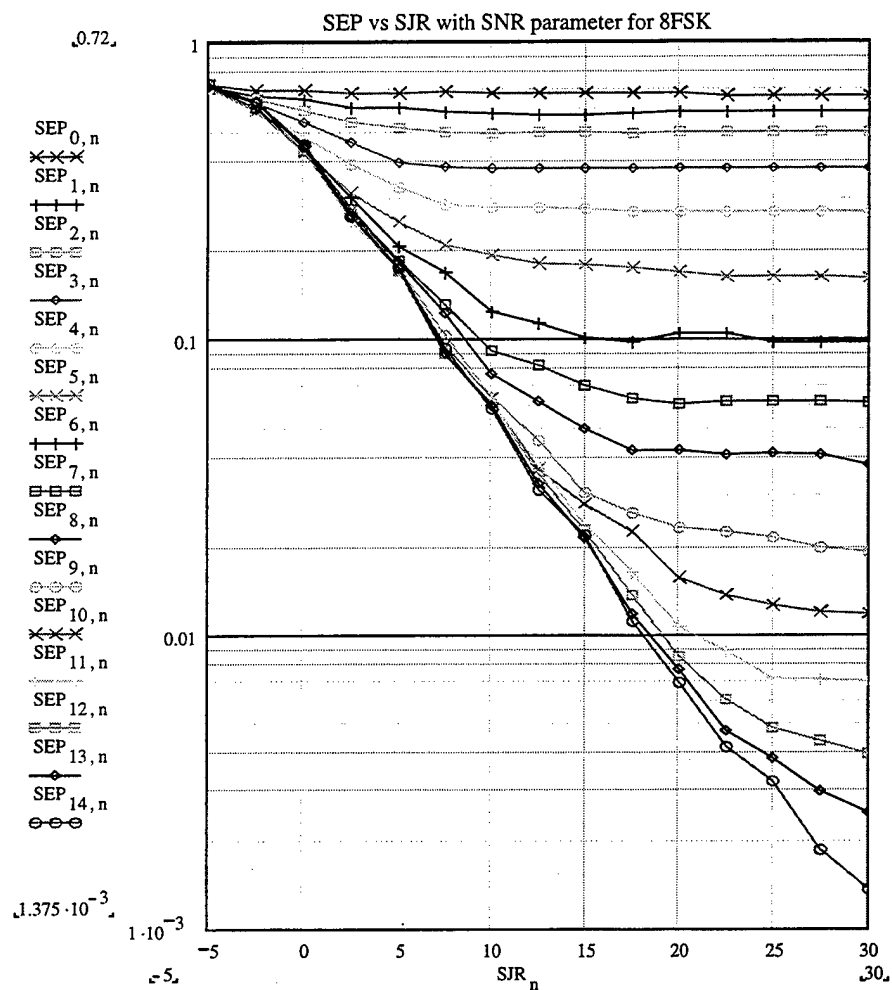
Figure 174. Simulation symbol error probability versus SJR with SNR as a parameter for coherent 8FSK, with Rician fading and R=1 for both MFSK signals (desirable and interfering).

The relative difference (percent "error") between the theory and the simulation is presented in Table 51. In Figure 175, the average difference for each curve is plotted versus SNR and SJR for each of the 15 previously presented curves.

251
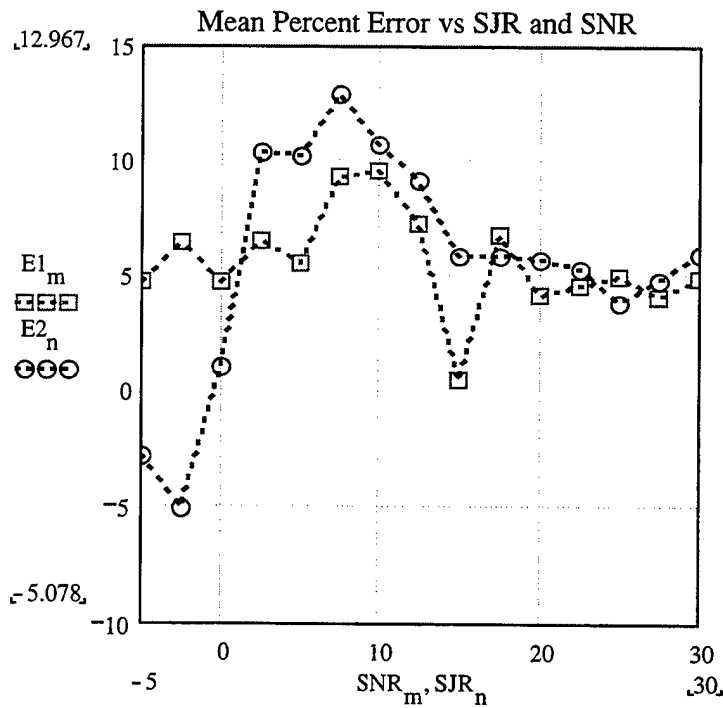
Figure 175. Mean percent difference as a function of SNR and SJR, respectively.

The two curves show how the mean difference varies with SNR and SJR. Each value of the mean difference is the average of the differences that correspond to the 15 points on each of the 15 curves for the symbol error probability as a function of SNR (with SJR as parameter) and SJR (with SNR as parameter), respectively.

	SYMBOL ERROR PROBABILITY	COHERENT 8FSK
1.	Root Mean Square Difference (%)	8.684
2.	Average Mean Difference (%)	5.598
3.	Maximum Difference (%)	20.848
4.	Minimum Difference (%)	-11.528
5.	Difference Deviation (%)	6.638

Table 51. Summary of the accuracy of the simulation for coherent 8FSK.

Observing the results for coherent detection of 2, 4, and 8FSK in a Rician fading channel and affected by AWGN and co-channel interference, we note that the simulation underestimates the theory for the cases of 2 and 8FSK and overestimates the theory for the case of 4FSK. The root mean square difference (in percent) is about 11% (in average) and the mean percent difference for all the cases is about 4%.

The average results for the coherent detection of 2, 4, and 8FSK are presented in Table 52.

	SYMBOL ERROR PROBABILITY	AVERAGE RESULTS FOR COHERENT 2, 4, AND 8FSK
1.	Root Mean Square Difference (%)	11.055
2.	Average Mean Difference (%)	4.079
3.	Maximum Difference (%)	24.866
4.	Minimum Difference (%)	-20.014
5.	Difference Deviation (%)	9.726

Table 52. Average results for the coherent detection of 2, 4, and 8FSK.

D. RICIAN FADING CHANNEL – NON-COHERENT DETECTION

In this section, we derive the symbol error probability for non-coherent detection of MFSK signals transmitted over a frequency-nonselective, slowly fading Rician channel in the presence of AWGN and co-channel interference. The Rician fading channel affects both the desired and interfering signals.

1. Theoretical Probability Of Symbol Error For NonCoherent Detection

The probability that the signal symbol will be received correctly is evaluated, again, separately for the following two cases:

- 1st case: the signal and the interference symbols are on the same branch.

- 2nd case: the signal and the interference symbols are on different branches.

Then, combining the two cases, we evaluate the total symbol error probability.

a) The Signal And The Interference Symbols Are On The Same Branch

The conditional probability of symbol error for non-coherent, orthogonal MFSK signals transmitted through a Rician fading channel, with AWGN and co-channel interference has been derived in Chapter V (equation (5.41)):

$$P1(r_j) = \int_0^\infty \sum_{k=1}^{M-1} \frac{(M-1)!}{k! \cdot (M-1-k)!} \cdot \frac{(-1)^{k+1}}{(k+1)} \cdot e^{\frac{-k}{2 \cdot (k+1)} \left(\frac{\sqrt{P_{dif}} \, y + r_j}{\sqrt{P_{noise}}} \right)^2} \cdot e^{\frac{-1}{2} \cdot (y^2 + 2 \cdot R)} \cdot I0\left(\sqrt{2 \cdot R \cdot y}\right) \cdot y \, dy \quad (6.31)$$

where r_j is the amplitude of the interfering MFSK signal.

The above symbol error probability is conditioned on the amplitude r_j of the interfering signal, which is assumed as a Rician random variable with the probability density function:

$$f(r_j) = \frac{r_j}{P_{j\_dif}} \cdot e^{\frac{-\left(r_j^2 + 2 \cdot P_{j\_dir}\right)}{2 \cdot P_{j\_dif}}} \cdot I0\left(\frac{\sqrt{2 \cdot P_{j\_dir}} \cdot r_j}{P_{j\_dif}}\right) \quad (6.32)$$

where:

P_{j_dir} is the power of the direct interfering signal component

P_{j_dif} is the power of the diffuse interfering signal component.

Integrating the product of the conditional probability of symbol error and the probability density function of the interfering signal's amplitude r_j over all possible values of r_j, and using the transformation of (6.22) we obtain the unconditional probability of symbol error for this case:

$$P1 = \int_0^\infty \int_0^\infty \left[\sum_{k=1}^{M-1} \frac{(M-1)!}{k! \cdot (M-1-k)!} \cdot \frac{(-1)^{k+1}}{(k+1)} \cdot e^{\frac{-k}{2 \cdot (k+1)}\left(y \cdot \sqrt{\frac{P_{dif}}{P_{noise}}} + z \cdot \frac{P_{j\_dif}}{P_{noise}}\right)^2} \right. $$
$$\left. e^{\frac{-1}{2} \cdot \left(y^2 + 2 \cdot R\right)} \cdot I0\left(\sqrt{2 \cdot R} \cdot y\right) \cdot e^{\frac{-\left(z^2 + 2 \cdot R_{jam}\right)}{2}} \cdot I0\left(\sqrt{2 \cdot R_{jam}} \cdot z\right) \cdot y \cdot z \right] dy dz \quad (6.33)$$

The above integral must be evaluated numerically.

255

b) The Signal And The Interference Symbols Are On Different Branches

The conditional probability of symbol error for this case has already been derived in Chapter V (equation (5.43)). This is given by:

$$P2(r_j) = 1 - \int_0^\infty \int_0^\infty \left[\left(1 - e^{-\frac{x^2}{2}}\right)^{M-2} e^{-\frac{1}{2}\left(x^2 + \frac{P_{dif}}{P_{noise}} \cdot y^2\right)} \left[\left(1 - e^{-\frac{1}{2}\left(x^2 + \frac{r_j^2}{P_{noise}}\right)} \cdot \sum_{p=0}^\infty \left(\frac{r_j}{x \cdot \sqrt{P_{noise}}}\right)^p \cdot In\left(p, \frac{r_j}{\sqrt{P_{noise}}} \cdot x\right)\right) \right] I0\left(\frac{\sqrt{P_{dif}}}{\sqrt{P_{noise}}} \cdot y \cdot x\right) \cdot e^{-\frac{1}{2}\left(y^2 + 2 \cdot R\right)} \cdot I0\left(\sqrt{2 \cdot R} \cdot y\right) \cdot x \cdot y \right] dxdy \quad (6.34)$$

Integrating the product of the conditional probability of symbol error and the probability density function of the interfering signal's amplitude r_j over all possible values of r_j and using again the transformation of (6.22), we get the unconditional probability of symbol error for this case:

$$P2 = 1 - \int_0^\infty \int_0^\infty \int_0^\infty \left[\left[\left(1 - e^{-\frac{1}{2}\left(x^2 + z^2 \frac{P_{j\_dif}}{P_{noise}}\right)} \cdot \sum_{p=0}^\infty \left(\frac{z \cdot \sqrt{P_{j\_dif}}}{x \cdot \sqrt{P_{noise}}}\right)^p \cdot In\left(p, z \cdot \sqrt{\frac{P_{j\_dif}}{P_{noise}}} \cdot x\right)\right)\right] \left(1 - e^{-\frac{x^2}{2}}\right)^{M-2} e^{-\frac{1}{2}\left(x^2 + \frac{P_{dif}}{P_{noise}} \cdot y^2 + y^2 + z^2 + 2 \cdot R + 2 \cdot R_{jam}\right)} I0\left(\frac{\sqrt{P_{dif}}}{\sqrt{P_{noise}}} \cdot y \cdot x\right) \cdot I0\left(\sqrt{2 \cdot R} \cdot y\right) \cdot I0\left(\sqrt{2 \cdot R_{jam}} \cdot z\right) \cdot x \cdot y \cdot z \right] dxdydz \quad (6.35)$$

The above triple integral has to be evaluated numerically.

256

c) Total Symbol Error Probability

The total symbol error probability, combining the two cases, is given by:

$$P_{total} = \frac{1}{M} \cdot P1 + \frac{M-1}{M} \cdot P2 \qquad (6.36)$$

where 1/M is the probability that the transmitted and the interfering symbols are at the same branch and (M-1)/M is the probability that the transmitted and the interfering symbols are at different branches.

Substituting equations (6.27) and (6.30) into equations (6.33) and (6.35), we are able to evaluate and plot the theoretical symbol error probability as a function of SNR, SJR and the ratio of the powers of the direct and diffuse signal components.

2. Simulink Model and Block Analysis

The schematic diagram of the Simulink model is the same as the block diagram shown in Figure 160 for coherent detection except that the block 'Coh MFSK demod baseband' has been replaced by the block 'Non-coherent MFSK demod baseband'.

3. Simulation Analysis And Performance Verification

In this section, simulation results are presented in order to verify the performance of non-coherent detection of MFSK signal corrupted by AWGN and co-channel interference in a Rician fading channel. Each simulation runs until at least 100 errors are observed. The data sequences are limited to 10^6 symbols for each simulation, to prevent 'out of memory' errors. As long as less than 100 errors are observed, the simulation sequence is repeated until a sufficient number of errors are counted.

a) Results For 2FSK

The theoretical and the simulation symbol error probabilities for non-coherently detected 2FSK are presented in Figures 176 and 177, respectively, as functions of average SNR in dB with SJR as a parameter. The values for the signal-to-noise and signal-to-interference ratios were chosen from −5 dB to +16 dB in increments of 1.5 dB.
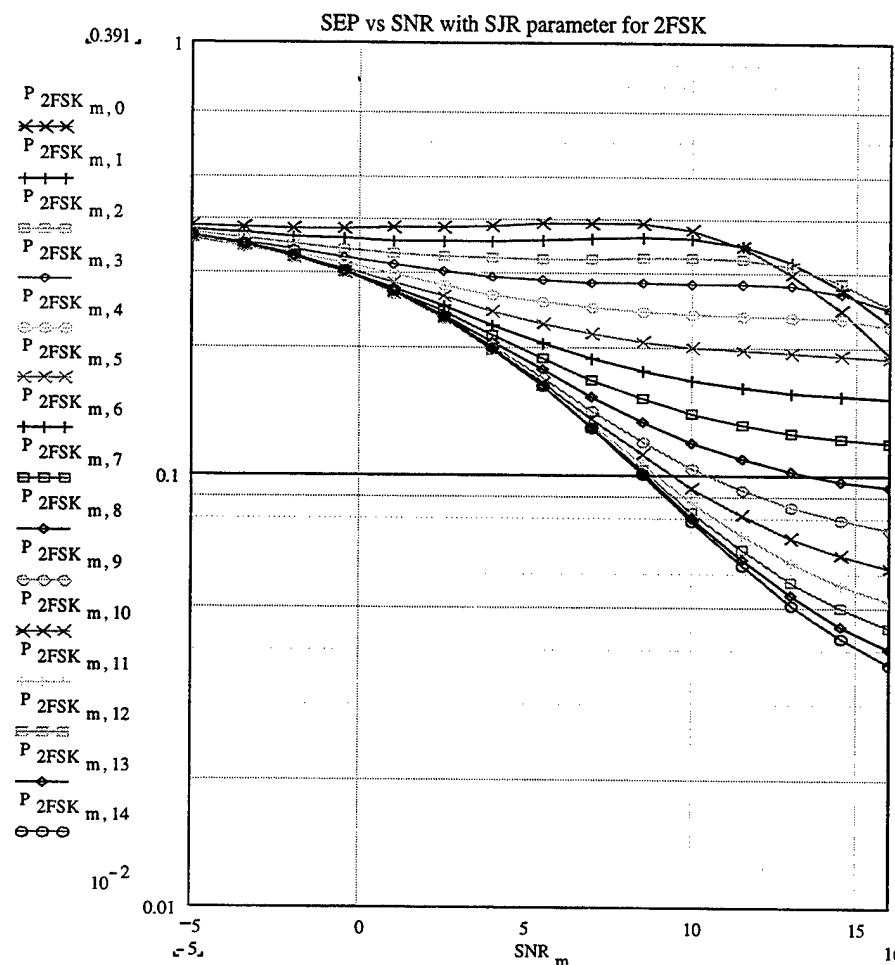
Figure 176. Theoretical symbol error probability versus SNR with SJR as a parameter.

258

for non-coherent 2FSK, with Rician fading and R=1 for both MFSK signals (desirable and interfering).

As evident from Figure 176 and 177, respectively, the curves tend to become flat as SNR increases that is they converge to a constant value determined by the value of SJR. The consequence of the signal fading is that the symbol error probability does not decrease as fast with the increase in either SNR (along a curve) or SJR (from curve to curve) as it does for the case of non-fading signals.
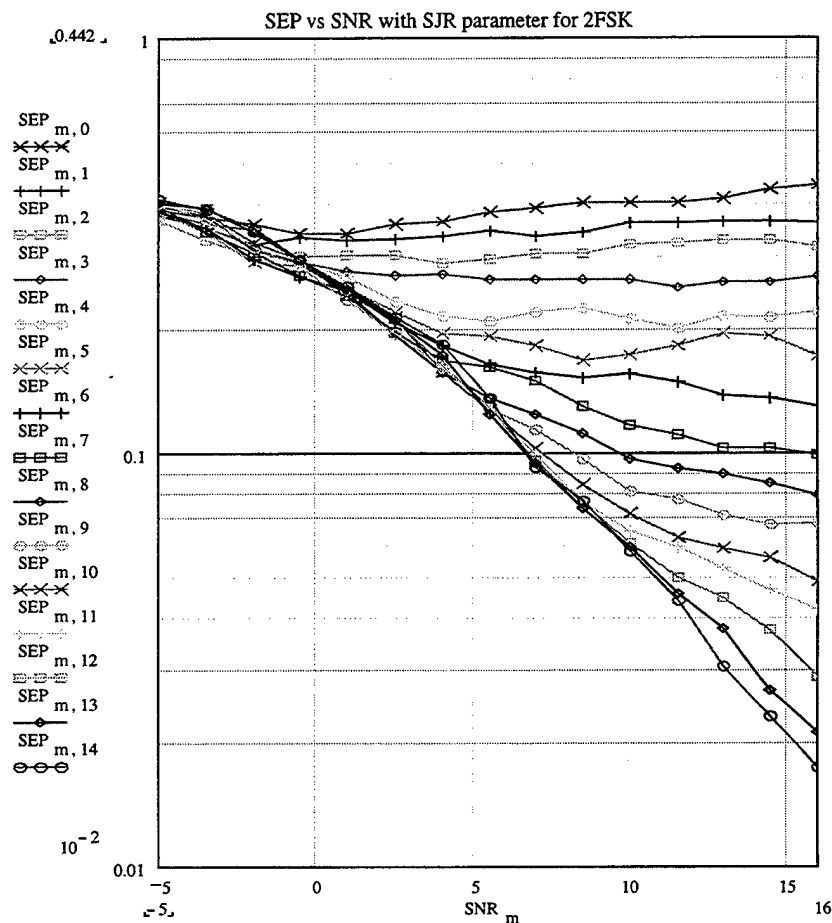
Figure 177. Simulation symbol error probability versus SNR with SJR as a parameter for non-coherent 2FSK, with Rician fading and R=1 for both MFSK signals (desirable and interfering).

259

In Figures 178 and 179, respectively, the theoretical and simulation results for the symbol error probability are presented as functions of SJR with SNR as a parameter.
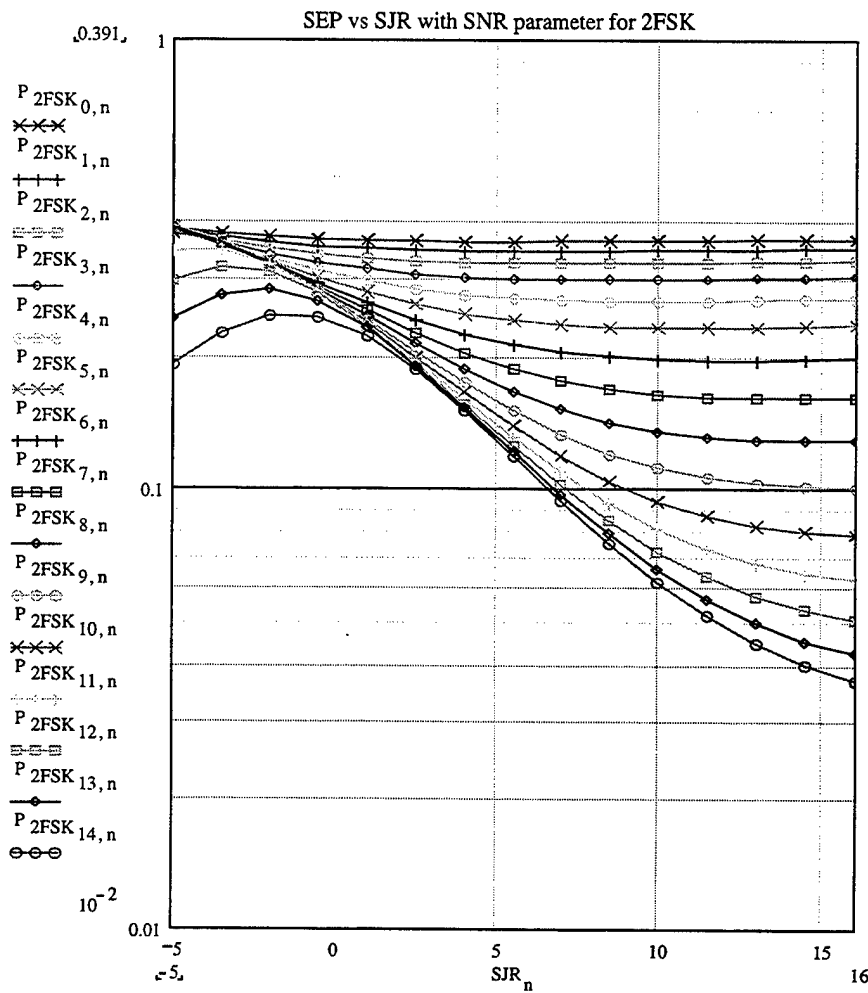
Figure 178. Theoretical symbol error probability versus SJR with SNR as a parameter for non-coherent 2FSK, with Rician fading and R=1 for both MFSK signals (desirable and interfering).

We note again the dramatic increase in the symbol error probability due to Rician fading and co-channel interference.
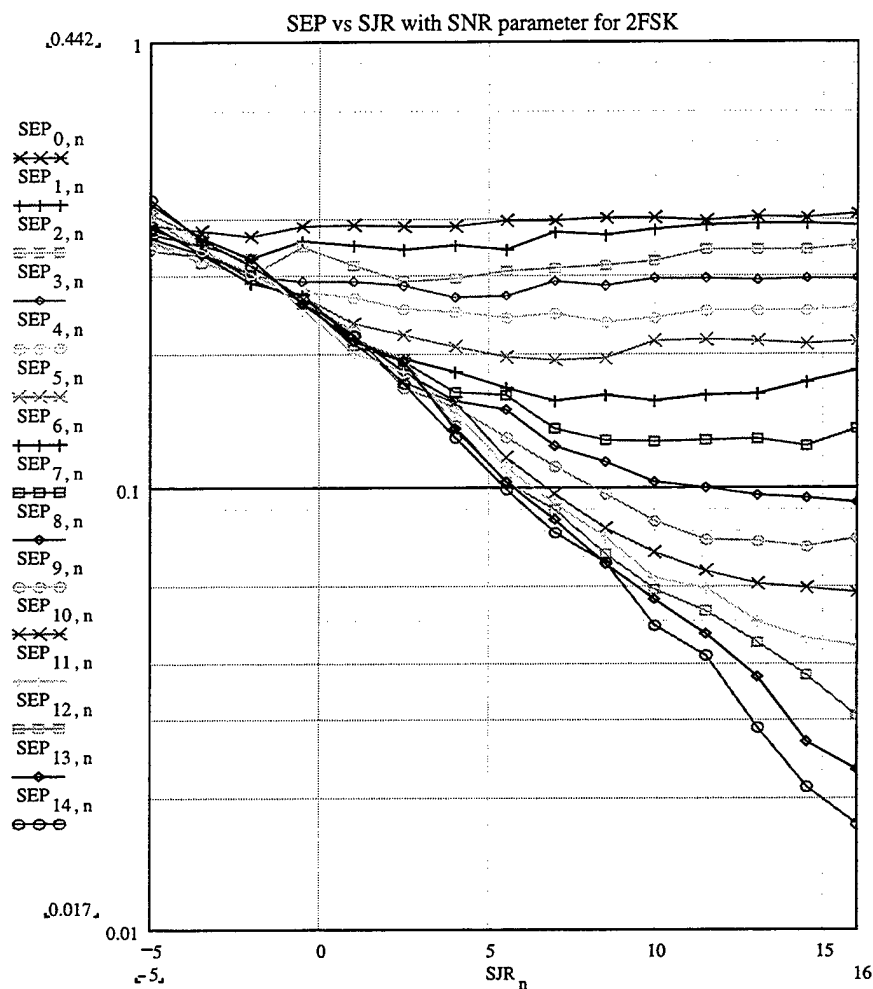
Figure 179. Simulation symbol error probability versus SJR with SNR as a parameter for non-coherent 2FSK, with Rician fading and R=1 for both MFSK signals (desirable and interfering).

The relative difference (percent "error") between the theory and the simulation is presented in Table 53. In Figure 180, the average error for each curve is plotted versus SNR and SJR for each of the 15 previously presented curves.

261
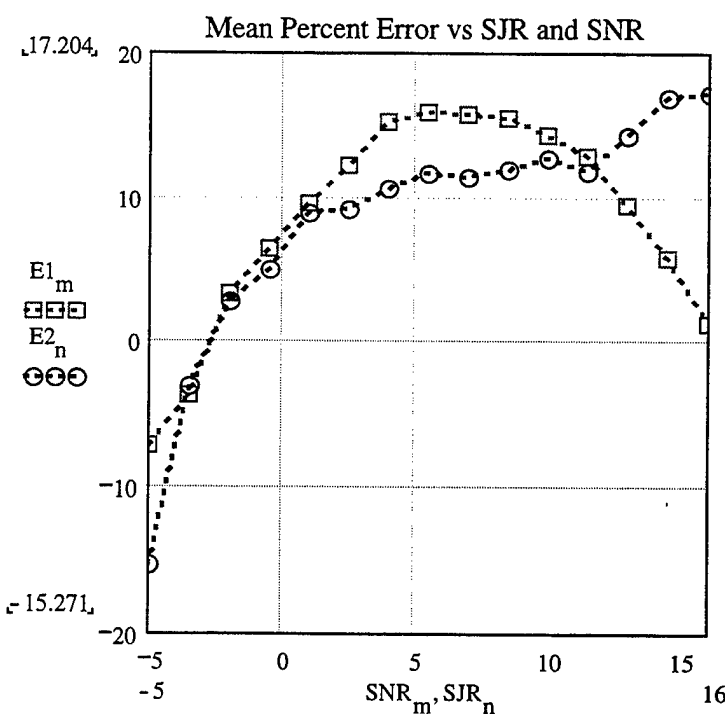
Figure 180. Mean percent difference as a function of SNR and SJR, respectively.

The two curves show how the mean difference varies with SNR and SJR. Each value of the mean difference is the average of the differences that correspond to the 15 points on each of the 15 curves for the symbol error probability as a function of SNR (with SJR as parameter) and SJR (with SNR as parameter), respectively.

	SYMBOL ERROR PROBABILITY	NON-COHERENT 2FSK
1.	Root Mean Square Difference (%)	19.325
2.	Average Mean Difference (%)	8.434
3.	Maximum Difference (%)	52.892
4.	Minimum Difference (%)	-129.912
5.	Difference Deviation (%)	17.387

Table 53. Summary of the accuracy of the simulation for non-coherent 2FSK.

b) Results For 4FSK

The theoretical and the simulation symbol error probabilities for non-coherently detected 4FSK are presented in Figures 181 and 182, respectively, as functions of average SNR in dB with SJR as a parameter. The values for the signal-to-noise and signal-to-interference ratios were chosen from −5 dB to +16 dB in increments of 1.5 dB.
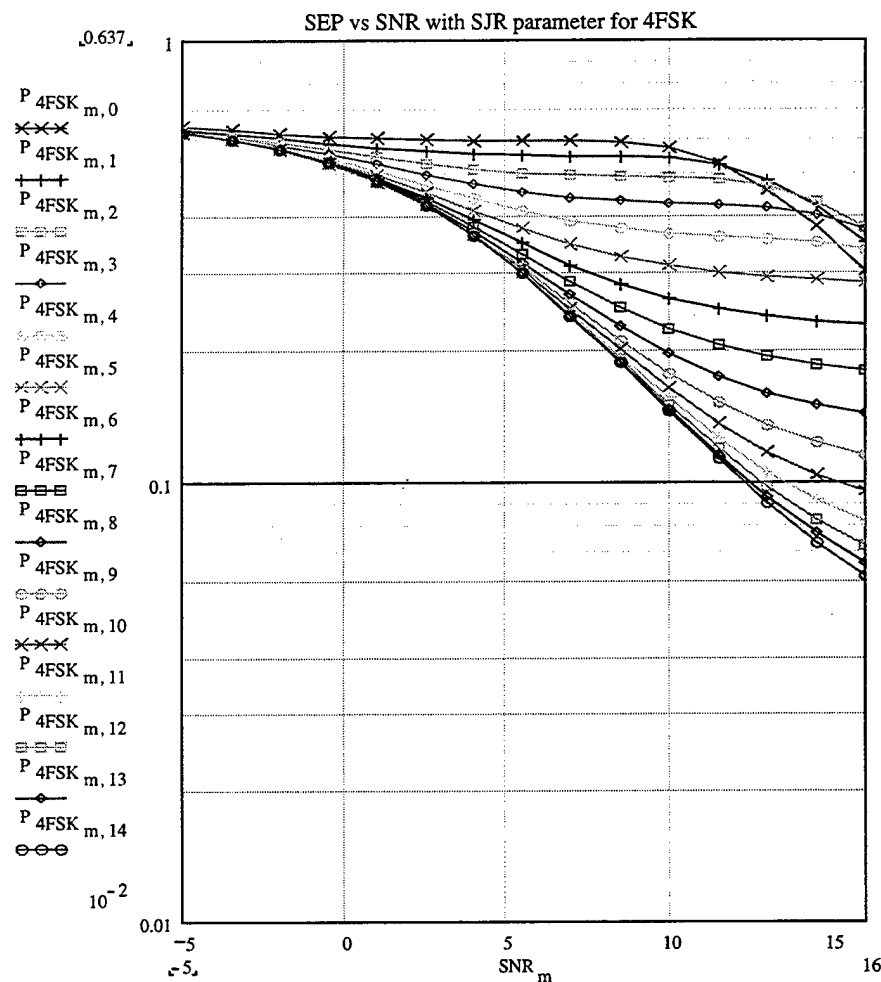

Figure 181. Theoretical symbol error probability versus SNR with SJR as a parameter for non-coherent 4FSK, with Rician fading and R=1 for both MFSK signals (desirable and interfering).
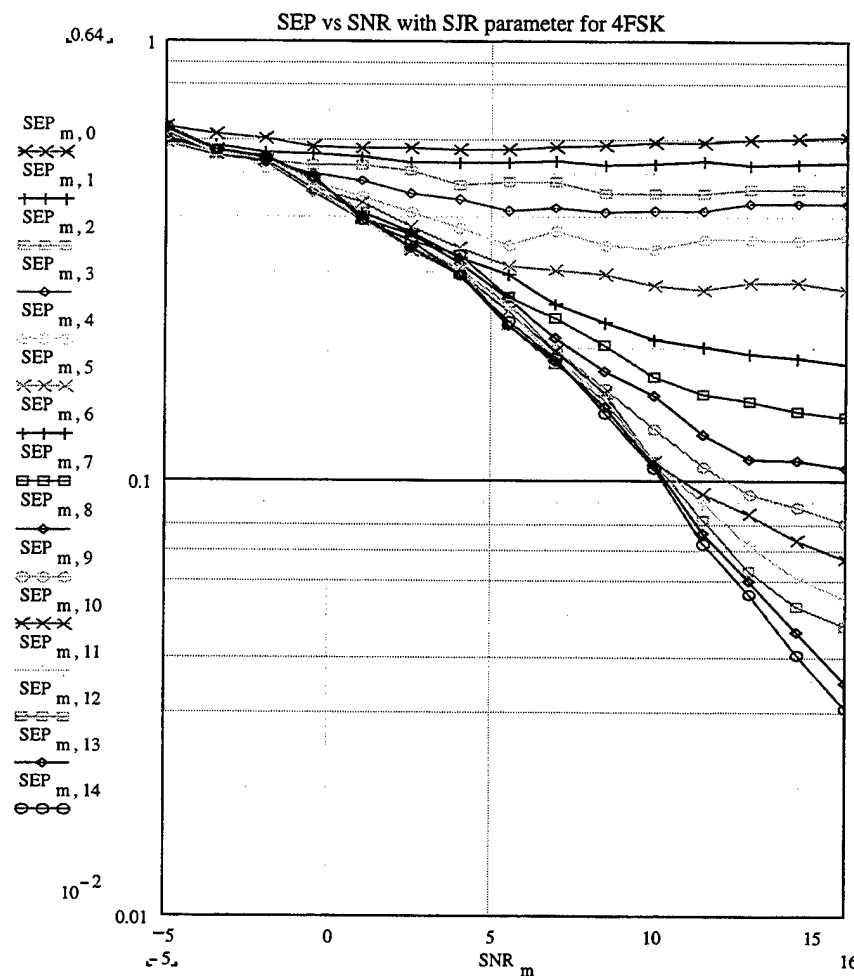
Figure 182. Simulation symbol error probability versus SNR with SJR as a parameter

for non-coherent 4FSK, with Rician fading and R=1 for both MFSK signals (desirable

and interfering).

In Figures 183 and 184, respectively, the theoretical and simulation results

for the symbol error probability are presented as functions of SJR with SNR as a
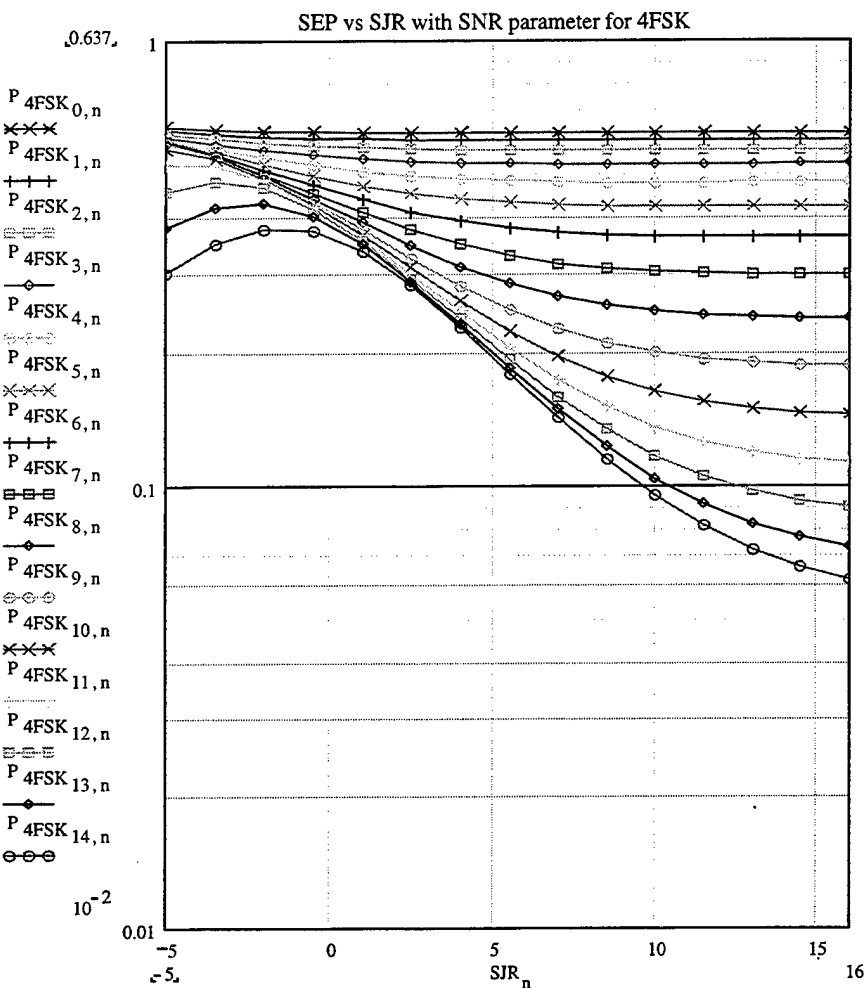
parameter.

Figure 183. Theoretical symbol error probability versus SJR with SNR as a parameter for non-coherent 4FSK, with Rician fading and R=1 for both MFSK signals (desirable and interfering).

We note again the dramatic increase in the symbol error probability due to Rician fading and co-channel interference.
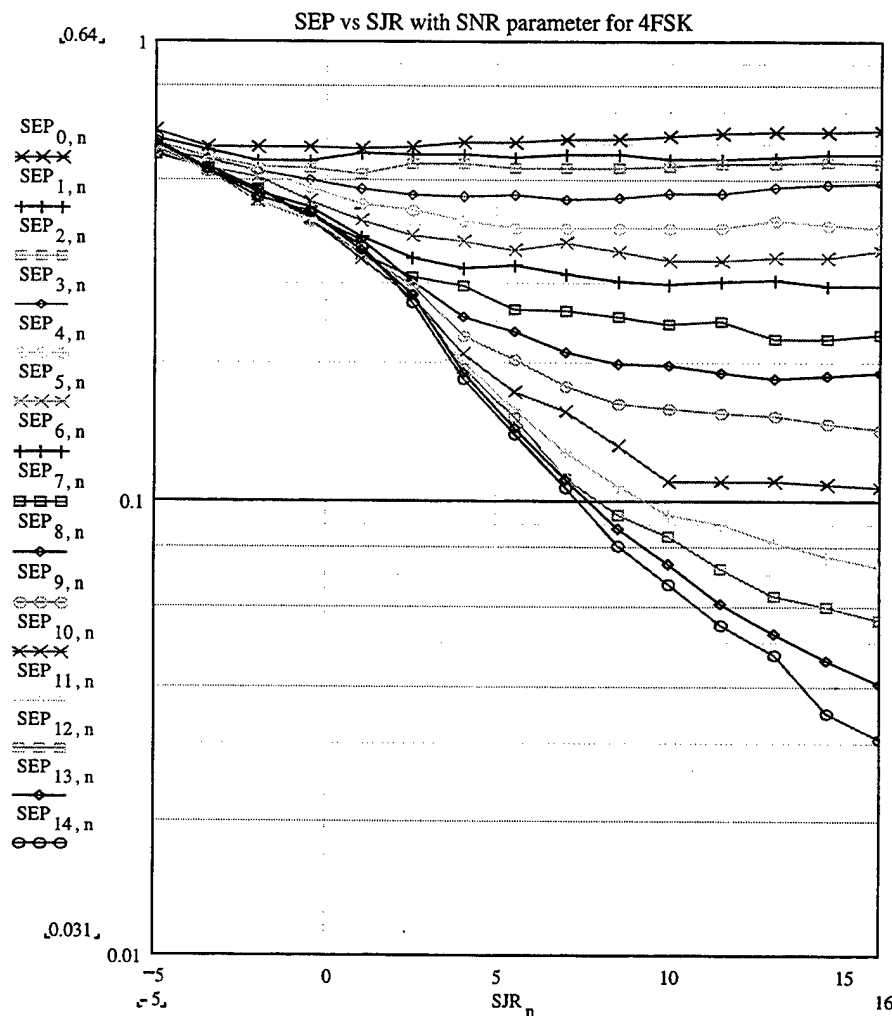
Figure 184. Simulation symbol error probability versus SJR with SNR as a parameter for non-coherent 4FSK, with Rician fading and R=1 for both MFSK signals (desirable and interfering).

The relative difference (percent "error") between the theory and the simulation is presented in Table 54. In Figure 185, the average error for each curve is plotted versus SNR and SJR for each of the 15 previously presented curves.
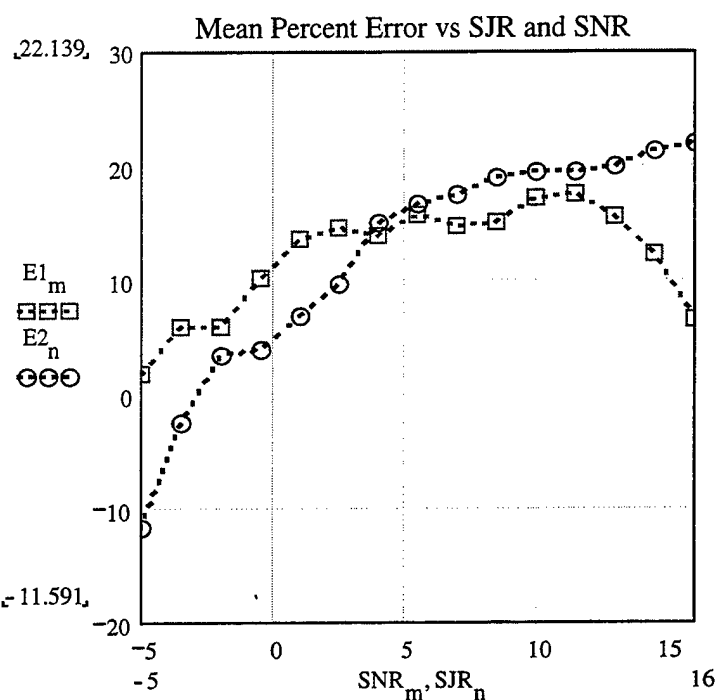
Figure 185. Mean percent difference as a function of SNR and SJR, respectively.

The two curves show how the mean difference varies with SNR and SJR. Each value of the mean difference is the average of the differences that correspond to the 15 points on each of the 15 curves for the symbol error probability as a function of SNR (with SJR as parameter) and SJR (with SNR as parameter), respectively.

	SYMBOL ERROR PROBABILITY	NON-COHERENT 4FSK
1.	Root Mean Square Difference (%)	19.771
2.	Average Mean Difference (%)	12.131
3.	Maximum Difference (%)	50.398
4.	Minimum Difference (%)	-101.574
5.	Difference Deviation (%)	15.612

Table 54. Summary of the accuracy of the simulation for non-coherent 4FSK.

267

c) Results For 8FSK

The theoretical and the simulation symbol error probabilities for non-coherently detected 8FSK are presented in the Figures 186 and 187, respectively, as functions of average SNR in dB with SJR as a parameter. The values for the signal-to-noise and signal-to-interference ratios were chosen from −5 dB to +16 dB in increments of 1.5 dB.
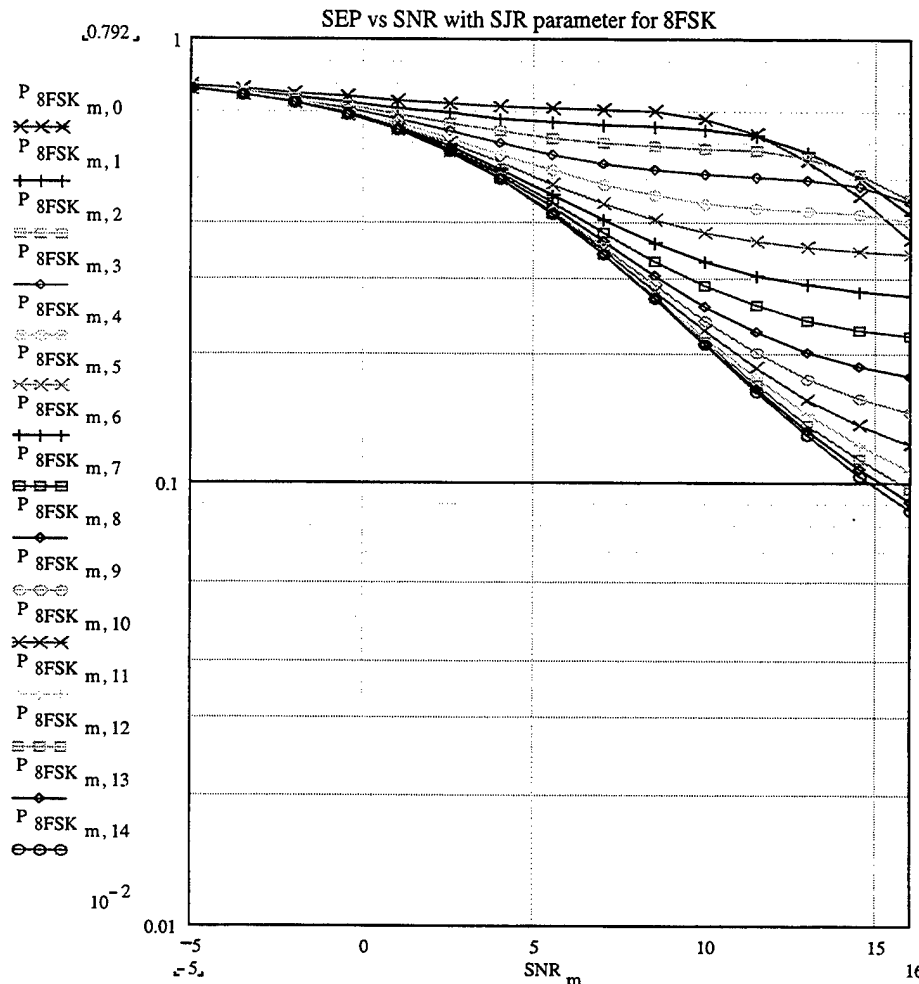

Figure 186. Theoretical symbol error probability versus SNR with SJR as a parameter for non-coherent 8FSK, with Rician fading and R=1 for both MFSK signals (desirable and interfering).
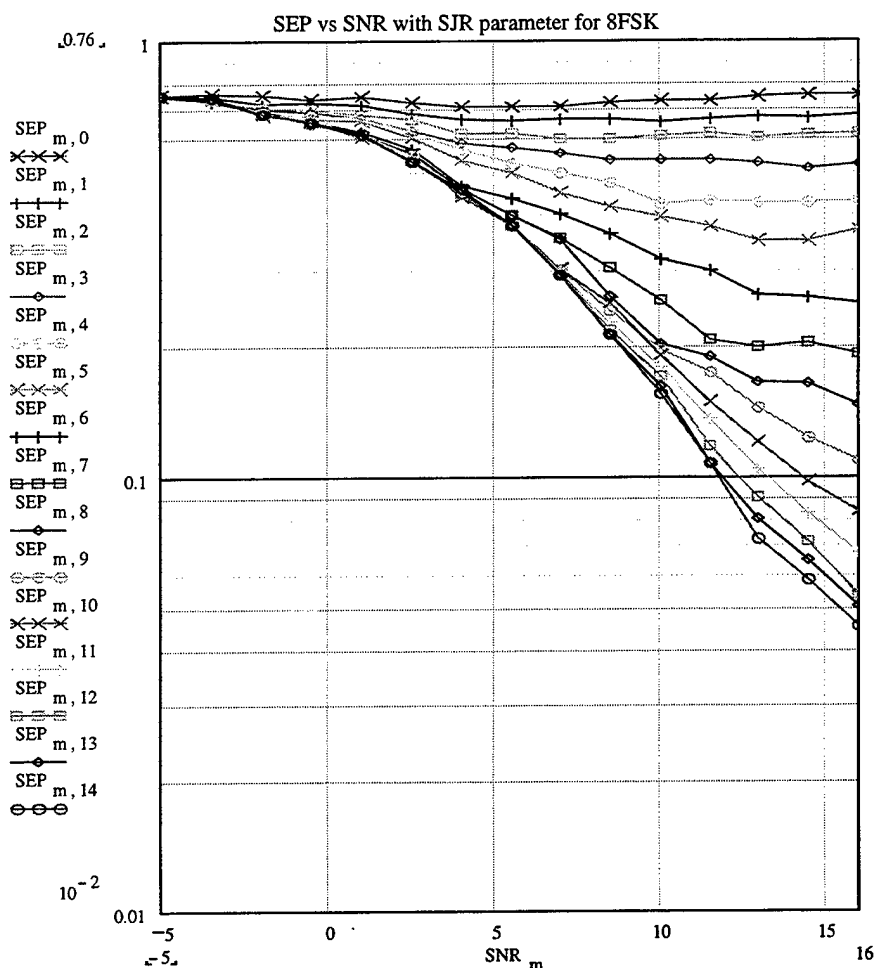
Figure 187. Simulation symbol error probability versus SNR with SJR as a parameter

for non-coherent 8FSK, with Rician fading and R=1 for both MFSK signals (desirable

and interfering).

In Figures 188 and 189, respectively, the theoretical and simulation results

for the symbol error probability are presented as functions of SJR with SNR as a

parameter.

269
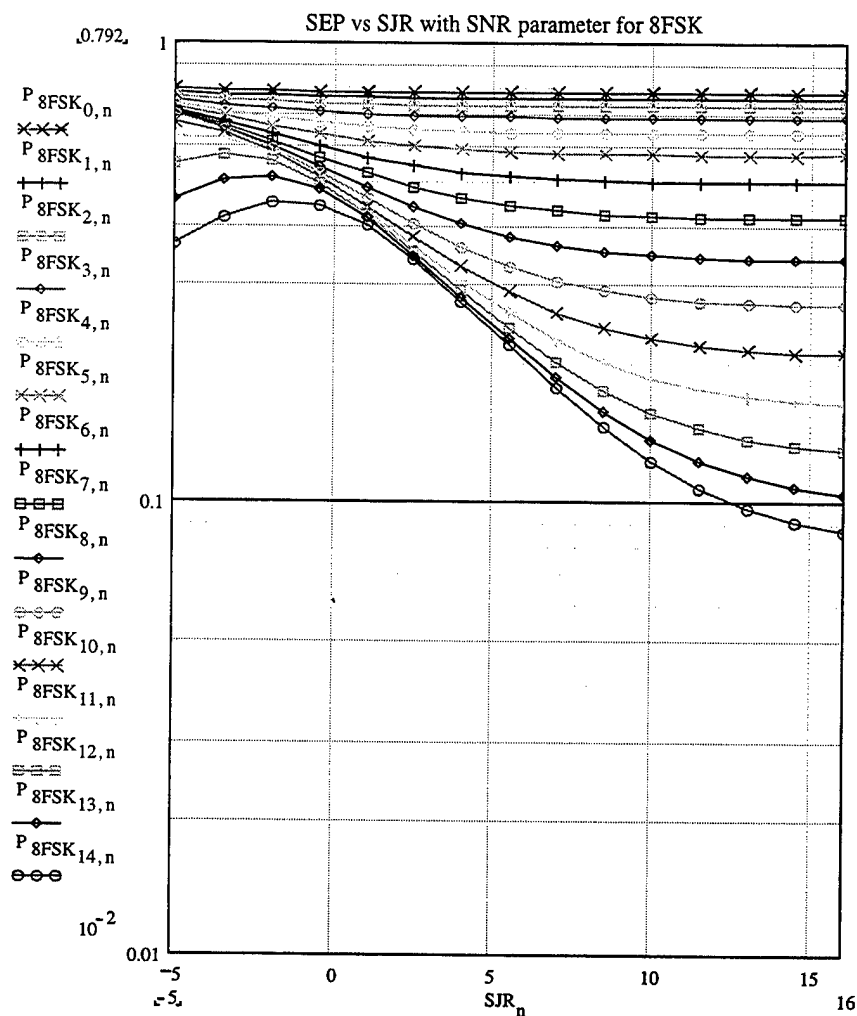
Figure 188. Theoretical symbol error probability versus SJR with SNR as a parameter for non-coherent 8FSK, with Rician fading and R=1 for both MFSK signals (desirable and interfering).

We note again the dramatic increase in the symbol error probability due to Rician fading and co-channel interference.
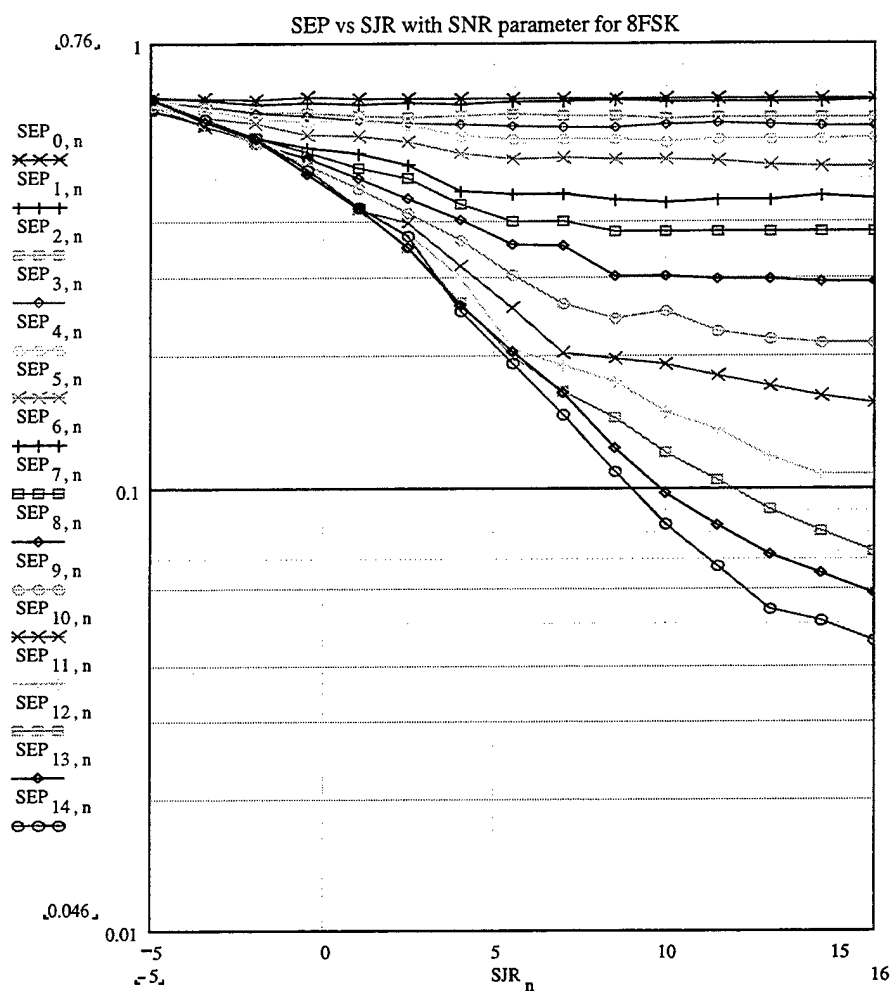
Figure 189. Simulation symbol error probability versus SJR with SNR as a parameter
for non-coherent 8FSK, with Rician fading and R=1 for both MFSK signals (desirable
and interfering).

The relative difference (percent "error") between the theory and the
simulation is presented in Table 55. In Figure 190, the average error for each curve is
plotted versus SNR and SJR for each of the 15 previously presented curves.

271
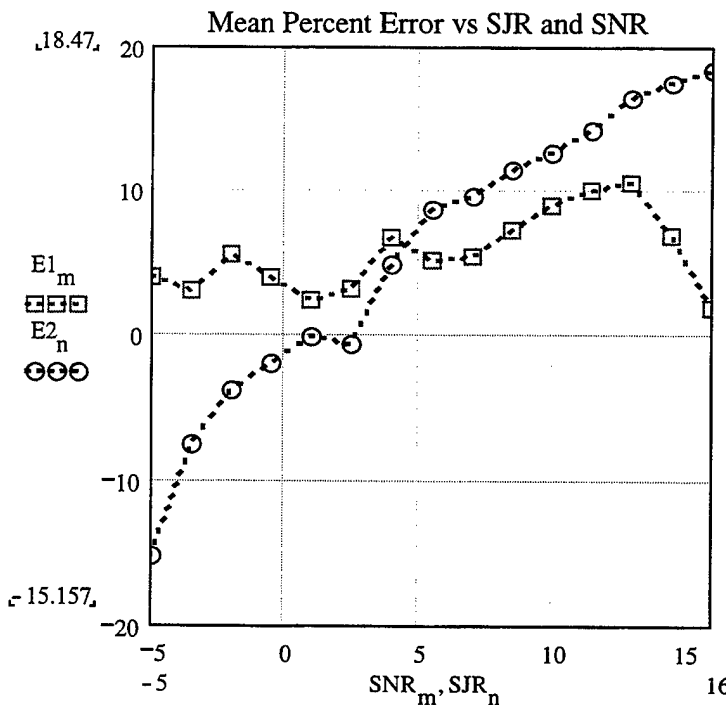
Figure 190. Mean percent difference as a function of SNR and SJR, respectively.

The two curves show how the mean difference varies with SNR and SJR. Each value of the mean difference is the average of the differences that correspond to the 15 points on each of the 15 curves for the symbol error probability as a function of SNR (with SJR as parameter) and SJR (with SNR as parameter), respectively.

	SYMBOL ERROR PROBABILITY	NON-COHERENT 8FSK
1.	Root Mean Square Difference (%)	16.827
2.	Average Mean Difference (%)	5.633
3.	Maximum Difference (%)	47.421
4.	Minimum Difference (%)	-105.789
5.	Difference Deviation (%)	15.856

Table 55. Summary of the accuracy of the simulation for non-coherent 8FSK.

Observing the results for non-coherent detection of 2, 4, and 8FSK in a Rician fading channel and affected by AWGN and co-channel interference, we note that the simulation underestimates the theory for all of the cases of 2, 4, and 8FSK. The root mean square difference (in percent) is about 18% (in average) and the mean percent difference for all the cases is about 9%.

The average results for the non-coherent detection of 2, 4, and 8FSK are presented in Table 56.

	SYMBOL ERROR PROBABILITY	AVERAGE RESULTS FOR NON-COHERENT 2, 4, AND 8FSK
1.	Root Mean Square Difference (%)	18.641
2.	Average Mean Difference (%)	8.733
3.	Maximum Difference (%)	50.237
4.	Minimum Difference (%)	-112.425
5.	Difference Deviation (%)	16.285

Table 56. Average results for the non-coherent detection of 2, 4, and 8FSK.

VII. SUMMARY AND RECOMMENDATIONS

A. SUMMARY

In this thesis the probability of symbol error is quantified for coherent and non-coherent detection of M-ary frequency-shift keyed (MFSK) signals affected by another, interfering, MFSK signal (co-channel interference), and additive white Gaussian noise (AWGN) in a fading channel.

First, the symbol error probabilities for coherent detection of 2FSK, 4FSK, and 8FSK have been determined by theoretical expressions as functions of SNR and SJR. Then, the same symbol error probabilities have been determined by performing time domain simulations based on SIMULINK and MATLAB/SIMULINK Communications Toolbox. Finally, the theoretical symbol error probabilities have been compared with the simulation results, the differences between them have been presented and the possible causes of these differences have been discussed.

All the theoretical expressions derived in Chapters IV, V, and VI as well as the closed form solutions in Appendices A, B, and C are original and their derivation was based on the concepts of coherent and non-coherent detection of MFSK signals.

The overall statistics for the difference (percent "error") between the theory and the simulation are presented in Table 57. The presented total results have been derived by averaging the statistics over all the values obtained for each case of MFSK detection.

	SYMBOL ERROR PROBABILITY	TOTAL RESULTS FOR 2, 4, AND 8FSK
1.	Root Mean Square Difference (%)	15.3756
2.	Average Mean Difference (%)	8.1325
3.	Maximum Difference (%)	38.4691
4.	Minimum Difference (%)	-45.0895
5.	Difference Deviation (%)	13.3638

Table 57. Overall statistics for the difference between theory and simulation of the detection of 2, 4, and 8FSK with AWGN and co-channel interference in fading channel.

The simulation required computational time to obtain values of the symbol error probability as small as 10^{-4} for 100 or so errors was about 3-4 hours maximum (on a 600 MHz PC). The numerical evaluation of the theoretical expressions, using MATHCAD8, required several seconds minimum and 7-8 hours maximum time (on a 600 MHz PC).

B.   RECOMMENDATIONS

The phase shift between the interference and the desired signal affects the detection process only for the case of the desired signal and the interference on same branch. In this work the assumption was made that the interference carrier has the same phase as the desired signal carrier, that is their phase difference has not been implemented in the Simulink model and not accounted for in the theoretical calculations. Inclusion of the phase difference between the carriers of the interfering and the desired signals adds another random variable to the model and increases the model complexity further, but it also represents a more realistic case. Further work should include the addition of a random variable representing the phase difference. The most likely case

276

would be that the phase difference is represented by a uniformly distributed random variable (between 0 and 2π).

Also, various ratios of the direct and diffuse powers (R) should be considered for the Rician interference model. In this work the special case R=1 (equal direct and diffuse powers) was considered. Note that the case of Rayleigh distributed interference and the case of constant interference power are the limiting cases when R tends to 0 and R tends to infinity, and these case have been addressed here. Nevertheless, it would be of interest to consider several cases of R between 0 and 1 (say 0.5, 0.25, etc.) and several cases of R between 1 and infinity (say 2, 4, etc.).

THIS PAGE INTENTIONALLY LEFT BLANK.

APPENDIX A. CLOSED FORM SOLUTION FOR THE SYMBOL ERROR PROBABILITY OF COHERENT BFSK WITH AWGN AND CO-CHANNEL INTERFERENCE

1. The Signal And The Interference Symbols Are On The Same Branch

The symbol error probability for coherent detection of MFSK with AWGN and co-channel interference with the signal and the interference symbols on the same branch of the receiver is given by equation (4.7). Applying M=2, we obtain the corresponding expression for BFSK:

$$P1 = 1 - \frac{1}{\sqrt{2 \cdot \pi}} \cdot \int_{-\infty}^{\infty} e^{\frac{-x^2}{2}} \cdot \left(1 - Q\left(x + \frac{S+J}{\sigma}\right)\right) dx \tag{A1}$$

We recall the following identities:

$$\int_{-\infty}^{\infty} e^{\frac{-x^2}{2}} dx = \sqrt{2 \cdot \pi} \tag{A2}$$

$$Q(x) = \frac{1}{2} \cdot \left(1 - erf\left(\frac{x}{\sqrt{2}}\right)\right) \tag{A3}$$

$$\int_{-\infty}^{\infty} e^{-\alpha \cdot x^2} \cdot erf\left(\frac{x+b}{\sqrt{2}}\right) dx = \sqrt{\frac{\pi}{\alpha}} \cdot erf\left(b \cdot \sqrt{\frac{\alpha}{2 \cdot \alpha + 1}}\right) \quad \text{with} \quad \alpha > 0 \tag{A4}$$

279

Applying (A2), (A3), and (A4) to equation (A1), we find the closed form solution:

$$P1 = Q\left(\frac{S + J}{\sqrt{2} \cdot \sigma}\right) \tag{A5}$$

Using (4.16), we express P1 as a function of SNR and SJR:

$$P1 = Q\left(10^{\frac{SNR}{20}} + 10^{\frac{SNR - SJR}{20}}\right) \tag{A6}$$

2.   The Signal And The Interference Symbols Are On Different Branches

The symbol error probability for coherent detection of MFSK with AWGN and co-channel interference with the signal and the interference symbols on different branches of the receiver is given by equation (4.14). Applying M=2, we obtain the corresponding expression for BFSK:

$$P2 = 1 - \frac{1}{\sqrt{2 \cdot \pi}} \cdot \int_{-\infty}^{\infty} e^{\frac{-x^2}{2}} \cdot \left(1 - Q\left(x + \frac{S - J}{\sigma}\right)\right) dx \tag{A7}$$

Applying (A2), (A3), and (A4) to equation (A7), we find the closed form solution:

$$P2 = Q\left(\frac{S - J}{\sqrt{2} \cdot \sigma}\right) \tag{A8}$$

Using (4.16), we express P2 as a function of SNR and SJR:

$$P2 = Q\left(10^{\frac{SNR}{20}} - 10^{\frac{SNR - SJR}{20}}\right) \tag{A9}$$

280

3. Total Symbol Error Probability

Applying (A6) and (A9) in (4.15), we find the symbol error probability for BFSK:

$$P_{BFSK} = \frac{1}{2} \cdot Q\left(10^{\frac{SNR}{20}} + 10^{\frac{SNR-SJR}{20}}\right) + \frac{1}{2} \cdot Q\left(10^{\frac{SNR}{20}} - 10^{\frac{SNR-SJR}{20}}\right) \quad (A10)$$

THIS PAGE INTENTIONALLY LEFT BLANK.

APPENDIX B. CLOSED FORM SOLUTION FOR EQUATION (5.15)

We recall equation (5.15) for the symbol error probability for non-coherent detection of MFSK signals transmitted over a frequency nonselective, slowly fading Rayleigh channel in the presence of AWGN and co-channel interference with the signal and the interference symbols on the same branch of the receiver (case 1):

$$P1 = \int_0^\infty \sum_{k=1}^{M-1} \frac{(M-1)!}{k! \cdot (M-1-k)!} \cdot \frac{(-1)^{k+1}}{k+1} \cdot e^{\frac{-k}{2 \cdot (k+1)} \cdot \left(y \cdot \frac{\sqrt{P_{sig}}}{\sqrt{P_{noise}}} + \frac{J}{\sqrt{P_{noise}}} \right)^2} \cdot e^{\frac{-y^2}{2}} \cdot y \, dy \quad (B1)$$

Moving the integral inside the summation and rearranging the terms, we obtain:

$$P1 = \sum_{k=1}^{M-1} \frac{(M-1)!}{k! \cdot (M-1-k)!} \cdot \frac{(-1)^{k+1}}{k+1} \cdot e^{-k \cdot \frac{J^2}{P_{noise}}}{2 \cdot (k+1)} \cdot \int_0^\infty y \cdot e^{-\left[\frac{k \cdot \frac{P_{sig}}{P_{noise}}}{2 \cdot (k+1)} + \frac{1}{2} \right] \cdot y^2 - \left[\frac{k \cdot \frac{\sqrt{P_{sig}}}{P_{noise}} \cdot J}{k+1} \right] \cdot y} \, dy \quad (B2)$$

We recall the following identity:

$$\int_0^\infty x^n \cdot e^{-p \cdot x^2 - q \cdot x} dx = \frac{(-1)^n}{2} \cdot \sqrt{\frac{\pi}{q}} \cdot \frac{d^n}{d q^n} \left(e^{\frac{q^2}{4 \cdot p}} \cdot \mathrm{erfc}\left(\frac{q}{2 \cdot \sqrt{p}} \right) \right) \quad (B3)$$

We let:

$$p = \frac{k \cdot \frac{P_{sig}}{P_{noise}}}{2 \cdot (k+1)} + \frac{1}{2} \qquad q = \frac{k \cdot \frac{\sqrt{P_{sig}}}{P_{noise}} \cdot J}{k+1} \quad (B4)$$

Applying (B3) and (B4), for n equal to 1, into (B2), we find the closed form solution:

$$P1 = \sum_{k=1}^{M-1} \frac{(M-1)!}{k! \cdot (M-1-k)!} \cdot \frac{(-1)^{k+2}}{2 \cdot (k+1)} \cdot e^{-k \cdot \frac{J^2}{P_{noise}} / 2 \cdot (k+1)} \cdot \left(\frac{\sqrt{q \cdot \pi}}{2 \cdot p} \cdot \exp\left(\frac{q^2}{4 \cdot p}\right) \cdot \mathrm{erfc}\left(\frac{q}{2 \cdot \sqrt{p}}\right) - \frac{1}{\sqrt{p \cdot q}} \right) \quad (B5)$$

Substituting back the values of p and q (equations (B4)) into (B5), we obtain:

$$P1 = \sum_{k=1}^{M-1} \frac{(M-1)!}{k! \cdot (M-1-k)!} \cdot \frac{(-1)^{k+2}}{2} \cdot e^{-k \cdot \frac{J^2}{P_{noise}} / 2 \cdot (k+1)} \cdot \left[\left(\frac{\sqrt{\frac{k \cdot \frac{\sqrt{P_{sig}}}{P_{noise}} \cdot J}{k+1}} \cdot \pi}{k \cdot \frac{P_{sig}}{P_{noise}} + k+1} \cdot e^{\frac{\left(k \cdot \frac{\sqrt{P_{sig}}}{P_{noise}} \cdot J\right)^2 / (k+1)}{2 \cdot \left(k \cdot \frac{P_{sig}}{P_{noise}} + k+1\right)}} \cdot \mathrm{erfc} \frac{k \cdot \frac{\sqrt{P_{sig}}}{P_{noise}} \cdot J / \sqrt{k+1}}{\sqrt{2} \cdot \sqrt{k \cdot \frac{P_{sig}}{P_{noise}} + k+1}} \right) + \frac{-\sqrt{2}}{\sqrt{\left(k \cdot \frac{P_{sig}}{P_{noise}} + k+1\right) \cdot \left(k \cdot \frac{\sqrt{P_{sig}}}{P_{noise}} \cdot J\right)}} \right] \cdots \quad (B6)$$

284

APPENDIX C. CLOSED FORM SOLUTION FOR EQUATION (5.41)

We recall equation (5.41) for the symbol error probability for non-coherent detection of MFSK signals transmitted over a frequency nonselective, slowly fading Rician channel in the presence of AWGN and co-channel interference with the signal and the interference symbols on the same branch of the receiver (case 1):

$$
P1 = \int_0^\infty \sum_{k=1}^{M-1} \frac{(M-1)!}{k! \cdot (M-1-k)!} \cdot \frac{(-1)^{k+1}}{(k+1)} \cdot e^{\frac{-k}{2 \cdot (k+1)} \cdot \left(\frac{\sqrt{P_{dif}} y + J}{\sqrt{P_{noise}}} \right)^2} \cdot e^{\frac{-1}{2} \cdot \left(y^2 + 2 \cdot \frac{P_{dir}}{P_{dif}} \right)} \cdot I0 \left(2 \cdot \sqrt{\frac{P_{dir}}{P_{dif}}} \cdot y \right) \cdot y \; dy \quad (C1)
$$

For practical purposes we define the following constants:

$$
\alpha = \frac{\sqrt{P_{dif}}}{\sqrt{P_{noise}}} \qquad b = \frac{J}{\sqrt{P_{noise}}} \qquad c = \frac{P_{dir}}{P_{dif}} \qquad (C2)
$$

Using (C2) and moving the integral inside the summation, we obtain:

$$
P1 = \sum_{k=1}^{M-1} \frac{(M-1)!}{k! \cdot (M-1-k)!} \cdot \frac{2 \cdot (-1)^{k+1}}{\left(k \cdot \alpha^2 + k + 1 \right)} \cdot e^{-\left[\frac{k \cdot b^2}{2 \cdot \left(k \cdot \alpha^2 + k + 1 \right)} + c \right]} \cdot \int_0^\infty \left[e^{-\left[y + \frac{k \cdot \alpha \cdot b}{\sqrt{2 \cdot (k+1) \cdot \left(k \cdot \alpha^2 + k + 1 \right)}} \right]^2} \cdot I0 \left(2 \cdot \sqrt{c} \cdot \frac{\sqrt{k+1}}{\sqrt{k \cdot \alpha^2 + k + 1}} \cdot y \right) \cdot y \right] dy \quad (C3)
$$

We recall the identity:

$$
I0(x) = \sum_{n=0}^{\infty} \frac{\left(\frac{x}{2} \right)^{2 \cdot n}}{(n!)^2} \qquad (C4)
$$

285

Substituting (C4) into (C3), we obtain:

$$P = \sum_{k=1}^{M-1} \sum_{n=0}^{\infty} \frac{(M-1)!}{k! \cdot (M-1-k)!} \cdot \frac{2 \cdot (-1)^{k+1}}{\left(k\alpha^2 + k + 1\right)} \cdot e^{-\left[\frac{k b^2}{2\left(k\alpha^2 + k + 1\right)} + c\right]} \cdot \left(\frac{1}{n!}\right)^2 \left[\frac{c \cdot (k+1)}{k\alpha^2 + k + 1}\right]^n \cdot \int_0^{\infty} e^{-\left[y + \frac{k\alpha b}{\sqrt{2(k+1) \cdot (k\alpha^2 + k + 1)}}\right]^2} y^{2n+1} dy \quad (C5)$$

Now, we make the following transformation of variable:

$$z = y + \frac{k \cdot \alpha \cdot b}{\sqrt{2 \cdot (k+1) \cdot \left(k \cdot \alpha^2 + k + 1\right)}} = y + \gamma \qquad (C6)$$

where γ is constant.

So, (C5) becomes:

$$P = \sum_{k=1}^{M-1} \sum_{n=0}^{\infty} \frac{(M-1)!}{k! \cdot (M-1-k)!} \cdot \frac{2 \cdot (-1)^{k+1}}{\left(k\alpha^2 + k + 1\right)} \cdot e^{-\left[\frac{k \cdot b^2}{2\left(k\alpha^2 + k + 1\right)} + c\right]} \cdot \left(\frac{1}{n!}\right)^2 \left[\frac{c \cdot (k+1)}{k \cdot \alpha^2 + k + 1}\right]^n \cdot \int_{\gamma}^{\infty} e^{-z^2} \cdot (z - \gamma)^{2n+1} dz \quad (C7)$$

To evaluate the integral of the above expression, we recall the binomial identity:

$$(z - \gamma)^{2 \cdot n + 1} = \sum_{m=0}^{2 \cdot n + 1} \frac{(2 \cdot n + 1)!}{m! \cdot (2 \cdot n + 1 - m)!} \cdot (-\gamma)^{2 \cdot n + 1 - m} \cdot z^m \qquad (C8)$$

Applying (C8) to (C7), we obtain:

$$P1 = \left[\begin{array}{l} \displaystyle\sum_{k=1}^{M-1} \sum_{n=0}^{\infty} \sum_{m=0}^{2 \cdot n + 1} \frac{(M-1)!}{k! \cdot (M-1-k)!} \cdot \frac{2 \cdot (-1)^{k+1}}{\left(k \cdot \alpha^2 + k + 1\right)} \cdot e^{-\left[\frac{k \cdot b^2}{2 \cdot \left(k \cdot \alpha^2 + k + 1\right)} + c\right]} \\[2em] \displaystyle \left(\frac{1}{n!}\right)^2 \cdot \left[\frac{c \cdot (k+1)}{k \cdot \alpha^2 + k + 1}\right]^n \cdot \frac{(2 \cdot n + 1)!}{m! \cdot (2 \cdot n + 1 - m)!} \cdot (-\gamma)^{2 \cdot n + 1 - m} \cdot \int_{\gamma}^{\infty} e^{-z^2} \cdot z^m dz \end{array} \right] \quad (C9)$$

Now, the integral of (C9) has the following solution:

$$\int_{\gamma}^{\infty} e^{-z^2} \cdot z^m \, dz = \frac{1}{2} \cdot \Gamma\left(\frac{1}{2} \cdot m + \frac{1}{2}, \gamma^2\right)$$

(C10)

Substituting into (C9), we get:

$$P1 = \left[\begin{array}{c} \displaystyle\sum_{k=1}^{M-1} \sum_{n=0}^{\infty} \sum_{m=0}^{2 \cdot n + 1} \frac{(M-1)!}{k! \cdot (M-1-k)!} \cdot \frac{(-1)^{k+1}}{\left(k \cdot \alpha^2 + k + 1\right)} \cdot e^{-\left[\frac{k \cdot b^2}{2 \cdot \left(k \cdot \alpha^2 + k + 1\right)} + c\right]} \\[2em] \left(\frac{1}{n!}\right)^2 \cdot \left[\frac{c \cdot (k+1)}{k \cdot \alpha^2 + k + 1}\right]^n \cdot \frac{(2 \cdot n + 1)!}{m! \cdot (2 \cdot n + 1 - m)!} \cdot (-\gamma)^{2 \cdot n + 1 - m} \cdot \Gamma\left(\frac{m+1}{2}, \gamma^2\right) \end{array} \right]$$

(C11)

The **complementary incomplete gamma function** $\Gamma(m+1/2, \gamma)$ is given by ((2.46) of Ref [9]):

$$\Gamma\left(\frac{m+1}{2}, \gamma^2\right) = \Gamma\left(\frac{m+1}{2}\right) - \gamma^{(m+1)} \cdot \sum_{p=0}^{\infty} \frac{(-1)^p \cdot \gamma^{2 \cdot p}}{p! \cdot \left(p + \frac{m+1}{2}\right)}$$

(C12)

The gamma function in (C12) is given by ((2.4) and (2.25) of Ref [9]):

$$\Gamma\left(\frac{m+1}{2}\right) = \left(\frac{m-1}{2}\right)! \qquad \text{for } m=1,3,5,7,9,\ldots$$

(C13)

$$\Gamma\left(\frac{m+1}{2}\right) = \frac{m!}{2^m \cdot \left(\frac{m}{2}\right)!} \cdot \sqrt{\pi} \qquad \text{for } m=0,2,4,6,8,\ldots$$

(C14)

287

LIST OF REFERENCES

1.   Konstantinos Tsiridis, *Time Domain Simulations of MFSK Communications System Performance in the Presence of Wideband Noise and Co-Channel Interference*, Master's Thesis, Naval Postgraduate School, Monterey, CA, December 1998.

2.   Lebaric Jovan, Course Notes for EC 4550 Digital Communications, Naval Postgraduate School, Monterey, CA, 1998.

3.   *Simulink User's Guide*, The Math Works Inc., Natick, MA, 1993.

4.   Bernard Sklar, *Digital Communications*, Prentice Hall, Englewood Cliffs, NJ, 1988.

5.   M. Jeruchim et al, *Communication System Simulation*, Plenum Press, New York, NY, 1992.

6.   Floyd M. Gardner and John D. Baker, *Simulation Techniques*, John Wiley and Sons Inc., New York, NY, 1997.

7.   The Matlab Expo, *An Introduction to Matlab, Simulink, and the Matlab Toolboxes*, Inc., Natick, MA, April 1993.

8.   W. Wang, *Communications Toolbox User's Guide*, The Math Works Inc., 2nd ed., Natick, MA, 1996.

9.   Larry C. Andrews, *Special Functions of Mathematics for Engineers*, McGraw-Hill, Inc., New York, NY, 1992.

INITIAL DISTRIBUTION LIST

No. Copies

1. Defense Technical Information Center..2
    8725 John J. Kingman Rd., STE 0944
    Ft. Belvoir, VA 22060-6218

2. Dudley Knox Library..2
    Naval Postgraduate School
    411 Dyer Rd.
    Monterey, CA 93943-5101

3. Chairman, Code EC..1
    Department of Electrical and Computer Engineering
    Naval Postgraduate School
    Monterey, CA 93943-5121

4. Professor Clark Robertson, Code EC/Rc......................................1
    Department of Electrical and Computer Engineering
    Naval Postgraduate School
    Monterey, CA 93943-5121

5. Dr Jovan Lebaric, Code EC/Le..2
    Department of Electrical and Computer Engineering
    Naval Postgraduate School
    Monterey, CA 93943-5121

6. Embassy of Greece..1
    Office of the Air Attaché
    2228 Massachusetts Avenue, N.W.
    Washington, DC 20008

7. Andreas Argyriou..1
    Menelaou 69 & Dionysou 5
    Ag. Dimitrios 17343
    Athens
    GREECE